REGULATION OF TRANSCRIPTION BY ULTRAVIOLET-B RADIATION IN *Arabidopsis thaliana*

Christos N. Velanis

Submitted in fulfilment of the requirements for the degree of Doctor of Philosophy

College of Medical Veterinary and Life Sciences
Institute of Molecular, Cell and Systems Biology
University of Glasgow

December 2014

“There is no royal road to science, and only those who do not dread the fatiguing climb of its steep paths have a chance of gaining its luminous summits”

Karl Marx, Das Kapital, Volume 1
Preface to the French Edition
London 1872

Abstract

Plants are sessile photo-autotrophic organisms and need to adapt constantly to a dynamic environment. Light is of utmost importance for plants to be able to monitor their surroundings. Ultraviolet-B radiation (UV-B; 280-315 nm) is an intrinsic part of sunlight and, depending on the wavelength and the fluence rate, it may be a stressful signal or an "informational" one. The so called photomorphogenic responses of plants to UV-B are largely mediated by the UV-B specific photoreceptor UV RESISTANCE LOCUS 8 (UVR8), which "senses" UV-B via a tryptophan based mechanism.

UVR8 is localised in the cytoplasm and the nucleus mainly as a homodimer. Upon UV-B irradiation it splits to its monomers and accumulates in the nucleus where it has been found to interact with the E3 Ubiquitin ligase COP1. In the nucleus UVR8 has been shown to associate with chromatin on loci of UV-B responsive genes, including that encoding for the bZIP transcription factor (TF) ELONGATED HYPOCOTYL 5 (HY5), a key effector of UVR8-dependent signalling pathways. The binding of UVR8 to chromatin appears to take place via interaction with histones (H2B in particular) rather than DNA itself. However, this association with chromatin seems not to be UV-B specific.

The above data suggest a mechanistic basis for an assumed function of UVR8 in the regulation of transcription. It is possible that UVR8 interacts with other proteins associated with chromatin to promote remodelling and/or recruits/activates TFs which in turn stimulate transcription of its target genes. The main objective of this study was to address the above working hypothesis. Chromatin immunoprecipitation (ChIP) experiments revealed that the loci of particular UVR8-regulated genes accumulate specific histone acetylation marks following UV-B illumination, and these enrichments were observed only under the presence of a functional UVR8. Moreover, Yeast One Hybrid (Y1H) screens were performed with the aim of identifying novel TFs which mediate the UVR8-dependent UV-B induced activation of *HY5* expression. Several interesting candidates were obtained, including members of the BBX family of transcriptional regulators and members of the R2R3 MYB family of TFs, and although none was found to be essential for the UVR8-mediated UV-B responses that were tested, the findings that emerged in the course of this study open new directions for future research.

TABLE OF CONTENTS

List of figures

Chapter 1

Chapter 2

Chapter 3

Chapter 4

Chapter 5

Chapter 6

Chapter 7

Chapter 8

List of tables

Chapter 2

Chapter 5

PREFACE

Part of the experimental work of this thesis has been included in the following publication:

Hayes, S., Velanis, C.N., Jenkins, G.I., and Franklin, K.A. (2014). UV-B detected by the UVR8 photoreceptor antagonizes auxin signaling and plant shade avoidance. Proc Natl Acad Sci U S A **111**: 11894–11899.

ACKNOWLEDGMENTS

This PhD thesis is the end (or perhaps I should say “a stop”, so that I can get some rest before I set out again) of a journey I started nearly four years ago driven by a long-lasting interest in Biology. It is not an easy journey, but it turns out to be very enjoyable, and I owe that to many inspiring people I was privileged to interact with along the way.

Firstly, I am very grateful to my supervisor, Prof. Gareth I. Jenkins, who gave me the opportunity to work on this project and guided me throughout my studies providing valuable advice, support and encouragement. Many thanks also to Prof. John M. Christie, who always had time to discuss with me and helped me to overcome many difficulties in my research.

I would additionally like to thank Dr Catherine Cloix, Dr Katherine Baxter, Dr Bobby Brown, and the two fellow PhD students at the time, Monika Heilmann and Andrew O’ Hara, who all welcomed me to the team and were always happy to assist me. Bobby was at all times a very reliable source of information, and Monika was “an example to follow” with her organisation and efficiency in the lab. Being a nocturnal worker himself , “Dr Andy” was a great company for me during the many nights I was struggling to keep track of my yeast clones, and he also took great care so that I don’t end up supporting the “wrong” football team in Scotland. Many thanks also to my colleagues Kirsty McInnes, Kirsten Findlay and Lisa Blackwood who all contributed in creating a nice, pleasant atmosphere to work in, and they never complained that their pipettes, pens, or timers were often mysteriously found lying on my bench. Moreover, I’m thankful that I met Ellen, Ashutosh and Bhavana half-way through my PhD, as they brought different expertise to the lab, and I am especially grateful to Ashutosh, my neighbour across the bench, who was a great source of humour in addition to providing instructive scientific feedback.

A special mention for Dr Stuart Sullivan and Dr Jan Petersen who were always available to discuss my results with me, and got me off the hook on numerous occasions with helpful troubleshooting tips. Particularly Stuart’s critical approach has been of great value in helping me to strengthen this thesis.

I’m also grateful to Dr Pieter Ouwerkerk (University of Leiden) for providing the vectors for the Y1H screens, to Dr Christopher Grefen (University of Tübingen) for his guidance in setting up my screens, to Prof Ferenc Nagy for sharing unpublished (at the time) information on the *HY5* promoter *cis*-regulatory elements, to Prof Michael Holdsworth (University of Nottingham) for providing a *BBX31* clone and to Prof Jeffrey Chen (University of Texas at Austin) for providing the *hd1* mutants. Many thanks also to Dr Eirini Kaiserli, Maria Papanatsiou, Mary Ann Madsen and to everyone else in the Bower Building for many helpful discussions, and to Elina Chrysanthou who on numerous occasions volunteered to help me with my experiments.

Family members and great friends I’ve met in Glasgow contributed very much to my well being by helping me out through difficult periods, by sharing with me wonderful moments and by reminding me that there is a life outside the lab. Mentioning them here would require a whole Chapter, not a section, and devoting only a couple of lines would be unfair. I will reserve my acknowledgments to them for a more personal, informal moment, that I think they would appreciate more.

Finally, I would like to express my gratitude to Prof. Milton A Typas (University of Athens) and to the “State Scholarship Foundation of Greece” for coordinating all issues related to my funding. The last four years have been extremely difficult for Greece, with the majority of the population experiencing severe financial cuts. Yet, not a single penny was ever cut from my funding, enabling me to complete my studies without any difficulties. For that, I am most deeply indebted!

Author's Declaration

I declare that, except where explicit reference is made to the contribution of others, this dissertation is the result of my own work and has not been submitted for any other degree at the University of Glasgow or any other institution.

During my studies, I was financially supported by the State Scholarship Foundation of Greece (Ιδρυμα Κρατικών Υποτροφιών, I.K.Y).

Christos N. Velanis

Ab	Antibody
3-AT	3-amino-1,2,4-triazole
ABCB19	ATP-Binding Cassette B19
ACE	ACTG-Containing Elements
ACT2	Actin 2
AD	Activation Domain
ADA1-5	Alterations/Deficiency in Activation 1-5
ADO	Adagio
ALY 2	Always Early 2
ANAC13	Arabidopsis NAC domain 13
ANOVA	Analysis Of Variance
Arg	Arginine
ATAF1	Arabidopsis Transcription Activation Factor
BBX	B-Box
BD	Binding Domain
bHLH	basic Helix Loop Helix
BiFC	Bimolecular Fluorescence Complementation
BLUS1	Blue Light Signalling 1
C4-pepc	C4-specific phosphoenolpyruvate carboxylase
CAM7	Calmodulin 7
CcoAOMT	CAFEOYL-CoA 3-O-methyltransferase
CCT	CONSTANS, CONSTANCE LIKE and TOC1
CD	Circular Dichroism
CDD	COP10-DDB1-DET1
cDNA	complementary DNA
CEN4	Centromere of chromosome 4
ChIP	Chromatin ImmunoPrecipitation
CHS	Chalcone Synthase
CIB1	Cryptochrome interacting basic helix-loop-helix 1
CK2	Casein Kinase 2
CNT/PHR	Cryptochrome N-terminal Photolyase-Related domain
CO	CONSTANS
COG1	COGWeel 1
Co-IP	Co-ImmunoPrecipitation
Col-0	Columbia ecotype
COP1	Constitutively Photomorphogenic 1
CPRF1	Common Plant Regulatory Factors 1

CRYs	Cryptochromes
CSN	COP9 signalosome
CUC	Cup shaped Cotyledon
CUL4-DDB1	Cullin4-Damaged DNA Binding Protein 1
DASH	Drosophila, Arabidopsis, Synchocystis and Homo
DCAFs	DDB1 and CUL4 Associated Factors
DDB1	Damaged DNA Binding Protein 1
DoF	DNA binding with One Finger
DWD	DDB1 binding WD40 domain
EGFP	Enhanced Green Fluorescent Protein
ELIP1	Early Light Induced Protein 1
EPP1	Enhanced Photomorphogenic 1
FAD	Flavin Adenine Dinucleotide
FAR1	Far-Red Impaired Response 1
FHL	FHY1-Like
FHY3	Far Red Elongated Hypocotyl 3
FKF1	Flavin-Binding Kelch Repeat F-box 1
FLC	Flowering Locus C
FLT	Flowering Locus T
FMN	Flavin Mononuclotide
FR	Far-Red
FRET	Fluorescence Resonance Energy Transfer
FVE	Flowering Locus VE
GBF1	G-box Binding Factor 1
G-boxes	ACTG-Containing Elements
GCN4	General Control Non-Repressible 4
GCN5	General Control Non-Repressible 5
GNATs	GCN5-related N-terminal Acetyltransferases
H2B	Histone 2 B
H3	Histone 3
H3ac	Acetylated Histone 3
H3K14ac	Acetylated Lysine 14 of Histone 3
H3K27me3	Trimethylated Lysine 27 of Histone 3
H3K36me3	Trimethylated Lysine 36 of Histone 3
H3K4me3	Trimethylated Lysine 4 of Histone 3
H3K56ac	Acetylated Lysine 56 of Histone 3
H3K9ac	Acetylated Lysine 9 of Histone 3

H3K9,14diac	Diacetylated Histone 3 at Lysines 9 and 14
H3K9me3	Trimethylated Lysine 9 of Histone 3
H4	Histone 4
H4ac	Acetylated Histone 4
HAC5	Histone Acetyltransferase of the CREB Binding Protein Family
HATs	Histone acetyltransferases
HD1	Histone Deacetylase
HDACs	Histone de-acetylases
HDC1	Histone Deacetylase Complex 1
HFR1	Long Hypocotyl in Far Red 1
HIR	High Irradiance Response
HKRD	Histidine Kinase Related Domain
HRP	Horseradish Peroxidase
HY5	Elongated Hypocotyl 5
HYH	HY5 Homologue
IP	ImmunoPrecipitation
K14	Lysine14
K36	Lysine 36
K4	Lysine 4
K9	Lysine 9
LAF1	Long After Far Red 1
Ler	Landsberg *erecta*
LFRs	Low Fluence Responses
LKP2	LOV Kelch Protein 2
LOV	Light Oxygen Voltage
LREs	Light -Responsive cis-regulatory Elements
LUC	Luciferase
LW	Low fluence rate White light
MIRS	miRNA-encoding genes
MREs	Myb Recognition Elements
mRNA	messenger RNA
MTHF	methenyltetrahydrofolate
MYB	Myoblastosis
MYST	MOZ,Ybf2/Sas2, Sas2 and Tip60
NAC domain	NAM, ATAF1, CUC domain
NAM	No Apical Meristem
NASC	Nottingham Arabidopsis Stock Centre

NF-Y	Nuclear Factor Y
NLS	Nuclear Localisation Signal
NO	Nitric Oxide
NPH3	Non-Phototropic Hypocotyl 3
NR	Nitrate Reductase
OBP3	OBPF4 Binding protein 3
OE	OverExpressing
ORF	Open Reading Frame
PAR 1	Phytochrome Rapidly Regulated 1
PAS	Per-ARNT-Sim
Pfr	Phytochrome Far-red absorbing form
PhANGs	Photosynthesis-associated nuclear genes
phot 1- phot 2	phototropins
PHR	Photolyase related
PHYA-PHYE	Phytochrome A-E
PIFs	Phytochrome Interacting Factors
PIN3	PIN-Formed 3
PKL	PICKLE
PKS	Phytochrome Kinase Substrate
PlantTFD	Plant Trancription Factor Database
PME	Pectin Methylesterase
Pr	Phytochrome Red light absorbing form
R	Red
RCC1	Regulator of Chromatin Condensation 1
RCD1	Radical induced Cell Death 1
ROS	Reactive Oxygen Species
RPD3	Reduced Potassium Deficiency 3
RT-PCR	Reverse Transcriptase Polymerase Chain Reaction
RuBisCo	Ribulose-1,5-bisphosphate carboxylase
RUPs	Repressors of UV-B Photomorphogenesis
SCL33	SC35-LIKE SPLICING FACTOR 33
SD , SE	Standard Deviation, Standard Error
SDS-PAGE	Sodium dodecyl sulfate PolyAcrylamide gel Electrophoresis
SHP2	Shatterproof 2
SNL	SIN3-LIKE 1
SPA	Suppressor of Phytochrome A
SPL	Squamosa Promoter-Like

STH2	Salt Tolerance Homologue 2
TAF_{II}	TATA Associated Factors
TAIR	The Arabidopsis Information Resource
TBP	TATA Binding Protein
T-DNA	Transfer DNA
TFIID	Transcription Factor IID
TFs	Transcription Factors
TPT	TransPlanta Collection
Trps	tryptophans
TSS	Transcription start site
UBQ5	Ubiquitin
UV-B	Ultra Violet B
UVR8	Ultra Violet Resistance Locus 8
VLFRs	Very-Low- Fluence Responses
W	tryptophans
WB	Western Blots
WNK	With No Lysine
Ws	Wassilewskija
Y1H	Yeast one hybrid
Y2H	Yeast two hybrid
Y3H	Yeast three hybrid
ZTL	Zeitlupe

CHAPTER 1 : INTRODUCTION

Life, at least in its most familiar forms manifested by the majority of Earth's ecosystems, is entirely dependent on a constant solar energy supply. As such, it is currently sustained by higher plants, the principal solar collectors that convert light energy to chemical energy, which they eventually store in the bonds formed when carbohydrates are photosynthesised from carbon dioxide and water (Ruban, 2014). Being sessile organisms, plants have no other alternative but to face the challenges posed by a highly fluctuating environment on the site they have established themselves. Thus, they have evolved intricate mechanisms for monitoring their surroundings, and modifying their physiology accordingly, as they maintain a remarkable developmental and overall phenotypic plasticity (Feher, 2014). Among the environmental cues utilised for the assessment of the changing external conditions, light is of utmost importance. In order to integrate light signals, plants employ a sophisticated suite of photoreceptors (Fig. 1-1) that enable them to detect spectral quality, quantity (defined as photon fluence rate), duration and direction of illumination. Moreover, the effects of light on plant growth and development are profound during the entire life cycle, as they contribute to the regulation of seed germination, seedling photomorphogenesis, vegetative growth (phototropism, gravitropism, shade avoidance, diurnal photoperiodic responses) and reproductive growth (induction of flowering) (Kami et al., 2010).

The stratospheric ozone layer effectively filters out those wavelengths of the sunlight spectrum that lie below 295 nm (McKenzie et al., 2003). Very little radiation above 1000 nm reaches the Earth's surface, because atmospheric water absorbs strongly above that threshold (Hill and Jones, 2000). Not surprisingly, therefore, the biologically relevant sunlight wavelengths range between **U**ltra **V**iolet -**B** (UV-B, 280 - 315 nm) and Far-Red light (700 - 800 nm). In this introductory section, a brief outline of the interactions between plants and visible light will be provided at first, before attempting a more detailed account of responses to UV-B radiation, which is the light quality that this work principally focused on. Subsequently, recent advances in light-regulated transcriptional networks will be summarised and, eventually, a synopsis of the aims of this work will be provided along with a model encapsulating the working hypotheses on which the whole project was founded.

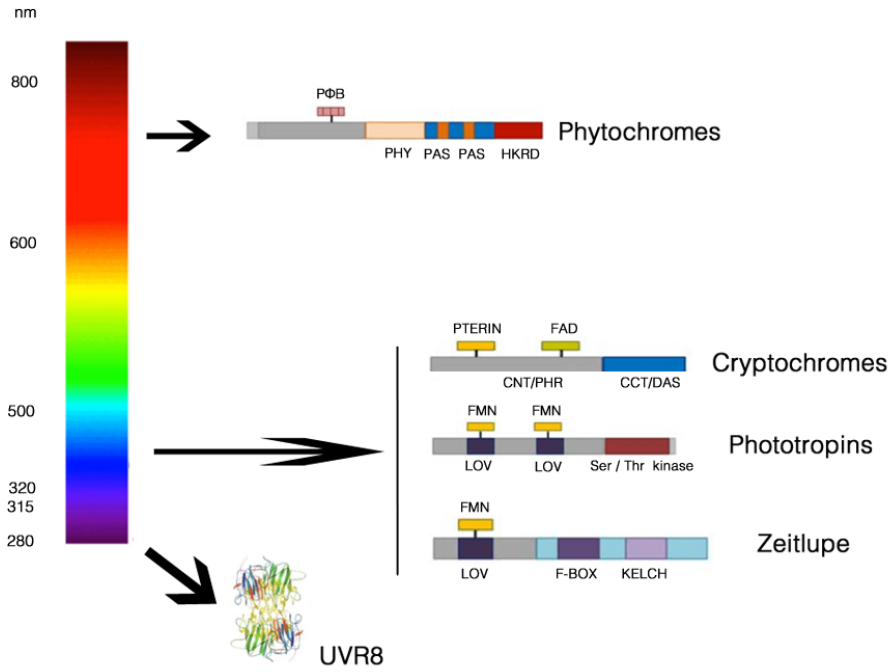

Fig 1-1. **Photoreceptor families in Arabidopsis**.
Phytochromes predominately absorb in the red and far-red region of the spectrum, whereas Cryptochromes, Phototropins and Zeitlupe proteins perceive blue light and UV-A wavelengths. UVR8 is the only known UV-B photoreceptor. **Phytochromes**: the N-terminal photosensory domain binds covalently the chromophore, a phytochromobilin (PΦB); the C-terminal domain contains several motifs important for signalling: **P**er-**A**RNT-**S**im (PAS) domain, **H**istidine **K**inase **R**elated **D**omain (HKRD). **Cryptochromes**: CNT/PHR domain, **C**ryptochrome **N**-**t**erminal **Ph**otolyase-**R**elated domain; CCT/DAS domain, less-conserved, intrinsically unstructured C-terminal domain; FAD, **F**lavin **A**denine **D**inucleotide chromophore. **Phototropins**: Photosensory N-terminal half consists of two **L**ight-**O**xygen-**V**oltage (LOV) domains binding the **F**lavin **M**ono**n**ucleotide (FMN), C-terminal half contains Serine / Threonine kinase function. **Zeitlupe**: Photosensory N-terminal half consists of one FMN-binding LOV domain, followed by an F-Box motif and six Kelch repeats (KELCH) in the C-terminal region. **UVR8**: a homodimeric photosensor of the WD40 family of proteins. Modified from Jiao et al., 2007

1.1 Phytochromes and Red / Far-Red light sensing

The phytochrome family of photoreceptors plays a crucial role in perceiving Red (R) and Far-Red (FR) light (600 - 800 nm), and its members contribute to the control of diverse light-regulated physiological responses (Kami et al., 2010). Among the latter, seed germination and shade avoidance are the ones that predominantly depend on phytochromes (Casal, 2013; Possart et al., 2014). There are five phytochrome genes in Arabidopsis (*PHYA - PHYE*), which encode for five distinct apoproteins (PHYA-PHYE), each consisting of two major domains: an N-terminal photosensory domain, whereupon a phytochromobilin chromophore is covalently bound (Fig 1-1), and a regulatory C-terminal region which includes a **H**istidine-**K**inase-**R**elated-**D**omain (Rockwell et al., 2006) as well as dimerisation and localisation domains (Chen and Chory, 2011). Phytochromes are synthesised in their R light absorbing form (Pr) and upon absorption of a photon the chromophore undergoes isomerisation that leads to the formation of the bioactive FR-absorbing form (Pfr) (Franklin and Quail, 2010). This photo-conversion is reversible and the regeneration of the Pr spectral state can be brought about either rapidly (upon absorption of light by the Pfr state), or by a prolonged period in darkness that allows enough time for a thermal process, known as “dark reversion”, to take place (Rockwell et al., 2006).

Contrary to other phytochromes, phyA is highly labile in its Pfr form. It is the predominant phytochrome in dark grown seedlings but, if the latter are transferred to light, PfrA undergoes rapid degradation to much lower steady-state levels (Clough and Vierstra, 1997). Nevertheless, when this equilibrium is reached the amount of PfrA remains sufficient for mediating the highly sensitive, non-reversible, **V**ery-**L**ow-**F**luence **R**esponses (VLFRs) that underlie de-etiolation upon soil emergence. On the other hand, in those cases in which the plants are continuously irradiated with wavelengths that establish a steady low percentage of Pfr (e.g continuous FR), phyA cycles stably between the two spectral forms and signals via the **H**igh **I**rradiance **R**esponse (HIR) mode (Nagy and Schäfer, 2002; Possart et al., 2014; Casal et al., 2014). Regarding the phytochromes phyB - phyE, they are light-stable in Arabidopsis and mediate the **L**ow **F**luence **R**esponses (LFRs); phyB in particular is the most abundant phytochrome in light-grown plants (Sharrock and Clack, 2002). Furthermore, some light stable phytochromes are known to be capable of forming

heterodimers. Whereas phyA, phyB and phyD form homodimers, phyC and phyE exist in seedlings only as heterodimers with phyB and phyD (Clack et al., 2009; Sharrock and Clack, 2004).

Concerning the signal transduction pathways of phytochrome-mediated responses, initial attempts to dissect them employed micro-injection experiments (reviewed in Hughes, 2013). Cells deficient in chromophore synthesis were injected with phyA or putative downstream signalling components, and phenotype rescue was assessed. Subsequently, focus shifted towards yeast two hybrid approaches (Schafer and Bowler, 2002) and forward genetic studies in Arabidopsis (Chen and Chory, 2011). These efforts led to the identification of mainly nuclear signalling components that phytochromes functionally interact with, following photoreception and rapid translocation from the cytosol to subnuclear entities called photo-bodies (Van Buskirk et al., 2012). The majority of those signalling effectors turned out to be either transcription factors or E3 ubiquitin ligases with regulatory effects over transcription factors. They will be dealt with, in more detail, in the introductory section that has been devoted to light-regulated transcription. Proteins of the **P**HYTOCHROME **K**INASE **S**UBSTRATE (PKS) family were notable exceptions, with PKS1 being the first member to be identified as a cytosolic interacting partner and phosphorylation substrate of phyA and phyB (Fankhauser et al., 1999). Subsequent research revealed that PKSs may represent important integration points for phytochrome and phototropin signalling (de Carbonnel et al., 2010; Demarsy et al., 2012), although their precise physiological role(s) remain elusive (Hughes, 2013).

1.2 Cryptochromes, Phototropins, Zeitlupe proteins and UV-A / Blue light sensing

DNA - photolyases comprise a vast and diversified gene family of photoactive enzymes, ubiquitously present across all major phylogenetic clades and primarily involved in repairing UV-induced damage to the genetic material. The cryptochromes (CRYs), first identified in Arabidopsis and later found in eubacteria, archaea and many eukaryotes, represent an important functionally distinct subfamily which, possibly with few exceptions, exerts a UV-A / blue light (320 - 500 nm) photosensory and signalling function rather than

mediating light-dependent DNA repair (Chaves et al., 2011). Structurally, all members of the cryptochromes / photolyases family share a relatively conserved N-terminal **Ph**otolyase - **r**elated (PHR) domain where two chromophores, a primary / catalytic flavin and a second light harvesting deazaflavin or pterin, are bound (Liscum et al., 2003). However, only cryptochromes possess an intrinsically unstructured carboxyl-terminal extension (C-terminal DAS domain CCT/DAS, Fig. 1-1), beyond the PHR domain, that varies considerably in length and sequence. Its functional significance has been connected to signalling, post-translational modifications, targeting to specific cellular compartments and protein–protein interactions (Fortunato et al., 2014). Arabidopsis currently is known to have three cryptochromes, cry1, cry2 and cry3, where the pterin derivative 5,10-methenyltetrahydrofolate (MTHF) has been proposed to mediate light harvesting (Chaves et al., 2011). Photoreceptive activity has been documented for cry1 and cry2, which contribute to entraining the circadian clock and to triggering developmental processes such as de-etiolation and induction of flowering (Kami et al., 2010; Möglich et al., 2010). As for cry3, which is a cry-DASH (**D**rosophila, **A**rabidopsis, **S**ynchocystis and **H**omo), it localises in chloroplasts and mitochondria (Kleine et al., 2003) and is implicated in DNA repair mechanisms (Zirak et al., 2009). In terms of their sub-cellular localisation, cry1 and cry2 display different patterns. Whereas cry1 is predominantly nuclear in the dark and undergoes light dependent accumulation in the cytosol, cry2 is constitutively nuclear (Lin and Shalitin, 2003).

Both cryptochromes can dimerise, and in the nucleus they have been reported to interact with **Co**nstitutively **P**hotomorphogenic **1** (COP1), a central switch in plant photomorphogenesis (Rosenfeldt et al., 2008; Sang et al., 2005; Yang et al., 2001). Upon UV-A / blue light perception, cry1 and cry2 undergo a photoexcitation-driven rapid phosphorylation (Bouly et al., 2003; Shalitin et al., 2002). This, in turn, triggers conformational changes of the C-terminal region and concomitant signalling events that lead to deactivation of COP1 and disruption of the negative regulatory effects that the latter has on photomorphogenesis promoting factors such as Elongated **Hy**pocotyl **5** (HY5) (Wang et al., 2001; Yang et al., 2001).

Alongside cryptochromes, plants can perceive UV-A / Blue light by employing two groups of photo-sensing proteins, namely phototropins and zeitlupe family proteins, which contain

the so called **L**ight **O**xygen **V**oltage (LOV) domains. LOV domains were first described as tandem sensor domains of phototropins (Christie et al., 1998), one year after the isolation of the first phototropin gene (Huala et al., 1997). Later it became evident that they are a subset of the diverse **P**er-**A**RNT-**S**im (PAS) domain superfamily, implicated in cellular signalling across all kingdoms of life, and that they are additionally present in fungi and bacteria (Crosson et al., 2003). Arabidopsis has two plasma-membrane-associated phototropins, designated phot1 and phot2, which have partially overlapping roles in regulating phototropism. Moreover, they mediate various light-induced responses which together serve to enhance photosynthetic performance and improve growth under weak light conditions (Christie, 2007).

Structurally, phototropins consist of an N-terminal photosensory segment (Fig 1-1), which harbours two LOV domains, each of which binds non-covalently a flavin-mononucleotide (FMN) chromophore. The C-termini have a serine / threonine kinase domain important for the signalling output (Briggs and Christie, 2002). Upon excitation, a covalent adduct between FMN and a conserved cysteine residue of the LOV domain is formed as an initial step of a reversible photocycle activation (Salomon et al., 2000). This light-dependent bond formation is coupled to kinase activation through induced conformational changes to the C-terminal region (Harper et al., 2003), thereby triggering rapid fluence rate-dependent autophosphorylation and signalling initiation.

Several signalling effectors have been identified for phototropin - mediated responses. Back in the early days of phototropin research, **N**ON-**PH**OTOTROPIC HYPOCOTYL **3** (NPH3) was identified as an interacting partner of phot1 (Motchoulski and Liscum, 1999), essential for auxin redistribution and phototropism. Not long ago, the auxin efflux transporter **A**TP-**B**INDING **C**ASSETTE **B19** (ABCB19) was reported to be a direct phosphorylation target of phot1 (Christie et al., 2011), active at and above the hypocotyl apex, where redistribution of auxin to the epidermal cells occurs. Phosphorylation of ABCB19 impairs its efflux activity and primes lateral fluxes that are channelled to the elongation zone via the auxin transporter **PIN**-FORMED **3** (PIN3). Recently, a Ser / Thr kinase named **BLU**E LIGHT **S**IGNALLING **1** (BLUS1) was identified as a phosphorylation substrate of phot1 during phototropin - mediated signalling in guard cells (Takemiya et al., 2013). Members of the PKS family, initially identified as phytochrome signalling intermediates, have also been reported to participate in phototropin - initiated signalling pathways (de Carbonnel et al., 2010; Demarsy et al., 2012).

The ZEITLUPE family of LOV domain-containing proteins currently consists of three members, namely Zeitlupe (ZTL, also known as Adagio, ADO), Flavin-binding Kelch Repeat F-box 1 (FKF1) and LOV Kelch Protein 2 (LKP2) (Demarsy and Fankhauser, 2009). The family owes its name to the implication of its members in flowering onset and circadian clock entrainment (Kim et al., 2007), by mediating light-controled ubiquitin-dependent protein degradation (Mas et al., 2003). Contrary to phototropins, the ZEITLUPE family proteins contain only one FMN-binding LOV domain (Fig 1-1), followed by an F-box domain and several Kelch repeats.

Concluding this brief introductory outline of the visible-light-responsive photo-sensing systems of higher plants, it is worth mentioning that there are a number of green light - mediated responses which cannot be accounted for based on known photoreceptors. Phytochromes, cryptochromes and phototropins are all capable of perceiving green light, but there is also evidence that a yet-to-be identified green-light-specific photoreceptor might be at play (Folta and Maruhnich, 2007; Wang et al., 2013; Zhang et al., 2011). In addition, the conventional classification of photoreceptors has been largely reliant on the chemical nature and photochromicity of the associated chromophores. In some lower plants such as ferns, however, a novel photoreceptor named neochrome has been identified, and it represents a chimeric form of the phytochrome photosensory domain fused to an entire phototropin (Christie, 2007). In ferns of the genus *Adiantum,* phototropism and chloroplast movements are regulated by red and blue light, and a functional neochrome is required.

1.3 UV-B induced responses in Arabidopsis

Ultraviolet (UV) light is part of the solar electromagnetic spectrum with wavelengths immediately below visible light. Traditionally, it is divided in three different types, categorised on the basis of distinct wavelength ranges : UV-C (< 280 nm), UV-B (280-315 nm) and UV-A (315-400 nm) (Li et al., 2013).

As already mentioned, the daylight spectrum is practically devoid of UV-C, and UV-B wavelengths below ~ 295 nm. Nonetheless, because of its relatively high energy, the UV-B portion that makes it through the ozone layer and actually reaches the surface of our planet has significant impact on the biosphere (Jenkins, 2009).

In general, the diverse plant responses to UV-B can be classified in two distinct categories: stress-related responses and photomorphogenic responses. In the first, UV-B is regarded as a potential damaging agent which plants need to cope with. In photomorphogenic responses, on the other hand, UV-B is utilised as an informative signal which enables plants to modify their physiology and development according to the prevailing environmental conditions. The type of the elicited response is primarily dependent on the fluence rate of UV-B exposure, and on whether the plants have been through an acclimation period prior to the exposure (Heijde and Ulm, 2012; Jenkins, 2009). High UV-B fluence rates (defined as the number of moles of photons impinging on a defined area in a given time, e.g., μmol m^{-2} s^{-1}) have the potential to damage macromolecules, including DNA, thus impairing vital physiological processes. Therefore, they tend to induce stress-related responses such as activation of pathways for DNA damage repair and production of reactive oxygen species (ROS) (Ulm and Nagy, 2005). Rather than being specific to UV-B, the signal transduction routes which underlie these processes are convergence points for responses triggered by various stressful stimuli (Brown and Jenkins, 2008; Jenkins 2009).

By contrast, low doses of UV-B have long been known to promote photomorphogenesis (Wellmann, 1976). The decrease in the rate of both hypocotyl elongation and primary root growth, and the promotion of cotyledon opening, are well documented developmental consequences of low fluence rate UV-B illumination (Boccalandro et al., 2001; Kim et al., 1998; Shinkle et al., 2004; Shinkle et al., 2010; Tong et al., 2008). Moreover, UV-B has long been known to trigger the biosynthesis of flavonoid compounds, which are important components of the UV-absorbing protective “sunscreen” that is deposited in the leaf

epidermis, thus reducing penetration of the potentially harmful radiation into the mesophyll tissue (Caldwell et al., 1983; Hahlbrock and Scheel, 1989; Ryan et al., 2001). The gene encoding for the key enzyme **ch**alcone **s**ynthase (CHS) is among the flavonoid biosynthesis genes whose transcription is stimulated by low doses of UV-B (Frohnmeyer et al., 1999; Hartmann et al., 2005; Jenkins et al., 2001). Intriguingly, low fluence rate UV-B also exerts a positive regulatory effect on genes encoding for enzymes that participate in damaged-DNA repair processes, and enzymes of the antioxidant and ROS-scavenging systems (Brown et al., 2005; Favory et al., 2009; Ulm et al., 2004). This is an important feature from an ecophysiological point of view, as it suggests that low doses of UV-B prime the plants to be better prepared for a potential subsequent dose elevation, thereby acclimating them and enabling them to ameliorate possible damage.

1.3.1 UVR8, a UV-B specific photoreceptor

Early biochemical and genetic approaches quickly revealed that photomorphogenic UV-B responses could not be attributed to any of the known photoreceptors (Ballaré et al., 1995; Christie and Jenkins, 1996; Frohnmeyer et al., 1998). In the meantime, the non-UV-B-specific signalling pathways, such as those for DNA damage, ROS, and wound/defence signalling which were known to be important for mediating a subset of UV-B responses, had been ruled out as unlikely to be involved in perceiving the photomorphogenic UV-B signal (A−H−Mackerness et al., 1999; Gadjev et al., 2006; Surplus et al., 1998; Ulm et al., 2004).

The possibility that plants possess a UV-B specific photoreceptor had intrigued scientists for many years, and various approaches had been employed attempting to identify it. Eventually, significant progress was made during a standard forward genetics approach where Arabidopsis mutants were screened for UV-B hypersensitivity phenotypes (Kliebenstein et al., 2002). An interesting mutant came out of that study, it was designated *uv-resistance locus 8 - 1* (*uvr8-1*) and the genetic locus to which the mutation mapped was also given the name *UVR8.* In that seminal report, UVR8 was characterised as displaying moderate homology with the human guanine nucleotide exchange factor Regulator of Chromatin Condensation 1 (RCC1) and was suggested to act in the signal transduction pathway that leads to the induction of flavonoids biosynthesis. Subsequent studies

identified additional *uvr8* alleles, demonstrated that UVR8 is the first UV-B-specific signalling component and highlighted its absolute requirement for photomorphogenic UV-B pathways (Brown et al., 2005; Favory et al., 2009). Meanwhile, as research around UV-B-elicited responses progressed, transcriptome analyses revealed that a broad range of genes with significant contribution to UV protection and repair of UV-induced damage were regulated in a HY5-dependent (Ulm et al., 2004) and a UVR8-dependent (Brown et al., 2005) fashion under photomorphogenic UV-B doses. Nowadays, the list of plant responses to UV-B that are orchestrated by genes which undergo a UVR8-mediated regulation is continuously updated, and extends beyond photomorphogenesis to include responses relevant to photosynthesis (Davey et al., 2012), morphology of older plants (Hectors et al., 2007; Wargent et al., 2009), tolerance against biotic stress causal agents (Demkura and Ballare, 2012), and regulation of stomatal aperture (Tossi et al., 2014). In addition, interesting findings have now emerged from research which tried to address questions related to the integration of UVR8 signalling with pathways known to be governed by other photoreceptors (Hayes et al., 2014; Vandenbussche et al., 2014).

With regard to its subcellular localisation, UVR8 was shown to be present in both the cytoplasm and the nucleus, with UV-B promoting its rapid nuclear accumulation without affecting the overall abundance of the protein which appeared to be constitutively expressed (Kaiserli and Jenkins, 2007). Interestingly, nuclear localisation was necessary but not sufficient to stimulate UVR8 function, since an engineered UVR8 variant harbouring a nuclear localisation signal (NLS) for constant presence in the nucleus still required UV-B stimulation to exert its regulatory role. This enhanced nuclear localisation in response to inductive UV-B illumination is reminiscent of the phytochrome mode of action, and raised suspicions that UVR8 could have photoreceptive capability (Jenkins, 2009). The intensified research towards testing this hypothesis peaked in 2011, with a breakthrough publication which declared UVR8 to be the long-sought-after UV-B-specific photoreceptor of higher plants (Rizzini et al., 2011), validating the computational predictions of a synchronous report (Wu et al., 2011). By taking advantage of *in vitro* and heterologous *in vivo* biochemical systems, Rizzini and co-workers demonstrated that a homodimeric form of UVR8 perceives the UV-B signal and undergoes rapid monomerisation. Moreover, the authors also proposed that a number of conserved

tryptophans are of utmost significance for the light sensing mechanism, with tryptophan W285 being the key residue.

1.3.2 Structure and molecular function of UVR8

Unlike other known Arabidopsis photoreceptors, no evidence has ever been presented that UVR8 binds an external chromophore (Jenkins, 2014b; Jenkins, 2014a). Hence, the discovery of its photo-sensing role sparked great interest towards elucidating the detailed three dimensional structure, with the aim, eventually, to resolve the mechanism of photoreception.

At first, structural modelling was based on the related RCC1 protein, which belongs to the large family of WD40 repeat-containing proteins, whose functions cover diverse signalling processes by acting as hubs in various cellular networks (Stirnimann et al., 2010; Xu and Min, 2011). RCC1 folds in a seven-bladed β-propeller, each blade consisting of four anti parallel β-sheets with loops in between (Renault et al., 1998). UVR8 was believed to assume a similar β-propeller fold, but the functional divergence between the two proteins (Brown et al., 2005) suggested that the UV-B photoreceptor would essentially possess several distinctive features. The crystal structure of Arabidopsis UVR8 (Fig 1-2) was obtained independently by two research groups (Christie et al., 2012; Wu et al., 2012), and the anticipated differences with the canonical WD40 repeat proteins were revealed. The propeller blades have three rather than four β- strands, and the first blade is composed of a contiguous N-terminal sequence instead of comprising both N-terminal and C-terminal sequences (Jenkins, 2014b). The unique structural properties of UVR8, however, are those related to the light sensing function.

The crystallised UVR8 corresponded to the homodimeric form and lacked 11 amino acids at the N-terminus and 59 amino acids at the C-terminus (Christie et al., 2012; Wu et al., 2012). The dimer interface is enriched in charged and aromatic amino acids, whose distribution pattern results in the establishment of an electrostatic potential complementarity across the horizontal plane that separates the two monomers, and allows the formation of an adhesive network of salt bridges to hold the two subunits together (Fig 1-2 C). The significance of at least some salt bridging residues in maintaining the dimeric structure has been demonstrated through experimentation with mutant UVR8 proteins.

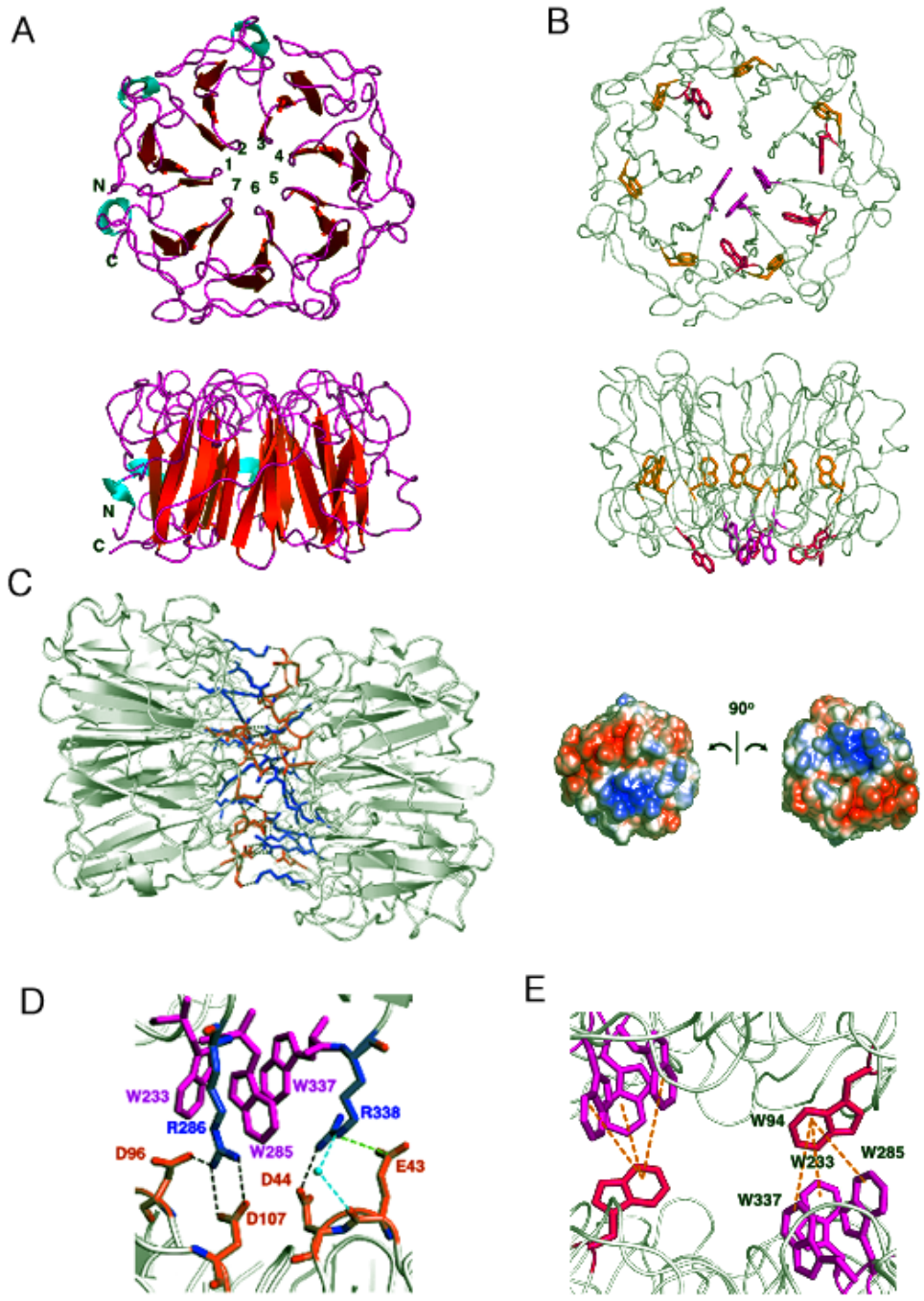

Fig 1-2. **Structural basis of UVR8 photoreception**.
A. UVR8 monomer from a dimerisation surface view (upper) and a side view (lower). The seven propeller blades are annotated. **B**. UVR8 tryptophans viewed from the dimerisation surface and from the side. Trps in the propeller blades are shown in orange, whereas those in the dimer interaction surface are coloured magenta (W233, W285, W337) or red. **C**. Left image : Basic (blue) and acidic (red) amino acids participating in the formation of the salt bridges at the dimer interface. Right image: Patches of complementary electrostatic potential at the dimer interaction surfaces of two monomers, separated and rotated towards the viewer. Basic amino acids contribute positive charge whereas acidic amino acids are negatively charged. **D**. Key interactions involved in maintaining the UVR8 dimer. **E.** Pyramidal arrangement of Trps across the dimer interface. Adapted from Jenkins, 2014(b)

In particular, if the interactions of R286 with D96 and D107 or those of R338 with E43 and D44 (Fig 1-2 D) are abolished, the result is a considerably weakened dimer (Christie et al., 2012; Huang et al., 2014b; Wu et al., 2012; Wu et al., 2013).

The photoreceptive activity of UVR8 is dependent on specific tryptophans (W or Trps) in its primary sequence, which function as intrinsic chromophores. At first, functional and computational data had highlighted the potential importance of W233, W285 and W337 (Rizzini et al., 2011; Wu et al., 2011). Subsequently, actual structural information supported the initial propositions, by revealing that these three Trps constitute a distinct "triad" (Christie et al., 2012) that forms the base of a pyramidal structure whose top is provided by W94 of the adjacent monomer (Fig 1-2 E). Mutagenesis experiments have demonstrated that whereas W337 and W94 have a relatively minor effect on UVR8 function (Christie et al., 2012; O'Hara and Jenkins, 2012; Wu et al., 2012), W285 and W233 are required for UV-B signal perception (Christie et al., 2012; Heijde et al., 2013; Huang et al., 2014b; O'Hara and Jenkins, 2012; Wu et al., 2012). The current consensus of opinion about the central roles of W285 and W233 in photoreception has been reached amid only slight discrepancies in the reported results. $UVR8^{W285A}$ is recovered as a dimer in size exclusion chromatography by Christie and co-workers regardless of illumination conditions, whereas Wu et al. (2012) detect a monomeric shoulder in UV-B treated samples, which they interpret as the result of a seemingly UV-B-weakened homodimer. Both reports agree that $UVR8^{W285A}$ appears constitutively monomeric when examined with semi-native (non boiled samples) SDS-PAGE, and circular dichroism (CD) spectra (Christie et al., 2012) present this mutation as a non-UV-B-responsive dimer. With regard to some *in planta* assays, however, there is ongoing debate as to what the true phenotype of $UVR8^{W285A}$ is. In particular, with the exception of one study (O'Hara and Jenkins, 2012), $UVR8^{W285A}$ has been found to exert a constitutively photomorphogenic phenotype (Heijde et al., 2013; Huang et al., 2013; Huang et al., 2014b). This controversy will be discussed in detail in the following section that deals with UVR8-dependent photomorphogenic UV-B signalling.

With regard to the details of the mechanism of photoreception, two alternative hypotheses have been put forward. The one (Christie et al., 2012) suggests that when the excitonically coupled "triad" Trps absorb a photon, an electron is transferred to adjacent Arg residues

destabilising the salt bridges in which the latter participate, thereby causing monomerisation and onset of signalling. Wu et al. (2012) on the other hand, highlight the potential importance of cation - π interactions between the "triad" and the neighbouring Args. To date, only computational approaches have addressed these hypotheses (Liu et al., 2014; Voityuk et al., 2014; Wu et al., 2014), but a detailed account is beyond the scope of this introduction and the reader is referred to a recent relevant review (Jenkins, 2014b).

Finally, for completion it is worth mentioning that a recent publication attempts to put a new spin on our understanding of how plants sense photomorphogenic UV-B light, by arguing in favour of a UVR8-independent process in which signals originate from UV-B absorption by DNA and lead to a cell cycle arrest (Biever et al., 2014).

1.3.2.1 UVR8-dependent photomorphogenic UV-B signalling

Research on UV-B signal transduction essentially paralleled the intensive study of UVR8, since it was first reported to be a UV-B-specific signalling component (Brown et al., 2005). The rapid nuclear accumulation following UV-B perception (Kaiserli and Jenkins, 2007) did not reveal any particular subnuclear patterns of localisation. Hints towards that direction came two years later, when UVR8 was found to interact with COP1 in a UV-B-dependent manner, and the complex appeared to aggregate in nuclear bodies of mustard hypocotyl cells (Favory et al., 2009). Previously, COP1 had been established as a repressor of photomorphogenesis which targeted positive regulators for proteasome-dependent degradation (Lau and Deng, 2012; Osterlund et al., 2000). The only suggestions towards a positive role in UV-B responses came from the findings of Oravecz et al., (2006), that following UV-B illumination COP1 promotes, and is required for, the expression of *HY5*. The latter is a major transcriptional effector in UVR8-dependent photomorphogenesis, as will be discussed in a following section. Nowadays COP1 is undisputedly regarded as a positive regulator of UV-B photomorphogenesis, and the illumination-dependent interaction with UVR8, both *in planta* and in heterologous yeast systems, is regularly employed along with other diagnostic assays to assess functional UVR8-mediated signalling. Moreover, it was recently demonstrated that a 27 amino acid region located towards the C-terminus of UVR8 is required for the interaction with COP1 (Cloix et al., 2012).

Notwithstanding the consistency among many independently obtained results regarding the physical interaction between the two proteins, the full understanding of the epistatic relationship of *UVR8* and *COP1* has been hampered by conflicting phenotypic observations. This has been especially evident in *in vivo* studies of UVR8 photoreception. For example, it has been found that $UVR8^{W285A}$ appears constitutively monomeric, interacts with COP1 regardless of UV-B illumination (Heijde et al., 2013; Huang et al., 2013; Huang et al., 2014b; O'Hara and Jenkins, 2012) but fails to complement the *uvr8-1* mutant phenotype (Huang et al., 2014b; O'Hara and Jenkins, 2012). With the exception of the work by O'Hara and Jenkins (2012), all other three studies report a *cop1*-like phenotype for $UVR8^{W285A}$ in darkness. On the basis of findings reported earlier by Favory et al. (2009), where overexpression of UVR8 was found to result in enhanced UV-B photomorphogenic response, O'Hara and Jenkins argued that an expected *cop* phenotype is absent in their results because the expression levels of the mutant UVR8 protein were close to those of the native in WT plants. Later, Heijde et al. (2013) and Huang et al. (2013) published their works simultaneously reporting the *cop*-like phenotype, but only Heijde et al. presented data on the protein expression levels and they were indeed found to be at least 30-fold higher than in WT plants. At this stage the discrepancy would have been resolved, but Huang et al. (2014) recently reported a mild constitutively photomorphogenic phenotype for $UVR8^{W285A}$ Arabidopsis lines whose mutant protein expression levels were found comparable to those of the native UVR8 in WT plants, indicating that further research is needed to reveal the truth of the matter.

The precise mechanism by which COP1 acts under UV-B is not understood (Jenkins, 2014a). In principle, the positive role of COP1 in UV-B responses could involve the initiation of degradation of a negative regulator, but no experimental evidence supports such option at present. COP1 is an E3 ubiquitin ligase and consists of a RING finger domain, a coiled coil domain and seven C-terminal WD40 repeats. All three domains mediate protein-protein interactions (Yi and Deng, 2005), therefore it is conceivable that COP1 might facilitate the indirect interaction of UVR8 with other proteins in the course of effectuating downstream UV-B signalling. In support of this notion, Arabidopsis **S**uppressor of **P**hytochrome **A**-105 (SPA) proteins were recently reported to associate with COP1 and UVR8 in a trimeric complex that acts to positively regulate photomorphogenic

UV-B responses (Heijde et al., 2013; Huang et al., 2013). Plants with multiple *spa* mutations displayed impaired response to UV-B, revising previous observations by Oravecz et al. (2006) according to which SPAs appeared to be dispensable for COP1 function in the UV-B photomorphogenic pathway and non-essential in UV-B responses. The exact role of SPAs is not clear but it appears that there is no direct association with UVR8 itself . Rather, COP1 acts as a bridging protein. Huang et al. (2013) elegantly demonstrated that upon UV-B exposure, COP1 and SPAs are diverted towards associating with UVR8, being withdrawn from their physical/functional association with the **CUL**LIN**4** - **D**AMAGED **D**NA **B**INDING PROTEIN **1** (CUL4-DDB1) E3 ubiquitin ligase complex, for which they are known contributors in substrate reception (Lau and Deng, 2012). This UV-B directed reorganisation of COP1-SPA-containing complexes stabilises the intracellular levels of HY5, which is a primary target of CUL4-DDB1 complexes. Furthermore, it has been suggested (Huang et al., 2014a; Jenkins, 2014a), that the UVR8-COP1-SPAx complex may inactivate the intrinsic E3 ubiquitin ligase activity of COP1 itself, similarly to the action of cryptochromes when they interact with SPAs (Fankhauser and Ulm, 2011).

As is usually the case with the operation of any signalling pathway, UVR8-dependent signalling has been reported to be kept under control by certain negative regulators. **R**epressors of **U**V-B **P**hotomorphogenesis **1** and **2** (RUP1 and RUP2) are two closely related WD40-repeat-containing proteins which redundantly act to prevent unbalanced stimulation of UV-B photomorphogenesis. Double mutant plants, in which the function of both RUPs was impaired, displayed increased UV-B induced flavonoid accumulation, elevated UV-tolerance after acclimation and a generally enhanced response to UV-B (Gruber et al., 2010). The UV-B induced, UVR8-mediated expression of specific genes, including *HY5*, was increased in *rup1rup2* plants and suppressed in RUP2 overexpressing lines. Interestingly, *RUP1* and *RUP2* genes were themselves found to be stimulated by UV-B under the control of UVR8, COP1 and HY5, suggesting the existence of a negative feedback loop (Gruber et al., 2010). The RUPs-mediated negative regulation involves direct physical interaction with UVR8, documented *in planta* (Gruber et al., 2010), and via heterologous yeast two hybrid assays which further revealed that the interaction is

mediated by the same C-terminal 27 amino acid region of UVR8 that binds COP1 (Cloix et al., 2012). Subsequent research came to add two important pieces in constructing the puzzle of UVR8-dependent signalling by demonstrating that the UVR8 dimer regeneration *in vivo* is mediated by the RUPs (Heijde and Ulm, 2013) and requires an intact C- terminus of UVR8 (Heilmann and Jenkins, 2013).

As things stand, and obviously having much more to learn, UVR8-dependent signalling can be summarised as follows (Fig 1-3): UV-B radiation causes monomerisation of the UVR8 homodimer, rapid accumulation of the monomers in the nucleus, and reorganisation of nuclear COP1-SPA-containing complexes favouring COP1-SPA association with UVR8 monomers. UVR8-COP1-SPA complexes positively regulate the transcription of target genes, among which are those encoding for the key transcription factors HY5 and its close homologue HYH, which in turn control the expression of many downstream genes that mediate UVR8-dependent responses. Meanwhile, as significant amounts of the nuclear COP1-SPA reserves are diverted away from the CUL4-DDB1 E3 ligase complexes, a post-translational stabilisation of HY5 is achieved. In due course, RUP1 and RUP2 accumulate as a result of the HY5-mediated transcriptional stimulation of their genes, and repress the pathway by competing with COP1-SPA for binding to the C-terminal region of UVR8 and by facilitating regeneration of the UVR8 homodimer.

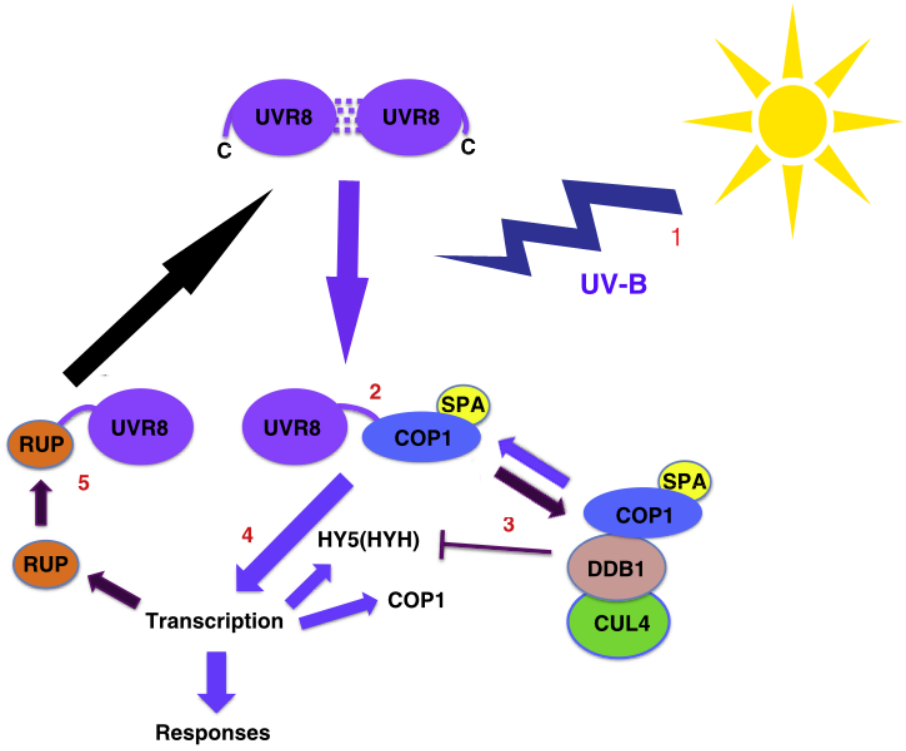

Fig 1-3. **Main events in the UVR8 signalling pathway**.

1. UV-B exposure causes monomerisation of the UVR8 dimer and a reorganisation of nuclear COP1/SPA containing complexes, favouring COP/SPA association with UVR8 monomers (**2**). This leads to stabilisation of the HY5 and HYH proteins (**3**). **4**. UVR8-COP1-SPA complexes positively regulate the transcription of many genes important for orchestrating photomorphogenic UV-B responses, including those encoding for COP1 and for the two homologue bZIP TFs HY5 and HYH. Moreover, in facilitating the formation of a negative-feedback regulatory loop, the transcription of the RUPs-encoding genes is also stimulated, thereby leading to accumulation of RUPs, which in turn compete with COP1/ SPA for binding to the C-terminus of UVR8 (**5**), a step required for UVR8 homodimer regeneration. Adapted from Jenkins, 2014(b)

1.4 Visible-light-regulated gene expression

Any balanced physiological response, including those mediated by light, depends on the coordinated activation and repression of certain genes through tightly regulated transcriptional networks (Jiao et al., 2007). Traditional genetic and molecular approaches have been very successful in identifying key individual positive and negative regulators. At the same time, the increasingly frequent utilisation of various ~omics technologies has revealed that large scale alterations of chromatin structure, dynamic changes in epigenetic landscapes and a massive reprogramming of the plant transcriptome are collectively underlying the sizeable developmental effects that light has on plants (Barneche et al., 2014; Li et al., 2012).

1.4.1 Light-Responsive cis-regulatory Elements (LREs) in transcriptional regulation.

Back in the mid- 1990s, at least 100 genes were known to undergo light-dependent transcriptional regulation, and there was considerable interest in identifying the *cis*-regulatory DNA elements that were involved (Terzaghi and Cashmore, 1995). The term used to describe these elements was "**L**ight-**R**esponsive **E**lements (LREs)", and in order to locate their relative position within known light-regulated loci, standard promoter deletion/ mutagenesis analyses were employed. Meanwhile, the binding motifs of light-responsive transcription factors were being determined through various molecular biology techniques such as footprinting, gel retardation assays, and methylation interference assays. No structural features common to all LREs could be identified (Arguello-Astorga and Herrera-Estrella, 1996), which led plant scientists to employ comparative phylogenetic approaches in an attempt to reduce the apparent diversity and to reveal any structural similarities that might lie concealed in dissimilar promoter regions with analogous functions (Arguello-Astorga and Herrera-Estrella, 1998). Whereas well defined, widely conserved core LREs could be identified as crucial for light responsiveness, it soon became evident that the minimal promoter determinants of light-regulated development should not be sought in individual LREs of universal presence, but in multipartite combinations of different cis-acting sequences (Chattopadhyay et al., 1998a; Puente et al., 1996).

Most information regarding LREs has been derived from studies on **ph**otosynthesis-**a**ssociated **n**uclear **g**enes (PhANGs) (Arguello-Astorga and Herrera-Estrella, 1998; Gilmartin and Chua, 1990b; Gilmartin and Chua, 1990a; Gilmartin et al., 1992), and from studies on photomorphogenesis (Jiao et al., 2007). A gene whose *cis*-regulatory elements have been functionally rather well characterised is ***CH****ALCONE* ***S****YNTHASE* (*CHS*), which encodes for a key enzyme in phenylpropanoid metabolism. At first, by taking advantage of a parsley protoplast system that responds accurately to light in terms of both *CHS* transcriptional activation and flavonoid biosynthesis, scientists employed in vivo footprinting which led to the identification of two separable light-responsive *cis*-acting "units", one TATA-proximal and one TATA-distal, each containing two footprint "boxes" (Schulze-Lefert et al., 1989a; Schulze-Lefert et al., 1989b). Clustered point mutations allowed the definition of the functional borders of Box II of the TATA-proximal Unit I, which was found to be highly similar to the G-box identified in numerous other plant promoters (Block et al., 1990). Subsequently, a 52 bp region encompassing Unit 1 was reported to be necessary and sufficient for light mediated gene activation (Weisshaar et al., 1991). Work on the *CHS15* promoter from *Phaseolus vulgaris* demonstrated that the G-box, and a proximal *cis*-element designated H-box, were necessary and in combination sufficient to stimulate expression triggered by the phenylpropanoid pathway intermediate *p*-coumaric acid (Loake et al., 1992). In due course, expression studies for the same promoter, undertaken in transgenic tobacco plants, revealed that a 39 bp region containing both elements could direct tissue specific expression and stress responsive activation (Faktor et al., 1997a; Faktor et al., 1997b). In addition, research on the *Sinapis alba CHS* promoter had revealed that UV-B- and UV-A/Blue light responsiveness were mediated by *cis*-regulatory elements with high homology to the first identified parsley counterparts (Kaiser et al., 1995). Hence, when the functional dissection of the Arabidopsis *CHS* promoter was reported (Hartmann et al., 1998), there were sufficient data to allow a first generalised conclusion (Weisshaar and Jenkins, 1998), according to which the combinatorial interaction of three types of elements conferred the promoter- and stimulus-dependent specificity in gene activation. These there types of elements were ACE- or G-box-like, genuine ACE or G-boxes (**A**CTG- **C**ontaining **E**lements), and MREs (**M**yb **R**ecognition **E**lements). In 2005, a study attempting to extend the analysis to several other

phenylpropanoid biosynthesis genes found that similar LREs, sufficient to drive light responsiveness, were present in all tested promoters (Hartmann et al., 2005). Moreover, the authors conducted a more thorough analysis of the *CHS* promoter and discovered a third *cis*- acting element, which, although dispensable for the promoter's light-driven activation, seemed to be important for tissue specific expression acting in combination with the MRE. Relatively recently, a research effort aimed at contributing to the current understanding of the *cis*- regulatory elements that orchestrate UV-B-induced expression led to the identification of a novel element, the UVbox of the *ANAC13* promoter (Safrany et al., 2008). Ongoing studies are currently refining our knowledge of the regulation of promoters containing other long- known LREs such as the GATA-, GT- and Z-boxes (Gangappa and Chattopadhyay, 2013; Gangappa et al., 2013c; Gangappa et al., 2013d).

Valuable as they still are, traditional experimental setups cannot compare with current genome-scale methodologies in terms of the wealth of information that can be extracted. Continuously refined computational approaches are being employed in order to map the dynamics of regulatory DNA and various transcription factor networks, thus generating genome-wide, condition- and tissue-specific maps of TF occupancy (Sullivan et al., 2014). Moreover, a recent study examined the DNA binding specificities of all major classes of plant transcription factors using protein-binding microarrays, and a remarkable finding was that almost half of the tested TFs were able to recognise secondary DNA motifs, which in many cases were completely unrelated to the primarily recognised element (Franco-Zorrilla et al., 2014). In addition, pairwise comparisons between UV-B inducible promoters identified a series of *cis*- elements, which are absent from promoters of genes for early phenylpropanoid metabolism, but might be conferring UV-B responsiveness (Brosche et al., 2002). Not too long ago, genome-scale expression data from microarray studies were utilised to gain more comprehensive insights into the enriched sequence elements among promoters of co-expressed or differentially expressed phyA-regulated genes (Hudson and Quail, 2003). Intriguingly, two distinct flanking consensus sequences were observed adjacent to the G-box core, one predominating in phyA-induced and the other in phyA-repressed promoters. Similarly, different flanking sequences around various LREs have been suggested to convey organ specificity in light regulation (Jiao et al. 2005). It appears, therefore, that different members of the same family of TFs can mediate gene induction or

repression with distinct spatial patterns (Jiao et al., 2007). Finally, valuable information on LREs has been gathered during the past decade through studies on the genomic binding sites of particular key transcription factors in light signalling, such as HY5, PIF1 and FHY3 (reviewed in Li et al., 2012).

1.4.2 Light-Responsive and light-quality-specific transcription factors

Only 5-6% of the Arabidopsis genome encodes for transcription factors (TFs) (Riechmann et al., 2000). However, a great proportion of the early light-responsive genes, especially shortly after light exposure when photomorphogenesis is barely observable, has been reported to correspond to transcription-factor-encoding genes (Li et al., 2012). Within one hour of FR (or R) light exposure, 44% (or 25%) of the functionally classifiable early light responsive genes were found to encode TFs. In the case of blue light illumination, 64 early responsive TFs were identified (Jiao et al., 2003; Tepperman et al., 2001; Tepperman et al., 2004). Similar trends were observed in UV-B-related transcriptomic studies, as will be discussed in a following section. Collectively, such findings highlight the potential significance of primary light-regulated transcriptional networks (Jiao et al., 2007)

Various transcription factors, both of positive and negative regulatory function, have been identified to act downstream of specific photoreceptors. **FAR**-RED IMPAIRED RESPONSE **1** (FAR1), **F**AR RED ELONGATED **HY**POCOTYL **3** (FHY3), **L**ONG **A**FTER **F**AR RED **1** (LAF1), and LONG **H**YPOCOTYL IN **F**AR **R**ED 1 (HFR1) all act in phyA signalling (Casal et al., 2014). FAR1 and FHY3 are both transposon derived transcription factors, which control the transcription of FHY1 and **FH**Y1-**L**ike (FHL), whose role is crucial for the light-induced nuclear import of phyA (Genoud et al., 2008). FHY1 in particular has been reported to guide phyA to target gene promoters and to co-activate transcription, but also to undergo a phyA-dependent phosphorylation which impairs its function (Chen et al., 2012). In a recent study, ChIP seq experiments revealed that nuclear FHY1 can act either in association or independently from phyA to activate the expression of distinct target genes (Chen et al., 2014). LAF1, on the other hand, is a R2R3-MYB family transcription factor which has been shown, together with HFR1 (a bHLH TF), to participate in FHY1- and FHL- containing complexes in vivo, thus transmitting phyA

signals for inhibition of hypocotyl elongation (Yang et al., 2009). Morover, LAF1 and HFR1 were recently reported to regulate largely independent signalling pathways from HY5, downstream of phyA (Jang et al., 2013).

Two transcription factors of the **D**NA binding with **o**ne **F**inger (DoF) family, namely **COG**WEEL **1** (COG1) and **OBP**F4 binding protein **3** (OBP3), have also been reported to be involved in red light signalling. The first is known to be a negative regulator downstream of both phyA and phyB, whereas OBP3 has been reported to act positively in the inhibition of hypocotyl elongation and negatively for cotyledon expansion in phyB signalling (Jiao et al., 2007)

Phytochrome **I**nteracting **F**actors (PIFs), constitute a small subset of the **b**asic **H**elix **L**oop **H**elix (bHLH) family of transcription factors, and are well established central players in phytochrome mediated light signalling networks (Leivar and Quail, 2011). In 1998, PIF3 was identified in a screen for phyB-interacting proteins and was shown to be capable of binding to the C-termini of both PHYA and PHYB (Ni et al., 1998). One year later, the full-length photoactive phytochrome B was found to bind PIF3 *in vitro,* only upon light-induced conversion to its active form, whereas photoconversion back to its inactive form caused dissociation of the complex (Ni et al., 1999). Later, PIF3 was documented to bind specifically to G-box-containing *cis*-regulatory DNA, and phyB, upon light-triggered conversion to its biologically active conformer, bound reversibly to G-box–bound PIF3 (Martínez-García et al., 2000). These findings led to the formulation of a hypothesis favouring a positive regulatory role of PIF3 in light signalling. However, subsequent research pointed towards a completely different direction. Loss of function *pif3* plants exhibited hypersensitivity to continuous R light, administered from germination onward (Kim et al., 2003). In addition, the light induced phytochrome entry in the nucleus, where it interacts with PIF3 in nuclear speckles, was found to result in rapid degradation of PIF3 (Bauer et al., 2004). Hence, a model of light induced proteolysis of a rather negatively acting PIF3 protein seemed to be gaining ground. A second PIF protein, namely PIF4, had been discovered shortly before through a combination of genetic and reverse genetic approaches (Huq and Quail, 2002,). Based on homology to PIF3, several other PIFs were subsequently identified, including PIF1, PIF5, PIF6 and PIF7. Recently, a quadruple *pif1pif3pif4pif5* mutant was found to display a constitutively photomorphogenic phenotype

providing compelling evidence that PIFs are repressors of photomorphogenesis (Josse and Halliday, 2008; Leivar et al., 2008; Shin et al., 2009). The molecular details of the action of PIFs during skotomorphogenic growth are far from clear (discussed in Leivar and Quail, 2011) but recent work has shed some light to that direction. Building on an earlier study (Leivar et al., 2009), Zhang and co-workers have now shown that in the dark the four PIFs whose function is impaired in the above quadruple mutant share occupancy of binding sites on target promoters. Promoter binding varies quantitatively from gene to gene, hence a mosaic of differential transcriptional responsiveness is generated. Upon exposure to light, phytochromes are activated and PIFs undergo rapid proteolysis leading to an overall reorganisation of the transcriptional networks towards de-etiolation (Zhang et al., 2013). It should be noted that although highly similar in sequence, PIFs do not completely overlap in their function. PIF3 has been reported to differentially mediate distinct branches of phyB signalling as a positive regulator of nuclear encoded photosynthetic genes and early chloroplast development (Monte et al., 2004). In addition, various modes of functional interactions have been reported between PIFs and other transcription factors. PIF1 was recently reported to interact with FHY3/FAR1 to regulate chlorophyll biosynthesis during de-etiolation (Tang et al., 2012), whereas both synergistic (Shin et al., 2007) and antagonistic (Toledo-Ortiz et al., 2014) relationships have been reported for PIFs and HY5.

With regard to blue light signalling, phototropins have a relatively minor contribution to transcriptional regulation (Ohgishi et al., 2004). Several TFs have been identified as components of the CRYs signalling pathways, and include OBP3 (common with phy-mediated signalling, discussed above), **C**ryptochrome **i**nteracting **b**asic helix-loop-helix **1** CIB1 (Liu et al., 2013), and two G- and Z- box binding transcription factors, namely MYC2 (bHLH family) and **G**-box **B**inding **F**actor **1** (GBF1) (Gangappa and Chattopadhyay, 2013; Gangappa et al., 2013c; Gupta et al., 2014; Sethi et al., 2014; Singh et al., 2012).

A pivotal transcription factor of major importance in light signalling is the bZIP family member HY5 (Oyama et al., 1997). Mutant *hy5* plants have been shown to display a partially etiolated phenotype in a wide spectrum of light qualities, suggesting that HY5 acts

downstream of all photoreceptors from a central, relatively high hierarchical position (Jiao et al., 2007). HY5 is constitutively nuclear and has been long known to bind to LREs in vitro (Chattopadhyay et al., 1998b). Given its great importance in photomorphogenesis, several studies have tried to identify its target genes on a genome-wide scale (Gao et al., 2004; Lee et al., 2007; Zhang et al., 2011a). Remarkably, it was found that ~44% of all genes in the Arabidopsis genome are HY5 targets, many among them are early light responsive transcription factors, and binding to some is regulated by light conditions whereas in other cases binding is light-independent. Earlier, it had been demonstrated that the direct effects of HY5 on light-mediated gene expression can be both positive and negative, and that ~20% of the Arabidopsis light-regulated genes are under its control (Ma et al., 2002). As *HY5* was a central focus of this study, more extensive discussion of the relevant literature has been included in various sections throughout this thesis.

1.4.3 Modes of regulation of transcription factors by light

Regulation at the transcript level, post-translational modifications, tightly controlled degradation and desensitisation through protein-protein interactions are all important facets of the light-mediated fine-tuning of transcription factor activity (Wu, 2014).

Common **P**lant **R**egulatory **F**actors 1 (CPRF1) is a light-induced transcription factor identified in parsley during early research that focused on the LREs of its *CHS* gene (Weisshaar et al., 1991). A subsequent study which focused on the functional characterisation of CPRF1 revealed that it might negatively regulate its own gene's transcription by binding to defined *cis*- elements on the promoter (Feldbrugge et al., 1994). Later work on various CPRF family members revealed that they could act either as activators or repressors, depending on the promoter context and the light stimulus. Intriguingly, it was also shown that controlled mechanisms of nuclear import and/or retention in the cytosol might contribute significantly to the regulation of the transcriptional activity of certain CPRFs and GBFs (Kircher et al., 1998).

The steady-state transcript levels of any given gene at a particular instant are additionally balanced through post-transcriptional processes. For example, many genes encoding for members of the various light signalling pathways are known to produce two or more

alternatively spliced transcript variants. Notably, an alternatively spliced *HYH* mRNA has been reported to produce a HYH protein (altHYH) that lacks the motif which is responsible for physical interaction with COP1 (Sibout et al., 2006). This leads to stabilisation of the intracellular levels of altHYH, which in turn has been suggested (Wu, 2014) that could, in principle, increase the expression of light-regulated genes. In addition to alternative splicing, pivotal roles in post-transcriptional regulation are played by small regulatory RNAs, including microRNAs (miRNAs) and small interfering RNAs (siRNAs). It was recently shown that several miRNA-encoding genes (*MIRs*) are directly activated by HY5 and at least eight genes were found to be targets of both HY5 and HY5-regulated *MIRs* (Zhang et al., 2011). Interestingly, *HY5* expression itself has been found to undergo light-mediated post-transcriptional control by the miRNA miR175d (Tsai et al., 2014).

For some transcription factors, phosphorylation is a common post-translational modification which can influence the ability of sequence specific promoter binding (Jiao et al., 2007). A usual suspect for phosphorylating light-responses-mediating transcription factors, thereby modifying their activity/stability, is **C**asein **K**inase **2** (CK2), a ubiquitous Ser/Thr kinase. HFR1, HY5 and PIF1 are a few examples of its substrates (Bu et al., 2011; Hardtke et al., 2000). Phosphorylation of transcription factors is very often coupled with ubiquitin-mediated proteolysis, which has lately been established as being an important regulatory mechanism of light signalling. Since it was first demonstrated (Osterlund et al., 2000), COP/SPA-mediated ubiquitination of photomorphogenesis-promoting transcription factors and their subsequent degradation via the 26S proteasome pathway have been undoubtedly documented on numerous occasions (Lau and Deng, 2012).

Finally, compelling evidence suggesting that the activity of many transcriptional regulators can be fine-tuned on the basis of their ability to form homo- and heterodimers has accumulated in recent years. For example, the DNA binding activity of PIF4 has been found reduced after physical interaction with **P**hytochrome R**a**pidly **R**egulated 1 (PAR1) (Hao et al., 2012). Similarly, both PIF4 and PIF5 have been reported to form heterodimers with HFR1, and the formation of these complexes impairs the PIF4/PIF5-triggered expression of cell elongation genes (Hornitschek et al., 2009). Lastly, the ability of FHY3/FAR1 to activate expression of *FHY1* and *FHL* has been shown to be compromised by HY5 binding to FHY3/FAR1 and/or associating with ACGT-containing elements on the the *FHY1* and *FHL* promoters (Li et al., 2010).

1.4.4 Chromatin dynamics and light

The large scale transcriptomic fluctuations which underlie the striking developmental transitions that plants undergo under the influence of light, inevitably require a fine balance between genome packaging and genome access. The genetic material is organised in a dynamic nucleoprotein configuration, the chromatin, whose structure, both fine and higher, often needs to be manipulated so that the required DNA-based processes can take place in an appropriately regulated fashion (Campos and Reinberg, 2009). For more than two decades, it has been known that chromatin-based mechanisms are of utmost importance for the proper manifestation of various light responses. Diverse types of post-translational histone modifications have been reported to contribute in the light-mediated alternations of chromatin between its two main compaction states, euchromatin and heterochromatin, thus facilitating the suitable transcriptional output (Barneche et al., 2014). Among the histone marks that are regularly reported in the relevant literature, acetylation, ubiquitination and methylation of specific residues are the most notable. Expectedly, mutant plants impaired in genes encoding for certain histone modifying enzymes have been demonstrated to display altered photomorphogenic phenotypes (Wu, 2014). Moreover, chromatin remodellers with nucleosome-stimulated ATPase activity have also been found to be involved in light signalling (Jing et al., 2013). The main body of the intensified research of the last couple of decades comes principally from studies on photomorphogenesis and particularly de-etiolation. Purposely, a detailed presentation of noteworthy studies has been avoided in this introductory section. Instead, because of their high relevance to approaches undertaken throughout this project, such works received a thorough account in subsequent chapters, where they can easily be reflected upon during the discussion of the obtained results.

1.5 UV-B dependent gene expression

The diverse effects of UV-B on plants involve differential gene expression (Jenkins, 2009). There have been quite a few transcriptomic profiling analyses, both in maize (Casati and Walbot, 2003; Casati and Walbot, 2004b; Casati et al., 2006) and Arabidopsis (Brosche et al., 2002; Brown et al., 2005; Kilian et al., 2007; Morales et al., 2013; Ulm et al., 2004), which have revealed a wide range of affected genes concerned with numerous cellular processes. Common to all studies was the finding that most genes displayed an increase in expression, but a substantial proportion appeared to be repressed by UV-B. Moreover, organ- and developmental stage- specificity was uncovered for many UV-B regulated genes (Casati and Walbot, 2004a). The response of many genes was found to be rapid and transient expression kinetics were noticed for some (Ulm et al., 2004; Kilian et al., 2007). Consistently with the two known distinct types of UV-B responses, high fluence rate illumination with short wavelengths induced many genes normally associated with stress responses, whereas even brief exposure to long wavelength, low fluence rate UV-B, stimulated the expression of genes involved in UV-protection (Jenkins, 2009; Kilian et al., 2007). It should be noted, however, that recent intriguing findings are suggesting that low- and high- fluence rate UV-B signalling pathways, albeit independent of each other (Brown and Jenkins, 2008), are both important for plants to achieve full UV-B tolerance (Gonzalez Besteiro et al., 2011).

During the course of this project, the focus was exclusively on the photomorphogenic UV-B responses of plants, which as already mentioned in a previous section are mediated by the UVR8 photoreceptor.

1.5.1 UVR8-dependent gene expression

UVR8 acts by regulating the transcription of many genes. The transcriptomic analysis by Brown et al. (2005) revealed that in mature leaf tissue the expression of at least 70 genes is altered upon UV-B illumination. The genes implicated in the amelioration of UV-damage were only a subset of the total number, which included genes involved in metabolism, signalling, transcriptional regulation, and the production of chloroplast-specific proteins. Subsequent work by Favory and coworkers (2009) expanded the list of UVR8-regulated genes to several hundreds, by using slightly different, more specific light conditions, and

whole Arabidopsis seedlings. Moreover, this work utilised sun simulators, thus strengthening the notion that UVR8 orchestrates responses required for survival in sunlight. Recently, further support to this idea was provided with experiments in the natural environment, where UVR8 was shown to promote growth under ambient solar UV-B, thereby contributing to the plants' acclimation so that they can subsequently tolerate higher exposure levels (Morales et al., 2013). Additionally, Morales and coworkers provided evidence for the regulation of expression of genes associated with combatting herbivore attack, thus expanding the catalogue of non UV-protection-related responses that are affected by UVR8 (mentioned in Section 1.3.1) as a consequence of its broader effects on cellular biochemistry.

The key effectors of UVR8-mediated transcriptional regulation are HY5 and its homologue HYH. The involvement of HY5 in UV-B-activated gene expression was first demonstrated in the genome-wide expression analysis by Ulm et al. (2004), where the transcripts of both homologues were found to accumulate rapidly after low doses of UV-B, along with those of several other transcription factors. Subsequently, utilisation of *hy5* mutant plants showed reduced UV-B tolerance highlighting its crucial role (Brown et al., 2005; Oravecz et al., 2006). In due course, it was demonstrated that the transcriptional activation of *HY5* by UV-B depends on UVR8 and COP1 (Brown et al., 2005; Oravecz et al., 2006; Favory et al., 2009). Expression analyses conducted with *hy5, hyh* and *hy5hyh* mutant plants revealed partial redundancy between the two transcription factors in mediating the regulation of downstream genes, with a dominant role of HY5 (Brown and Jenkins, 2008). Interestingly, in a recent study which focused on the entrainment of the Arabidopsis circadian clock by UV-B (Feher et al., 2011), it was reported that there is a subset of UVR8- and COP1-dependent genes whose regulation is not under the control of HY5/HYH.

Another recently reported positive transcriptional regulator of UV-B photomorphogenesis is FHY3, a transposon-derived TF which together with FAR1 plays a crucial role in phytochrome signalling. *FHY3* expression is induced by UV-B and the *fhy3* plants display impaired UV-B induced hypocotyl growth and reduced tolerance to UV-B damage (Huang et al., 2012). Unexpectedly, FAR1 appeared non-essential in the UV-B photomorphogenic pathway, as *fhy3/far1* double mutants did not suffer more severe effects, and *far1* plants displayed no visible phenotypic alterations. Intriguingly, in the same study FHY3 and HY5

were found to bind directly to distinct *cis*-regulatory elements on the *COP1* promoter, driving the UV-B induced expression of *COP1*.

Finally, it is worth mentioning that HY5 activity in UV-B responses in negatively affected by a transcriptional effector of the B-BOX zinc finger family, namely BBX24 (Jiang et al., 2012). It has been suggested that BBX24 functions in concert with **R**ADICAL INDUCED **C**ELL **D**EATH 1 (RCD1), which is an additional negative regulator of UV-B signalling (Jenkins, 2014a; Jiang et al., 2009; Jiang et al., 2012). In the course of this project, the results that came out drove particular attention to the BBX family of transcriptional regulators, hence the relationship of BBX24 with UV-B signalling is thoroughly discussed in a subsequent chapter.

1.5.2 Molecular details of UVR8-regulated transcription

Presently, the events that follow the interaction of UVR8 with COP/SPA and lead to transcriptional activation of target genes remain obscure. Hints as to which direction research should turn to, in order to shed some light on this facet of UV-B signalling, have been available for almost a decade. Yet, the progress achieved so far is disproportionate compared to the wealth of information gathered for other aspects of photomorphogenic UV-B responses (Jenkins, 2014a).

Brown et al. (2005) were the first to report association of UVR8 with chromatin through its ability to bind histones. It was shown that UVR8 can bind strongly to histone-containing agarose beads, and its elution required high salt concentrations. Later, histone H2B appeared to be the preferential target of UVR8, since it was the most effective competitor in disturbing the UVR8-histone-agarose association (Cloix and Jenkins, 2008). Moreover, numerous studies have reported the in vivo detection of UVR8 on plant chromatin via **Ch**romatin **I**mmuno**p**recipitation (ChIP) assays (Brown et al., 2005; Cloix et al., 2012; Cloix and Jenkins, 2008; Favory et al., 2009; Kaiserli and Jenkins, 2007). Intriguingly, the binding of UVR8 to chromatin is observable regardless of UV-B illumination, but it has been argued that without quantitative data it is not possible to conclude that UV-B stimulates this phenomenon (Jenkins, 2014a). Although it is possible that UVR8 might appear on chromatin as a member of a multipartite protein complex, currently no experimental data are available in support of such a view. A candidate which has been

investigated in that respect is COP1, but it appears to be dispensable for UVR8-chromatin association (Cloix et al., 2012; Favory et al., 2009). Moreover, ChIP assays have revealed that chromatin binding appears only for a subset of the genetic loci occupied by UVR8-regulated genes, and although the association has been clearly detected on promoter regions, it appears not to be restricted to them. For *HY5* particularly, the UVR8-chromatin interaction spans the entire locus, covering promoter, coding and 3' non coding regions (Cloix and Jenkins, 2008). These data have been interpreted to imply that UVR8 might be directly, physically involved in promoting gene expression by participating in processes that keep chromatin in a transcriptionally active euchromatic conformation. Indeed, it is conceivable that UVR8, by associating with chromatin on target loci, could act as a recruiting agent for protein complexes with histone modifying or chromatin remodelling activity. It is unclear why only some target loci and not others are observed to display the UVR8-chromatin interaction in ChIP experiments, but as is the case with many assays, ChIPs have certain detection limits that may leave unnoticed some weak/transient, yet true and physiologically effective chromatin associations. On the other hand, it is worth keeping in mind that the association of UVR8 with chromatin might be unspecific, resulting from UVR8's ability to stick to histones.

There is good evidence in the literature which can be viewed as encouraging to the functional UVR8-histone complex hypothesised above. Studies in maize, and Arabidopsis, have highlighted the significance of UV-B-mediated chromatin-based processes coupled to transcriptional regulation. Genome-wide analysis of high altitude maize ecotypes and of RNAi knock down plant lines suggested that certain chromatin remodelling proteins are important mediators of UV-B responses (Casati et al., 2006). In particular, plants from high altitude locations, where the exposure to UV-B is naturally higher, appeared to have elevated levels of chromatin-remodelling-proteins-encoding transcripts. On the other hand, RNAi transgenic plants with lower expression of certain genes encoding for such chromatin remodelling proteins exhibited hypersensitivity to UV-B, which could be observed in increased leaf arching, leaf chlorosis and necrosis, and altered UV-B regulation of selected genes. In a later study, it was demonstrated that acetylation of histones H3 and H4 correlated with increased transcription of several UV-B responsive genes in maize (Casati et al., 2008). Not surprisingly, subsequent research in Arabidopsis revealed that the

promoter regions of two UVR8-regulated genes, namely *HY5* and ***E**arly **L**ight **I**nduced **P**rotein 1* (*ELIP.1*), are enriched in diacetylated histone H3 at lysine K9 and K14 (H3K9,14diac) (Cloix and Jenkins, 2008). Relatively recently, another study was published which claimed that histone acetylation is important in the DNA repair processes that follow UV-B irradiation (Campi et al., 2012). Given that there are many histone modifications which are of functional relevance to diverse plant responses to light (Barneche et al., 2014; Fisher and Franklin, 2011), it would be informative and valuable for subsequent research to pinpoint those modifications which are physiologically significant for photomorphogenic UV-B responses, and to assess how, if at all, their appearance is regulated by UVR8. A significant amount of time and effort during this project was dedicated to that goal.

An equally important, and largely unresolved, issue in our understanding of the molecular details of UVR8-regulated transcription is the lack of knowledge on the identity of the transcription factors that mediate the UV-B-induced increase in *HY5* transcripts. *HY5* expression is increased rapidly after UV-B illumination, and levels peak after ~ 2h (Brown et al., 2009), but the TFs effectuating the response remain elusive. Recently, it was reported that **CA**L**M**ODULIN7 (CAM7), a unique member of the calmodulin family, interacts physically with HY5 and both are capable of binding to the *HY5* promoter, albeit on different *cis*- elements (Abbas et al., 2014). The authors did not include UV-B light in their study, but employed other light conditions to demonstrate that HY5 and CAM7 act in concert to fine-tune the optimal *HY5* promoter activation during photomorphogenesis. While this thesis was in the final stages of editing, an interesting report was published on HY5 activity over its own promoter under photomorphogenic UV-B conditions (Binkert et al., 2014). Revealingly, HY5 was found to control the transcription of its own gene following UV-B illumination by binding to the same *cis*- element reported by Abbas et al. (2014). Nevertheless, the authors in their discussion emphasise the necessity of directing research efforts towards identifying additional TFs, which presumably would act either jointly with or in opposition to HY5, in order to mediate a regulated UV-B-induced expression of the *HY5* gene. In a rationale similar to the one described earlier, the enigmatic association of UVR8 with the chromatin might have something to do with the recruitment and/or activation of such particular TFs. It is important, therefore, for gaining a deeper understanding of these obscure events, to identify the involved transcription factors

and to investigate whether UVR8 has any contribution to the mechanisms by which they are guided to their site of action. Substantial time and effort throughout this project was devoted to that end.

1.5.3 Summary of the aims of this study

In conclusion, there were two principal aims in this study: to address questions related to the nature of the chromatin-based events that underlie UVR8-stimulated transcription, and to identify novel TFs that might be significant for the UVR8-mediated UV-B-induced transcriptional upregulation of *HY5*. Although distinct, these two research directions were approached under a central unifying working hypothesis: that the functional significance of the UVR8-chromatin association may lie in its requirement for the recruitment/activation of chromatin modifying complexes and/or transcription factors (Fig 1-4).

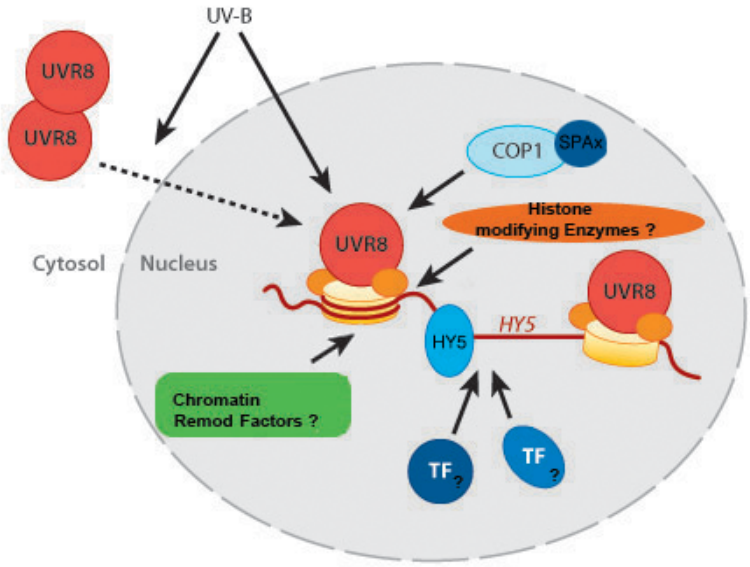

Fig 1-4. Model encapsulating the research questions that this study attempted to address and the working hypothesis which guided our experimental approach. Following UV-B perception, UVR8 monomerizes and accumulates rapidly in the nucleus where it controls the expression of various genes, including *HY5*. The molecular mechanisms by which this gene-regulatory function is achieved are currently unclear, but the association of UVR8 with chromatin might be a requirement for the recruitment and/or activation of particular chromatin modifiers and/or transcription factors. With this working hypothesis in mind, this study aimed at shedding light in the chromatin based-events that underlie UVR8-stimulated transcription and at identifying novel TFs required for the UVR8-mediated UV-B-induced activation of *HY5*. Modified from Jenkins, 2009.

CHAPTER 2 : MATERIALS & METHODS

2.1 Plant materials

The **W**ild-**T**ype (WT) *Arabidopsis thaliana* plants used throughout this study were of the Landsberg *erecta* (L*er*), Columbia (Col-0) and Wassilewskija (W*s*) ecotypes, seeds of which had been initially obtained from The European Arabidopsis Stock Centre (NASC, Nottingham, UK). Prof. Daniel Kliebenstein (UC Davis, CA, USA) provided the *uvr8-1* (L*er*) mutant seeds. The *hy5 ks-50 /hyh* and *hd1* mutants (W*s*) were supplied by Prof. Xing Wang Deng (Yale University, CT, USA) and Professor Jeffrey Chen (University of Texas, Austin, USA) respectively. Seeds of the T-DNA insertional mutants, or of the **T**RANSL**P**LAN**T**A (TPT) collection conditional overexpressors, described in Chapters 4, 6, and 7, were purchased from NASC. Their accession numbers and parent lines are given in Table 2.1. Whenever used, the WT *Nicotiana* plants were of the species *Nicotiana benthamiana.*

T-DNA insertional mutant	NASC accession number	Parent Line
gcn5	N674989	SALK_048427
hac5	N667192	SALK_122443
taf1	N660015	SALK_088103
fve	N878321	SAIL_1167_E05
sth2-1 & sth2-3	N654361 & N657768	SALK_113836 & SALK_107948
sth3	N605367	SALK_105367
myb31	N865157	WiscDsLoxHs080_11H
myb61-3	N686619	SALK_106556
myb61-1	N117564	SM_3.30853
myb50	N436625	GK-382E01
nf-yc9	N558903	SALK_058903
anac083	N643793	SALK_143793
TPT OE	**NASC catalogue number**	**Parent Line**
MYB61 cOE 1	N2101453	TPT_1.09540.1B
MYB61 cOE 2	N2101454	TPT_1.09540.1D
MYB61 cOE 3	N2101455	TPT_1.09540.1F

Table 2.1 Seed-stock accession numbers and parent lines of various T-DNA mutants and of conditionally overexpressing lines purchased from the European Arabidopsis Stock Centre

2.2 Chemicals and reagents

Unless otherwise stated, the reagents and chemicals used during this study were purchased from Sigma-Aldrich Ltd. (Poole, Dorset, UK), Thermo Fisher Scientific Ltd. (Loughborough, Leicestershire, UK) or Bio-Rad laboratories (California, USA). Yeast media and drop-out supplements were purchased from Takara-Clontech (2 Avenue du Président Kennedy, France). Yeast One Hybrid bait sequences were synthesised by Genscript Inc. (NJ, USA) and all primer sequences were synthesised by Life-Technologies (3 Fountain Drive, Inchinnan Business Park, Renfrew PA4 9RF).

2.2.1 Primer sequences

The primer sequences used throughout this project were designed in the Geneious Software (Geneious version 8.0 created by Biomatters. Available from http://www.geneious.com) using *Primer3,* apart from the genotyping primers which were obtained from the SALK T-DNA primer design website http://signal.salk.edu/tdnaprimers.2.html. All primers are listed in Table 2.2. Because of the large number of sequences, the table is organised in sub-tables according to the applications in which primers were used. The Tm values used throughout the project were calculated according to recommended (*Primer3)* algorithms.

Primer sequences for ChIP	Primer Name
TCCCCTATCCATTATTCACCG	qChIP p.r *HY5* Fw
TTGCGAGACATTTTGGGAAGG	qChIP p.r *HY5* Rev
AGTTCAGGAAACAACTCGACC	qChIP p.r *ELIP.1*Fw
ATGTTGAACGATGCTGTTGCC	qChIP p.r ELIP.*1* Rev
CGAAATGATTCGTGTCTGTCG	qChIP p.r *ACT2* Fw
TGTTCTTCTCTGTCAAGTCGC	qChIP p.r *ACT2* Rev
AAGGATCGAGAAGCAGAGAAC	qChIP p.r *WRKY30* Fw
TTGCATGGCTTCTGGAAACTG	qChIP p.r *WRKY30* Rev
ACGAGTTGCAGACTTTGAGTG	qChIP p.r *HYH* Fw
CCAGTTTTGTGCTTCTTGTGG	qChIP p.r *HYH* Rev
CTAACCTACCACACTCTCATC	qChIP p.r *CHS* Fw
ATCCAAAGAAGAAGCACCAGC	qChIP p.r *CHS* Rev

Table 2.2 Primer sequences used throughout this study.

Primer sequences for ChIP	Primer Name
TCCCAACGAGTGATCTCATTG	qChIP t.r *HY5* Fw
TTCTTTTCCGACAGCTTCTCC	qChIP t.r *HY5* Rev
AATGACCAGCTCGAAGAGAAG	qChIP t.r *HYH* Fw
CACTGAACAATGGATTAAAGGG	qChIP t.r *HYH* Rev
GTGAGCACAAAGTTTAGCGAC	qChIP t.r *ELIP.1* Fw
ACTTGGACTCAACGCTTATGC	qChIP t.r *ELIP.1* Rev
GTATTGTGCTGGATTCTGGTG	qChIP t.r *ACT2* Fw
GAGGTAATCAGTAAGGTCACG	qChIP t.r *ACT2* Rev
CAGACAGGACATCGTGGTGGT	qChIP t.r *CHS* Fw
ACATGAGTGATCTTTGACTTGG	qChIP t.r *CHS* Rev
TCGAAGAAGTCAATGCCAAGG	qChIP t.r *WRKY30* Fw
TCTCCAACTGAATCCATCGTC	qChIP t.r *WRKY30* Rev
ATAATCTTCAGCAGCCGTTGC	qChIP t.r *UBQ5* Fw
GAAAATCAATCGCTGCTGGTC	qChIP t.r *UBQ5* Rev
CACATCAGTCTGTCACCATCAAG	qCHIP *CEN4* Fw
CTACTCCAAATCTTACAAACCC	qCHIP *CEN* Rev
TGGTAAGATGTATCATTCGTGAAACCT	ChIP *AtCCoAOMT7* Fw
AGAATGATACATATTACCAAACGGTT	ChIP *AtCCoAOMT7* Rev
GACGGCATGATCGTTACCAATCC	ChIP *AtPME* Fw
CGATGTGTTTATATAGATGTGGGGACT	ChIP *AtPME* Rev
Primer sequences for Direct Y1H , Y2H or Y3H assays	**Primer Name**
ATATTGAATTCATGGAAGAGATTTCGACGGA	*COP1*-pGBKT7 Fw
ATTGTCGACCTACTAGAATCACGCAGCGAGT	*COP1*-pGBKT7 Rev
AAAGAATTCATGAGCGTATGGAACTACGCC	*DDB1b*-pGBKT7 Fw
AAAGGATCCTCAGTGAAGCCTAGTGAGTTCTTCAAC	*DDB1b*-pGBKT7 Rev
AAACCATGGAAATGAGTTCAACGAGGAGCAG	*DDB2*-pGBKT7 Fw
TTTGTCGACTACATAACGACCTTCTTCACTC	*DDB2*-pGBKT7 Rev
ATAGAATTCATGCCTCTGTTTGAGCTTTTCAGG	*PIF3*-pGBKT7 Fw
ATAGTCGACATGTCACGACGATCCACAAAACTG	*PIF3*-pGBKT7 Rev
TTTGAATTCTGCGCCGACGAAGCTGCTCTCTGTC	*BBX24*-pGBKT7 Fw
ATTGTCGACGTCTACACATAGATTACATATAGCTT	*BBX24*-pGBKT7 Rev
TTTCATATGATGGGGAGACATTCTTGCTGTTAC	*MYB61*-pGBKT7 Fw
ATAGGATCCGCTAAAGGGACTGACCAAAAGAGAC	*MYB61*-pGBKT7 Rev
TATCATATGCATTGCAACATGAAGAGACATTCTTGT	*MYB50*-pGBKT7 Fw
TAAGGATCCAAAGAAACTAAAGGGTCTGACCACCA	*MYB50*-pGBKT7 Rev
AAAACATATGATGCAGGAACAAGCGACTAG	*HY5*-pGADT7 Fw
AAAAATCGATAGAAGAAGAAGGAGATCAAAGG	*HY5*-pGADT7 Rev
AATACATATGATGGAGAGCGACGAAGCAG	*FVE/MSI4* -pGADT7 Fw
TATAATCGATCTCTTAAGGCTTGGAGGC	*FVE/MSI4*-pGADT7 Rev
AAAGAATTCAGCTCATGGAACTACGTTGTTAC	*DDB1a*-pGADT7 Fw
ATATTATCGATGCGTTGATTGATGATTGATTTGAC	*DDB1a*-pGADT7 Rev
AAAGAATTCATGAAGATCAGGTGCGACGTCTGC	*STH2*-pGADT7-Fw
AAAGAGCTCGATCAAAGTTGGGAGAAATGAAGGAG	*STH2*-pGADT7-Rev
TTTCATATGCATTGTTGTACTCTCATGGTATCTG	partial*HAC5*-pGADT Fw
TTTATCGATTCATTCAGGAGTGGAGGCCGTTG	partial*HAC5*-pGADT7 Rev
TATCATATGCATTGCAACATGAAGAGACATTCTTGT	*MYB50*-pGADT7 Fw
TAAGGATCCAAAGAAACTAAAGGGTCTGACCACCA	*MYB50*-pGADT7 Rev

Table 2.2 Primer sequences used throughout this study.

Primer sequences for Direct Y1H , Y2H or Y3H assays	Primer Name
TTTCATATGATGGGTAGACCACCTTGTTGCGAG	*MYB31*-pGADT7 Fw
ATAATCGATTTATTTTAACTCCTCTAAAGACACGTC	*MYB31*-pGADT7 Rev
TTTCATATGATGGGGAGACATTCTTGCTGTTAC	*MYB61*-pGADT7 Fw
ATAATCGATGCTAAAGGGACTGACCAAAAGAGAC	*MYB61*-pGADT7 Rev
TAGCATATGATGGATAATGTCAAACTTGTTAAGAATG	*NAC83*-pGADT7 Fw
TATATCGATTCATCTGAAACTATTGCAACTACTGGTC	*NAC83*-pGADT7 Rev
TTAGAATTCATGGACGCCCTGCTTCAAGTTTC	*Gras-like TF*-pGADT7 Fw
AAACTCGAGCTCACGGGATCAAACATATTCTAC	*Gras-like TF*-pGADT7 Rev
ATTCCCGGGGGATACTGGCGGCAATTCGCTG	*HD1*-pGADT7 Fw
TATCTCGAGGAAATTAGAAGCTCCGAGTCTTATG	*HD1*-pGADT7 Rev
AATGAATTCTCAGAAATGGGGGATTCCGACAGG	*NF-YB2*-pGADT7 Fw
TTTATCGATTCACCAATCTTTGTTAAGTCCTTG	*NF-YB2*-pGADT7 Rev
AAACATATGATGGATCAACAAGACCATGGACAGTC	*NF-YC9*-pGADT7 Fw
TTTATCGATAGTTTCTTGCTAATTTTCCTGGTCAG	*NF-YC9*-pGADT7 Rev
AAACATATGATGGAGGGTGGTGCGAGTAATGAAG	*SHP*-pGADT7 Fw
TATATCGATTCAAACAAGTTGCAGAGGTGGTTGG	*SHP*-pGADT7 Rev
TTTGAATTCATGGACTGCAACATGGTATCTTCGTC	*SPL11*-pGADT7 Fw
ATTATCGATCTATTTTGGTACAACATCATATGAACAG	*SPL11*-pGADT7 Rev
TTTCATATGATGAAGATTCAGTGTAACGTTTGTGAG	*STH3*-pGADT7 Fw
AAAATCGATAAGATAATTACAAATGCTAGAACCGTC	*STH3*-pGADT7 Rev
TAACATATGGCTGACTTCGTCCAGAAAGATCCCAC	*WNK10*-pGADT7 Fw
TTCATCGATTCATCAACTCAGCTTCATCCACTTCC	*WNK10*-pGADT7 Rev
AGGCCATGGAGGCCATGAGTTCAACGAGGAGCAG	*DDB2*-pGADT7 FW
TTTCTCGAGTACATAACGACCTTCTTCACTC	*DDB2*-pGADT7 Rev
ATAATCGATGCGAAAGAAAATGCATGTCAGGCTTG	*PICKLE*-pGADT7 Fw
TTTGGATCCTTCAATGGTGCCTCGGTTTATGAGC	*PICKLE*-pGADT7 Rev
AAACATATGCACCAAGGTTGGAGTTTTGAGGAGAAT	*PIF4*-pGADT7-Fw
AAAATCGATACCTAGTGGTCCAAACGAGAACCGTC	*PIF4*-pGADT7 Rev
ATACATATGGGCTGTGGATCAAATTCTGGGTGG	partial*TAF1*-pGADT7-Fw
ATAATCGATTGCCTATCCCAAATCTCATGACAC	partial*TAF1*-pGADT7-Rev
TTTGAATTCGAAGATAATTTTCACATGTCCACTA	*PIF5*-pGADT7 Fw
ATTGGATCCTCAGCCTATTTTACCCATATGAAGAC	*PIF5*-pGADT7 Rev
AAAGAATTCATGTCGAATTATGGAGTTAAAGAGC	*PIF7*-pGADT7 Fw
AATGGATCCCAATAATACTAGGTCGCTAGACTAATC	*PIF7*-pGADT7 Rev
AAACATATGATGAAGATACAATGTGATGTGTGTG	*BBX25*-pGADT7 Fw
ACTATCGATCTTAGTAGATTCATCCATAGTTTAG	*BBX25*-pGADT7 Rev
AAACATATGATGTGTAGAGGCTTGAATAATGAAG	*BBX31*-pGADT7 Fw
ATAATCGATTCAGAGAAAAACAAACGGAACCTC	*BBX31*-pGADT7 Rev
ATTGCGGCCGCAATGGGGAGACATTCTTGCTGTTAC	*MYB61*-pBRIDGE Fw
AAAAGATCTGCTAAAGGGACTGACCAAAAGAGAC	*MYB61*-pBRIDGE Rev
Primer sequences for Y1H screens	**Primer Name**
GAGTGCTCTATCGCTAGGG	pINTHIS3/NB-bait seq primer
GAAGATACCCCACCAAACCC	Y1H screen clones sequencing (pGADT7) Fw
GCCAAGATTGAAACTTAGAGG	Y1H screen clones sequencing (pGADT7) Rev
CCTTACGGTCTCTAGATGGTTG	*PCD6* bait seq primer
TACTAGGGCTTTCTGCTCTG	*HIS3* Bait seq primer

Table 2.2 Primer sequences used throughout this study.

Primer sequences for Genotyping	Primer Name
AAACGTCTTACCTGGTTGCAC	*gcn5* LP
ACGTATCAGTTTCTGATCCGG	*gcn5* RP
AGGCCAGGTAAGCTAACGAAG	*hac5* LP
ACAGCCAGCGGTCAAGAC	*hac5* RP
GCAGCCTGCTCACTTGATATC	*taf1* LP
TTCCACTTGGGTTGAACACTC	*taf1* RP
GGAAGTGGGAGTAGGAACTCG	*ddb2* LP
TTTTCCCTCCATTTTTAACCG	*ddb2* RP
GGAATCGAGGAAATCCTCAAC	*sth2-1* LP
TCAAACAATCGAATGGAATGC	*sth2-1* RP
AGTCCCACTTGGTTCGATACC	*sth2-2* LP
TTAGAGGCGAGTTTGTTAGCG	*sth2-2* RP
TGCTTAAACCATAAACCTCAAGC	*sth3* LP
CCAAAAGCCACAAGATTCATC	*sth3* RP
CTATTGGAGCAGTTCCTGCAG	*nf-yc9* LP
AACCAGTCTCTTCCCCTTCAG	*nf-yc9* RP
CCCACGAGGTGTATATCATGG	*fve* LP
TTACCTGCAATGTTCCACCTC	*fve* RP
GACTAATTACCTTCGTCCCGG	*myb31* LP
ATCGACTTGACCACAAGCAAG	*myb31* RP
GAAATTTAAATTTGGCTCTGTTTG	*myb61-1* LP
AAAGGCCATCTGATTTATCCG	*myb61-1* RP
TGTTAGCTTTGCACAGCATTG	*myb61-2* LP
TCTGAAATTCCCAGTTTGGTG	*myb61-2* RP
CTTCAGCAACACCGTTTAAGC	*anac083*
TGAGGTGGTTTGCCTTTGTAG	*anac083*
TACGAATAAGAGCGTCCATTTTAGAGTGA	3' dSpm (SM Lines LB)
ATTTTGCCGATTTCGGAAC	LBb1.3 (SALK Lines LB)
TAGCATCTGAATTTCATAACCAATCTCGATACAC	LB3 (SAIL Lines LB)
AACGTCCGCAATGTGTTATTAAGTTGTC	p745 WiscDsLoxHs T-DNA specific

Primer sequences for generating GFP-tagged TFs	Primer Name
AAAGAATTCATGAAGATCAGGTGCGACGTCTGC	*STH2*-GFP Fw
CTCGTCGACCAGAAAGATCTAAACTTTTTATTAG	*STH2*-GFP Rev
ATAGAATTCATGAAGATTCAGTGTAACGTTTGTGAG	*STH3*-GFP Fw
AAAGTCGACAACCGTCGCCGCCGTTTCCCAACCC	*STH3*-GFP Rev
ATAGAATTCATGGATCAACAAGACCATGGACAGTC	*NF-YC9*-GFP Fw
TTTGTCGACTTTTCCTGGTCAGGTTGGTCAGGTG	*NF-YC9*-GFP Rev
TTTGAATTCATGGGGAGACATTCTTGCTGTTAC	*MYB61*-GFP Fw
AAAGGATCCAGGGACTGACCAAAAGAGACGGCC	*MYB61*-GFP Rev
TAGGAATTCATGGATAATGTCAAACTTGTTAAGAATG	*ANAC83*-GFP Fw
AAAGTCGACCATCTGAAACTATTGCAACTACTGG	*ANAC83*-GFP Rev
ATAGTCGACATGGGTAGACCACCTTGTTGCGAG	*MYB31*-GFP Fw
ATAGGATCCTTTAACTCCTCTAAAGACACGTCGATG	*MYB31*-GFP Rev
ATAGTCGACATGAAGAGACATTCTTGTTGTTAC	*MYB50*-GFP Fw
AAAGGATCCAGGGTCTGACCACCAAAAGAG	*MYB50*-GFP Rev

Primer sequences for RT-PCR	Primer Name
GCGGATTCTCATGGTCTATCCCA	*MYB61*-Fw 3-ter
CTGACCAAAAGAGACGGCCATTC	*MYB61*-Rev 3-ter
CTTCTTACTCACATCACCAATCAC	*MYB61*-Fw 5-ter
GCATGAAGTTCGACGATGAGATTC	*MYB61*-Rev 5-ter
GGCTGAAGAGGTTGTTGAGGAAC	*HY5*-Fw
AGCATCTGGTTCTCGTTCTGAAGA	*HY5*-rev
GTGAGCACAAAGTTTAGCGAC	*ELIP.1* Fw
ACTTGGACTCAACGCTTATGC	*ELIP.1* Rev
GTATTGTGCTGGATTCTGGTG	*ACT2* Fw
GAGGTAATCAGTAAGGTCACG	*ACT2* Rev
CAGACAGGACATCGTGGTGGT	*CHS* Fw
ACATGAGTGATCTTTGACTTGG	*CHS* Rev

Table 2.2 Primer sequences used throughout this study.

2.2.2 Antibodies

ChIP experiments, Immunoblots (Western Blots, WB), and Co-IPs were carried out with commercial antibodies from several manufacturers or with non-commercial antibodies kindly donated by other researchers. They are presented in Table 2.3

Antibody	Application & Working Dilution	Source (Company and Cat Number, or Principal Ivestigator)
anti-H3	ChIP, 1/200	Abcam, Cat # : ab1791
anti-H3K9,14 Diac	ChIP and ChIPseq, 1/200	Millipore, Cat # : 06-599
anti-H3K4me3	ChIP, 1/200	Active Motif, Cat # 39159 - 60
anti-H2Bub	ChIP, 1/200	Dr Ali Shilatifard Northwestern University Feinberg School of Medicine. Chicago USA
anti-H3K36me3	ChIP, 1/200	Abcam, Cat # : ab9050
anti-H3K9me3	ChIP, 1/200	Millipore, Cat # : 07-442
anti-H3K56	ChIP, 1/200	Active Motif, Cat # : 39281
anti-CHS	WB 1/1000	Santa Cruz, Cat # : sc 12620
anti-HA	WB and Co-IP 1/5000	Abcam, Cat # : ab9110
anti-cMYC	WB 1/1000	Santa Cruz Cat # : 9E10 sc-40
anti-C'-terUVR8	WB and Co-IP, 1/5000	Prof Gareth I Jenkins MVLS , University of Glasgow, UK
Anti-GFP	WB and ChIP, 1/5000, and 1/200 respectively	Abcam Cat # : ab290 Clonetech Cat # 632375 Myltenyi Biotech Cat # 130-091-833

Table 2.3 Antibodies employed in various experimental procedures during this project.

2.2.3 Plasmid Vectors

A number of plasmid vectors were used throughout the study for standard molecular biology procedures and/or specialised assays. They are listed in Table 2.4, along with information regarding their availability, the particular applications they were utilised for during this project, and their selection markers in bacteria and/or yeast

VECTOR	AVAILABLE FROM	APPLICATION	SELECTION	MARKER
			In Bacteria	In yeast
pCR2.1 TOPO	Invitrogen	Standards for qPCR	Ampicilin or Kanamycin	-
pCR4 TOPO	Invitrogen	Standards for qPCR	Ampicilin or Kanamycin	-
pGBKT7	Clontech	Y2H	Kanamycin	Leu deprival
pGADT7	Clontech	Y2H, Direct Y1H	Ampicilin	Trp deprival
pBridge	Clontech	Y3H	Ampicilin	Trp deprival
pEZRL(N)	Prof G.I.Jenkins Lab. University of Glasgow	GFP-tagging of proteins for transient or stable plant transformations	Kanamycin	-
pINT-HIS3NB	Dr Pieter Owerkerk Institute of Biology, Leiden University	Y1H screens	Carbenicilin or Ampicilin	Geneticin G418
pGWB15	Prof G.I.Jenkins Lab. University of Glasgow	HA-tagging of proteins for transient or stable plant transformations	Kanamycin	-

Table 2.4 Plasmid vectors used in various experimental procedures throughout the study.

2.2.4 Enzymes

Unless otherwise stated, the enzymes used for restriction digestions, ligations and standard PCR applications were purchased from New England Biolabs Inc. KOD-hot start polymerase (Novagen Cat # : 71086-3) was used when a proof-reading polymerase activity was desired; qPCR reactions were set up using the Brilliant III Ultra-Fast SYBR master mix (Agilent technologies Cat # : 600882). All enzymes were used according to the instructions provided in their accompanying documentation.

2.2.5 Antibiotics

Ampicillin and gentamycin were purchased from Melford Ltd. (Ipswich, Suffolk, UK). Kanamycin was obtained from Sigma-Aldrich and chloramphenicol from Duchefa Biochemie B.V. (Haarlem, The Netherlands). Geneticin G418 (Cat # 10131-035) was purchased from Life Technologies. The working concentrations of the antibiotics are given in Table 2.5.

Antibiotic	Working Concentration
Kanamycin	50 μg/ml for bacteria, 100 μg/ml for plants
Ampicillin	50 μg/ml for bacteria
Gentamycin	30 μg/ml for bacteria
Chloramphenicol	34 μg/ml for bacteria
Geneticin G418	150-200 μg/ml fror yeast

Table 2.5 Working concentrations of antibiotics

2.3 Bacterial and yeast strains

E.coli TOP10 cells were used for all standard cloning / sub cloning procedures, unless otherwise stated. The GV3101 *A. tumefaciens* strain was used for transient expression studies (transient transformation of *N. benthamiana*) or stable transformations of Arabidopsis plants. Regarding the yeast - based experiments, the AH109 strain was used for the Y2H assays, the Y187 strain was used for the direct Y1H assays, and the Y2HGold was employed for the Y3H assays. All yeast strains were obtained from Clontech Inc.

2.4 General laboratory procedures

2.4.1 pH Measurements, Centrifugations, Sterilisations

The pH value of solutions and media was measured with a Jenway 3320 pH Meter or, when only an approximation was sufficient, with pH indicator strips. Centrifugations were performed with an Eppendorf 5415 D bench-top centrifuge (up to 2 ml eppendorf tubes), SORVALL LEGEND RT Centrifuge (15 ml and 50 ml Falcon Centrifuge tubes), and SORVALL EVOLUTION RC Centrifuge (≥ 50 ml volumes). Unless otherwise stated, solutions, media and equipment were sterilised for 15 min at 120 °C and 1 atm, with a bench-top autoclave (Prestige Medical, Model 220140). In case of heat - labile substances, filter sterilisation was performed by filtration through a 0.2 μM pore diameter Nalgene filter.

2.4.2 Standard molecular biology and biochemical procedures

2.4.2.1 Crude DNA extraction from Arabidopsis leaves and genotyping

Crude gDNA extraction was performed as described in (Kotchoni and Gachomo, 2009). In brief, approximately 10-15 mg of Arabidopsis leaf tissue were placed in a micro centrifuge tube and macerated with a small pestle, without extraction buffer. Subsequently, 500 μl of extraction buffer (1 % SDS, 0.5 M NaCl, no pH adjustment needed) were added in the tube, the mixture was vortexed for 20 sec and then spun down, full speed (16000g), at room temperature. The supernatant was precipitated for 5 min with isopropanol, centrifuged, and the resulting pellet was washed with 75% ethanol, air -dried and resuspended in 50 μl of H_2O. 1 μl was then used as template for the genotyping PCR. The latter was performed as described in the SALK T-DNA primer design website http://signal.salk.edu/tdnaprimers.2.html. Briefly, two combinations of primers were used for each template. One primer pair, designated LP and RP, targeted the genomic regions that flank the T-DNA from the left and right side respectively, and should not yield a product if the insertion is present. The second primer pair, designated LB and RP, consists of a T-DNA specific primer (LB) and the RP genomic primer. It should only result in a PCR product if the T-DNA insertion is at the expected genetic locus.

2.4.2.2 Phenol - chloroform extraction of DNA, RNA isolation from plant tissues, quantification of nucleic acids and agarose electrophoresis

Phenol - Chloroform extraction of DNA from aqueous solutions was performed as described in (Sambrook et al., 2001) with the following deviation : the phenol extraction step was omitted. Instead, two extraction steps were performed, one with a 1:1 mixture of phenol and chloroform : isoamyl-alcohol (24:1), and one with chloroform : isoamyl-alcohol (24:1) alone. No alterations were made to the rest of the procedure.

RNA isolation from plant tissues was performed with the QIAGEN RNeasy Plant mini kit, Cat # 74904, according to the manufacturer's instructions. On - column DNase treatment was performed with the QIAGEN RNase - Free DNase Set, Cat # 79254 according to provided recommendations .

Quantification of nucleic acids was performed spectrophotometrically. In brief, 2 μl of DNA or RNA were diluted in 70 μl of dH2O and the absorbance at 230, 260 as well as 280 nm was measured (Eppendorf Bio Photometer) in comparison to a dH2O blank sample. An absorbance A=1 at 260 nm corresponds to a concentration of 50 μg/ml double-stranded DNA or 40 μg/ml of single-stranded DNA or RNA (Sambrook et al., 2001). The absorbance ratios 260/230 and 260/280 were recorded as indicative of the purity of the sample ($A_{230/260/280}$ should be approximately 1/1.8/1 for DNA and 1/2.0/1 for RNA).

Electrophoresis of nucleic acids was routinely performed on 1% agarose gels supplemented with ethidium bromide. Gels were prepared by melting agarose in 1 x TAE buffer (40 mM Tris-HCl, 1 mM EDTA), adding ethidium bromide (0.2 μg/ml) at a final concentration of 0.01% (v/v), pouring in an appropriate casting tray, and finally leaving to set at room temperature. DNA samples were then mixed with 4 x loading buffer (Promega), loaded on a set gel, already immersed in TAE buffer, and subjected to electrophoretic separation at 100 Volts.

2.4.2.3 DNase treatment of RNA samples, Reverse Transcriptase - mediated cDNA synthesis and RT-PCR

Although a first DNase treatment was always being performed during the RNA isolation itself, with the use of on-column DNA digestion, experience showed that for high yielding isolations this step was not enough to eliminate DNA contamination of the RNA samples. Thus, eluted RNA samples were given an additional DNase treatment. In brief, the following procedure was followed. Approximately 2 μg of RNA were diluted in 1 x DNase I buffer and incubated, for 1.5 h at 37 °C, with 2 units of DNase. The reaction was then terminated, by adding DNase Inactivation Reagent to the samples and leaving them for 5 min at room temperature, before pelleting the inactivation reagent by centrifugation. Efficiency of the DNase treatment was subsequently tested by a 35 cycle PCR reaction using primers for *ACTIN2*. Absence of PCR product was indicative of an efficient DNase treatment, which allowed proceeding to first strand cDNA synthesis. Otherwise, the DNase treatment was repeated until no PCR products could be detected.

Synthesis of first strand cDNA was performed using SuperScript® III First-Strand Synthesis System for RT-PCR (Life technologies). In short, 20 μl of DNA-free RNA were incubated with 4 μM oligo-dT primers (dTTT…T_{20}) at 68 °C for 10 min. The mixtures were cooled down on ice for 5 min. Subsequently, 1 x Reverse Transcriptase Reaction Buffer, 0.6 mM dNTPs, 20 units RNase inhibitor, 6 mM DTT, and 100 units SuperScript® III RT were added. The reactions were allowed to proceed at 48 °C for 50 min, and an enzyme heat-inactivation step (5 min at 95 °C) followed. The cDNA samples were stored at -20 °C or immediately used for RT-PCR.

Equivalent amounts of cDNA, estimated on the basis of RT-PCR product accumulation when *ACTIN2* primers were used, were employed as templates in the semi-quantitative RT-PCR-based gene expression experiments. The following PCR protocol was used : Step 1 (initial denaturation), 3 min at 95 °C ; step 2, 30 sec at 95 °C ; step 3 (annealing and extension), 1.5 min at 62 °C ; step 4, cycle to step 2 for 24 cycles (*ACTIN2, ELIP1*), 26 cycles (*CHS*) or 29 cycles (*HY5*); step 5, 5 min at 68 °C ; step 6 10 °C until collecting the reactions. All reactions were set up with New England Biolabs reagents, according to the accompanying instructions. For measuring transcript abundance via qPCR, RNA samples were validated according to the MIQE guidelines (Bustin et al., 2009) and cycling conditions were identical to those described is Section 2.7.4.

2.4.2.4 Restriction digestions, ligations, transformations and plasmid minipreps

In routinely performed restriction digestions, 0.5 to 3 μg of DNA were digested using commercial enzymes (Section 2.2.4), and appropriate buffers at concentrations and incubation times recommended by the manufacturer. Digests were column-purified using the QIAGEN QIAquick PCR Purification Kit (Cat # 28104) or, if first separated by agarose electrophoresis, with the QIAGEN QIAquick Gel extraction Kit (Cat # 28704), according to supplied protocols.

Purified digested DNA (PCR products or linearised plasmid DNA) with complementary single stranded "sticky ends" were subsequently used for ligations. An approximate 3:1 insert:vector ratio was calculated following spectrophotometric quantification, or judged empirically on the basis of the band intensities following electrophoretic separation in agarose gels. Reactions were performed at 10 μl final volume, containing 1x ligation buffer and 10 units of T4 DNA ligase (NEB). The ligation mix was incubated at room temperature for 1 h. 2-5 μl of the ligation mix was used for heat-shock-based transformation of 50 μl chemically competent *E. coli* cells (TOP10), which had been prepared in advance according to published protocols (Inoue et al., 1990).

In the cases of transformation of *Agrobacterium tumefaciens*, the preferred method was electroporation. Firstly, electro-competent Agrobacteria were prepared with the following procedure : Agrobacterium cells (GV3101strain) were inoculated in a 10 ml subculture of LB medium containing 30 μg/ml gentamicin, and left to grow for 20-24 h at 28 °C with constant shaking (200 rpm). Subsequently, one litre of gentamycin-containing LB medium was inoculated with the O/N subculture and grown until it reached OD_{600} = 0.5 - 0.8. Cells were then pelleted at 2,000 g for 10 min at 4 °C. The supernatant was discarded and the pellet was gently resuspended in 100 ml ice-cold sterile 10% (v/v) glycerol. Centrifugation and resuspension were repeated twice, changing the 10% glycerol resuspension volume (10 ml and finally 1 ml). 50 μl aliquots were snap-frozen in liquid Nitrogen and stored at -80 °C.

For the transformation itself, 1-2 μl of plasmid DNA were added in 50 μl of electro-competent Agrobacteria, and the cell suspension was incubated for 20-30 min on ice. Cells were then transferred into a pre-chilled electroporation cuvette (Bio-Rad) and

pulsed with 2.2 kV using a MicroPulserTM Electroporator (Bio-Rad). Immediately following the electric pulse, 1 ml of LB medium was added to the cells, which were then transferred to a 15 ml centrifuge tube and incubated at 28 °C with constant shaking (200 rpm) for 3 h. For the purpose of avoiding crowded growth on the petri dishes, 50 μl of 1/100 and 1/1000 dilutions were spread onto LB agar plates containing appropriate selective antibiotics. Plates were incubated at 28 °C for 2-3 days.

For plasmid isolations, putative transformants were selected from the LB agar plates and used to inoculate 5-10 ml of liquid LB media, supplemented with the appropriate antibiotics. After O/N growth for *E.coli* (or 20-24 h for Agrobacteria), the cells were pelleted via centrifugation and subjected to alkaline lysis following the instructions accompanying the QIAGEN Qia-prep Spin Miniprep kit (Cat # 27104). Recovered plasmid DNA aliquots were usually subjected to diagnostic restriction digestions to ensure the presence of appropriately sized insert DNA, and sent for sequencing (GATC-biotech Germany).

2.4.2.5 Protein extraction, protein quantification, SDS-PAGE, immunoblotting (western blots)

For protein extractions, Arabidopsis plants were ground on ice, using mortar and pestle, while soaked in protein micro-extraction buffer {(20 mM HEPES pH 7.8, 450 mM NaCl, 50 mM NaF, 0.2 mM EDTA, 25% (v/v) glycerol, 0.5 mM PMSF, 1 mM DTT and protease inhibitor (PI) mix (Complete Mini, Roche)}. The homogenate was subsequently centrifuged at 16,000g for 10 min at 4°C, and the supernatant was transferred to a fresh tube.

Regarding *N. benthamiana* plants, leaf tissue was snap-frozen in liquid nitrogen and ground to fine powder with mortar and pestle. The tissue powder was transferred to a pre-chilled microcentrifuge tube and approximately 1-3 volumes of protein extraction buffer {(25 mM Tris-HCl pH 7.5, 1 mM EDTA, 150 mM NaCl, 10% v/v glycerol, 10 mM DTT, 0.1% (v/v) Nonidet-P40, 2% (w/v) PVPP, PI cocktail and/or 0.5 mM PMSF)} was added. The mixture was then vortexed to obtain a homogenate and left on ice for 10 min, during which an additional vortexing was performed. Samples were then centrifuged at 16,000g for 15 min at 4 °C and the supernatant was transferred to a fresh tube.

Protein quantification was performed via the Bradford colorimetric assay, using bovine serum albumin (BSA) as a standard. Bradford assay solution (Bio-Rad, UK) was diluted five-fold with distilled water and filter sterilised to remove suspended particles. 1 µl of protein extract was added to 1 ml of Bradford solution and mixed well to obtain a homogenous colour. The absorbance at 595 nm was recorded with a spectrophotometer (Eppendorf, Germany) against a blank sample (Bradford solution without added protein). The concentration of each sample was calculated based on the equation derived from a standard curve, which had been generated using BSA standard solutions of known concentrations (1, 2, 4, 6, 8, 10 µg/µl).

SDS Polyacrylamide Gel Electrophoresis was performed according to the following procedure : Protein samples were denatured by adding the required amounts of 4 x SDS protein sample buffer {250 mM Tris-HCl pH 6.8, 2% (w/v) SDS, 20% (v/v) β-mercaptoethanol, 40% (v/v) glycerol, 0.5% (w/v) bromophenol blue} and subsequent boiling for 10 min at 95 °C. Depending on the size of the protein of interest, either 7.5% or 10% polyacrylamide separating gels were used, with a 4% polyacrylamide stacking gel on top {Separating: 7.5%, 10% (w/v) bis-acrylamide, 0.38 M Tris-HCl pH 8.8, 0.1% (w/v) SDS, 0.05% (w/v) APS, 0.07% (v/v) TEMED; Stacking: 4% (w/v) bis-acrylamide, 132 mM Tris-HCl pH 6.8, 0.1% (w/v) SDS, 0.05% (w/v) APS, 0.15% (v/v) TEMED}. Electrophoresis was performed at 200 V, for a duration of approximately 1 h , in SDS running buffer {25 mM Tris-HCl pH 8.5, 190 mM glycine and 0.1% (w/v) SDS}. An estimation of molecular weights was possible by comparison to the migration patterns of pre-stained molecular weight markers (Cat # P7708, New England Biolabs and/or Cat # 26616 Thermo Fisher Scientific).

For immunoblotting, protein extracts separated by SDS-PAGE were transferred, in the presence of transfer buffer {25 mM Tris-HCl pH 8.5, 190 mM glycine and 20% (v/v) methanol}, onto nitrocellulose membranes (Bio-Rad, UK), at 400 mA for 45 min. Membranes were then stained with Ponceau S solution {0.1% (w/v) Ponceau S, 1% (v/v) acetic acid} to demonstrate equal loading of protein samples. Subsequently, membranes were immersed for 1 h in blocking solution {(8% (w/v) non-fat dried milk in TBS-T (25 mM Tris-HCl pH 8, 150 mM NaCl, 2.7 mM KCl, 0.1% (v/v) Triton-X)}, to prevent non-specific binding of the antibodies. Primary antibodies were used in the working dilutions,

prepared with blocking solution, shown in Table 2.3. Incubation time varied from 1 h at room temperature to overnight (O/N) at 4 °C. Membranes were then washed 4 times with TBS-TT {(25 mM Tris-HCl pH 8, 150 mM NaCl, 2.7 mM KCl, 0.1% (v/v) Triton-X, 0.05% (v/v) Tween)} and once with TBS-T for a total of 25 min. Depending on the organism in which the primary antibodies had been produced, secondary anti-rabbit, anti-mouse (both Promega, Cat # W401B and W402B respectively), anti-rat (Cat # P0450, Dako Denmark A/S, Glostrup, Denmark) or anti-goat (Cat # A5420, Sigma) HRP conjugated antibodies, were used in 1:5000 (Promega Abs), 1:7500 and 1:7500 dilutions respectively, all prepared in blocking solution. The incubation time was 1 h followed by five washes with TBS-TT and 1 wash with TBS for a total of 35 min. For detection of Chemiluminescent signals, ECL Plus Western Blotting Detection Reagent (Amersham or Pierce Fisher) was used according to the manufacturer's instructions.

In cases where it was desirable to re-probe a particular membrane with different primary antibody, a stripping procedure was applied. To that end, membranes already subjected to chemiluminescent detection were washed in TBS and then incubated at 50 °C, immersed in stripping buffer {(100 mM β-mercaptoethanol, 2% (w/v) SDS, 62.5 mM Tris-HCl pH 6.8)}, for 30 min with gentle agitation (30 rpm). Subsequently, they were washed at least three times with TBS-T, for at least 20 min at room temperature. Immunolabeling and detection was then performed as described above.

2.5 Light treatments.

2.5.1 Light sources

Warm white fluorescent tubes L36W/30 (Osram, Munich, Germany) were used for white light, whereas for UV-B light, narrowband UV-B tubes Philips TL20W/01RS (Philips, Aachen, Germany) were employed. This narrowband UV-B source has a maximal emission at 311 nm (Fig 2-1), and it has been demonstrated, via the use of various cut-off filters, that the very low levels of emitted UV-A and blue light are insufficient to induce a UV-A/blue light specific response (Brown et al., 2009). White light fluence rates were measured using a LI-250A light meter, on which a LI-190 quantum sensor (LI-COR, Lincoln, NE, USA) was attached. UV-B fluence rates were measured using either a RS232 or a Spectro Sense

2 SKL904 meter, fitted with appropriate UV-B Sensors (SKU 430/SS2) (Skye Instruments, Powys, UK).

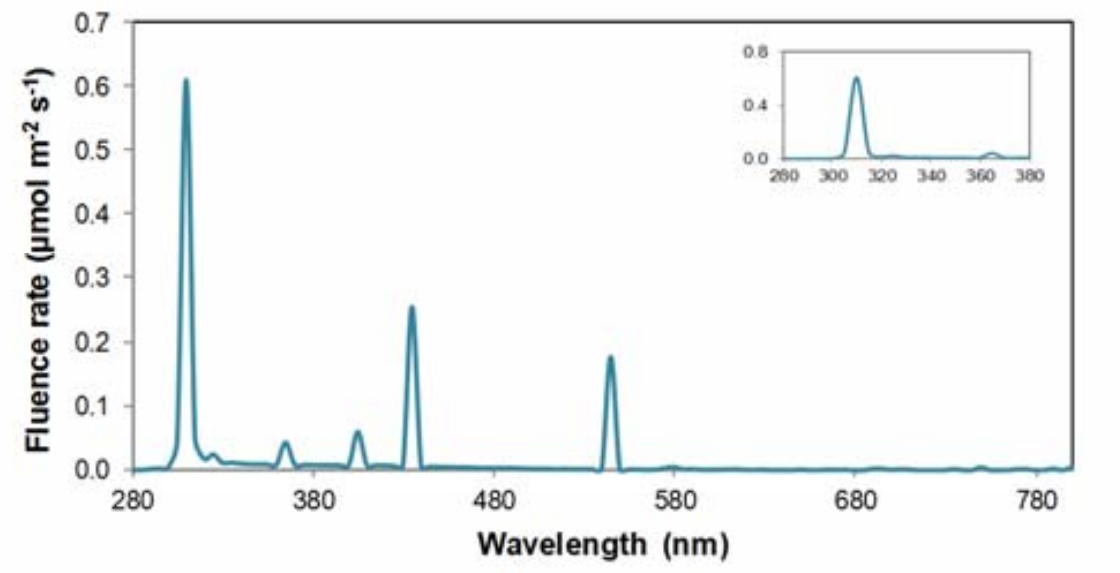

Fig 2-1 Spectrum of the narrowband UV-B tubes, Philips TL20W/01RS . (From Monika Heilmann, PhD thesis, University of Glasgow)

2.5.2 Plant UV-B treatments for gene expression studies and ChIPs

For gene expression studies, on the day before the UV-B treatment, 3 weeks old plants which had been grown under constant white light (=60 μmol m^{-2} s^{-1}) were transferred and kept in darkness O/N. On the next day, the plants were separated into two groups, one to serve as a control, and one to receive the UV-B treatment. Control plants were illuminated with **L**ow fluence rate **W**hite Light (LW, = 15 μmol m^{-2} s^{-1}) for 3 h, whereas the other group received 1 - 1.5 μmol m^{-2} s^{-1} narrow band UV-B light for 3 h. Upon completion of treatment, leaf tissue was collected, snap frozen in liquid nitrogen and stored at -80 °C.

For Chromatin Immuno-precipitation (ChIP) experiments, the light treatments were identical to the aforementioned, except that the duration which ranged between 4 and 5 h. Furthermore, upon completion of treatment leaf tissue was collected and kept on ice until fixation (usually performed approximately 30 minutes after harvesting). Fixation is described, along with a detailed description of the ChIP procedure, in a following section.

2.6 Plant growth and standard plant-based procedures

2.6.1 Plant growth on soil or agar plates.

Arabidopsis seeds were sown on the surface of pots containing compost soaked in insecticide solution {(0.2 g/l Intercept (Scotts, Ipswich, Suffolk, UK)}. The pots were kept under a humidifier during a stratification period of 3 days (4 °C), employed to break seed dormancy, and for one additional week following germination in the growth chambers. The latter had been programmed to sustain optimum light, temperature and humidity conditions (50-120 μmol m^{-2} s^{-1}, 20-22 °C, up to 75% humidity).

For aseptic growth on agar plates, seeds were first subjected to a surface sterilisation step, which consisted of a 5 min treatment with 50% (v/v) sodium hypochlorite solution followed by five washes with sterile dH2O. The sterilised seeds were then sown on 0.8% agar plates, which contained 2.15 g/l Murashige and Skoog salts (1⁄2 MS) and had adjusted pH = 5.7. The seed-containing plates were subjected to stratification and then transferred to the growth cabinets.

2.6.2 Hypocotyl elongation assays

For hypocotyl elongation assays, sterilised and cold-stratified seeds were germinated under low fluence rate white light (LW 1.5 μmol m^{-2} s^{-1}) without any measurable UV-B (control plants), or under LW supplemented with 1.5 μmol m^{-2} s^{-1} narrow band UV-B. Hypocotyl lengths from at least 25 seedlings were measured 5 days after germination and results were presented as mean values ± SE. From the remaining seedlings of each treatment, protein was extracted and immunoblots aimed at detecting expression levels of CHS were performed, as described in Section 2.4.2.4.

2.6.3 Stable transformation of Arabidopsis and generation of transgenic lines

Transformation of Arabidopsis plants and subsequent manipulation for identification of transgenic lines was carried out according to Davis et al., (2009), with minor deviations. In short, Agrobacteria harbouring the desired construct were grown in 500 ml YEBS medium (1 g/L yeast extract, 5 g/ L beef extract, 5 g/L sucrose, 5 g/L bacto-peptone, 0.5 g/L magnesium sulphate; adjusted pH 7) until stationary phase. 200 μl of Silwett L77 were then added in the culture and recently bolting plants, without many fully formed siliques, were dipped directly into the mixture for 20 seconds. Plants were covered with transparent bags to maintain high humidity and were transferred to the growth cabinets for a day. Subsequently, the bags were removed and after 3-4 days the dipping was repeated, using the same culture mixture which had been stored at 4°C after its initial use. Seeds were collected 4-5 weeks after the second dipping and sown, without undergoing surface sterilization, on petri dishes containing 1/4 MS-saturated chromatography sand {(1.1 g/L MS basal salt, 0.5 g/L MES; adjusted pH 5.7) Silicon dioxide Cat # 84880}, supplemented with the appropriate antibiotic. Resistant seedlings (T1) were identified within 4 days from germination, rescued on soil and grown until seed production (T2 seeds). T2 seeds, in turn, were sown on 1/4 MS-saturated chromatography sand and scored for antibiotic resistance segregation. Those lines which displayed a 3:1 ratio of resistant:sensitive phenotype where considered as having a single-locus T-DNA insertion and were checked under the confocal laser scanning microscope (Zeiss LSM510) for GFP expression levels. Eventually, lines for which satisfactory expression was observed were taken further to the T3 generation for identification of homozygous lines on the basis of 100% antibiotic resistance.

2.6.5 Transient transformation of *N. benthamiana* plants.

A single colony of Agrobacterium cells, freshly transformed with the desired construct, was inoculated in 10 ml of liquid LB medium supplemented with appropriate antibiotics. After O/N growth at 28 °C under constant 200 rpm shaking, when cell densities had reached OD_{600} values ranging between 0.6 - 1.0, cells were pelleted by centrifugation at 2,000g for 10 min. The pellet was then resuspended up to OD_{600} = 0.3-0.4 in infiltration medium (10 mM MgCl2, 10 mM MES pH 6.5), and the resulting suspension was left at room temperature for 3 hours. The Agrobacterium suspension was then infiltrated in *N. benthamiana* leaves with a needle-less syringe, using areas of the abaxial side as entry points. Afterwards, the infiltrated plants were moved back to the growth cabinets, at 28 °C, where they were left for 1.5 days before assessing gene expression by confocal microscopy (GFP-tagged constructs), or proceeding to protein extraction (HA-tagged constructs). For GFP visualisation, excitation was at 488 nm and light was reflected by a secondary NET 545 dichroic mirror. GFP fluorescence was collected as the light passed through a 505-530 broad pass filter. Long pass filter at 650 nm was used to allow collection of chloroplast autofluorescence (Chlorophyl fluorescence detected and rendered in the red channel).

2.6.6 Co-Immunoprecipitation experiments following transient expression in *N. benthamiana.*

For the Co-Immunoprecipitation experiments, the leaves of 4-5 weeks old *N. benthamiana* plants were infiltrated with mixed cell suspensions, which consisted of Agrobacteria harbouring either of the two constructs encoding for the proteins of interest. After 2 days, leaf discs were excised from the infiltrated leaves and were observed under the confocal microscope, in order to ascertain satisfactory expression of the GFP-tagged protein. If satisfactory signal levels were detected, 3-4 leaf disks were homogenized in 150 µl SDS loading buffer and boiled at 95°C for 10 min, before being centrifuged at full speed in a bench-top microcentrifuge. Following the latter step, 25 µl of the supernatant were subjected to SDS-PAGE and immunoblotting against the HA-epitope tag, in an attempt to assess the level of expression of the HA-tagged protein. If both putative interacting partners (the GFP-fused and the HA-fused proteins) were found to be satisfactorily expressed, the procedure was taken further to performing the GFP-immunoprecipitation.

To that end, protein was extracted from the infiltrated leaves, and quantified as described in Section 2.4.2.5. Subsequently, approximately 10 mg of total protein, topped up to 1ml final volume with IP wash buffer (same as protein extraction buffer but without the PVPP), were used for immunoprecipitating the GFP-fusion protein with 50 µl magnetic anti-GFP micro-beads (µMac beads, 130-091-370, Miltenyi Biotech). 1/10 of the amount used for IP was kept aside to serve as the input sample. The procedure was performed according to manufacturer's recommendations, with the following alterations: The magnetic microcolumn was equilibrated with 200 µl IP wash buffer, before the extract-micro beads mixture was applied on the column. Non-GFP tagged proteins were allowed to flow through the column, whereas the GFP-tagged proteins, together with any interacting proteins, were retained on the column via the magnetic interaction of a strong magnet with the micro-breads. The column was washed five times with 200 µl IP wash buffer. Elution was then performed as instructed in the kit's manual. The eluted material represents the IP sample. Eventually, Input and IP samples were subjected to SDS-PAGE and immunoblotting against GFP (IP signal) and HA (CoIP signal).

2.6.7 Cross pollination of Arabidopsis.

Crosses between different Arabidopsis mutants were carried out exactly as described elsewhere (Weigel and Glazebrook, 2005), with no deviations from the recommended procedure.

2.7 Chromatin Immunoprecipitation (ChIP)

The light treatments of plants and tissue harvesting prior to fixation have been described in Section 2.5.2.

2.7.1 Fixation and chromatin isolation

Approximately 2g of leaf tissue were immersed in 1% v/v formaldehyde and underwent a 15 min vacuum infiltration. Glycine was then added, in order to quench the fixation reaction, at a final concentration of 0.125 M, and allowed to penetrate the tissue by prolonging vacuum infiltration for 5 additional minutes. Subsequently, infiltrated tissue was washed with water, air dried to the best possible extent, and snap frozen in liquid N_2.

Frozen tissue was ground to very fine powder, which was resuspended in 30 ml of extraction buffer 1 {0.4 M sucrose, 10 mM Tris-HCl pH 8, 10 mM MgCl2, 5 mM β-mercaptoethanol, 0.1 mM PMSF, one tablet PI (Complete mini EDTA-free Roche)} and left horizontally on ice, under gentle agitation, for 15 min. Afterwards, the suspension was filtered twice through a double layer of miracloth, and the flow-through was centrifuged for 20 min at 3500g, 4 °C. The pellet was resuspended in 1 ml of extraction buffer 2 {0.25 M sucrose, 10 mM Tris-HCl pH 8, 10 mM MgCl2, 1% TritonX-100, 5 mM β-mercaptoethanol, 0.1 mM PMSF, PI (Complete mini EDTA-free Roche)}, and the resulting suspension was centrifuged 10 min at 16000g, 4°C. The new pellet was resuspended in 500 µl of extraction buffer 3 {1.7 M sucrose, 10 mM Tris-HCl pH 8, 2 mM MgCl2, 0,15% TritonX-100, 5 mM β-mercaptoethanol, 0.1 mM PMSF, PI (Complete mini EDTA-free Roche)}, and the suspension was carefully layered upon 500 µl of fresh extraction buffer 3. The resulting two-layered heterogeneous mixture was subjected to 1 h full speed (16000g) centrifugation in a bench-top centrifuge, at 4°C. The pellet was resuspended in 500 ml nuclei lysis buffer (50 mM Tris-HCl pH 8, 10 mM EDTA, 1% SDS, 0.1 mM PMSF and PI). 10 µl were put aside to serve later as non-sonicated chromatin sample. The remainder was subjected to sonication, in order to shear the chromatin, by repeating 5 times a {(15 sec ON - 10 sec OFF) x 1 min)} sonication cycle (Sanyo Soniprep150 sonicator). Samples were then centrifuged at full speed (16000g) for 10 min, 4°C, and the supernatant was transferred to a fresh tube. 10 µl of sonicated chromatin were run on an agarose gel along with the 10 µl non-sonicated aliquot saved on a previous step, in order to ascertain successful shearing of chromatin to fragments ranging between 200 - 800 bp.

2.7.2 Immunoprecipitation

20 μl of each sample were saved to be used as Input, whereas the remainder was diluted to 3 ml (or 2 ml if poorly performing antibody was to be used) with ChIP dilution buffer (16.7 mM Tris-HCl pH 8, 1.2 mM EDTA pH 8, 1.1 % Triton X - 100, 167 mM NaCl). Subsequently, 3 (or 2) equal volume aliquots (1 ml each) were transferred to clean microcentrifuge tubes. As a pre-clearing step, 50 μl of protein A-coated magnetic beads were added in each sample and the mixtures were left for approximately 2.5 h at 4 °C, under rotation. Afterwards, the magnetic beads were removed and 5 μl of the desired antibody were added in each sample intended to be an IP sample, whereas nothing was added to the remaining sample which would serve as the "No antibody" or "mock" control. All samples were left for O/N incubation, under low speed rotation, at 4 °C. On the following day, 50 μl of protein A-coated magnetic beads were added in every sample and incubation was allowed to continue for 1-3 additional hours.

2.7.3 Washes, elution of immunocomplexes, reversal of cross-links and DNA isolation

After binding to the chromatin-antibody immunocomplexes, the protein A-coated magnetic beads were subjected to four consecutive double washes of increasing stringency. First, a 5 min low salt wash (150 mM NaCl, 0.1% SDS, 1% Triton X-100, 2 mM EDTA pH 8, 20 mM Tris-HCl pH 8) was performed twice, followed by two repeats of a 5 min high salt wash (500 mM NaCl, 0.1% SDS, 1% Triton X-100, 2 mM EDTA pH 8, 20 mM Tris-HCl pH 8). Subsequently, a double 5 min wash with LiCl washing buffer was performed (0.25 M LiCl, 1% Na-deoxycholate, 1% Nonidet-P40, 1mM EDTA, 10 mM Tris-HCl pH 8), and finally two 5 min washes with TE washing buffer (10 mM Tris-HCl pH 8, 1 mM EDTA pH 8) were carried out. The immunocomplexes were then eluted twice from the magnetic beads, by suspending the latter in 250 μl elution buffer (1% v/v SDS, 0.1 M $NaHCO_3$) and incubating for 15 min at 65 °C. Meanwhile, 480 μl of elution buffer had been added to the 20 μl of Input chromatin saved on a previous step, and 20 μl 5 M NaCl were added in all samples (Input and eluted IPs). Cross-links were reversed by O/N incubation at 65 °C. On the following day, 30 μl Proteinase K solution (20 μg proteinase K in 10 μl 0.5 M EDTA and 20 μl 1 M Tris-HCl pH 6.5) were added to every sample and they were incubated 1 h at 45 °C. The DNA was recovered by Phenol-Chloroform extraction (Section 2.4.2.2.).

Ethanol precipitation was performed in the presence of 1 μl glycogen, pellets were washed with 75% ethanol, air dried and resuspended in 50 μl dH_2O.

2.7.4 qPCR analysis of immunoprecipitated DNA

The recovered DNA was analysed via quantitative real-time PCR (Applied Biosystems StepOnePlus) employing absolute standard curve-mediated quantification. To that end, the PCR products of each primer pair were subcloned in the pCR2.1 TOPO vector (or pCR4 TOPO, both from Life technologies) according to the manufacturer's instructions. Seven serial 1/10 dilutions of each construct, with the highest concentration being 10 pg/μl of plasmid, were analysed invariably on every qPCR plate, for the purpose of generating a 7 points standard curve, from the slope of which a satisfactory 95-105% efficiency of amplification was ascertained. The equation of the standard curve was used to ascribe a DNA quantity to each obtained Ct value, provided that the latter would not be higher than the Ct obtained from the most diluted standard sample, and from that quantity an absolute target copy number could be calculated. All samples were run in two technical replicates on every plate. Moreover, a dissociation curve was performed after every run, in order to assess whether the obtained fluorescence signals (particularly of high Ct values) corresponded to the desired product and not to accumulation of primer dimers or unspecific products. The cycling conditions, identical for all target sequences, were the following : 95 °C 2 min, (95 °C 10 sec, 62 °C 30 sec) x 40 cycles. For the melting curve, products were denatured at 95 °C for 1 min, allowed to re-anneal at 60 °C for 30 sec, and then the temperature was gradually raised up to 95 °C, with data collection at every + 0.3 °C increment.

In order to express the relative enrichment of a specific histone mark over a particular genomic locus of interest, a double normalisation approach was employed (Morohashi et al., 2009), according to which the IP DNA quantity was first normalised against the corresponding Input DNA quantity (% of Input) and the obtained ratio was afterwards normalised against the similar ratio obtained with a reference primer set (either *ACTIN2* or *UBQ5*). Therefore the final normalisation was done using the formula

$$\frac{(ChIPedDNA_{target} / InputDNA_{target})}{(ChIPedDNA_{reference} / InputDNA_{reference})}$$

Independent biological ChIP experiments were always performed with the same lot of extraction buffers and solutions, and, whenever possible, the recovered DNA was analysed with the same qPCR master mix, to reduce the risk of added, technical in its origin, variation. Nevertheless, as ChIP experiments tend to be inherently highly variable, results were presented with standard deviation (SD) error bars, which emphasise variability and have been proposed to be more appropriate in reporting quantitative ChIP data (Struhl, 2007). Two tailed Student's t-tests, resulting in p values, were employed to assess statistical significance between pairs of values, with the p value threshold representing the lowest acceptable confidence limits being set to $p < 0.1$ (Guo et al., 2008). When it was suspected that a combined effect of differential light treatments and different genotypes might be at play, two way ANOVA was performed to address such possibilities. Statistical analysis was performed with Wizard (Version 1.5.1 (101) available from Apple store).

2.8 Yeast Two Hybrid (Y2H) and Yeast Three Hybrid (Y3H) assays

Y2H assays were performed in the AH109 yeast strain whereas the Y3H assays were performed either with AH109 or Y2HGold yeast strains.

For Y2H, yeast competent cells preparation and subsequent transformations with pGBKT7 and pGADT7 constructs were carried out as described in Owerkerk and Meijer 2001 and 2011. Five to seven distinct large colonies (2-4 mm) were picked from each plate of transformed yeast and were pooled together in a 30 ml universal tube containing 5 ml of liquid SD-L-W supplemented with 50 μg/ml kanamycin. Universal tubes were then incubated O/N at 30 °C with rigorous shaking (250 rpm). On the next day, the OD_{600} value of each liquid culture was measured, 2 ml were set aside for protein extraction, and 1 ml was harvested by spinning down the cells in a bench top microcentrifuge for 30 sec at maximum speed. The supernatant was removed and the cells were washed by resuspending in 1 ml of sterile dH2O. Cells were then pelleted again (30 sec max speed) and resuspended in adequate volume of 1x TE buffer, calculated from the OD_{600} value of the original culture, so that for the resulting yeast suspension $OD_{600}=1$.

Two 1/10 serial dilutions of every yeast suspension were prepared and 8 μl were immediately spotted on the different plates along with 8 μl of the undiluted sample. Non selective SD-L-W plates were used as a control for the viability of the spotted yeast. Low stringency SD-L-W-H plates were used to detect weak interactions and high stringency

SD-L-W-H-A plates were employed for detection of stronger interactions. All media were supplemented with 50 μg/ml kanamycin as a precaution against bacterial contamination. After spotting, the plates that were supposed to remain in darkness were wrapped with tin foil and all plates were transferred in a 30 °C incubator under 0.1 μmol m^{-2} s^{-1} of narrowband UV-B light. Photographs of yeast were taken with a Nikon COOLPIX100 digital camera after 48 h (SD-L-W) , 72 h (SD-L-W-H) and 96 h (SD-L-W-H-A).

For protein extraction, the 2 ml culture saved in an earlier step was spun down, full speed (16000g), with a bench-top microcentrifuge and the pellet was resuspended (100 μl for OD_{600}=1) in Lyse and Load buffer (50 mM Tris-HCl pH 8, 4% SDS, 8 M Urea, 30% Glycerol, 0.1 M DTT, 0.005% w/v Bromophenol blue). The resulting suspension was incubated at 65 °C for a period of 1 h, after which cell debris were spun down and 20 μl of the supernatant were loaded on gels for SDS - PAGE and subsequent immunoblotting.

For the Y3H assays the experimental procedures were essentially the same, with minor adjustments to meet the auxotrophic and selection requirements which are specific to the assay. The most important change is that AH109 cells and Y2HGold cells were maintained for 2 weeks in methionine lacking medium, before being used to produce competent cells, as they tend to lose their capability to survive without externally provided Met unless regularly subjected to such selective pressure. If AH109 cells were used, the selection for interactions was applied with SD-L-W-M-H media, whereas if Y2HGold cells were used a slightly more stringent selection could be applied (SD-L-W-M-H +Aureobasidin).

2.9 Yeast One Hybrid (Y1H) Screen

The Y1H screen was performed by using a "Mate & Plate Library - Universal *Arabidopsis* (Normalized)" (Clontech, Cat # 630487), which has been engineered by Clontech, primarily to be used with the "Matchmaker GAL4 Two Hybrid systems". According to the manufacturer's description, this yeast two-hybrid library has been constructed from mRNA isolated from 11 *Arabidopsis* tissues, mixed in equal quantities and transformed into the yeast strain Y187, using the pGADT7 recAB plasmid as vector (Leu selection marker in yeast). The cDNA was normalized prior to library construction, in order to reduce the copy number of abundant cDNAs derived from highly represented mRNAs, thereby increasing the representation of low copy number transcripts. The normalization process has been performed in a way that reduces the number of clones that must be screened, thereby facilitating the identification and characterization of novel protein-protein interactions. As the Y187 strain is of the *MAT***a** mating type, this library can readily be mated with a *MAT****a*** GAL4 reporter strain, such as AH109 or Y2HGold, for screening. This latter particular characteristic was taken advantage of, in order to modify a standard one - hybrid screening protocol (Ouwerkerk and Meijer, 2001; Ouwerkerk and Meijer, 2011) by introducing a mating step which brought "bait" DNA and "prey" proteins in the same (diploid) cell, thereby extending the suitability of the library to include one-hybrid applications (Lopato et al., 2006; Pyvovarenko and Lopato, 2011). A detailed account of the steps involved in the screening procedure is given in the following sections.

2.9.1 Generation of yeast reporter strains and assessment for background growth

Three "bait" DNA sequences were synthesised (Genscript, USA), each corresponding to tandem repeats of defined *cis*-regulatory elements of the *HY5* promoter. The "bait" DNAs were designated b1, b2 and b1.2, and their sequences were :

b1 : GCGGCCGCATCTAACGGCTAAATCTAACGGCTAAATCTAACGGCTAAACTAGT
b2 : GCGGCCGCCCCACGTTCCCCCACGTTCCCCCACGTTCCACTAGT
b1.2 : GCGGCCGCATCTAACGGCTAAAATCCACCCACGTTCCATCTAACGGCTAAAATCCACCCACGTTCCACTAGT.

Each "bait" was cloned in the *Not*I-*Spe*I sites of the pINT1-HIS3NB (GenBank accession AY061966) binary (shuttle) vector, located conveniently in front of a minimal

promoter containing the TATA box transcription start site and a *HIS3* reporter gene that follows immediately. Recombinant pINT-HIS3NB vectors carrying the desired baits were sequenced, after which linear fragments of interest were excised via a double restriction digestion with *Nco*I and *Sac*I. The resulting linearised sections represented the so called "integration fragments", because they contained, apart from the "bait-reporter" system, additional sequences important for integration into the yeast genome and subsequent selection (Fig 2-2).

Fig 2-2 Integration fragments resulting from the digestion of pINT-HIS3NB with *Nco*I and *Sac*I. At an approximate distance of 1.7 Kb downstream of the "bait-*HIS3* reporter" system follows the dominant selection marker gene *APT1,* which confers resistance to the antibiotic Geneticin G418. The "bait-*HIS3* reporter" - *APTI* cassette is flanked on either side with sequences derived from the yeast *PDC6* gene locus, which is non-essential for survival. It is via these sequences that a double-crossover - mediated homologous recombination event occurs, resulting in the integration of the "bait-*HIS3* reporter" system into the yeast genome and the generation of a "yeast-reporter" strain.

100 - 500 ng of integration fragment were transformed in competent AH109 yeast cells, according to the protocols described in (Ouwerkerk and Meijer, 2011) without any alterations. The cells were plated on YAPD medium supplemented with 150 mg/ml G418, and colonies were obtained after 3-4 days. Colony PCRs were performed on putative transformants using appropriate primers (Table 2.2) to verify successful integration, and the PCR products were sequenced to validate the generation of yeast - reporter strains harbouring error - free "bait" sequences. Finally, these yeast reporter strains were assessed for background, leaky growth, by streaking on His-lacking medium supplemented with increasing concentrations of 3-amino-1.2.4-triazole (3-AT).

2.9.2 Mating of yeast-reporter strains with the universal, normalised, Mate & Plate Arabidopsis Library. Calculation of the number of screened clones

One large (2-3mm) colony of the desired "bait-reporter" strain (AH109) was inoculated into 50 ml of G418 containing liquid YPDA medium (1% w/v yeast extract, 2% w/v peptone, 2% w/v Bacto agar, 2% w/v glucose, 20 mg/l adenine hemisulfate). The culture was incubated under rigorous shaking (250 rpm) at 30 °C until OD_{600} = 0.8. Cells were pelleted at 1000g for 5 min and the pellet was resuspended in 4-5 ml YPDA (= 1 x 10^8 cells / ml).

1ml of library strain (Y187) was thawed in a room temperature water bath, and 10 µl were removed for titering on SD - L plates. To that end, 1/100, 1/1000 and 1/10000 dilutions were prepared and spread onto SD - L plates. Colony forming units (cfu) were counted 3 days later, and the titer of the library was determined (should be ≥ 2 x 10^7 cells / ml , for a healthy library aliquot). The thawed library aliquot was combined with the 4 - 5 ml of "bait-reporter" strain in a sterile 2 l flask, and 45 ml of 2 x YPDA were added (with 50 µg / ml kanamycin to prevent contamination from bacteria). The cells from the library vial were rinsed twice with 1 ml 2 x YPDA and the rinses were added to the 2 l flask. This "mating culture" was incubated at 30 °C for 24 h, under slow shaking (40 rpm). After approximately 20 h, a droplet of the culture was checked under the microscope (40 X magnifying lens) for the presence of zygotes, the morphology of which is shown in Fig. 2-3. If zygotes were present, the entire culture was spun down (1000 g for 10 min). Meanwhile, the 2 l flask was rinsed twice with 50 ml 0.5 x YPDA (with 50 µg / ml kanamycin), the rinses were combined and used in the next step to resuspend the cell pellet. The cell suspension was then centrifuged again (1000 g for 10 min), the supernatant was discarded, and all pelleted cells were resuspended in exactly 10 ml of 0.5 x YPDA + Kan medium. The total volume of the cell suspension was measured and recorded.

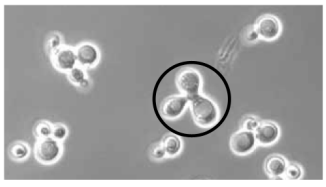

Fig 2-3 Microscopic identification of zygotes. A diploid cell in the process of dividing is encircled. *(Adapted from Matchmaker Y2Hgold Y2H system user manual)*

From the mated cells suspension, 100 μl of 1/10, 1/100, 1/1000 and 1/10000 dilutions were spread on Kan^+ agar plates containing either of the following: a) SD-L (selection for prey + diploids viability), b) YPDA + G418 (selection for bait + diploids viability), or c) SD-L + G418 (selection for diploids-only viability). The plates were then incubated at 30 °C for 3-4 days. The remaining mated-cells suspension was plated on SD-L-H + Kan + G418 + 7.5 mM 3AT large petri dishes (200 μl plated on each petri dish) and the plates were transferred in a 30 °C incubator for 10-14 days.

The number of screened clones was calculated by the number of viable diploid cfu, counted on the SD-L+G418 selective plates, and extrapolated to the entire volume of the mated-cells suspension. The mating efficiency was calculated by expressing the viability of the diploid cfu as a % ratio of the viability of the limiting mating partner (which is either the "bait" or the "prey", depending on which one gave the least viable cfu).

2.9.3 First round of elimination of false positive clones

After 10 - 14 days of incubation, putative positive clones outgrowing a background of small leaky-growth colonies could be clearly seen on the fully selective screen plates. All those clones were picked with sterile toothpicks, re-streaked on plates with identical selective medium supplemented with X-α-Gal, and returned to the incubators for another 10-14 days. After this period, a substantial number of clones were turning blue in colour, as a result of the hydrolysis of X-α-Gal in the medium, mediated by the activity of α-galactosidase. The latter, in the AH109 yeast strain, and, after the mating by necessity in the diploid screened cells as well, is encoded by the *MEL1* reporter gene which is under the transcriptional control of GAL4-responsive **U**pstream **A**ctivating **S**equences (UAS). Thus, only if a TF is not recognising specifically the plant-derived "bait" of interest, but is also binding to the UAS elements preceding *MEL1,* would the respective clone turn blue in colour. Therefore, all blue clones were discarded as false positives.

2.9.4 Plasmid rescue from the putative positive white clones, PCR and sequencing

Following the blue-white selection, colony PCR was performed on the white clones. A small quantity of cells was scrapped off the clones and resuspended in 30 µl of SPZymo Buffer (0.1 M potassium phosphate, 1.2 M sorbitol, 2.5 mg / ml zymolase 100T). The suspension was incubated for 30 min at 37°C, following by a zymolase-killing step at 95 °C for 5 min. At this stage the yeast cell wall had been degraded by zymolase leaving a large population of spheroplasts. 1 µl was used for PCR with proofreading polymerase and primers flanking the cloning sites of the library cDNAs in the pGADT7-RecAB vector, and the PCR products were sent for sequencing. Sequencing results were aligned with the annotated Arabidopsis genome and the identity of each cDNA clone was obtained.

In an alternative approach, undertaken only for a few clones that failed to give PCR products, 10 ml of SD-L + G418 medium were inoculated with cells from a single clone and incubated at 30 °C until OD_{600} =1. Subsequently the cells were pelleted, resuspended in 200 µl P1 buffer from the QIAGEN Qia-prep Spin Miniprep kit (Cat # 27104), and treated with 100 µl zymolase. The resulting spheroplasts were subjected to alkaline lysis, according to instructions in the kit's protocol. The recovered plasmids were sequenced, and the identity of the Arabidopsis cDNA insert was revealed.

2.9.5 Confirmation of Y1H interactions

Among the identified clones, those which represented annotated Arabidopsis transcription factors were considered of potential interest for further analysis. For the purpose of confirming the interactions with the "bait" DNAs of interest, all interesting TFs were cloned in the pGADT7 vector, full length and in frame with the GAL4-AD. Meanwhile, new yeast-reporter cells were prepared in the Y187 yeast strain, according to the procedures already described. Furthermore, three additional yeast-reporter cells were generated, which carried mutated versions of the "bait" DNAs used during the screens. All yeast-reporter strains ("baits" of interest and mutated "baits"), generated in the Y187 yeast strain, were tested for background growth on HIS-lacking media

supplemented with rising concentrations of 3-amino-1.2.4-triazole (3-AT). Eventually, once the minimum 3-AT concentration required to suppress leaky growth was established for every individual yeast-reporter strain, transformations with the pGADT7-TFs constructs were performed and the direct Y1H assays were carried out. The purely technical aspects of the assays are identical to those described for Y2H, with proper adjustments for auxotrophic requirements and selection media.

The sequences of the mutated “bait” DNAs were the following :

mb1 : GCGGCCGCATCGCCATTATAAATCGCCATTATAAATCGCCATTATAAACTAGT
mb2 : GCGGCCGCAAACATGGAAAAACATGGAAAAACATGGAAACTAGT
mb1.2 : GCGGCCGCATCGCCATTATAAAATCCAAAACATGGAAATCGCCATTATAAAATCCAAAACATGGAAACTAGT

CHAPTER 3 : INVOLVEMENT OF UVR8 IN THE EPIGENETIC CONTROL OF GENE EXPRESSION

3.1 Introduction

One important aspect of the physiological role of UVR8, downstream of the photo-sensory event, is the regulation of transcription of a diverse set of genes. An initial study demonstrated, via microarray analysis, that the expression of over 70 genes is stimulated in a UVR8-dependent manner in the leaves of UV-B treated Arabidopsis plants (Brown et al., 2005). A subsequent work, using whole seedlings and a narrow band UV-B source, expanded the catalogue of UVR8-regulated genes to several hundreds (Favory et al., 2009). Such large-scale changes in the transcriptomic profile, when occurring in response to a single stimulus, are usually preceded by processes that affect the dynamic state of chromatin in the nucleus. Alterations in the methylation status of DNA, rearrangements of the positions of nucleosomes, changes in the covalent modifications of protruding histone tails, are all common phenomena which ensure that the DNA will remain in a loosely packed euchromatic state. Thus, the access, assembly and function of the transcriptional machinery on the target genetic loci is greatly facilitated. One of the main goals of our research was to investigate whether UVR8 is implicated in chromatin remodelling processes, when it exerts its regulatory function after sensing UV-B light. The principal focus was on the histone modifications facet of chromatin plasticity, because prior research had already provided some interesting initial findings (Casati et al., 2008; Cloix and Jenkins, 2008). ChIP-qPCR was employed to validate and expand the previous observation that UV-B might be linked to the deposition of acetyl moieties on lysines K9 and K14 of histone H3 (H3K9,14diac). Subsequently, in an attempt to identify other histone marks, whose accumulation on certain genetic loci might be regulated in a UVR8-dependent manner during photomorphogenic UV-B responses, a narrowed down list of potential candidates was formulated based on published literature on genome-wide epigenetic mapping. Such studies had revealed that certain histone modifications tend to co-appear in some epigenetic landscapes, whereas others tend to be mutually exclusive (Charron et al., 2009; Roudier et al., 2011; Zhang et al., 2009)

We chose to perform ChIP assays using antibodies against H3K4me3, H3K9me3, H3K36me3 and H3K56ac, all of which mark actively transcribed euchromatin. In addition, as UVR8 has been shown to associate preferentially with histone H2B, it was decided to examine whether it affects monoubiquitination of H2B, a modification recently shown to be involved in photomorphogenesis (Bourbousse et al., 2012). As a control, for the purpose of ascertaining that any observed differences in ChIP signals can be safely attributed to differential enrichment levels, rather than altered nucleosome densities caused by the UV-B treatment, ChIP assays using an antibody against an invariant domain of histone H3 were performed. Specific UVR8-dependent UV-B induced genes, such as *CHS, ELIP.1, HY5* and *HYH,* were focused on during the qPCR analysis of the immunoprecipitated DNA. *ACT2* and/or *UBQ5* were used as reference genes for normalisation of the amount of ChIPed material. *WRKY30*, a gene induced through stress-related UVR8-independent UV-B responses, was chosen as a control intended to demonstrate that the threshold separating the photomorphogenic from the stressful stimulus was not exceeded during the UV-B treatments. Finally, since all the histone modifications under investigation are known to be marking euchromatin, a genomic region located close to the centromere of chromosome 4, which is usually tightly packed in a heterochromatic state, was utilised as a technical negative control for the ChIP-ing procedure.

3.2a UV-B does not cause ChIP - detectable changes in nucleosome density on the genetic loci of the assayed genes.

The structural organisation of eukaryotic genomes is of a highly dynamic nature, which enables the organisms to respond promptly to varying endogenous and exogenous stimuli. The nucleosomes, being the structural units of chromatin, are the usual targets of "chromatin remodelling" events. The modifications that take place are not only chemical in nature. Local displacements, re-positioning and even complete dissociation from DNA, leading to altered nucleosome density in the respective genetic locus, are commonly documented upon transcriptional activation. In *Saccharomyces cerevisiae,* nucleosome depletion has been reported at active regulatory regions on a genome-wide scale. Revealingly, the most heavily transcribed genes were found to display partial loss of H3 and H4 tetramers from their coding regions (Lee et al., 2004). In a recent study on mouse and human embryonic stem cells, nucleosome occupancy was found to undergo local changes around regulatory regions during cell differentiation and reprogramming (West et al., 2014). In plants these phenomena have yet to be addressed with similar rigour. Nevertheless, it has been reported that the density of H2A.Z-containing nucleosomes is a core feature of the thermo-sensory mechanism of Arabidopsis (Kumar and Wigge, 2010), which is probably evolutionarily conserved since similar observations were also made for budding yeast. Temperature is, therefore, an example of an environmental signal that induces changes in nucleosome occupancy, which plants have evolved to utilise in order to monitor their surroundings and modify their physiology and development accordingly. On the basis of the above information, it was a serious concern that transcriptional responses to UV-B might be accompanied by locus specific, if not genome-wide, UVR8-dependent alterations in nucleosome density. As interesting a finding as this might be on its own, it would pose a hurdle in the subsequent ChIP analysis. It would be difficult to distinguish whether the observed differences in the immunoprecipitated material indicate differential enrichments in specific histone modifications, or whether they result from differences in nucleosome occupancy. For that reason, ChIP experiments using antibody against an invariant domain of histone H3 were performed (Fig 3-1). UV-B treatment and the overall

experimental set up was essentially identical to the one followed when antibodies against various histone modifications were used. The results revealed no ChIP-detectable differences of the nucleosome density in the genetic loci of interest, when control and UV-B light treatment conditions we compared. Thus, at least under our particular experimental set up, any differences in signals obtained via histone mark - specific antibodies can be confidently accredited to actual differences in the enrichment in the corresponding modifications. It should be noted, however, that nucleosome occupancy may be assayed via alternative, more direct approaches, and it is possible that differences which lie below the sensitivity of the ChIP approach might still be present.

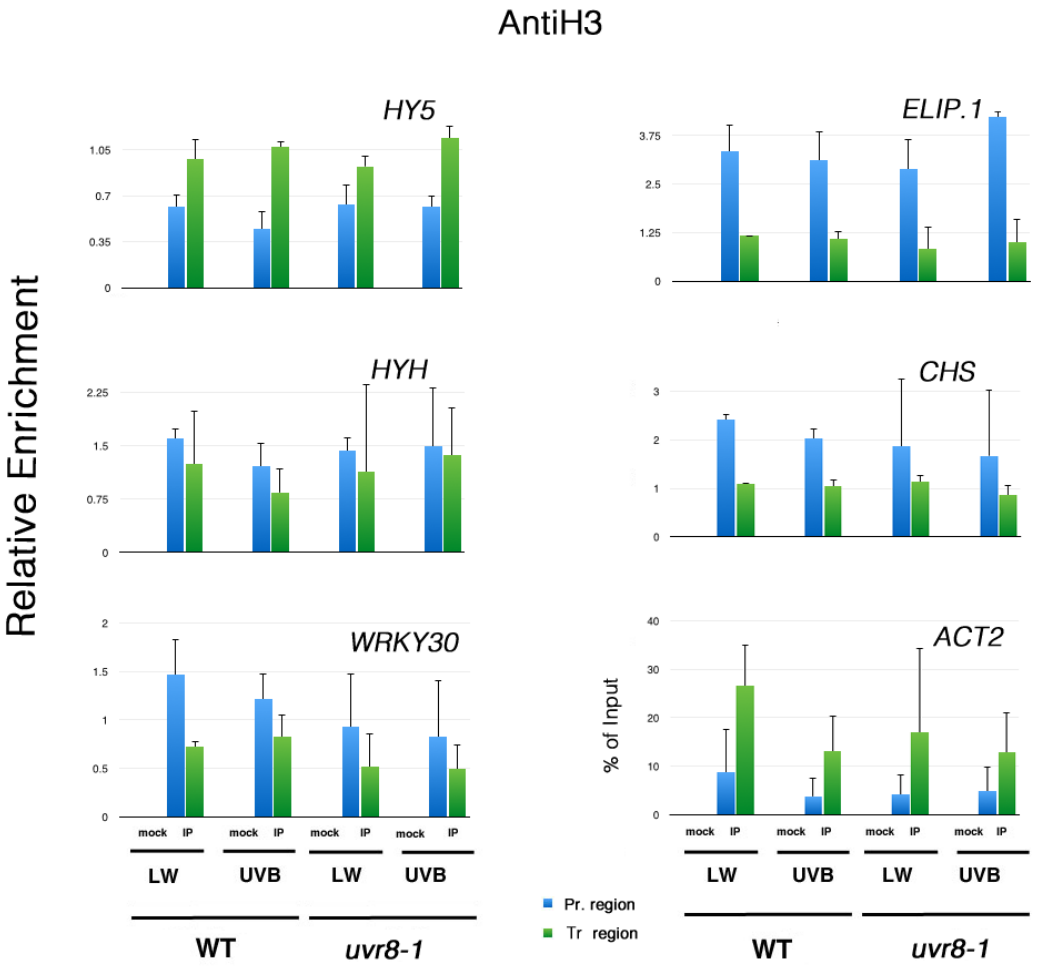

Fig. 3-1 : UV-B does not cause ChIP - detectable alterations in nucleosome density in the assayed genetic loci. Each graph displays the relative enrichment over promoter (blue) and transcribed region (green) DNA of the designated genes, expressed as % of Input normalised against *ACT2*. For *ACT2* itself, no normalisation was performed and enrichment is given as % of Input. Wt and *uvr8-1* plants were exposed to UV-B or control light treatments. LW: low fluence rate white light (15 µmol m^{-2} s^{-1}). UVB: 1.5 µmol m^{-2} s^{-1} narrow band UV-B for 4h. Mock: No Ab control. IP: Immunoprecipitated material. Error bars represent SD from two independent experiments.

3.2b A sequence known to appear exclusively in heterochromatin was not present in the immunoprecipitates recovered by any of the used antibodies

Although the majority of the antibodies used in this project were purchased from commercial suppliers and were accompanied by quality assurance documentation, none was raised against plant-specific immunogens and many were derived from polyclonal sera. This feature facilitates the detection of low abundance targets, as more than one epitopes are recognised by the antibody, but might also decrease specificity. Moreover, different antibody batches have distinct properties, which might affect performance under the experimental conditions followed during the ChIP protocol. For example, the input chromatin sample might have a high concentration of inhibitory factors, which could either decrease the efficiency of epitope binding, or they might favour unspecific interaction with non-target substrates (Haring et al., 2007). As the optimum performance of the antibodies is the most crucial factor for a successful ChIP, it was decided to perform control experiments which would assure that non-target chromatin is not recovered in the immunoprecipitated material. For this reason, chromatin preparations were made from 3 weeks old WT plants grown under low fluence rate white light. Subsequently, ChIP experiments were performed with all the antibodies and the recovered DNA was analysed via qPCR for the presence of two sequences (Fig 3-2). One, designated as +ve control, corresponded to either *ACT2* or *UBQ5,* which are two genes that were used for normalisation of the IP signals in subsequent ChIPs, and were expected to harbour detectable levels of the corresponding histone modifications. The second sequence, designated as *CEN4,* was derived form a region close to the centromere of chromosome 4, for which published information has revealed that the histone modifications of interest are practically absent (Roudier et al., 2011). The results confirmed that for all tested antibodies the unspecific precipitation is negligible relative to the signal that corresponded to the +ve control sequences. In the case of the anti-H2Bub antibody, which was not from a commercial supplier and was therefore not accompanied by quality assurance documentation, less stringent washes were employed during the ChIP protocol, in an attempt to increase a potentially low signal. This led to an increase of *CEN4* DNA, relative to the +ve control DNA, in the IP samples.

Nonetheless, the *CEN4* IP signal was comparable to the one recovered in its mock counterpart, which was not the case for the +ve control IP.

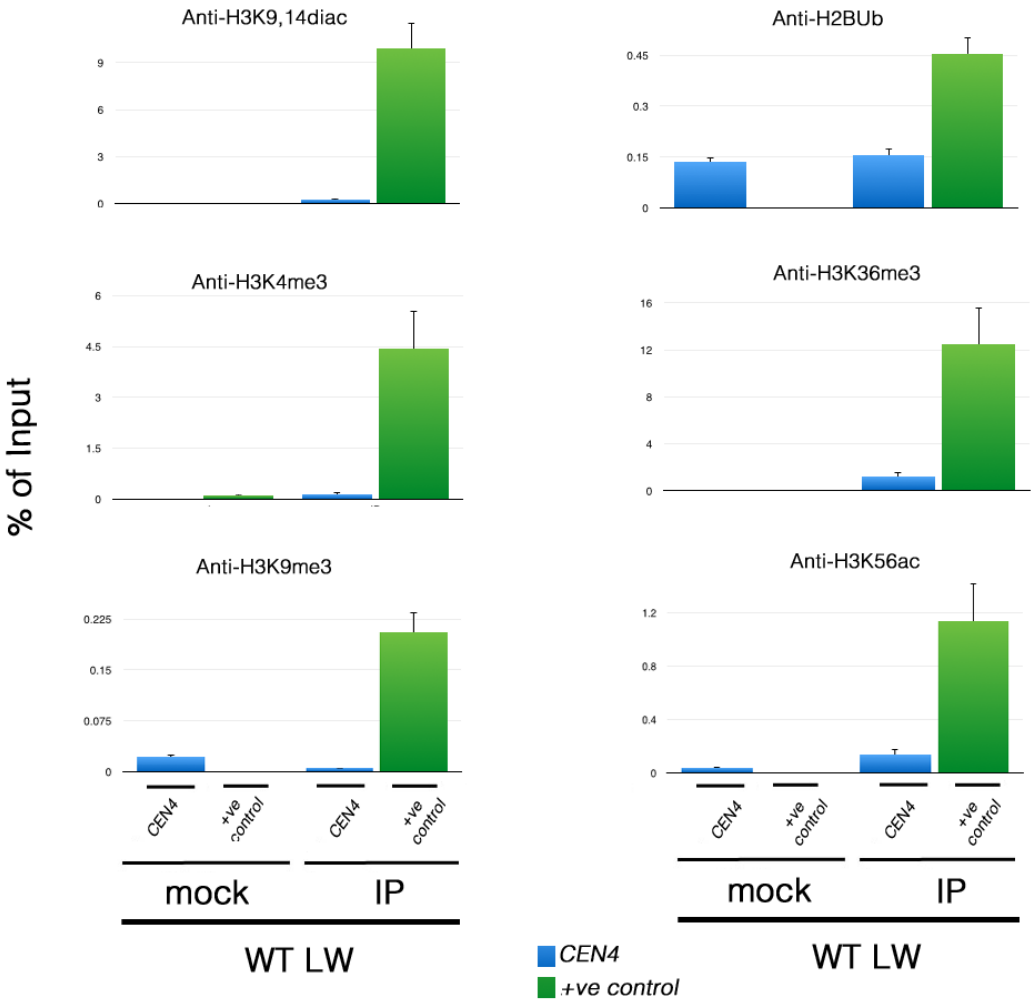

Fig. 3-2 : Non-target chromatin is not present in the immunoprecipitates.
Each graph displays the enrichment for the designated histone marks, presented as % of Input, over two sequences; a heterochromatin-associated centromeric sequence, *CEN4* (blue) and a +ve control sequence (green). The +ve control sequence was *UBQ5* for H3K9me3 and *ACT2* for the rest. Experiments were performed only for WT plants under low fluence rate white light (LW) 15 µmol m^{-2} s^{-1}. Mock: No Ab control. IP: Immunoprecipitated material. Error bars represent SD from two independent experiments.

3.3 UVR8 affects the acetylation status of lysines K9 and K14 of histone H3, on the chromatin of some UVR8-regulated UV-B-responsive genes

In agreement with numerous studies in plants, which have highlighted the major role of histone acetylation in the epigenetic control of transcription (reviewed by Ma et al., 2013 and Boycheva et al., 2014), Cloix and Jenkins reported that H3K9,14diac might be involved in the regulation of transcription by UV-B radiation (Cloix and Jenkins, 2008). However, since only WT plants were assayed, no conclusion could be drawn for the possible involvement of UVR8. Moreover, the immunoprecipitated material was analysed via end-point PCR which, although useful for "yes or no" answers, can potentially be very misleading if relied upon for comparative statements. In order to consolidate and extend the initial findings, three weeks old WT and *uvr8-1* mutant plants, grown since germination under low fluence rate white light (LW), were transferred to 1.5 μmol m^{-2} s^{-1} UV-B for 4h. Chromatin was immunoprecipitated with antibody recognising H3K9,14diac and the recovered DNA was analysed via real time qPCR, as described in detail in the "Materials and Methods" section. For each gene, sequences from the promoter as well as the transcribed region were assayed for enrichment. Results are summarised in Fig 3-3, with SD error bars, which highlight the variability between independent experiments and have been suggested as more suitable for presenting quantitative ChIP data (Struhl, 2007).

In partial consonance with the findings of Cloix and Jenkins, the promoter region of *ELIP. 1,* but not of *HY5, HYH* or *CHS,* was found to be significantly enriched in H3K9,14diac after UV-B exposure of the WT plants. No such response was monitored for the *uvr8-1* mutants. For the increase in signal on the *ELIP.1* promoter a Student t-test revealed $p = 0.09$, whereas for the *HY5, HYH* and *CHS* promoters the p-values were found to be higher than the threshold of 0.1 (*HY5* $p = 0.17$, *HYH* $p = 0.14$, *CHS* $p = 0.2$). The threshold of $p < 0.1$ is not common in scientific practice, but because of the inherent variability of ChIP assays, it has been used to claim significance over quantitative ChIP results with the lowest acceptable confidence limits (Guo et al., 2008). It is worth mentioning, however, that H3K9,14diac levels over the *HY5, HYH* and *CHS* promoters were consistently higher in UV-B-irradiated WT plants compared to plants kept under control light conditions. Similar trend was not observed for *uvr8-1* plants. It is therefore possible that variation between

individual experiments may have masked a mild but biologically important difference, which would only occur as statistically significant after many repetitions.

Regarding the transcribed regions, only WT plants exhibited significant increase in enrichment levels after UV-B treatment, over the loci of *HY5* ($p = 0.08$), *ELIP.1* ($p = 0.02$), *HYH* ($p = 0.04$) and *CHS* ($p = 0.02$). No similar observations were made for *uvr8-1* plants. As expected, both WT and *uvr8-1* behaved in similar fashion when *WRKY30* was assayed. Collectively, the results suggest that an intact UVR8 protein is required for the UV-B-induced accumulation of H3K9,14diac over the assayed genetic loci, and imply a novel mechanism of action of UVR8 during photomorphogenic UV-B responses.

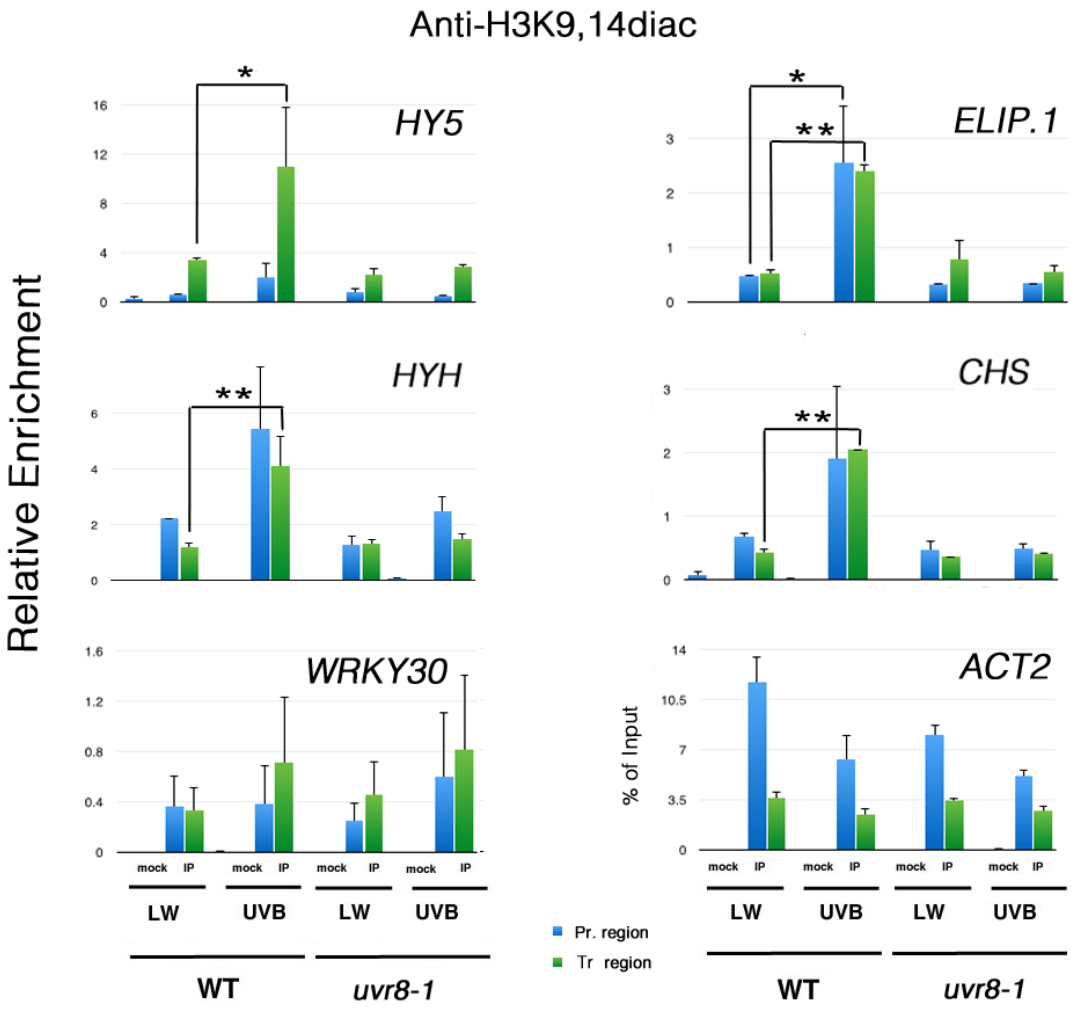

Fig. 3-3 : UVR8 affects the acetylation status of lysines K9 and K14 of histone H3. Each graph displays the relative enrichment in H3K9,14diac for both WT and *uvr8-1,* on promoter (blue) and transcribed regions (green) of the designated genes. LW: low fluence rate white light (15 µmol m^{-2} s^{-1}). UVB: 1.5 µmol m^{-2} s^{-1} narrow band UV-B for 4h. Mock: No Ab control. IP: Immunoprecipitated material. Results are expressed as % of Input normalised against *ACT2*. For *ACT2* itself, no normalisation was performed and enrichment is given as % of Input. Error bars represent SD (n=3). * $p < 0.1$; **: $p < 0.05$

3.4 UVR8 has no effect on either monoubiquitination of H2B or trimethylation of lysine K4 of histone H3 at the assayed genetic loci

According to the initial articulation of the "histone code hypothesis", distinct post-translational modifications of the histone tails could act either sequentially or in combination to regulate downstream processes (Strahl and Allis, 2000; Jenuwein and Allis, 2001). As refined tools for genome wide approaches became increasingly available, numerous studies have highlighted the importance of directing research towards elucidating the functional significance of the crosstalk among co-existing histone marks (Schwammle et al., 2014). After obtaining the first results with H3K9,14diac, it was desirable to investigate the possibility of UVR8 being important for the presence of other modifications existing in parallel. Since UVR8 is known to associate preferentially with histone H2B, one intriguing option was to check whether monoubiquitination of H2B is an important histone modification in UV-B responses. In addition, it is still unclear whether the interaction with COP1 has any functional significance for the association of UVR8 with chromatin. COP1 is an E3-ubiquitin ligase which has been suggested to be capable of modulating its substrates' activity, besides solely targeting them for degradation (Yan et al., 2011). Hence, it was intriguing, albeit probably slightly over-ambitious too, to speculate that COP1 might be involved in H2B monoubiquitination. H2Bub has been shown to be related to actively transcribed genes during photomorphogenesis (Bourbousse et al., 2012) and has also been reported to have high association with H3K4me3 along the Arabidopsis genome (Roudier et al., 2011). Moreover, H3K4me3 has been shown to significantly correlate with H3K9ac on the same loci, suggesting a mechanism of controlling gene expression changes via coordinated deposition of distinct histone marks (Ha et al., 2011) (Jang et al., 2011). Hence, ChIP experiments were performed with antibodies targeting these two modifications (Fig 3-4 and Fig 3-5). The results showed that although both histone marks were detectable at the genetic loci of interest, no significant differences were observed between WT plants and *uvr8-1* mutants when the enrichment levels of LW and UV-B treated plants were compared. The findings suggest that low fluence rate photomorphogenic UV-B, detected by the UVR8 photoreceptor, has no regulatory

impact on the deposition and/or dissipation of either H2Bub or H3K4me3 on the genetic loci of interest, at least under the conditions that define our experimental design.

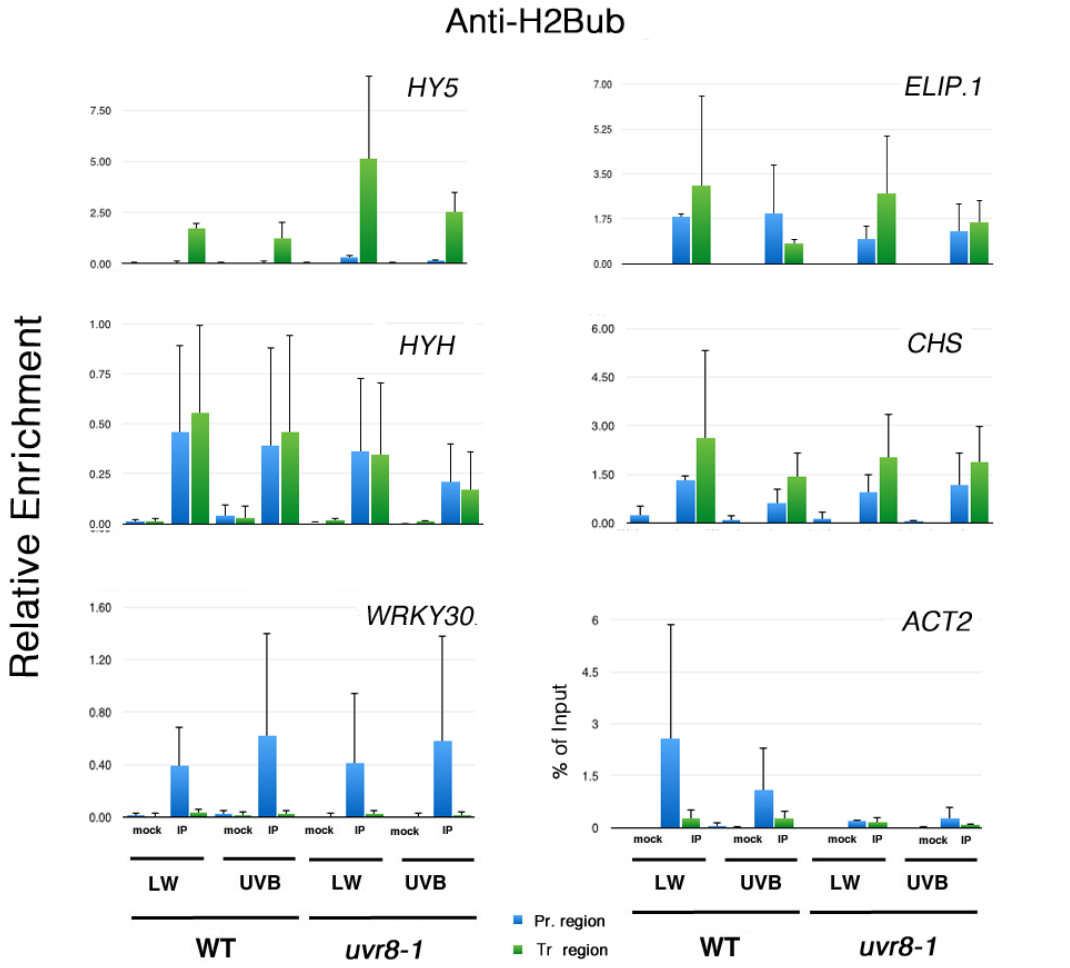

Fig. 3-4 : Results of ChIP with Anti-H2Bub antibody. Each graph displays the relative enrichment in H2Bub, for both WT and *uvr8-1,* on promoter (blue) and transcribed regions (green) of the designated genes. LW: low fluence rate white light (15 µmol m^{-2} s^{-1}). UVB: 1.5 µmol m^{-2} s^{-1} narrow band UV-B for 4h. Mock: No Ab control. IP: Immunoprecipitated material. Results are expressed as % of Input normalised against *ACT2*. For *ACT2* itself, no normalisation was performed and enrichment is given as % of Input. Error bars represent SD from two independent biological replicates.

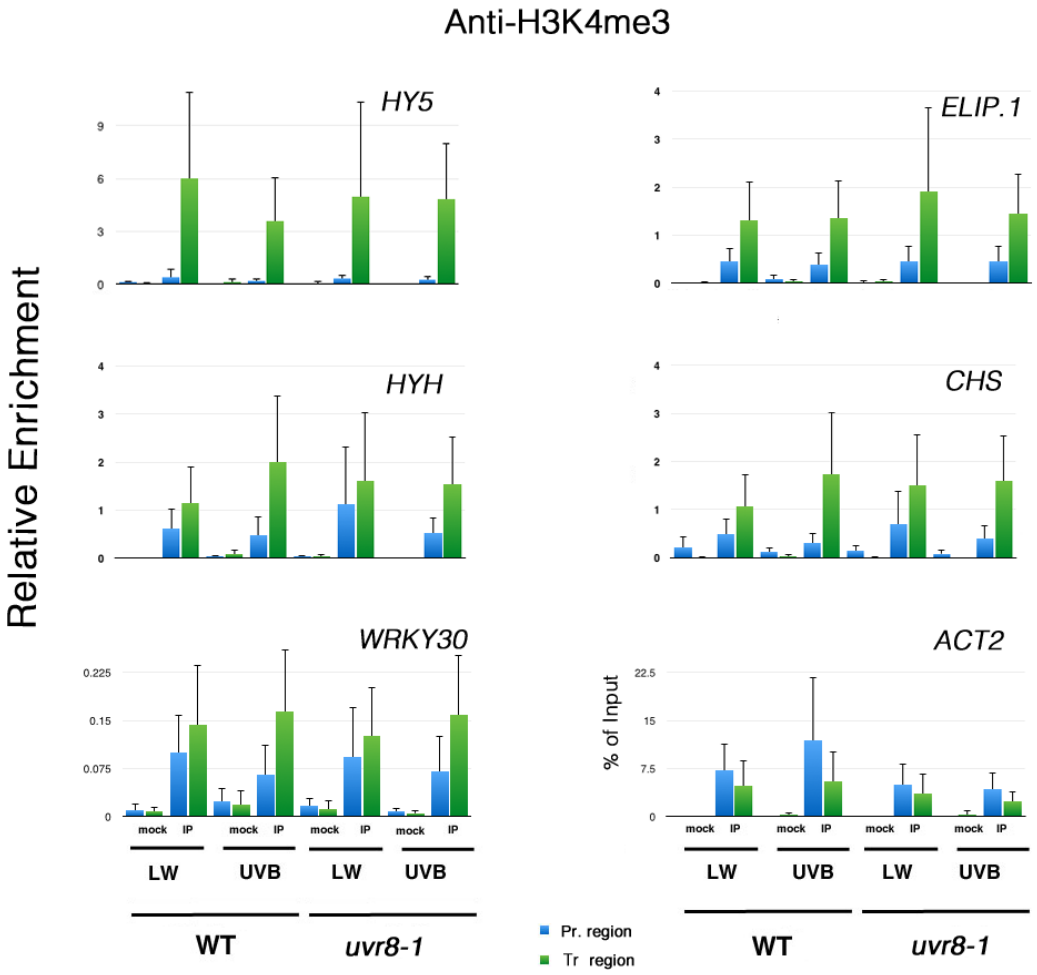

Fig. 3-5 : Results of ChIP with Anti-H3K4me3 antibody. Each graph displays the enrichment in trimethylated Lys 4 of H3 for both WT and *uvr8-1* plants, under low white light and UV-B irradiation, for promoter (blue) and transcribed region (green) of the designated genes. LW: low fluence rate white light (15 µmol m^{-2} s^{-1}). UVB: 1.5 µmol m^{-2} s^{-1} UV-B for 4h. Mock: No Ab control. IP: Immunoprecipitated material. Results are expressed as % of Input normalised against *ACT2*. For *ACT2* itself, no normalisation was performed and enrichment is given as % of Input. Error bars represent SD (n=3)

3.5 Trimethylation of Lysine 36 (K36) of H3 at the genetic loci of interest is not regulated by UV-B in a UVR8-dependent manner

As already mentioned, results from competition experiments have suggested that histone H2B is probably the preferred interacting partner for UVR8 during its association with chromatin. However, unequivocal *in planta* evidence for such a preference has yet to be provided. Unfortunately, the ChIP experiments against H2Bub and H3K4me3 did not result in findings that might help in formulating a relevant working hypothesis. Nonetheless, both histone marks were readily detected at the loci occupied by the genes of interest. If the UVR8-H2B preferential association is true *in planta*, it does not necessarily have to mediate the monoubiquitination / deubiquitination of H2B itself or the cross-talk with H3K4me3. It is conceivable that the deposition of another correlated histone mark, which arrives later on the scene, might be influenced.

Recently, remarkable effort has been put into providing integrative genome-wide epigenetic maps for Arabidopsis, with the aim of acquiring a comprehensive index of different chromatin states (Roudier et al. 2009). Such studies have revealed clusters of highly associated histone marks, on the basis of which trans-histone crosstalk is currently being investigated. One candidate, which appeared worthy of incorporation in our study on the basis of published literature, was H3K36me3. This particular modification, has been reported to be highly associated with H2Bub and H3K4me3 along the genome of Arabidopsis (Roudier et al., 2011). In yeast, it is essential for proper transcriptional elongation (Carrozza et al., 2005) and, interestingly, cycling of H2B between the monoubiquitinated and deubiquitinated states is essential for the sequential recruitment of the methyltransferases which mediate the deposition of the H3K4me3 and H3K36me3 histone marks (Weake and Workman, 2008). In plants, the proposed model suggests that H3K4me3 appears prior to H2B ubiquitination and deubiquitination, whereas H3K36me3 occurs afterwards (Schmitz et al., 2009). The results of the ChIP experiments performed with anti-H3K36me3 showed similar behaviour for WT and *uvr8-1* plants, with no significant differences in the enrichment levels between the two distinct light conditions (Fig 3-6). It can be therefore concluded that photomorphogenic UV-B and UVR8 exert no effect on the trans-histone crosstalk for the aforementioned modifications, at least not in a

way identifiable by the experimental set up of our study, which reflects a "snapshot" of the chromatin state at a particular time point and does not incorporate the temporal dimension of histone crosstalk dynamics.

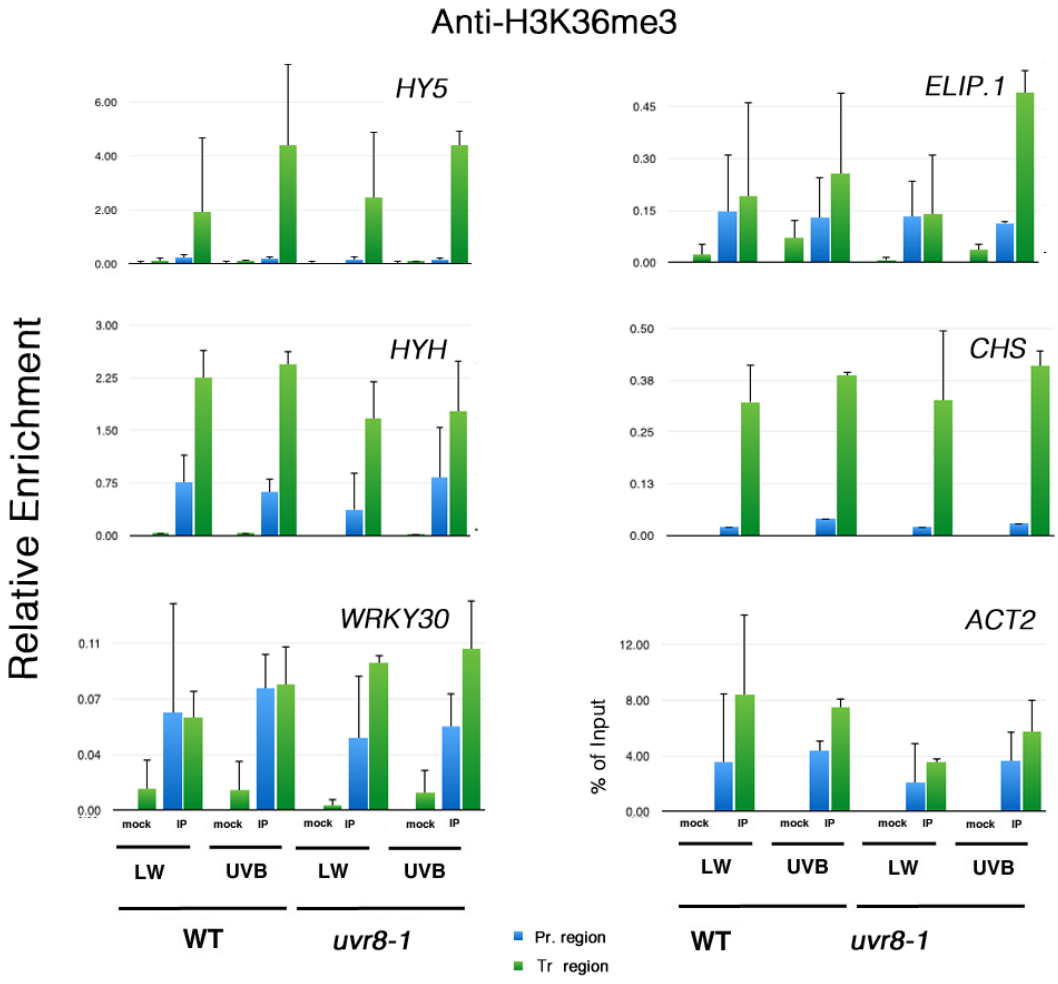

Fig. 3-6 : Results of ChIP with Anti-H3K36me3 antibody. Each graph displays the enrichment in trimethylated Lys 36 of H3 for both WT and *uvr8-1* plants, under low white light and UV-B irradiation, for promoter (blue) and transcribed region (green) of the designated genes. LW: low fluence rate white light (15 µmol m^{-2} s^{-1}). UVB: 1.5 µmol m^{-2} s^{-1} UV-B for 4h. Mock: No Ab control. IP: Immunoprecipitated material. Results are expressed as % of Input for *ACT2,* and normalised % of Input against *ACT2* for all other genes. Error bars represent SD from two independent biological replicates.

3.6 The relatively low levels of H3K9me3 found over well known UVR8-regulated genes are not altered upon UV-B illumination

The histone modification to which we turned our focus next was H3K9me3. In animals it is known to mark mainly heterochromatin, with only a few studies reporting atypical association with actively transcribed regions (Vakoc et al., 2005; Squazzo et al., 2006). In plants, studies on the epigenetic regulation of vernalization have ascribed a repressive function to H3K9me3, along with H3K27me3 (Schmitz et al., 2009). Later studies, however, have placed H3K9me3 among the activating marks (Charron et al., 2009), that precisely target translational start sites and are predominantly involved in transcriptional elongation (Roudier et al., 2011). It has been proposed that H3K9me3 might serve different outcomes depending largely on the particular genomic and/or chromatin context. Whether this histone mark plays a crucial role in regulating transcription remains debatable and no consensus has been reached. Revealingly, disparities in the published reports indicate that elucidation of the functional significance of H3K9me3 may turn out to be a very tedious task. For example, whereas a very high degree of co-appearance with H3K27me3, a silenced-euchromatin mark, has been reported by Charron et al., no such correlation was observed in another study despite the significant overlap in the analysed gene sets (Turck et al., 2007). Moreover, no signal, or very low enrichment levels, were observed for H3K9me3 over the *HY5* and *HYH* loci during the dark-to-light developmental transition. Together with other findings, the latter was indicative of a mild effect of H3K9me3 in transcriptional activation, more suggestive of a role in keeping a basal threshold level of expression (Charron et al., 2009). In contrast, an opposite role seems to be implied by the results of epigenetic mapping of chromosome 4, where H3K9me3 appears to mark highly expressed genes, and enrichment levels correlated positively with increases in gene expression (Roudier et al., 2011).

Based on the above information, it was decided to include H3K9me3 in our analysis. The hypothesis was that the low levels of enrichment over *HY5*, *HYH* and their downstream targets, expected under low fluence rate white light, might raise upon UV-B illumination underlying the concomitant increase in transcript abundances.

Unfortunately, our results revealed no such response (Fig 3-7). Enrichment levels in promoter regions were practically beyond detection for most assayed loci, whereas low signals could be observed for the transcribed regions, in agreement with H3K9me3 being viewed mainly as a mark for transcriptional elongation. No significant differences were found between WT and *uvr8-1* plants under the two distinct light conditions.

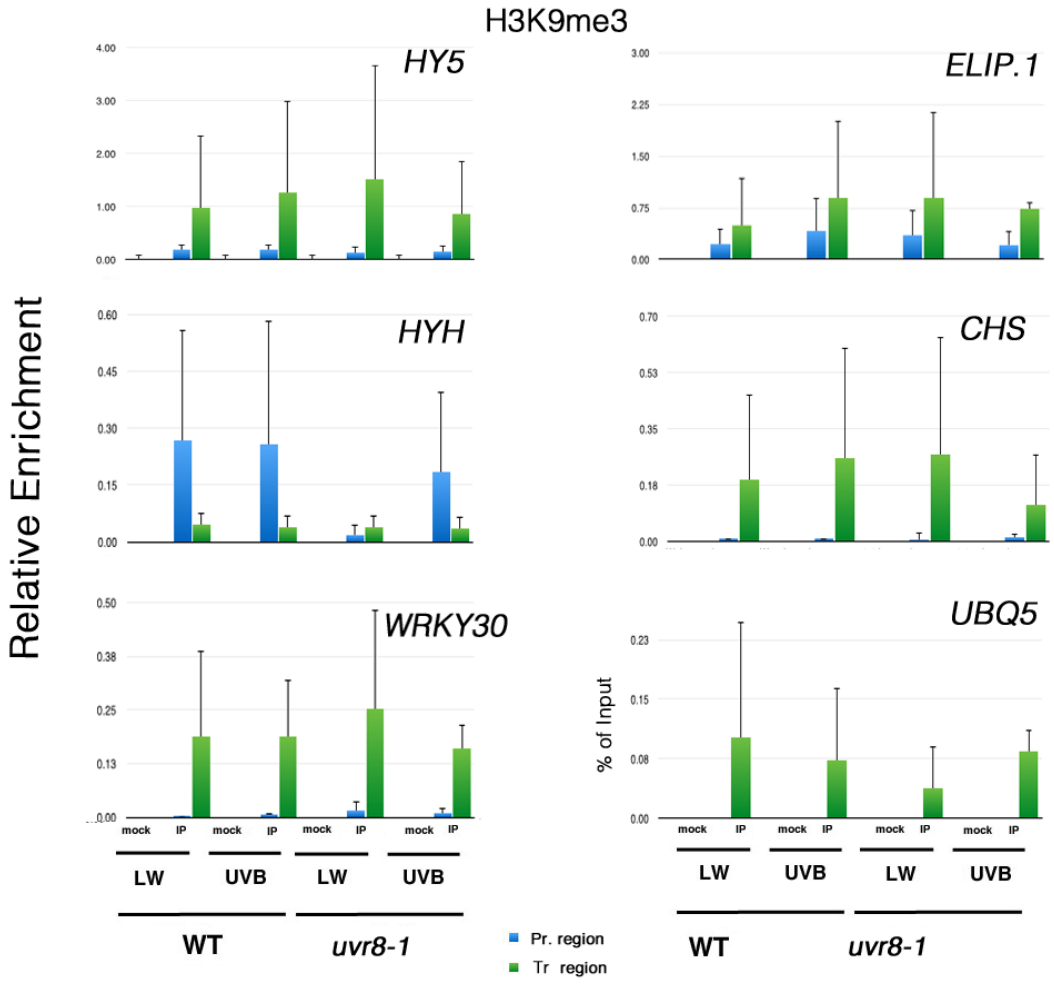

Fig. 3-7 : Results of ChIP with Anti-H3K9me3 antibody. Each graph displays the enrichment in H3K9me3 for both WT and *uvr8-1* plants, under low white light and UV-B irradiation, for promoter (blue) and transcribed region (green) of the designated genes. LW: low fluence rate white light (15 µmol m^{-2} s^{-1}). UVB: 1.5 µmol m^{-2} s^{-1} UV-B for 4 hours. Mock: No Ab control. IP: Immunoprecipitated material. Results are expressed as % of Input normalised against *UBQ5*. For *UBQ5* itself, no normalisation was performed and enrichment is given as % of Input. Error bars represent SD from two independent biological replicates.

3.7 UVR8 might be linked to a locus-specific accumulation of H3K56ac, for a subset of the UVR8-dependent UV-B responsive genes

The last histone modification for which potential correlations with UVR8-dependent UV-B responses were explored was H3K56ac. An initial report mapped this particular histone mark at promoter-proximal regions in plants, with enrichment levels peaking 0-100bp upstream of the coding region (Tanurdzic et al. 2008). Subsequently, as tight association with H3K4me3 was revealed, significant accumulation of H3K56ac was observed in short domains residing around the 5' end of the transcribed regions of expressed genes (Roudier et al., 2009). Moreover, the discovery and first characterisation of H3K56ac in yeast implicated it, among other processes, with the recruitment of chromatin remodelling factors and gene activation (Xu et al., 2005). Later, replication-independent, transcription-promoting nucleosome rearrangements were also proposed to be mediated by this particular histone mark (Rufiange et al., 2007). Such proposed functions, taken together with the increased correlation with H3K4me3 which was readily detected in our ChIP experiments, although without displaying any interesting UVR8-mediated fluctuations upon UV-B illumination (Fig 3-5), singled H3K56ac out as a promising candidate for inclusion in our analysis.

Interesting results came out of the ChIP experiments (Fig 3-8). In general, higher levels of enrichment were observed at the transcribed regions of the genes of interest, compared to the promoter regions. For *HY5,* both WT and *uvr8-1* plants seem to undergo a decrease in the enrichment over the transcribed region upon UV-B illumination, but the differences were not statistically significant. Regarding *HYH,* roughly equal enrichment levels were found under the two light conditions for both types of plants.

Concerning *ELIP.1,* comparing the average of the enrichment signals of the two distinct light conditions over the transcribed region revealed a significantly higher value for WT plants compared to *uvr8-1* (t-test, $p = 0.005$). Hence, it seems that a functional UVR8 is required for keeping adequate levels of H3K56ac over this locus. More specifically, WT plants displayed a UV-B-elicited significant increase in the relative enrichment of H3K56ac on the promoter region (t-test $p = 0.01$). No such response was monitored for

the *uvr8-1* mutant plants. Upon UV-B illumination, a significant decrease (t-test, p = 0.01) in the relative enrichment levels on the transcribed region of *ELIP.1* was observed for *uvr8-1* plants, whereas no such pattern was followed by WT plants. Interestingly, the relative enrichment level for UV-B-illuminated *uvr8-1* plants was found significantly lower than that of UV-B illuminated WT plants (t-test p = 0.01). In addition, a two-way ANOVA suggested that the combined influence of UVR8 loss-of-function and UV-B illumination appears to result in a cumulative effect in decreasing the average relative enrichment levels of H3K56ac over the transcribed region of ELIP.1 (p = 0.05 , 94% Confidence). It can therefore be concluded, that there might exist an underlying link between UVR8 and the accumulation of H3K56ac on the DNA of the *ELIP.1* gene.

Finally, with regard to *CHS*, WT plants displayed significantly higher enrichment levels compared to *uvr8-1* plants, when the cumulative signals for the two light conditions over the transcribed region were compared (t-test p = 0.008). Again, this might indicate that a functional UVR8 protein could be necessary for keeping sufficient levels of H3K56ac on this particular gene. Moreover, signal levels were significantly higher in the promoter and transcribed region of UV-B irradiated WT plants, when compared to similarly treated *uvr8-1* mutant plants (p = 0.017 for pr. region; p = 0.020 for tr. region). Under low fluence rate white light, no significant differences were detected between the two genotypes on either the promoter or the transcribed region. Additionally, UV-B illumination did not affect significantly the enrichment levels for neither WT plants nor *uvr8-1* when signals under LW and UV-B were compared within each genotype. No combinatorial effect of absence of UVR8 and UV-B illumination could be detected via two-way ANOVA.

On the basis of the above observations, it is conceivable that for at least a subset of the UVR8-regulated genes, H3K56ac is contributing to the increased gene expression that follows UV-B illumination, and the deposition and/or removal of this histone mark might be linked to UVR8.

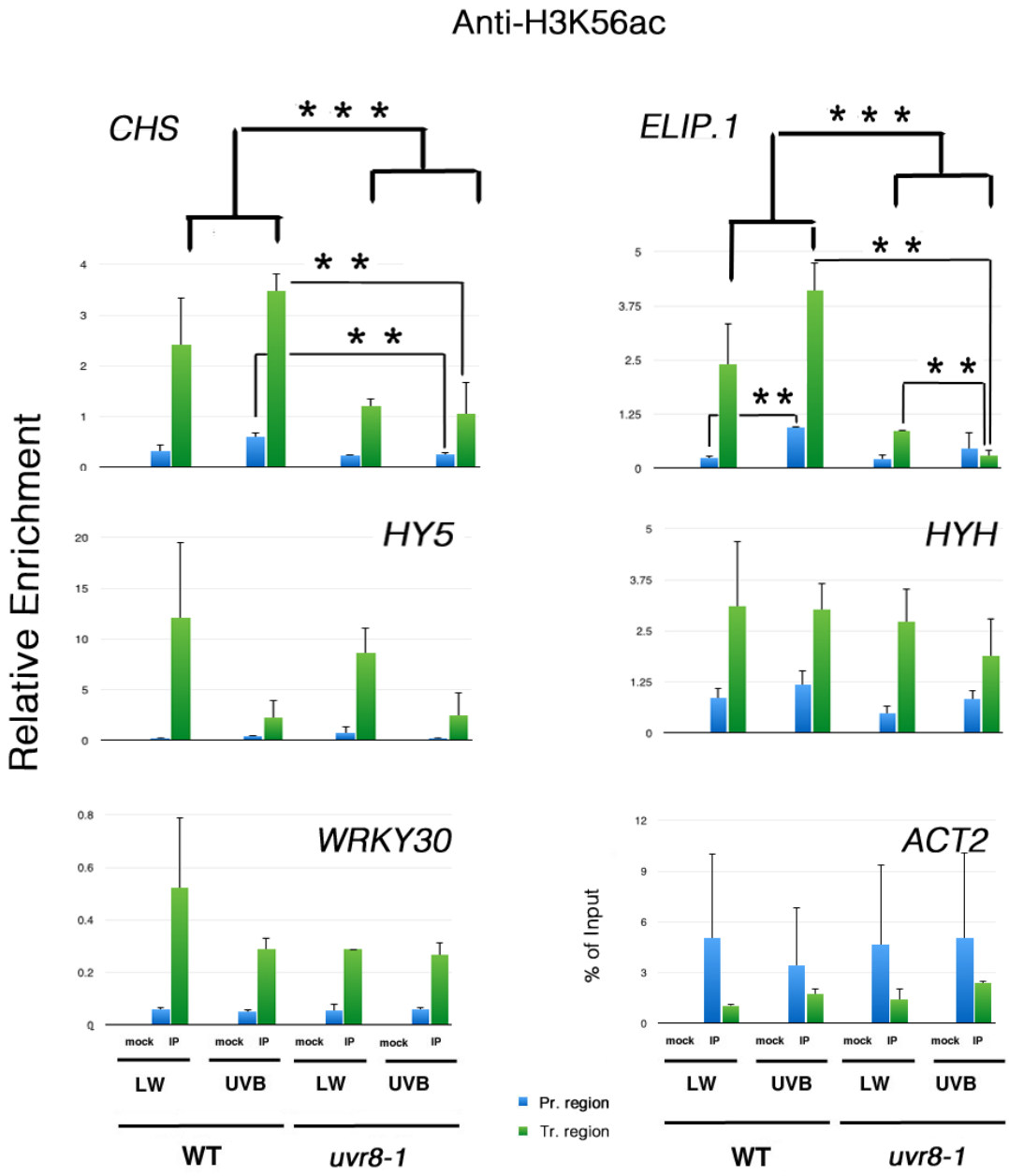

Fig. 3-8 : UVR8 might be linked to a locus-specific accumulation of H3K56ac, for a subset of the UVR8-dependent UV-B responsive genes. Each graph displays the enrichment in H3K56ac for both WT and *uvr8-1* plants, under low fluence rate white light and UV-B irradiation, for promoter (blue) and transcribed region (green) of the designated genes. LW: low fluence rate white light (15 µmol m^{-2} s^{-1}). UVB: 1.5 µmol m^{-2} s^{-1} UV-B for 4h. Mock: No Ab control. IP: Immunoprecipitated material. Results are expressed as % of Input normalised against *ACT2*. For *ACT2* itself, no normalisation was performed and enrichment is given as % of Input. Error bars represent SD from two independent biological replicates. ** : $p \leq 0.05$, *** : $p \leq 0.01$

3.8 Discussion.

Two distinct, tightly regulated processes are known, through which a temporary relaxation of the DNA-histones compaction can be effected in order to facilitate transcription (Li et al., 2007). One involves protein complexes, generally referred to as chromatin-remodeling complexes, which utilise ATP hydrolysis to unwrap the DNA from the histone octamers, or to form protein-free DNA loops, to promote nucleosome sliding and even, in some cases, to mediate eviction of histones from the nucleosome. The second, alternative process, entails post-translational modifications of the side chains of particular amino acids found on the histone molecules. Both the N-terminal tails, which are protruding from the nucleosome core particle, and the centrally positioned globular domains of histones may undergo such modifications. The result is a partial charge neutralisation of the histone molecules, and a concomitant disruption of the electrostatic interactions that contribute to the stability of the nucleosome core particle and of higher order chromatin structure (Campos and Reinberg, 2009).

Following photoreception, UVR8 rapidly accumulates in the nucleus (Kaiserli and Jenkins, 2007) where it mediates, via a yet unresolved mechanism, the expression of a set of genes among which are *HY5, HYH, ELIP1.1* and *CHS*. The association of UVR8 with chromatin (Brown et al., 2005; Favory et al., 2009), which intriguingly has been observed regardless of whether the plants have perceived UV-B (Cloix and Jenkins, 2008), has provided the basis for the formulation of a working hypothesis according to which there might be a link between UVR8 and any of the two aforementioned processes involved in chromatin relaxation. During this project, we primarily focused on histone modifications, building on previously published literature. There is a great diversity in the possible modifications that histones may undergo, thus potentially interesting candidates were sought among histone marks with documented involvement in light signalling (Fisher and Franklin, 2011). The majority of the relevant studies have focused on de-etiolation, and histone H3 acetylation and/or methylation have been by far the most frequently reported modifications.

Initially, studies in pea (*Pisum sativum*) demonstrated that the enhancer of the plastocyanin gene, *PetE,* acts through influencing H3ac and H4ac levels over the promoter and coding region (Chua et al., 2003). Two subsequent studies in maize (*Zea mays*), focusing on the C4-specific phosphoenolpyruvate carboxylase gene (*C4-pepc*), demonstrated that histone acetylation events precede rather than follow transcriptional activation (Offermann et al., 2006) and that light induction of acetylation is controlled by regulating the activity of histone deacetylaces (Offermann et al., 2008). Not long ago, it was reported that, particularly for H3K9ac, the enrichment levels over well known light-responsive genes are affected by light intensity and light wavelength, and that distinct photoreceptor systems mediate the effects of different light qualities (Guo et al., 2008). In a follow-up study, where a genome-wide approach was undertaken, H3K9ac emerged as potent contributor to light- regulated genome expression through its activating action on *HY5, HYH* and their downstream targets (Charron et al., 2009). Relatively recently the *phyA* locus was shown to be significantly enriched in H3K9,14diac upon its activation in darkness (Jang et al., 2011). It should be noted at this point, for proper interpretation of the results compared to the rest of the literature, that in both this latter study and our work, the antibody used for the ChIP assays was raised again diacetylated histone and does not distinguish between the two acetylated lysine residues. As there have been reports demonstrating that such antibodies, raised against bivalent immunogens, may have undocumented preference over one of the two modifications (Perez-Burgos et al., 2004), caution is advisable when reaching conclusions. As far as our work is concerned, and in the light of a recent report (Schenke et al., 2014), it is most likely that the observed acetylation differences are caused by an H3K9ac rather than an H3K14ac enrichment. Schenke and coworkers performed their experiments on Arabidopsis cell cultures, used UV-B doses sufficient to trigger photomorphogenic responses, employed antibodies specific to either of the two modifications, and eventually reached similar findings to the ones reported here only for the H3K9ac histone mark.

With regard to UV-B light specifically, histone modifications have been studied in maize and Arabidopsis, and good evidence has accumulated to support the contribution of chromatin-based processes to transcriptional regulation (Casati et al., 2006; Casati et al., 2008; Cloix and Jenkins, 2008; Schenke et al., 2014). Results presented in this chapter (Fig 3-3) stand in agreement with the already published literature, and extend the available information by implicating UVR8 in the UV-B-induced accumulation of H3K9,14diac over the chromatin loci occupied by the tested UVR8-regulated genes. The mechanistic details of UVR8 involvement are not clear, and their elucidation would be an interesting direction for future studies. One puzzling point, for example, is that UVR8 is not found on the chromatin of all genes it regulates. Whereas it could be detected on chromatin positions spanning the entire *HY5* locus, no signal was visible for the *HYH* and *CHS* promoter regions, and no data were provided on what the case for *ELIP.1* is (Cloix and Jenkins, 2008). Assuming that no misleading artefacts are at play, and that the results truly reflect the *in planta* situation, one feels tempted to speculate that in some cases UVR8 itself might be directly, physically involved in the accumulation of H3K9,14diac, whereas in other cases a downstream effector might undertake that role. A possible candidate would be HY5, which has previously been reported to be involved in the regulation of H3K9ac levels (Guo et al., 2008), and it has been proposed to mediate the transcription of downstream targets synergistically with *HYH* and histone acetylation (Charron et al., 2009). This hypothesis could be tested be performing ChIP assays using *hy5, hyh* and *hy5hyh* mutant lines. Since histone acetylation can be detected independently of transcription, and it is regulatory of, rather than consequential to gene expression, if such ChIP experiments lead to results similar to those observed for *uvr8-1* plants, it would suggest that HY5 and/or HYH are the directly involved agents in the regulation of H3K9,14diac accumulation. Moreover, data that might shed light on the above questions are expected from a ChIP-seq results analysis, that is currently under way. Six independent ChIP experiments with the antiH3K9,14diac antibody were performed. The samples were then pooled together, in order to obtain sufficient IP quantity for sequencing, and the expected results for *HY5* and *ELIP.1* were verified by qPCR (Fig 3-9) before sending an aliquot of the material to be sequenced. No more genes were looked at, as it would be a waste of template that may be later needed for confirmation of any ambiguous ChIP-seq

results. The aim behind this attempt is to identify, on a genome wide scale, as many genes as possible, which would appear to display, upon UV-B illumination, the UVR8-dependent pattern of H3K9,14diac accumulation that was observed for *HY5, ELIP.1, HYH* and *CHS*. Subsequently, this set of genes may be compared with similar sets that have come from microarray experiments, and have revealed how many genes are UVR8-regulated, or *HY5*-regulated, or UV-B regulated in general.

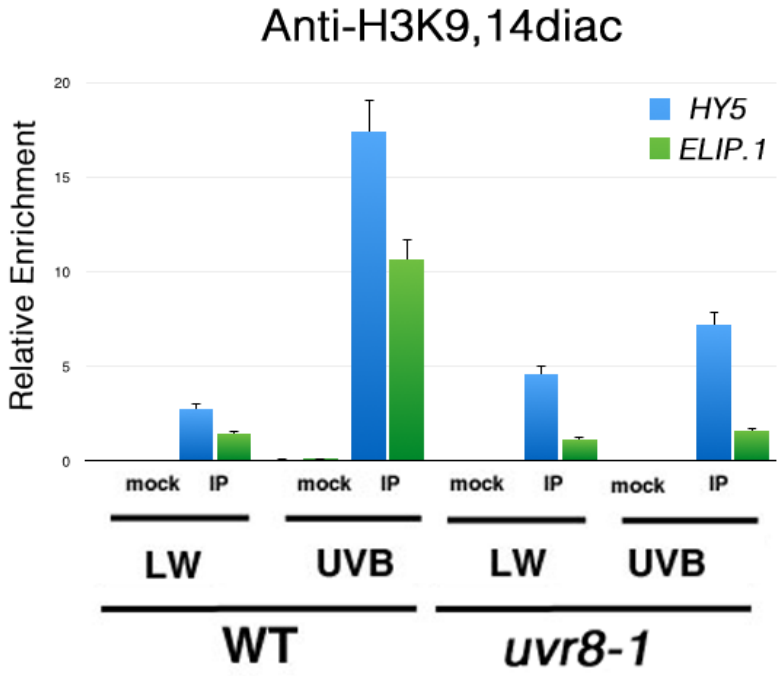

Fig. 3-9 : Confirmation of the expected results for the relative enrichment of H3K9,14diac over the transcribed regions of HY5 and ELIP.1, before sending the samples for ChIP-seq. The bar-chart displays the relative enrichment in H3K9,14diac for both WT and *uvr8-1* plants, under low fluence rate white light and UV-B irradiation, for the transcribed regions of *HY5* (blue) and *ELIP.1* (green). LW: low fluence rate white light (15 µmol m^{-2} s^{-1}). UVB: 1.5 µmol m^{-2} s^{-1} UV-B for 4h. Mock: No Ab control. IP: Immunoprecipitated material. Results are expressed as % of Input normalised against *ACT2*. Error bars represent SD (n=3) from three technical replicates for each sample on the qPCR plate

Our attempt to identify other histone marks that might exist in parallel with H3K9,14 diac, and might be regulated in a UVR8-dependent manner during UV-B responses, did not result in any interesting candidates, except H3K56ac which is discussed below. Obviously, it was practically impossible to perform an exhaustive research that would cover all potentially interesting histone modifications. Priority was given to those which consistently appeared in light signaling-related literature and/or were expected to co-localise with H3K9ac on the basis of epigenomic mapping reports. The rationale behind each individual choice has already been explained in the relevant results section. Nonetheless, there are important candidates that are certainly worthy of future investigation. Among them, H3K27ac could turn out to be interesting, because it has been reported to be highly correlated with H3K9ac, and has been found important for the high expression of *PHYA i*n darkness(Jang et al., 2011). This mark was left out of our analysis, only on the basis of its apparently minor role in *HY5/HYH* related de-etiolation processes (Charron et al., 2009). Photomorphogenic UV-B signalling, however, involves processes that are quite distinct from de-etiolation and it is possible that H3K27ac might be involved. Another interesting candidate is H3K27me3, which is widely regarded as a repressive histone modification, contributes significantly to gene silencing, and its removal from the enriched loci is needed for gene activation (Crevillén et al., 2014). Its inclusion in future analyses would address the interesting possibility of UVR8 (or of a downstream effector of it) being involved not only in the accumulation of activating marks on the genes it regulates, but also in the elimination of a silencing one.

Finally, with regard to H3K56ac, it was an unexpected and intriguing finding to observe a locus-specific involvement of UVR8 in the distribution of this histone mark upon UV-B illumination (Fig 3-8). Seemingly distinct patterns were obtained for the *HY5* compared to the *HYH* locus. This might reflect separate “histone code” annotations for the two homologues under photomorphogenic UV-B, although more independent biological replications are required to consolidate such a claim. The differences in the enrichment over the transcribed region of *HY5*, when low fluence rate white light was compared to UV-B, were close to but above an accepted statistical significance threshold. For *ELIP.1* the findings were more persuasive, and seem to imply that, under UV-B, a UVR8-dependent regulation of H3K56ac levels on the *ELIP.1* locus is at play.

No quantitative data are available on whether UVR8 associates with chromatin on the *ELIP.1* gene, hence the observations may result from the direct involvement of a downstream effector rather than of UVR8 itself. As discussed for H3K9,14diac, ChIP experiments on *hy5, hyh*, and *hy5hyh* mutants might help in resolving this point. Regarding *CHS*, the results were indicative of a similar general trend as the one observed for *ELIP.1*. Again, the intrinsic variability of ChIP assays may have masked biologically important differences by rendering them not statistically significant after only two repeats. For example, whereas for both *ELIP.1* and *CHS* the enrichments on the transcribed regions were significantly higher for UV-B-illuminated WT plants compared to UV-B-illuminated *uvr8-1* mutants, the corresponding differences for the two genotypes under LW were not statistically different. More repetitions could resolve what the case under LW conditions is, and the alternative interpretations could be different depending on the outcome. If it turns out that under LW conditions the enrichment for WT plants is comparable to that of *uvr8-1* plants, it will be safer to claim that the observed effects under UV-B truly relate to UVR8-dependent UV-B signalling. If, in contrast, WT plants appear to be significantly more enriched than *uvr8-1* under LW as well, then in light of the data that have demonstrated a UV-B-independent association of UVR8 with chromatin, one might be tempted to speculate a structural role of UVR8 in the recruitment of the acetylating and/or deacetylating agents.

In conclusion, the data presented in this chapter are consistent with a long held belief that histone acetylation is an important facet of the transcriptional regulation that follows photomorphogenic light stimuli, and have contributed to the existing information by implicating the recently discovered UVR8 photoreceptor. Some preliminary, first attempts, to address questions related to the nature of UVR8 involvement are the subject of the following chapter.

CHAPTER 4: INVESTIGATION OF THE POSSIBLE ROLE OF CERTAIN HATS AND/OR HDACS IN UVR8-DEPENDENT PHOTOMORPHOGENIC UV-B RESPONSES.

4.1 Introduction

Following the observations that the acetylation status of specific histone H3 residues might be implicated in the transcriptional regulation of photomorphogenic UV-B responses mediated by UVR8, it was decided to proceed with attempts aiming at identifying the particular histone acetyltransferases (HATs) and/or histone de-acetylases (HDACs), that were likely to be involved. Central to our approach was the working hypothesis that UVR8 could be physically, directly involved in the recruitment of the relevant histone modifying enzymes, which if confirmed would provide the first insights into the functional significance of the enigmatic UVR8-chromatin association.

At first, yeast two hybrid (Y2H) assays were undertaken, in order to address the possibility of interactions between UVR8 and candidate HATs / HDACs with documented involvement in light signalling. In due course, proteins which have no histone modifying activity themselves, but whose presence is important for HATs / HDACs to fulfil their role, were also included in the analysis. Furthermore, solely on the basis of published literature, a substantial number of proteins could be regarded as being potentially good candidates for direct interaction with UVR8 in a chromatin context. It was practically impossible to test them all within the time constraints of the project, however a subset was considered for analysis and included in the Y2H assays.

Having in mind that *in planta* experiments would be essential to consolidate any outcomes of the approaches in yeast, T-DNA insertional mutants of major HATs / HDACs were obtained from publicly available Arabidopsis germ-plasm banks. Many of the lines were segregating for the desired mutation. Hence, subsequent generations were subjected to genotyping analysis until homozygous individuals could be identified. The severity of the mutations was then assessed at the transcript level and, where possible, only null mutants were considered for further analysis. Eventually, the resulting mutant lines were assayed for altered phenotypes in standard UVR8-regulated UV-B responses.

4.2 Neither GCN5 itself nor the functionally related pair of transcriptional co-activator homologues, ADA2a and ADA2b, interact with UVR8 in yeast

The first HAT, which we turned our attention to, was **G**eneral **C**ontrol **N**ondepressible protein 5 (GCN5). The original identification of GCN5 came from genetic selections in yeast (Georgakopoulos and Thireos, 1992), where it was found to functionally interact with the transcriptional activator GCN4. During the same period, and via a similar approach, a group of potent transcriptional co-activators designated as ADA1-5 (**A**lterations/ **D**eficiency in **A**ctivation) were identified (Berger et al., 1992). GCN5 was later demonstrated to be capable of acetylating primarily H3, and to a lesser extend H4, at specific lysines. Interestingly, lysine K9 appeared to be the preferred acetylation position for newly synthesised yeast H3 *in vivo*, whereas in *in vitro* assays K14 appeared to be predominantly acetylated (Kuo et al., 1996). However, it soon became apparent that GCN5 alone is unable to exert HAT activity, and in order to effect the acetylation of nucleosomal histones it needed to form a heterodimer with ADA2 (Grant et al., 1997).

In the Arabidopsis genome there is one *GCN5* gene and two *ADA2* homologues, designated as *ADA2a* and *ADA2b*. The HAT activity is exhibited by GCN5, and both ADA2a and ADA2b interact with GCN5 in vitro and in Y2H assays (Stockinger et al., 2001). Acetylation levels of histones H3 and H4 have been reported to be generally lower in *gcn5* mutant plants, which also displayed reduced light-inducible gene expression. Moreover, H3K9ac and H3K14ac in particular were found to require a fully functional GCN5 protein (Benhamed et al., 2006). Intriguingly, in a subsequent high-throughput approach the authors demonstrated that the expression of a substantial number of genes might be dependent on both GCN5 and HY5 binding to the respective promoters (Benhamed et al., 2008). In the light of this information, a direct interaction of UVR8 with GCN5 appeared plausible, and a Y2H assay was employed to investigate this option (Fig 4-1). The well established interactions between GCN5 and ADA2a / ADA2b were used as controls, in order to demonstrate that all recombinant proteins were functional and behaved as expected during the assay. The UVR8-COP1 interaction, which is expected to be observed only when yeast cells are UV-B treated, was included to ensure the effectiveness

of the UV-B illumination. The results revealed that neither GCN5 nor any of the ADA2 members could interact with UVR8 in yeast.

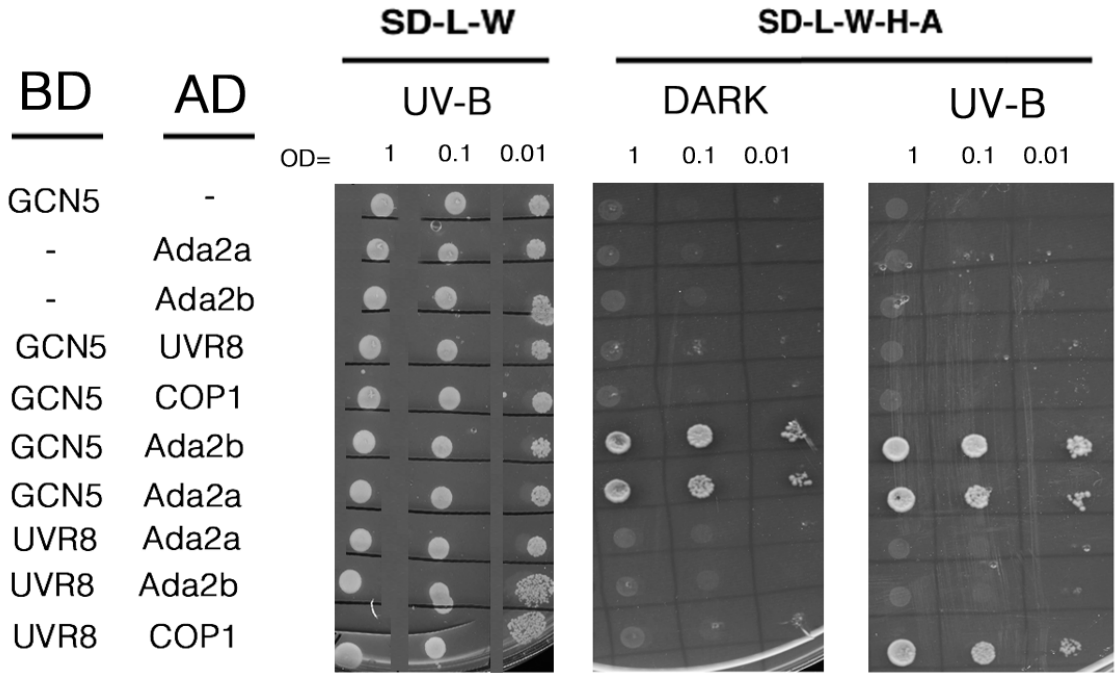

Fig. 4-1: Neither GCN5 nor its interacting partners ADA2a and ADA2b interact with UVR8 in yeast. The UVR8-COP1 interaction was used as a control of the effectiveness of the UV-B treatment, whereas the interactions between GCN5 and the two ADA2 proteins were employed to show that all constructs behave as expected. SD-L-W medium was used as a control for the viability of the spotted cells. Interactions were assessed only on high stringency selection plates (SD-L-W-H-A). Yeast spottings were performed from cell suspensions with three different cell densities (OD=1 , 0.1 and 0.01). Results are representative of three independent biological replicates.

4.3 UVR8 does not interact with HD1/HD19, or with the core TAF1/HAF2 protein.

As no interesting findings were revealed after the Y2H attempts with GCN5 and the functionally related ADA2 transcriptional co-activators, focus was turned upon two other histone modifying proteins, which have been consistently correlated with light signalling in plants.

TATA **B**inding Protein (TBP) - **A**ssociated **F**actors (TAF_{II}) are transcription associated proteins which, together with TBP, form the **T**ranscription **F**actor IID (TFIID) in human and Drosophila cells (Martinez, 2002). One member of this group is TAF1, which possesses HAT activity and, in Arabidopsis, is represented by the products of two homologous genes designated as *HAF1* and *HAF2* (Pandey et al., 2002). The two proteins are partially redundant, but the one synthesised by *HAF2* (TAF1/HAF2, hereafter referred to simply as TAF1) appears as the major player in plants (Bertrand et al., 2005). The Arabidopsis TAF1 protein has been reported to be required for the integration of light signals in orchestrating a balanced transcriptional response, as *haf2* mutant plants exhibited lower chlorophyll accumulation, reduced light-regulated transcripts and promoter activities. Moreover, hypocotyl length measurements in double mutant plants, in which both Phytochromes and TAF1 or Cryptochromes and TAF1 were affected, revealed that TAF1 is a positive regulator of the response, acting downstream of the photoreceptors. Additionally, *taf1/hy5* double mutants revealed synergistic effects for TAF1 and HY5 (Bertrand et al., 2005). Not long ago, TAF1 was also found to be required for H3K9ac, a histone mark on which it had a cumulative effect together with *GCN5* (Benhamed et al., 2006).

On the other hand, an important feature of the so called "acetylation code" of nucleosomal histones, which renders histone acetylation a versatile contributor to the mechanisms of controlling gene expression, is that it is dynamic and reversible. At any particular moment, the acetylation level over a genetic locus is the result of a dynamic equilibrium established between the contrasting activities of HATs and HDACs. Therefore, a hypothesis alternative to the one which places UVR8 as a recruiter of a particular acetyltransferase on selective loci, could be that it might as well be preventing the activity of an antagonistic deacetylase by interacting with it.

An appealing candidate to include in our analysis, with the aim of testing the above possibility, was HD1, a member of the Arabidopsis RPD3 family of HDACs, which has been thus named on the basis of sequence similarities with the **R**educed **P**otassium **D**eficiency 3 (RPD3) family of yeast deacetylaces. HD1 from Arabidopsis is known to have pleiotropic developmental effects (Tian et al., 2003), and has been proposed to act antagonistically to GCN5 in regulating H3K9ac levels on the promoters of various light regulated genes. Indeed, far red light - grown *gcn5/hd1* double mutants displayed a restored WT hypocotyl length phenotype, in contrast to the alterations, in opposing directions, caused by the single mutations (Benhamed et al., 2006). Moreover, Guo et al have reported that HD1 might be involved in the maintenance of H3K9ac levels in a light-dependent manner (Guo et al., 2008).

The Y2H experiments were carried out under both UV-B and UV-B-free conditions (Fig 4-2 B.) using the UVR8-COP1 interaction as a control. TAF1 and HD1 were cloned in the pGADT7 Y2H vector as translational fusions with the GAL4-AD, whereas UVR8 was fused with GAL4-BD in the pGBKT7 vector. In the case of HD1, the full length protein was cloned. In contrast, it was decided not to attempt a full length cloning of TAF1, whose coding sequence is almost 5.5 Kbp and its integration in the yeast vector might be problematic. Instead, a central portion of approximately 620 aa of the primary sequence of TAF1, including domains likely to mediate protein-protein interactions and excluding the C-terminal bromo-domain which is responsible for the recognition of the acetyl-lysines on the nucleosomal histones, was cloned. In order to demonstrate sufficient expression of the recombinant proteins in the transformed yeast cells, immunoblots against the HA-epitope tag were performed on protein extracts (Fig 4-2 A.). Both the partial TAF1 - GAL4 AD fusion (pTAF1/AD) and the HD1 - GAL4 AD fusion (HD1/AD) were detected as bands of the expected size. Figure 4-2 additionally shows the results of a Y2H assay performed to test the possibility of UVR8 interacting with the partial length of another HAT, namely HAC5. This is a **H**istone **A**cetyltransferase of the p300/**C**REB Binding Protein family (HAC), which according to **T**he **A**rabidopsis **I**nformation **R**esource (TAIR) database can acetylate either lysine K9 or K14 of histone H3. HAC5 was a late inclusion in our analysis, after a partial length clone was pulled out from a Y1H screen as being potentially capable to recognise *cis*-regulatory elements of the *HY5* promoter (Chapter 5 of this thesis). This

partial length clone (pHAC5) consisted of only the last 307 aa of the protein. Nevertheless, within that region there are domains that mediate protein-protein interactions, and it was decided to check wether this small portion is capable of binding to UVR8. Our results revealed that neither HD1, nor pTAF1, nor pHAC5 could interact with UVR8 in yeast.

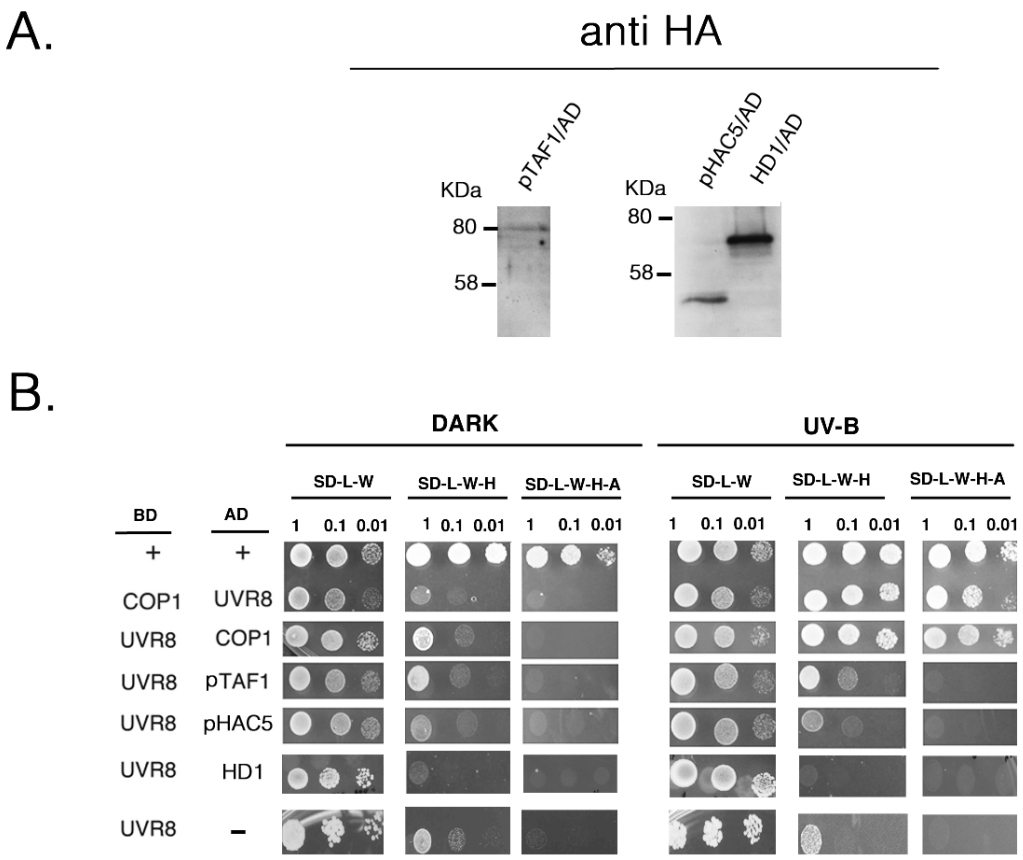

Fig. 4-2: UVR8 does not interact with HD1, a partial sequence of TAF1 (pTAF1) or the C-terminal sequence of HAC5 (pHAC5). **A.** Immunoblots with anti-HA antibody for detection of the recombinant proteins of interest in the yeast cells. **B.** The interaction between the murine p53/GAL4BD fusion protein (+ve BD) and the SV40 large T-antigen/GAL4AD fusion protein (+ve AD) was used as a general positive control for the Y2H assay. The interaction between UVR8-COP1 interaction was used as a control for the effectiveness of the UV-B treatment. SD-L-W medium was used as a control for the viability of the spotted cells. Interactions were assessed on low (SD-L-W-H) and high (SD-L-W-H-A) stringency selection plates. Yeast spottings were performed from cell suspensions with three different cell densities (OD=1, 0.1 and 0.01). Results are representative of three repeats.

4.4 UVR8 seems to interact weakly with FVE, under UV-B-free conditions, in a Y2H assay.

A combination of biochemical analyses and genetic screens performed for the isolation of Arabidopsis mutants involved in light-regulated seedling development, has led to the identification of a group of potent negative regulators of photomorphogenesis known as the COP/DET/FUS group (Yi and Deng, 2005). Three distinct multimeric biochemical entities, all of which are implicated in the degradation of photomorphogenesis-promoting factors by the proteasome, are known to consist of members of the above group. Namely, the COP1-SPA complexes, the **C**OP9 **s**ig**n**alosome (CSN), and the **C**OP10-**D**DB1-**D**ET1 (CDD) complex, are all linked to the ubiquitination/proteasome-mediated degradation of positive regulators of photomorphogenesis, via the CULLIN4 (CUL4) - DDB1 E3 ubiquitin ligase (Bernhardt et al., 2006; Chen et al., 2006; Chen et al., 2010). The functional interaction is mediated by the so called **D**DB1 and **C**UL4 **A**ssociated **F**actors (DCAFs), which are also sometimes referred to as **D**DB1-binding **WD**40 domain - containing proteins (DWD) (Chen et al., 2010; Lee and Zhou, 2007). However, the biological role of **D**amaged **D**NA Binding **P**rotein 1 (DDB1) is not restricted to being an important structural "adaptor" protein. In animal cells DDB1, together with the closely related DDB2, has been reported to interact with histone acetyltransferase complexes (Datta et al., 2001). In Arabidopsis, a model has been proposed (Schroeder et al., 2002) according to which DET1, being in a heterodimeric complex with DDB1, associates in a nucleosomal context with the N-terminal tail of histone H2B (Benvenuto et al., 2002) to repress transcription. Upon illumination, DDB1 is thought to recruit HATs which acetylate the N-terminal tail of H2B, thereby leading to the dissociation of both DET1 and DDB1 from chromatin and a concomitant transcriptional up-regulation.

In a relatively recent report, DDB1 was found to interact with the **F**lowering Locus **VE** (FVE) protein, which promotes flowering via the autonomous pathway and is involved in chromatin remodelling processes (Pazhouhandeh et al., 2011). Intriguingly, the interaction appeared to be mediated by the WD40 domain of FVE and affected **F**lowering **L**ocus **T** (FLT) expression by regulating the levels of H3K27me3. In an earlier study, FVE had been found to participate in a protein complex which represses the expression of ***F****lowring* ***L****ocus* ***C*** (*FLC*) via a histone deacetylation mechanism (Ausín et al., 2004).

DDB1 is represented by two homologues in Arabidopsis, designated as DDB1a and DDB1b. Together with DDB2 they constitute the DDB complex and appear to be important for UV-B tolerance and genomic integrity (Biedermann and Hellmann, 2010). Indeed, *ddb2* mutant plants are known to be impaired in DNA repair mechanisms and demonstrate increased sensitivity to high levels of UV-B radiation (Koga et al., 2006). Intriguingly, *fve* mutant plans were recently reported to have reduced levels of histone acetylation following UV-B treatment, and accumulated cyclobutane pyrimidine dimers (Campi et al., 2012).

Taking together the findings from all the aforementioned studies, a plausible hypothesis worthy of investigation was that UVR8 might be involved in a direct physical interaction with any of the DDB1, DDB2 or FVE. In order to test this, DDB1b and DDB2 were cloned in the pGBKT7 Y2H vector, fused with the GAL4-BD, whereas FVE and DDB1a were cloned in the pGADT7 vector as translational fusions with the GAL4-AD. The interaction between DDB1b and FVE (Pazhouhandeh et al., 2011) was used as a control to demonstrate that the recombinant proteins were behaving as anticipated. A weak interaction between UVR8 and FVE was detected, when yeast cells were not receiving any UV-B (Fig 4-3). It should be noted, however, that the assays were repeated four times and on two occasions the yeast growth on full selective medium was too slow to be convincingly regarded as indicative of interaction, whereas in the other two repeats (of which Fig 4-3 is representative) a weak but confidently detectable interaction was observed. Such variations are commonly observed in Y2H assays for borderline interactions, and are usually attributed to differences in the expression levels of the proteins within the yeast cells and/or to batch-to-batch differences in the quality and concentrations of the supplemented dropout mediums. As things stand, a weak/transient interaction between UVR8 and FVE in yeast should not be ruled out, and whether this also occurs *in planta* needs to be demonstrated with plant-specific approaches. As for the other candidates, none was observed to interact with UVR8 (Fig 4-3 and Fig 4-4).

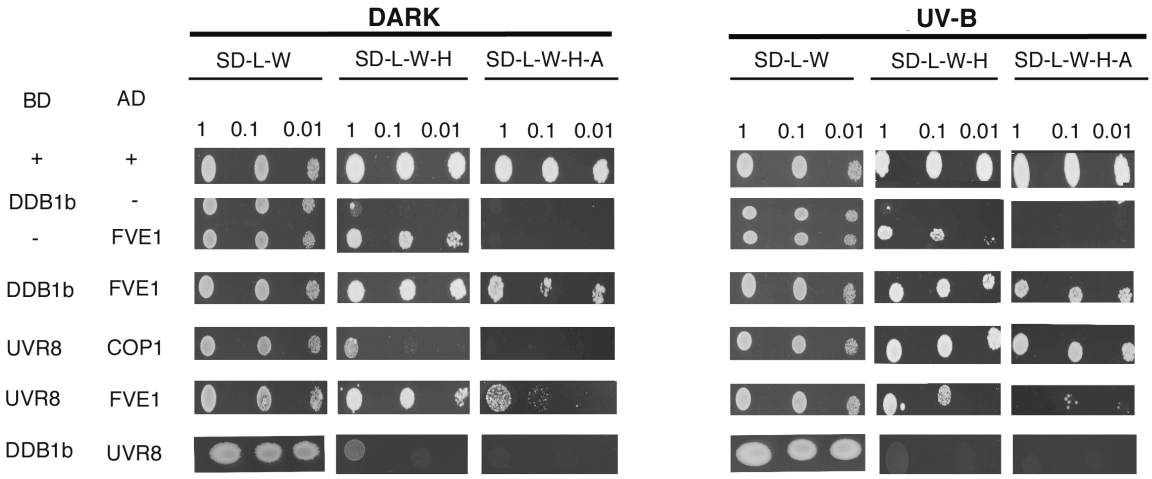

Fig. 4-3: UVR8 appears to interact weakly with FVE. The interaction between the murine p53/GAL4BD fusion protein (+ve BD) and the SV40 large T-antigen/GAL4AD fusion protein (+ve AD) was used as a general positive control for the Y2H assay. The interaction between UVR8-COP1 interaction was used as a control for the effectiveness of the UV-B treatment. The control interaction between FVE and DDB1b {Pazhouhandeh et al., 2011, #99979} was employed to demonstrate proper behaviour of the recombinant proteins in yeast. SD-L-W medium was used as a control for the viability of the spotted cells. Interactions were assessed on low (SD-L-W-H) and high (SD-L-W-H-A) stringency selection plates. Yeast spottings were performed from cell suspensions with three different cell densities (OD=1, 0.1 and 0.01). Results are representative of at least two repeats.

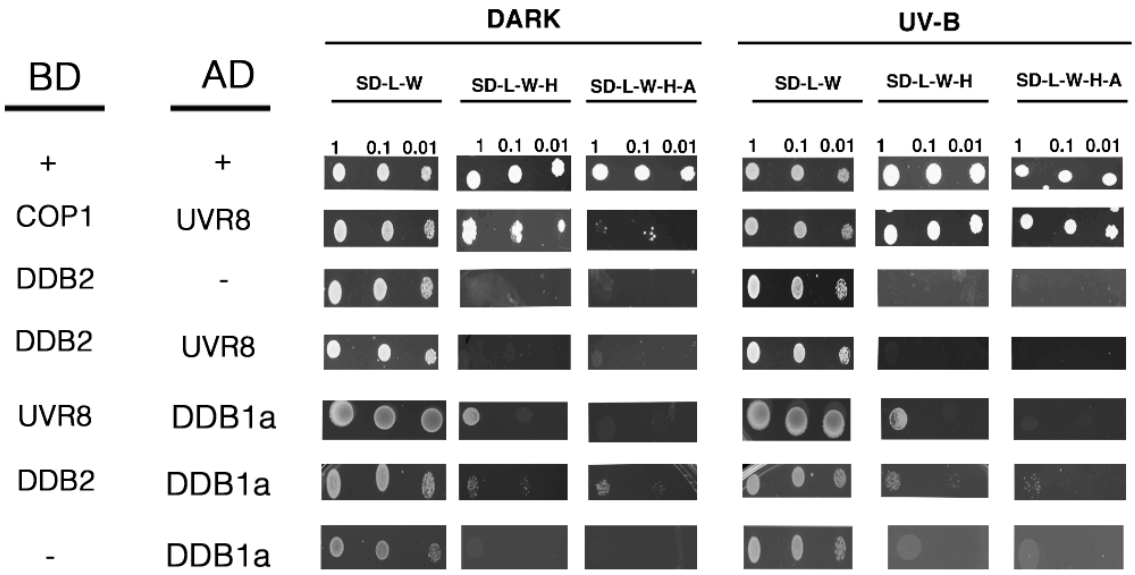

Fig. 4-4: UVR8 does not interact with DDB2 or DDB1a in yeast. The interaction between the murine p53/GAL4BD fusion protein (+ve BD) and the SV40 large T-antigen/GAL4AD fusion protein (+ve AD) was used as a general positive control for the Y2H assay. The COP1-UVR8 interaction was used as a control for the effectiveness of the UV-B treatment. The anticipated weak interaction of DDB2 with DDB1a in yeast {Dumbliauskas et al., 2011, #71146} was employed to demonstrate that the recombinant proteins behaved as expected. SD-L-W medium was used as a control for the viability of the spotted cells. Interactions were assessed on low (SD-L-W-H) and high (SD-L-W-H-A) stringency selection plates. Yeast spottings were performed from cell suspensions with three different cell densities (OD=1, 0.1 and 0.01). Results are representative of three independent repeats.

4.5 No direct interaction could be detected between UVR8 and various PIFs

As discussed in detail in the "General Introduction" section of this thesis, PIFs are bHLH TFs which play pivotal roles in phytochrome signalling, and are generally considered to exert negative regulatory function. The bZIP transcription factor HY5, on the other hand, has been long established as a photomorphogenesis-promoting protein. In a recent study, which focused on the transcriptional control of photosynthetic genes resulting from the integration of light and temperature stimuli, HY5 and PIFs were regarded as potent antagonists binding to similar cis-regulatory promoter elements (Toledo-Ortiz et al., 2014). Evidence has now started to accumulate that one of the targets of HY5 is its own promoter (Abbas et al., 2014; Binkert et al., 2014; Chapter 6 of this thesis) and it is plausible that, under photomorphogenic UV-B perceived by the UVR8 photoreceptor, a positive regulatory loop might be operating at the *HY5* locus. Furthermore, an intriguing finding, which shed some light on the mechanistic facets of the repressive roles of PIFs, was that PIF3 appears to interact physically with the histone deacetylase HDA15 (Liu et al., 2013). Compellingly, in the meantime UVR8 had been observed, in a collaborative study, to inhibit shade avoidance responses in Arabidopsis, which are positively mediated by stabilised levels of certain PIFs in the plant body (Hayes et al., 2014). It was therefore decided to address the possibility of whether UVR8 could be directly interacting with certain PIFs. The rationale in relation to this project, was that by the documented capability of at least one PIF, namely PIF3, to interact with a histone deacetylase, a putative interaction with UVR8 would take us one step further in gaining insights on how UVR8 performs its regulatory function.

The hypothesis was tested via a Y2H assay (Fig 4-5). PIF3 was cloned in the pGBKT7 vector fused to the GAL4-BD. In contrast, PIF4, PIF5 and PIF7 were cloned in the pGADT7 vector, in fusion with the GAL4-AD. The capability of PIFs to form heterodimers was exploited to confirm, by control interactions, the functionality of the recombinant proteins. Unfortunately, the results revealed no interactions of UVR8 with any of the tested PIFs.

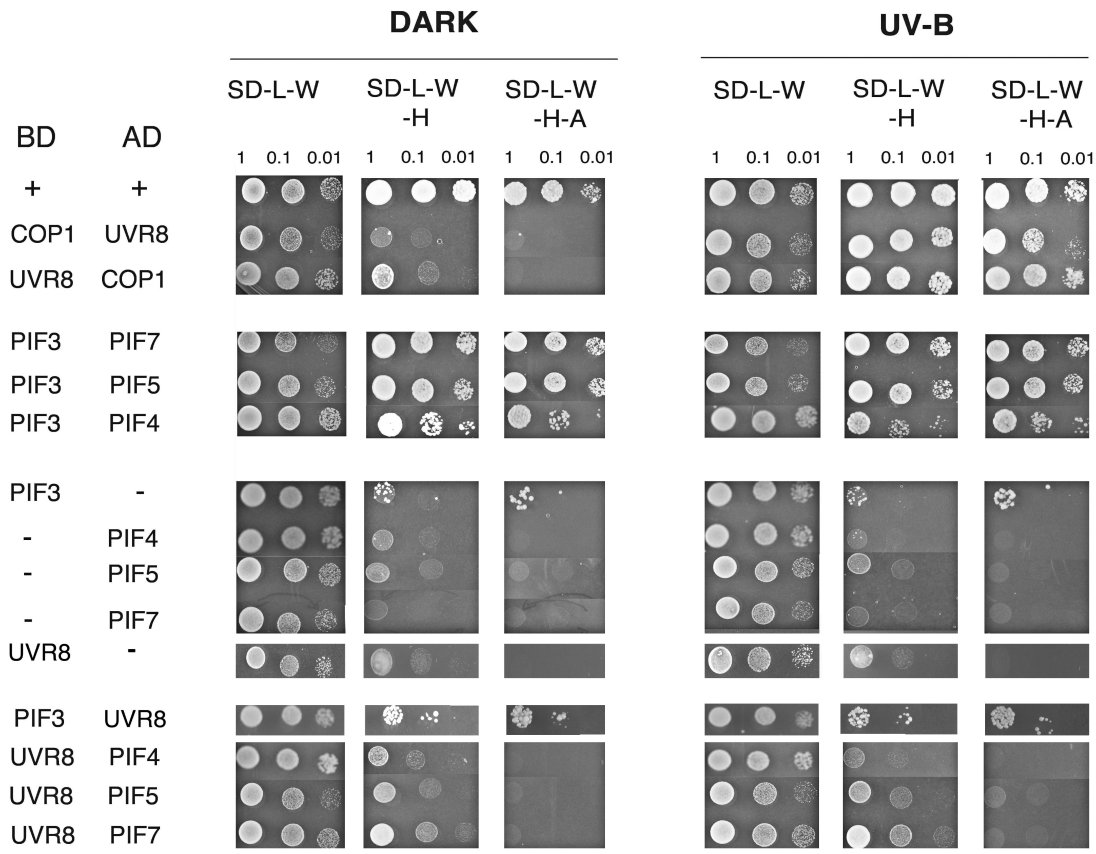

Fig. 4-5: UVR8 does not interact with selected PIFs. The interaction between the murine p53/GAL4BD fusion protein (+ve BD) and the SV40 large T-antigen/GAL4AD fusion protein (+ve AD) was used as a general positive control for the Y2H assay. The COP1-UVR8 interaction (in both fusion domain combinations) was used as a control for the effectiveness of the UV-B treatment. Heterodimerisation of PIFs was taken advantage of, in order to demonstrate that all recombinant PIF proteins behaved as expected during the assay. SD-L-W medium was used as a control for the viability of the spotted cells. Interactions were assessed on low (SD-L-W-H) and high (SD-L-W-H-A) stringency selection plates. Yeast spottings were performed from cell suspensions with three different cell densities (OD=1, 0.1 and 0.01). Results are representative of four repeats (Adapted from Hayes et al., 2014).

4.6 The Chromatin Remodelling Factor PKL/EPP1 does not interact with UVR8 in yeast.

Although the main focus throughout this project was almost exclusively on the post-translational modifications of nucleosomal histone molecules in trying to assess whether UVR8 is involved in the regulation of transcription at the epigenetic level, a relatively recent report brought a chromatin remodeller to our attention. **P**IC**KL**E (PKL), also known as **E**nhanced **P**hotomor**p**hogenic 1 (EPP1), possesses a nucleosome-stimulated ATPase activity, and it was shown to suppress photomorphogenesis (Jing et al., 2013). Interestingly, however, its function did not involve direct inhibitory effects on photomorphogenesis-promoting genes. Instead, PKL appeared to fulfil its role by keeping the levels of H3K27me3 (a repressive histone mark) low, upon the promoters of skotomorphogenesis - promoting genes (e.g genes involved in cell elongation). A compelling finding of this study was that HY5 was also found to associate with the promoters of the same genes, exerting an inhibitory effect on their expression both directly, by an intrinsic transcription-repressing activity, and indirectly by increasing the levels of H3K27me3. In addition, PKL and HY5 were shown to interact physically, thus promoting the hypothesis that they are antagonising each other for the dominating effect on the expression of the skotomorphogenesis - promoting genes. *PKL* expression was found to be decreased by light in a photoreceptor - dependent manner, but the authors did not include UVR8 and photomorphogenic UV-B in their study. It was therefore decided to investigate the possibility of a direct interaction between PKL and UVR8, which if present would reveal a novel functional pathway for UVR8. To this end, *PKL* coding sequence was cloned in the pGADT7 vector and tested against the UVR8-BD fusion for interaction under both UV-B supplemented and UV-B free conditions (Fig 4-6). No interaction could be detected. Repeated attempts to detect the PKL-AD fusion protein in protein extracts from transformed yeast were unsuccessful. However, when plasmid was rescued out of the yeast cells and sequenced, the construct appeared to be mutations-free. It is also unlikely that there is a mutation in the vector itself, as the very same aliquot of vector had been used for other constructs without any problems. Most probably, the PKL-AD fusion is not tolerated at high amounts in the yeast cells and the protein levels are kept low, below the limit of

detection of the immunoblotting procedure, but still sufficient for an interaction to be observed, if such interaction is present (Tucker et al., 2009).

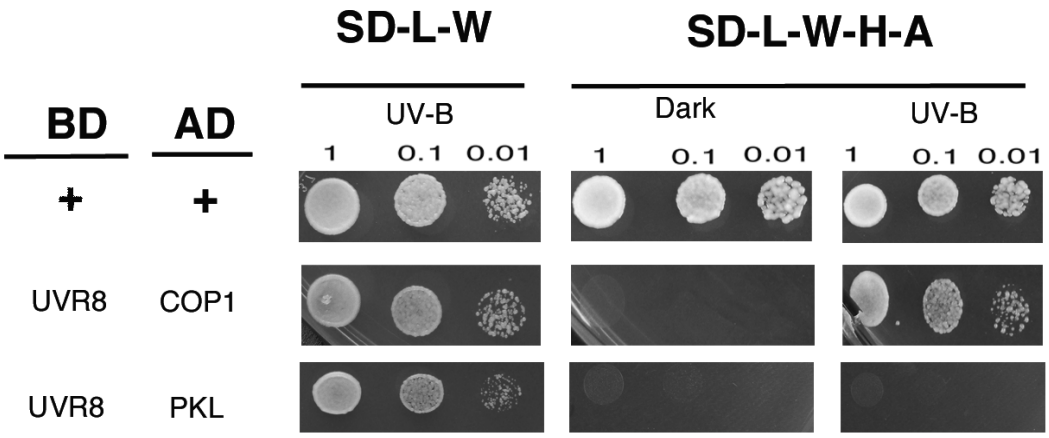

Fig. 4-6: UVR8 does not interact with PKL The interaction between the murine p53/ GAL4BD fusion protein (+ve BD) and the SV40 large T-antigen/GAL4AD fusion protein (+ve AD) was used as a general positive control for the Y2H assay. The UVR8-COP1 interaction was used as a control for the effectiveness of the UV-B treatment. SD-L-W medium was used as a control for the viability of the spotted cells. Interactions were assessed only on high stringency (SD-L-W-H-A) selection plates. Yeast spottings were performed from cell suspensions with three different cell densities (OD=1, 0.1 and 0.01). Results are representative of two repeats.

4.7 Functional analysis of Arabidopsis T-DNA-insertion mutant lines for certain HATs and HDACs.

After obtaining no interesting results with the targeted Y2H assays, with the possible exception of FVE, for which, as argued in the relevant section, the findings need to be validated via alternative approaches, it was decided to proceed to *in planta* functional analyses for the HATs and HDACs of interest. There was hesitation to exclude candidates from further consideration simply on the basis of a lack of interaction in yeast. A possible involvement of a particular HAT and/or HDAC in UVR8-mediated responses does not necessarily have to be mediated by a direct physical interaction with UVR8 itself. Indeed, histone acetylation and/or deacetylation are commonly performed by large protein complexes, where the subunits with the actual catalytic activity are surrounded by numerous adaptor proteins that contribute to the structural integrity of the complex. Therefore, subsequent analysis was undertaken for all the histone modifying proteins of interest.

T-DNA insertional mutant lines were identified (Fig 4-7), all in the Col (0) background except *hd1* which is in the Ws background. Homozygosity for the insertions was ascertained by PCR-based genotyping (Fig 4-7 A.). For *hd1* in particular, this step was omitted as it is a published line (Tian et al., 2003), which was kindly provided to us by the corresponding author of the study. The severity of the mutational effect was assessed, for each line, by comparing the transcript abundance levels of the affected gene in mutant and WT plants (Fig 4-7 B.) The results indicated that the *gcn5*, *taf1*, *hac5* and *fve* lines were all "knock out" mutants. Regarding *hd1* plants, RT-PCR analysis led to the detection of a greatly reduced full length *HD1* transcript. This is in agreement with the findings of Tian et al., who, when characterising this mutant line, found trace amounts of the HD1 protein on immunoblots. Strictly speaking such a line should be considered a "knock down" mutant, but the authors regarded it as being "practically null".

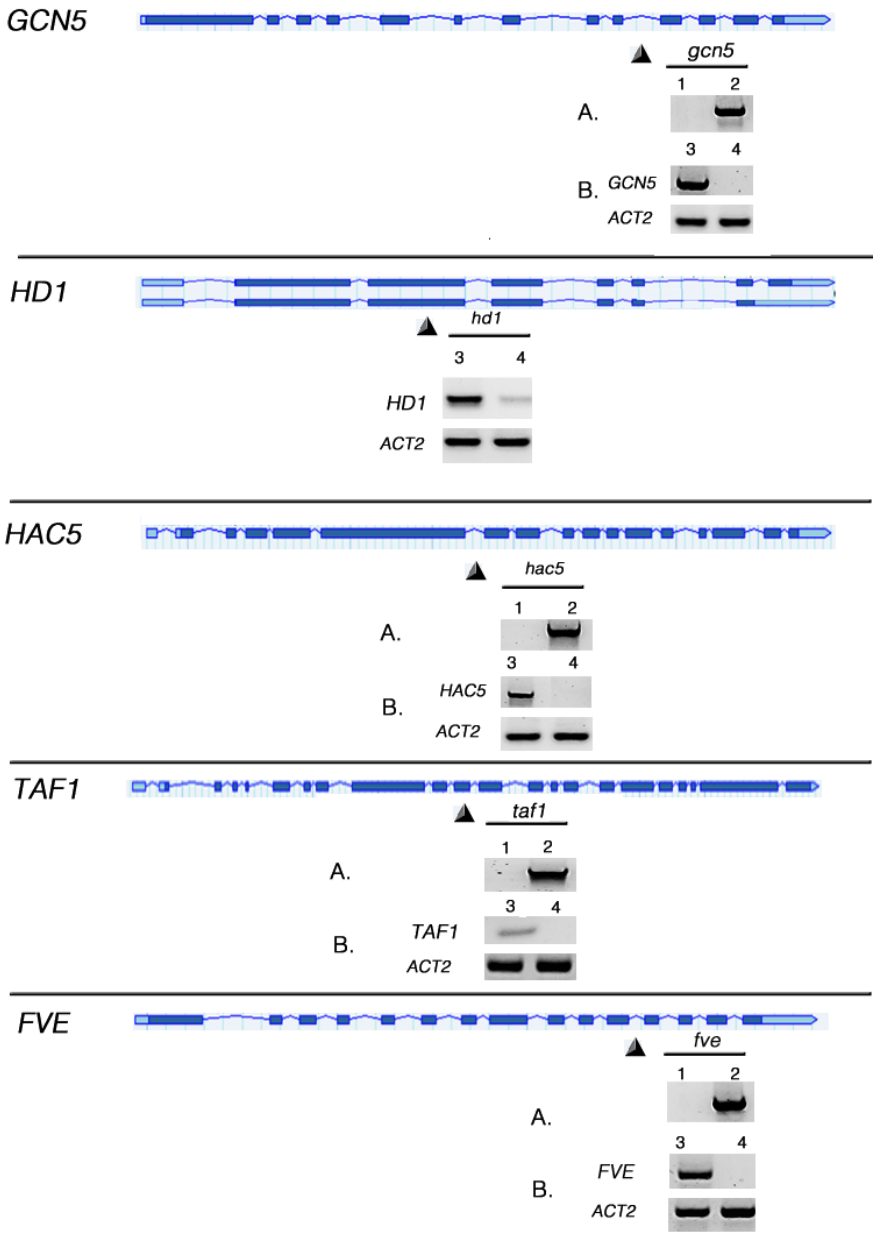

Fig. 4-7: Identification of T-DNA insertion mutant lines for the HATs and HDACs of interest.

A genome browser view of each gene is presented, and the approximate location of every T-DNA insertion (according to TAIR database) is annotated with a triangle. Exons are depicted as dark blue thick lines, untranslated regions as light blue thick lines and promoters or introns as slim lines. For each gene, Panel A shows the genotyping results. Lane 1 corresponds to the PCR outcome when primers flanking the T-DNA insertion were used, and it should not give product if an insertion is present; Lane 2 shows the PCR product when a Left Border T-DNA-specific primer and a locus-specific primer are used. Panel B shows the results of RT-PCR using gene specific primers, which amplify the full length coding sequence of each gene, and *ACT2* primers as a control. Lane 3 : WT cDNA Lane 4 : mutant line cDNA.

4.7.1 All mutant lines showed WT phenotypes in standard UV-B responses

Having available "loss of function" mutant plants for the histone modifying proteins under consideration, they were subjected to experimentation to assess their behaviour in a set of typical UVR8-mediated photomorphogenic UV-B responses. Firstly, hypocotyl elongation assays were undertaken to observe the effect of UV-B light on the rate of hypocotyl elongation. WT Col(0) plants were used as a reference against which the mutant lines were compared, whereas *uvr8-1* and *hy5/hyh* plants, which are known to display a hypo-sensitive response for this assay, were used as negative controls. WT L*er* and WT Ws plants were also included to account for differences between the Arabidopsis ecotypes, since the *uvr8-1* mutants are in the L*er* background while the *hy5/hyh* and *hd1* mutants are in the Ws background. Each genotype received two different light treatments, one in which the plants were germinated under low fluence rate white light (approximately 1.5 μmol m^{-2} s^{-1}), without any measurable UV-B (-), and one supplemented with 1.5 μmol m^{-2} s^{-1} narrow band UV-B (+). Hypocotyl lengths were measured 5 days after germination in a sample of at least 25 seedlings. In addition, as under this particular experimental setup CHS protein levels are known to increase substantially in a UVR8-dependent manner following UV-B illumination, protein was extracted from the remaining seedlings and immunoblots with anti-CHS antibody were performed. The results revealed (Fig 4-8 A and B) that all mutant lines of interest appeared to be UV-B responsive, exhibiting at least 3-fold shorter hypocotyls under UV-B, similarly to their WT counterparts. In detail, the UV-B (-) / UV-B (+) ratio of hypocotyl lengths was higher than 3.5 for WT Col(0) , *taf1*, *hac5*, and *fve* and equal to 3 for *gcn5*. For Wt Ws, WT L*er*, and *hd1* the ratio was between 3 and 3.5. Not surprisingly, *uvr8-1* and *hy5/hyh* mutants displayed a UV-B (-) / UV-B (+) ratio of hypocotyl lengths lower than 1.6, consistent with their hypo-sensitive phenotype. In support of the above findings, CHS protein levels were found markedly increased, upon UV-B illumination, in all mutant lines of interest (Fig 4-8 C.). It should be clarified at this point, that in young developing seedlings CHS expression is also subject to regulation by UV-B-independent developmental cues. This sometimes leads to the detection of faint signals in protein extracts from non UV-B-treated plants, or from UV-B treated *uvr8-1* mutants (Fig 4-8 C.).

Finally, the transcript abundance of three well known UV-B responsive UVR8-regulated genes, namely *HY5, ELIP.1* and *CHS,* was examined in gene expression assays. Three weeks old plants of all different genotypes, grown under continuous low fluence rate white light ($\leq$ 20 μmol m^{-2} s^{-1}), were transferred to 3 μmol m^{-2} s^{-1} narrow band UV-B for 4 hours. Total RNA was then isolated, cDNA was synthesised and the transcript levels were assessed via semi-quantitative RT-PCR. Only the *uvr8-1* mutants did not show the UV-B-induced accumulation of the aforementioned transcripts (Fig 4-9). Taken together, our data imply that none of the HATs/HDACs of interest is essential for the UV-B responses which we tested. The conclusion to which the analysis points is that either they are not involved at all, or they have a dispensable role which is fulfilled, in their absence, by a functionally related histone modifying protein.

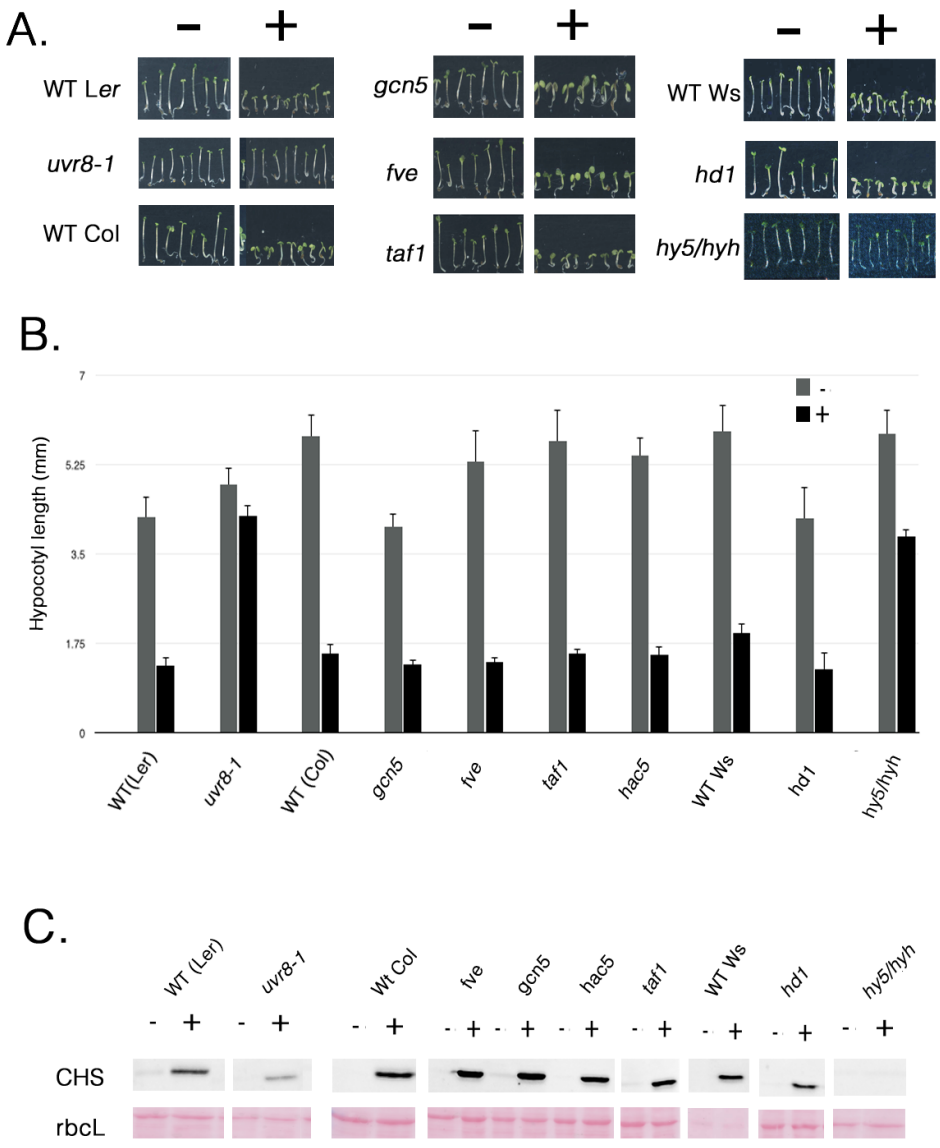

Fig. 4-8: Hypocotyl assay and CHS protein abundance. **-** : Low fluence rate white light (1.5 µmol m^{-2} s^{-1}), no measurable UV-B ; + : Low fluence rate white light supplemented with 1.5 µmol m^{-2} s^{-1} narrow-band UV-B. **A.** Photographs of representative seedlings from each line, which were germinated and grown for 5 days under UV-B-supplemented or UV-B-free light. **B.** Bar-chart of the average hypocotyl length values for each line, under the two distinct light conditions of the assay, 5 days after germination. Error bars represent SE ($n \geq 25$) . **C.** Anti-CHS antibody immunoblots on protein samples prepared from crude protein extracts of 5 days-old seedlings, subjected to the light treatments described above. Ponceau staining of the large subunit of RuBisCo (rbcL) is presented as a loading control. All tested lines, except *uvr8-1* and *hyh5/hyh* which served as negative controls, displayed UVR8-dependent, UV-B stimulated increase of the levels of immunoreactive CHS protein. Results are representative of three independent repeats.

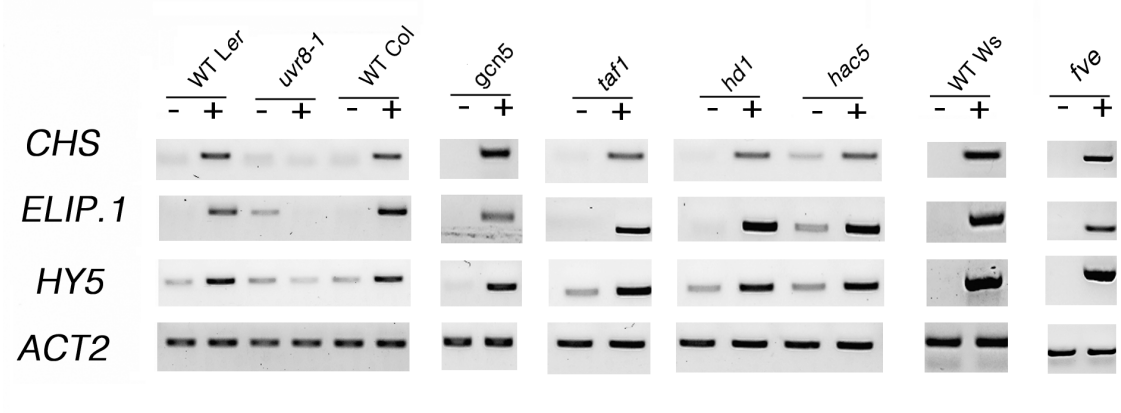

Fig. 4-9: Gene expression assay using semiquantitative RT-PCR. All tested lines appeared UV-B responsive.

- : Low fluence rate white light (20 µmol m^{-2} s^{-1}); + : 3 µmol m^{-2} s^{-1} narrow band UV-B for 4 hours.The transcript abundance of three genes, which respond to UV-B in a UVR8-dependent manner, was determined. All tested lines, except *uvr8-1* which was employed as a negative control, displayed accumulation of *HY5*, *ELIP.1* and *CHS* transcripts following UV-B exposure. *ACT2* was used as a control to demonstrate that equal amounts of starting cDNA template was used for the PCRs. Results are representative of three independent experiments.

4.8 Discussion

The results presented in this chapter summarise our findings from the attempts made to elucidate the nature of UVR8 involvement in the regulation of histone acetylation over certain UV-B responsive loci (Chapter 3). Yeast two hybrid assays were undertaken as the preferred preliminary approach in looking for direct interactions of candidate histone modifying proteins with UVR8, because these assays need the least optimisation compared to alternative *in vitro* or *in vivo* procedures (e.g pull-down assays, Co-IPs, BiFC etc).

On the basis of their sub-cellular localisation, and their preferred targets, HATs are divided into two classes: HAT-A and HAT-B. The first are nuclear and acetylate nucleosomal core histones, whereas type B HATs are found predominantly in the cytoplasm and catalyse the acetylation of free histones (Boycheva et al., 2014). There are at least 10 different HAT-A acetyltransferases in Arabidopsis, and they are grouped in four (Pandey et al., 2002) or five (Boycheva et al., 2014) families. Among them are the family of **G**CN5-related **N**-terminal **A**cetyl**t**ransferases (GNATs), the **M**OZ, **Y**bf2/Sas3, **S**as2 and **T**ip60 (MYST) - related HATs, the p300/**C**REB **B**inding **P**rotein (CBP) -related HATs and, finally, the TAF1. Plant HDACs, on the other hand, are slightly less diverse being classified in three distinct groups depending on homology to yeast HDACs. Nevertheless, Arabidopsis appears to have no less than 17 different individual HDACs (Ma et al., 2013). Essentially, therefore, our strategy had to rely on selective, targeted attempts, against specific members which appeared relevant to our working hypothesis in the light of published information. Obviously, the inevitable disadvantage is that there is a practical limit on how many candidates can be thus investigated, with a high risk of missing a truly interacting partner which might support the initial hypothesis. Nonetheless, this appeared as the most viable approach at the time and it was followed.

From the tested proteins, only FVE gave an encouraging result implying a weak interaction with UVR8 under UV-B free conditions (Fig 4-3). Yet, the fact that this finding was not consistently observed in all biological repetitions of the experiment raises suspicions that it might reflect an artefact, pointing towards the necessity of employing alternative techniques to resolve the truth of the matter. To that end, FLAG-tagged FVE constructs (Jeon and Kim, 2011) have been kindly donated by Prof Jung-mook Kim (Chonnam

National University Of Korea), and attempts are currently under way to perform Co-Immunoprecipitation assays with variously tagged (HA, GFP) UVR8.

As already argued, the involvement of a particular HAT/HDAC in UVR8-regulated UV-B responses could be taking place without direct physical interaction with the UV-B photoreceptor. Furthermore, the recruitment of the HAT and/or HDAC complexes to the appropriate loci might be mediated by a downstream effector of the UVR8-initiated signalling. Interesting hints to that direction are given by the hypocotyl length phenotypes of *taf1/hy5* plants under various light qualities (Bertrand et al., 2005), which revealed that the long hypocotyl *hy5* phenotype becomes markedly increased when TAF1 is not present. Conversely, the *gcn5/hy5* plants displayed a less severe hypocotyl length phenotype compared to the *hy5* single mutant plants, thus suggesting a different relationship between GCN5 and HY5 (Benhamed et al., 2006). It would be interesting to perform Y2H assays to address the possibility of direct physical interactions between HY5 and these two HATs. Even more informative, though time consuming, would be the generation of *uvr8-1/taf1* and *uvr8-1/gcn5* double mutants and their functional analysis under UV-B along with the *taf1/hy5* and *gcn5/hy5* plants, as well as the respective single mutants. Would TAF1 still display synergistic effects with HY5 under UV-B? And if so, what would the epistatic relationship with the *UVR8* locus be? The answers to these questions, and to similar ones for GCN5 and HD1 which have documented antagonistic functions in light signalling (Benhamed et al., 2006), may not be straight forward as functional redundancy might impose the need of triple, quadruple, or even multiple mutants. Nonetheless, clear effects might be observable and valuable insights might be gained for the formulation of alternative working hypotheses.

The *in-planta* assays performed after obtaining the “loss of function” mutants for the HATs/HDACs of interest did not reveal any interesting findings. Of course, this conclusion only applies to the particular tested responses, and it is possible that, had other UV-B-related phenotypic traits been investigated, clearly observable differences might come out. For example, the inhibition of primary root elongation by UV-B (Tong et al., 2008) has been used to demonstrate that *fve* plants are less responsive to UV-B than the WT (Campi et al., 2012). Eventually, however, if one wishes to make claims about direct involvement of the HATs/HDACs of interest in the deposition of the H3K9,14diac and H3K56ac histone

marks over specific UVR8-regulated genetic loci, ChIP assays with the same setup as described in Chapter 3 would have to be performed on WT plants and the single mutants described in this chapter. Unfortunately, as genotyping of successive generations had to be performed, these mutant lines became available quite late during this project, and even when seeds from homozygous individuals were obtained, the material was hardly enough for performing enough biological repetitions of ChIP assays, which are quite demanding in starting tissue. Seeds are currently being bulked up with the intention of performing as soon as possible these ChIP assays, at least for *fve*, *gcn5, taf1* and *hd1*. It is nonetheless worth keeping in mind that, firstly, functional redundancy might again mask the effects of single members' loss of function, and secondly, global alterations in the histone acetylation levels in these mutant lines may need to be taken into account when interpreting the results. FVE is known to act in partial redundancy with its homologue MSI5 (Gu et al., 2011) and ChIP assays on double mutants might be necessary. The same applies to the homologue pairs TAF1 - TAF2 and HD1 - HDA6. With regard to GCN5, trying to tackle functional redundancy would probably be more difficult, although there is not a close homologue in Arabidopsis. Instead, there are various GCN5-related proteins in the GNAT family that might be able to compensate for a GCN5 loss-of-function. For the pair HD1-HDA6 in particular, an attractive alternative approach would be to consider using mutant and/or over-expressing plants of the recently identified **H**istone **D**eacetylase **C**omplex 1 (HDC1), which is represented by one gene copy in the Arabidopsis genome, interacts physically with HD1 and HDA6, and has been demonstrated to affect H3K9,14diac levels on selected loci (Perrella et al. 2013). Hence, HDC1 would also be a candidate to test for direct interactions with UVR8 and HY5. Finally, if any promising findings come out of the above approaches, direct ChIP assays which would target the candidate HAT and/or HDAC on the respective chromatin loci might be employed to consolidate the results. This might require the use of transgenic lines, where the candidate histone modifying protein would be tagged to an epitope for which ChIP grade antibodies are commercially available.

With regard to the PIFs, no direct physical interactions with UVR8 were observed (Fig 4-5), providing no links to the working hypotheses dealt with in this project. It was later demonstrated that photomorphogenic UV-B, perceived by UVR8, triggers degradation of PIF4 and PIF5, and stabilises growth-repressing DELLA proteins, thus leading to

inhibition of auxin biosynthesis via a dual mechanism (Hayes et al. 2014). Moreover, recent work by colleagues in our laboratory has implicated high temperature with the UVR8 dimer -monomer kinetics. PIF4 is an important component of plant high temperature signalling and has been found to be important for the integration of diverse environmental cues during plant development (Koini et al., 2009). Together these findings show that UVR8 signalling is closely integrated with pathways where PIFs are major effectors, and it would be interesting to know in more detail the molecular basis of these crosstalks.

Regarding DDB1a, DDB1b and DDB2, which were also found not to interact with UVR8 (Fig 4-3 and Fig 4-4), *in planta* assays on their respective single mutants, similar to those undertaken for the HAT and HDACs single mutants (Fig 4-8 and Fig 4-9), might be informative. Seeds from homozygous *ddb2* plants have been obtained, but they were not examined closely for altered UV-B responsiveness, as substantial time and effort had to be invested in pursuing the second goal of this project, namely identifying novel transcription factors involved in the UV-B induced up-regulation of *HY5*. The three remaining chapters of this thesis summarise the most interesting findings from this research.

CHAPTER 5 : YEAST ONE HYBRID SCREENS

5.1 Introduction

The intensive research that followed the identification of UVR8 as a UV-B specific photoreceptor has unraveled various aspects of the photomorphogenic UV-B responses of higher plants. However, some facets of these responses have monopolised the scientific interest while others have received relatively little attention. For example, the elucidation of the structure of UVR8 was the main focus following the discovery that the protein can detect UV-B radiation (Rizzini et al., 2011). Once the structure became available (Christie et al., 2012; Wu et al., 2012), a unique photochemistry was implied by the fact that UVR8 does not need external chromophores in order to exert its function, and the focus shifted towards the clarification of the mechanistic details of photoreception (Liu et al., 2014; Wu et al., 2014). Moreover, various features of UV-B signalling have become clearer (Huang et al., 2014). Preliminary studies of the kinetics of the photocycle and the regeneration of the photoactive dimeric form have already been published (Heilmann and Jenkins, 2013; Heijde and Ulm, 2013). On a more integrative level, current information on the role of UVR8 in broader physiological and ecophysiolgical phenomena is regularly being updated (Singh et al., 2014; Tossi et al., 2014). Nevertheless, there is one aspect of UVR8 research that has remained almost static during the past few years. Namely, how does UVR8 regulate transcription? On this question, our understanding has remained relatively poor and one has remarkably little to say. Shedding some light on this side of UVR8 function has been the main goal of this project. In the previous chapters, some interesting results implicating UVR8 with chromatin remodelling processes were presented. In the following chapter we attempt to address a different question. In particular, although it is well established that HY5 and its homologue HYH are the two transcription factors that are the key effectors of UVR8-regulated UV-B photomorphogenic responses, little data are available as to which transcription factors mediate the expression of *HY5* and *HYH* themselves (Abbas et al. 2014; Binkert et al 2014). These early transcriptional events remain largely unclear. In order to improve current understanding, a Y1H approach was undertaken. The rationale is essentially the same as that of a Y2H screen. A known target

protein is employed as a “bait”, in order to retrieve potentially interacting partners from a pool of “prey” proteins which are usually available as a cDNA library. The difference in the case of a Y1H screen is that the “bait” target is a DNA sequence. Thus, the retrieved clones are likely to be novel transcription factors interacting specifically with the “bait” DNA.

Although HY5 and HYH are partially redundant in regulating UV-B responses, HY5 is the major effector. For this reason, only target DNA sequences corresponding to the promoter of *HY5* were used as “baits”. Generally, if no information is available about the candidate *cis*-regulatory elements of a promoter sequence, the whole promoter can be used as a “bait”. This, however, increases the likelihood of retrieving many false positive clones and lowers the resolution of the method, since no conclusions can be drawn as to which specific sequence of the “bait” promoter is recognised by a particular clone. Fortunately, for *HY5* in particular, a team of collaborators had already carried out preliminary work towards identifying the *cis*-regulatory elements that might be crucial for the UV-B control of *HY5* expression. By undertaking a “linker scan” approach, successive sequences of the promoter of *HY5* were mutated in a stepwise manner, and the resulting mutant versions were assayed for UV-B responsiveness. This led to the identification of two sequences, located relatively close to one another, which were designated as UV-B box1 and UV-B box2 (Fig 5-1). The first, located approximately at position -105 from the transcriptional start site, displays sequence similarity to **M**yb **R**ecognition **E**lement (MRE) boxes. The second, positioned at -87 from the transcriptional start site, is similar to **A**CGT- **C**ontaining **E**lement (ACE) boxes. These data were kindly provided by Prof Ferenc Nagy (University of Edinburgh) as unpublished information, and both putative cis-regulatory elements were employed as “baits” in the Y1H approach that was undertaken. Shortly before the completion of this thesis the above data were included in the study published by Binkert et al. (2014), where UV-B box1 and UV-B box2 were renamed as ACG-box and T/G-box respectively. Nonetheless, it was decided to keep the original designations throughout the thesis, as they highlight the functional involvement of the two cis-elements in UV-B responses.

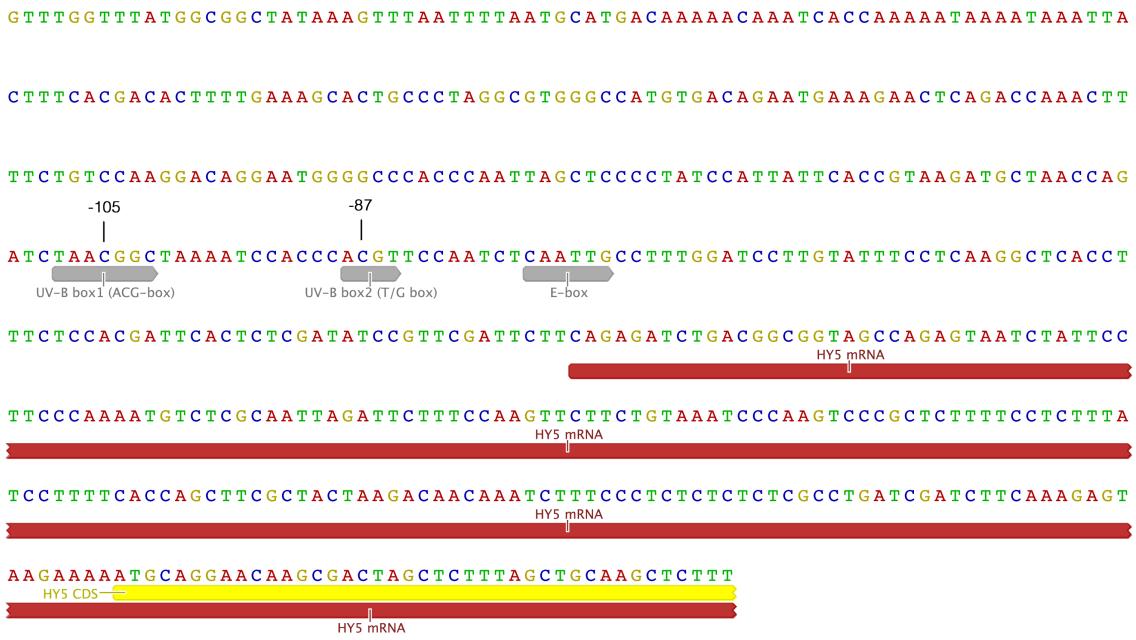

Fig. 5-1 : Genome browser view of the genetic locus of the promoter of *HY5*. The functionally characterised *cis*-regulatory elements of the *HY5* promoter are annotated in grey. UV-B box1 (ACG-box) and UV-B box2 (T/G box), positioned at -105 and -87 from the transcriptional start site respectively, are the ones that are primarily involved in UV-B responses (Binkert et al 2014). The E-box is a *cis*-regulatory element located downstream of UV-B box2 and is involved in light signalling (Abbas et al. 2014) but has minor contribution to UV-B responses (Binkert et al. 2014). For the Y1H screens of this project only UV-B box1 and UV-B box2 were considered for construction of "bait" DNA sequences. Part of the mRNA and the CDS of *HY5* are also visible (red and yellow annotations respectively). (*Image created via the Geneious software, Biomatters Ltd,*)

5.2 Construction of "bait" sequences and generation of yeast reporter strains

The selection of suitable "bait" sequences is of utmost importance for a successful Y1H screen. Since UV-B box1 and UV-B box2 had already been identified as potentially crucial for the UV-B regulation of *HY5* expression, they were used, individually and in combination, as target DNAs for the screens. Moreover, in order to increase the possibility of detecting weakly interacting TFs which bind to the UV-B boxes transiently, each particular "bait" DNA was synthesised in such a way that it contained tandem repeats of the UV-B boxes. Usage of repeats (usually 3-4) has also been reported to be beneficial by providing an optimal distance between the plant regulatory elements being tested and the core promoter of the yeast *HIS3* gene, which immediately follows separating them from the reporter gene (Lopato et al., 2006). Additionally, the three bases that naturally flank each side of the UV-B boxes were included in the "bait". The reason for this inclusion was that the bases surrounding the core sequence, at least for some *cis*-regulatory elements, have long been known to be important in stabilising the interaction with particular TFs (Meshi and Iwabuchi, 1995). Including more flanking bases could increase stability but it would also favour false positive interactions, especially since tandem repeats of the UV-B boxes were used. Thus, the threshold for the additional flanking bases was arbitrarily set to three. Eventually, the three target DNA sequences that were employed in the Y1H approach were : "bait UV-B box1", hereafter referred to as b1, consisting of three tandem repeats of UVB-box1 with its flanking bases on either side; "bait UV-box2", hereafter referred to as b2, comprising three tandem repeats of UVB-box2 including the three flanking bases on each side; finally, "bait UV-B boxes 1&2", hereafter b1,2, containing two tandem copies of UV-B box1 and UV-B box2 separated by their native intermediate DNA sequence, with the inclusion of the three flanking bases upstream of UV-B box1 and the three flanking bases downstream of UV-B box2 (Fig 5-2, A.). Two instead of three copies were used for b1.2 because the presence of the intermediate sequence, which naturally separates the two UV-B boxes in the *HY5* promoter, substantially increases the length of the "bait" and might favour the detection of more false positive clones if repeated excessively.

All three baits were cloned into the pINT-His3/NB integration vector and were subsequently integrated into the yeast (strain AH109) genome via homologous recombination with the *PDC6* gene, which is non-essential for yeast survival (Fig 5-2, B.). The resulting transformed yeast cells are referred to as yeast reporter strains (Ouwerkerk and Meijer, 2011) since they carry the *HIS3* reporter gene under the transcriptional control of the "bait" and the core promoter of the *HIS3* gene. Successful integration was confirmed via PCR using a forward primer that anneals with a genomic region downstream of the *PCD6* gene and a reverse primer that anneals within the *HIS3* reporter gene (Fig 5-2, C.) All PCR products were sequenced to verify that all yeast reporter cells carried the correct "bait" sequence.

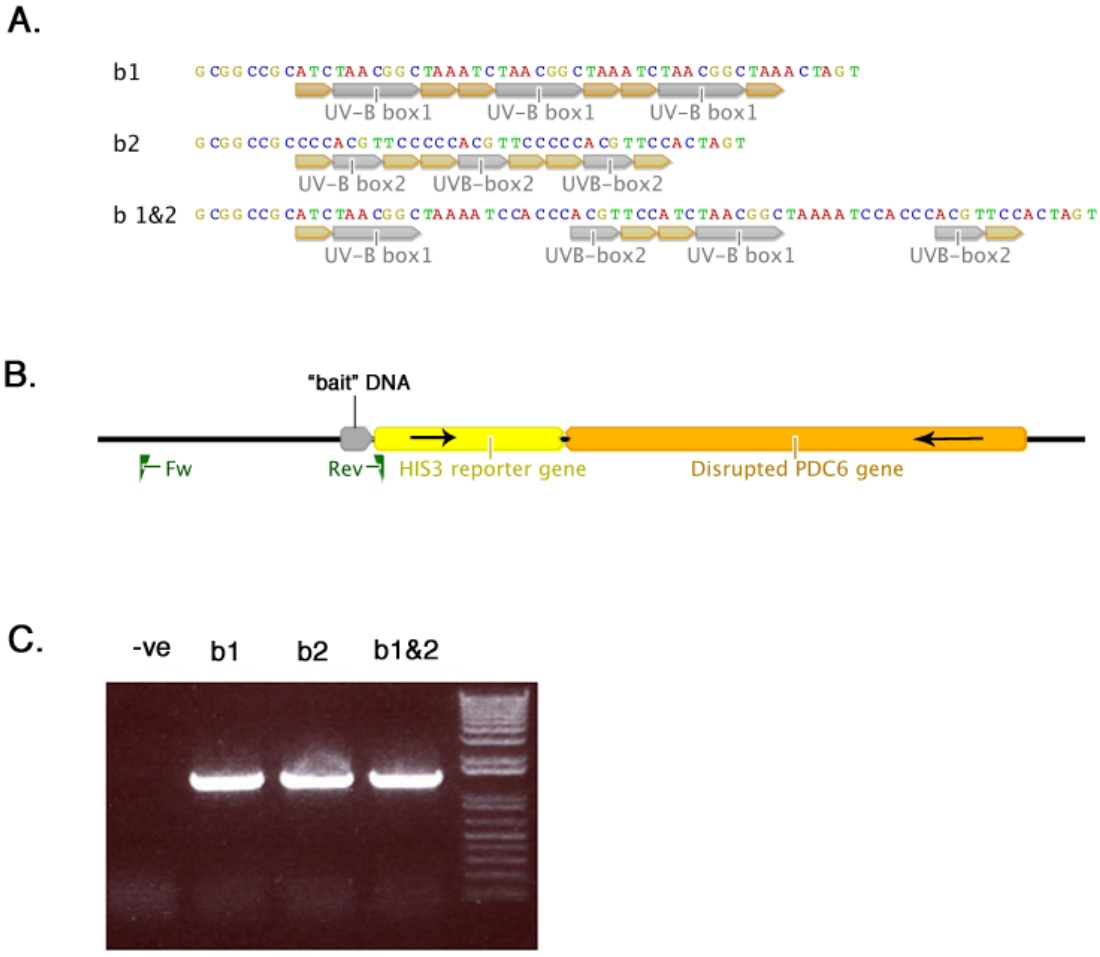

Fig. 5-2 : A. Sequence detail of the three bait sequences used in the Y1H screens. The UV-B boxes are annotated (gray) together with the there flanking bases (brown). **B.** Schematic view of the integration site of the "bait-reporter" construct into the yeast genome. The construct is introduced in the locus of the non essential *PDC6* gene. The arrows denote the orientation of the respective genes. The annealing sites of the primers used for determining successful integration are shown in green. **C**. Colony PCR on selected yeast reporter strain cells, with the primers shown in B**.** This particular combination of primers can give a PCR product only if the "bait-reporter" construct has been effectively introduced into the correct site in the yeast genome. Untransformed AH109 yeast cells were used as negative control.

5.3 Assessment of the yeast reporter strains for background growth on His-lacking medium

The *HIS3* reporter gene in the yeast reporter strains is preceded by a defined *cis*- acting sequence, which contains the heterologous plant regulatory elements and the core promoter of the homologous *HIS3* gene. It is possible for the latter to be recognised by native TFs of the yeast cells, thereby switching on the expression of the *HIS3* reporter gene. Moreover, the heterologous plant regulatory elements that are used as "baits" could also be recognised by some yeast transcription factors that have functional homology to plant transcription factors, resulting to "leaky" expression of the reporter gene. Such background growth would interfere with the subsequent screen. Hence, it was necessary to assess the growth characteristics of the yeast reporter cells on His-lacking medium. For that reason, 3-amino-1,2,4,-triazole (3-AT), a competitive inhibitor of the His3p enzyme, was used. The minimum concentration of 3-AT required to eliminate the background growth of every yeast reporter strain was determined via a titration experiment (Fig 5-3). Cells were streaked on plates containing various concentrations of 3-AT, rising with an increment of 2.5 mM (Lopato et al., 2006). All yeast reporter strains exhibited strikingly reduced growth when 2.5 mM 3-AT was present in the growth medium, with b1 showing some residual growth even at 5 mM 3-AT. However, the efficiency of the inhibitor has been reported to be dependent, among other factors, on the plating density of the cells (the higher the density the higher the required concentration of 3-AT, Ouwerkerk and Meijer, 2001). Due to the fact that when saturating screens are performed the plating density is extremely high, 7.5 mM of 3-AT was chosen as an optimum concentration for reducing the background growth during our screens.

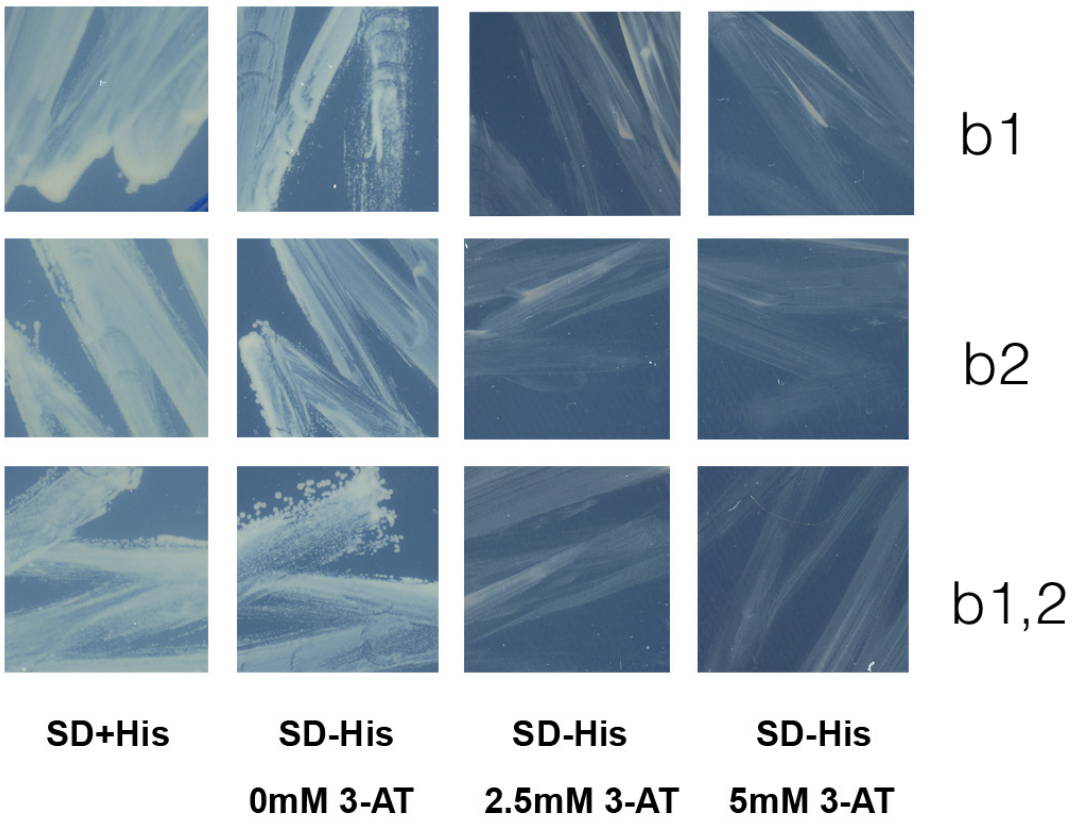

Fig. 5-3 : Titration experiment for determination of the optimal 3-AT concentration required under screening conditions. b1, b2 and b1,2 refer to the yeast reporter strains carrying the respective "bait" target DNA sequences. SD+His is complete growth medium used as +ve control to demonstrate the viability of the streaked cells. SD-His is His-lacking growth medium. 3-AT was supplemented in rising concentration with an increment of 2.5 mM. Results are representative of two independent repeats.

5.4 Yeast One Hybrid Library Screening

The actual screening procedure was performed by mating the yeast reporter strains (AH109) with the yeast strain in which the library was constructed (Y187). The library was a "Normalised , Universal Arabidopsis Mate & Plate" Library purchased from Clontech. The term "normalised" means that highly abundant housekeeping genes have been significantly reduced in copy number, whereas low abundance genes are increased in frequency and are relatively well represented. The term "universal" refers to a collection of cDNAs that have been prepared from appropriate mixtures of tissues, so that the broadest possible gene representation is provided. According to the manufacturer, the above features reduce up to three-fold the number of clones that need to be screened, with the recommended number being at least 10^6 clones.

Three individual screens (hereafter referred to as S1, S2 and S1.2) were performed, one for each "bait". Before the first screening attempt, a control mating experiment was undertaken in order to optimise the mating protocol in achieving the recommended (by the manufacturer) mating efficiency (2-5%). The same mating protocol was followed thereafter. In preparation for every screen, the first step was the validation of the optimum viability of the library, by ensuring that the number of colony forming units (cfu) present per ml of library cells was within the range recommended by the manufacturer (at least $2x10^7$ cells). Once satisfactory viability was ascertained, the library cells were used for mating with the yeast reporter strain. The presence of zygotes in the mating culture was established via microscopic observation and an aliquot of the culture was set aside for estimation of the number of diploid clones which were about to be screened. Once a saturating screen was confirmed (Fig 5-4 A.), the mated culture was plated on selective plates. After 10 to 14 days of growth, putative positive clones were visible as big colonies of yeast cells, in a background of much smaller ones (Fig 5-4 B.). All clones were subsequently re-streaked on selective medium supplemented with X-α-gal, as a first step of eliminating putative false positive clones via blue-white selection (Fig 5-4 C.).

Finally, colony PCR was performed on the clones that remained white after the second selection round and the resulting PCR products (Fig 5-4 D.) were sent for sequencing. The sequences were tested in a BLAST comparison against the Arabidopsis genome and the identity of each clone was determined.

A.

Screen	Library	Number of clones screened
S1	Normalised Universal Arabidopsis Mate & Plate Library	≃ $30x10^6$
S2	Normalised Universal Arabidopsis Mate & Plate Library	≃ $25x10^6$
S1.2	Normalised Universal Arabidopsis Mate & Plate Library	≃ $2x10^6$

B.

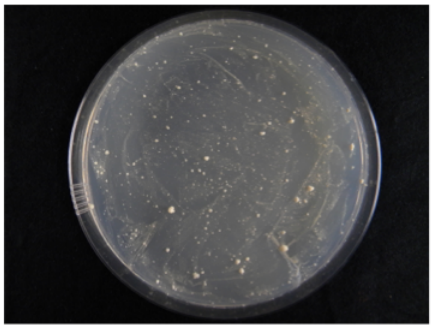

C.

D.

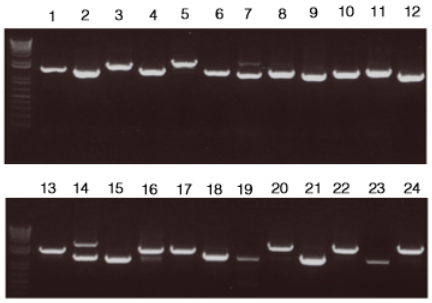

Fig. 5-4 : Main steps of the Y1H screening procedure. A. Sufficient number of clones was screened with all three "baits". The saturation threshold of 10^6 clones was exceeded in all three screens . **B**. Representative selective plate of a screen showing putative positive clones outgrowing a background of smaller "leaky" colonies. This also confirms that 7.5 mM of 3-AT had a balanced inhibitory effect. **C.** Representative plate from the 2nd round of screening via blue-white selection. Only white clones (red circle) were considered for further analysis. **D.** Typical PCR result from 24 random white clones. The PCR products vary, as different clones harbour different Arabidopsis cDNAs. PCR products were purified and sequenced to obtain the identity of each individual clone.

5.5 Putative positive clones identified by the Y1H Library Screens

The blue-white selection of clones proved to be an efficient early step towards elimination of false positives. More than 200 clones grew on the original selective plates for each screen, but the number of those considered for further analysis was reduced to less than a hundred after the blue-white selection. Thus, colony PCRs were performed on 96-well plates, an aliquot was run on agarose gels post-amplification to ensure the presence of product (Fig 5-4 D.) and the remainder of the PCR reaction was sequenced.

The sequencing results highlighted some interesting features of the technicalities around cDNA library construction. First, after performing a BLAST analysis of every sequence, the vast majority of clones were identified as cDNAs corresponding to genes that have no known function in specific DNA binding. Amongst them there were many "housekeeping" genes involved in photosynthesis, in primary or secondary metabolism, genes encoding structural proteins of the cytoskeleton, genes encoding proteins of the endo-membrane system, genes expressed only in specific organelles etc. This demonstrated that although a "normalised" library was used, the claimed "equalisation" in the representation of the cDNAs is only partial. Second, many of the sequenced products corresponded to partial rather than full length cDNAs. This is usually due to technical limitations of the library construction methodology, such as premature termination of the reverse transcription reaction (Zhu et al., 2001), but it might also reflect a true *in planta* condition, such as a high frequency of mis-splicing for a particular mRNA. Finally, a large number of clones (almost 2/3) were found not to be in frame with the Gal4-AD in the library vector, a direct consequence of an unspecific cloning strategy which renders only a random number of 1/3 of cloning events to be in the right **O**pen **R**eading **F**rame (ORF).

As the objective of the Y1H screens was the identification of novel transcription factors that might be involved in the UV-B regulation of *HY5* expression, only clones that represented annotated TFs were considered for further characterisation. Among them there were two R2R3 **My**o**b**lastosis (MYB) related transcription factors, AtMYB31 and AtMYB61, one **A**rabidopsis **NAC**- domain (ANAC) containing protein, AtANAC083, one **B**-**B**o**x** (BBX) containing protein, AtBBX21, also known as **S**alt **T**olerance **H**omologue 2 (STH2), one **S**quamossa **P**romoter-**L**ike (SPL) protein, AtSPL11, one member of the GRAS family of TFs (Gras-like TF), one MADS-box transcription factor, **Sh**atter**p**roof 2

(AtSHP2), one **W**ith **N**o Lysine (**K**) protein (AtWNK10) and finally two members of the **N**uclear **F**actor **Y** family (AtNF-YB2 and AtNF-YC9). Moreover, in the light of the results presented in chapter 3 where a UVR8-dependent regulation of the histone acetylation status on the promoters of some UV-B responsive genes was implied, two clones, corresponding to a **h**istone **ac**etyltransferace (AtHAC5) and a **h**istone **d**eacetylase (AtHD1) respectively, were also included in subsequent analysis (Table 5-1).

	YIH clones considered for further analysis	
S1	**S2**	**S1.2**
AT1G27360 *AtSPL11*	AT5G13180 *AtANAC083*	AT1G64630 *AtWNK10*
	AT1G74650 *AtMYB31*	AT3G12980 *AtHAC5*
	AT1G09540, *AtMYB61*	AT1G75540, *AtBBX21, AtSTH2,*
	AT1G08970, *AtNF-YC9*	AT5G59450, Gras-like TF
	AT5G47640, *AtNF-YB2*	AT4G38130, *AtHD1*
		AT2G42830, *AtSHP2, AtAGL5*

Table 5-1. Summary of the putative positive clones which were considered for further characterisation. The clones are listed according to which screen they were obtained from. All genes encode annotated Arabidopsis transcription factors with DNA binding specificity, except *AtSTH2* (green) which is a transcriptional co-regulator, and the two shown in red which encode a histone acetyltransferase (*AtHAC5*) and a histone de-acetylase (*AtHD1*). TAIR Annotation numbers are given for each clone.

5.6 Confirmation of Y1H interactions

As mentioned in the previous section, many of the clones recovered from the screens were truncated versions of the full length cDNAs and/or not in frame with the GAL4 activation domain. In fact, all clones listed in Table 5-1 were both partial length and out of frame. However, there are two major reasons not to exclude such clones from further analysis. First, yeast cells are reported to tolerate frameshift events during translation. These may occur as controlled ribosomal frame-shifting, largely affected by the secondary or tertiary structure of a particular mRNA (Dinman et al., 1997), or be increased in frequency by the use of specific antibiotics (such as the Geneticin G418 employed in our screens) which interfere with normal ribosomal function (Panchal et al. 1984). Second, even if a clone appears not to be in frame with the GAL4 activation domain, cryptic promoter elements in the bait plasmid may favour transcription of the cloned cDNA. If the latter encodes a transcription factor, its native activation domain could be sufficient to activate the *HIS3* core promoter and switch on the reporter gene. Thus, it is highly recommended (Ouwerkerk and Meijer, 2001) to validate the observed interactions by re-cloning the candidate clone in frame with the GAL4 activation domain and repeating the assay. To that end, the full length cDNAs of all genes listed in Table 5-1, except *AtHAC5*, were cloned in frame with GAL4-AD, in the Y2H vector pGADT-7. This vector is different from the one in which the library had been constructed (pGADT7-RecAB), but the essential features of both vectors are identical. Moreover, having the clones in the pGADT7 vector allowed their utilisation in subsequent Y2H experiments. In the case of *AtHAC5,* it was decided to clone only the partial length cDNA due to the relatively large size of the entire molecule (5kb).

Although the blue-white selection screened out those clones which interacted with yeast sequences as well as with the "bait" DNA, it did not provide any clues as to whether there is specificity of interaction within the "bait". The use of tandem repeats gives rise to sequence motifs that are not naturally present in the plant DNA. It is possible that such sequences give rise to apparently positive interactions which are in fact artificial and do not reflect true recognition of the *cis*-regulatory elements of interest. To account for this possibility, mutant "bait" target DNA sequences were synthesised and included in the confirmation assays (Fig 5-5). For consistency, these mutant "bait" sequences (hereafter

mb1, mb2 and mb1.2) were chosen to be identical with the mutations which led to the identification of the two UV-B boxes during the initial promoter linker scan assays (Data kindly provided by Prof. Ferenc Nagy).

Fig. 5-5 : Mutated "bait" target DNA sequences used during the confirmation of the Y1H screening results. Comparison of each bait with its mutant counterpart reveals that for mb1 and mb1.2 only the UV-B boxes of interest are mutated. In contrast, for mb2 the entire "bait" construct is different. As stated in the text, this is not ideal if one wishes to test the specificity of interaction against a defined cis-regulatory element. At the time at which these experiments were designed, however, the only known mutations that impaired the ability of UV-B box2 to function in UV-B signalling included the flanking bases on either side of the element. This inevitably led to alteration of the entire "bait" construct when the mutant "bait" was synthesised.

Two alternative approaches could be undertaken for the Y1H confirmation assays. One option was to follow a similar workflow with the screening procedures, by generating the yeast reporter cells in one strain (AH109) and introducing the candidate transcription factors in a strain of the opposite mating type (Y187). The two strains are then allowed to mate and the growth of diploid cells is assessed on selective medium. This procedure, however, introduces an unnecessary mating step, which is inevitable only if library screens are performed. Instead, a more straightforward protocol was adopted. All reporter cells were generated in one strain, they were subsequently transformed with the candidate transcription factors and, finally, possible interactions with the "bait" DNAs were determined by assessing growth on selective medium. The yeast strain of choice was Y187, because AH109 has been designed by Clontech mainly for Y2H assays and already possesses a *HIS3* reporter gene under the transcriptional regulation of yeast regulatory elements. Successful integration of all "baits" into the genome of the new yeast reporter strains (Y187) was confirmed via colony PCR (Fig 5-6 A.) as described previously (section 5.2 of this chapter). Due to the fact that "leaky" expression of the *HIS3* gene depends considerably on the genotype of the yeast strain (Ouwerkerk and Meijer, 2001), a new titration experiment to assess the required inhibitory amount of 3-AT was performed (Fig 5-6 B.). Finally, the expression of all recombinant transcription factors was tested via western blots against the HA epitope tag in yeast protein extracts (Fig 5-6 C.) Bands corresponding to the correct sizes could be detected for all but one transcription factor, namely AtWNK10, for which a band of almost half of the expected size was consistently obtained. This band presumably reflected a specific degradation product of WNK10. It was never present in protein extracts from untransformed yeast cells and when the WNK10-pGADT7 construct was rescued and sequenced, no problems could be detected with either the cloned gene or the plasmid. Similarly, the sequence obtained for the ANAC083-pGADT7 construct was as expected, even though the signal obtained in the blots was always very faint.

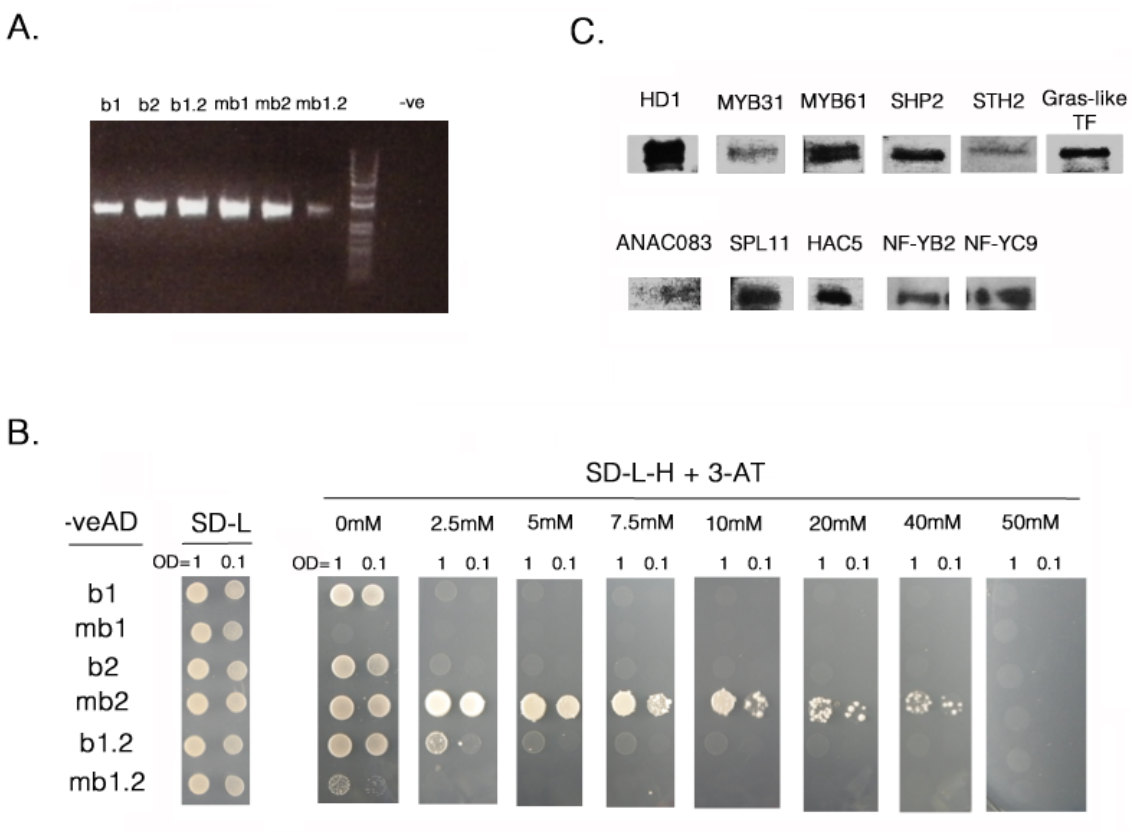

Fig. 5-6 : Basic steps before performing the direct Y1H assays for confirmation of the screening results . A. Colony PCR for confirmation of successful construction of Y187 "bait-reporter" strains. Untransformed Y187 cells were used as negative control. All PCR products were purified and validated by sequencing. **B.** Assessment of the "leaky" expression of the *HIS3* reporter. All different "bait-reporter" strains were transformed with the empty pGADT7 vector (-veAD) and their growth was monitored on His-lacking medium supplemented with different concentrations of the 3-AT inhibitor (SD-L-H + 3-AT). Histidine rich medium (SD-L), deprived only of Leucine for selection of the pGADT7 plasmid, was used as a control for the viability of the spotted cells. Spottings were performed with two different cell densities (OD= 1 and 0.1). **C.** Immunoblot results with anti-HA antibody on protein extracts of yeast cells transformed with the various pGADT7-TF recombinant vectors. With the exception of WNK10, for which no band of the correct size could be detected, all other HA-tagged transcription factors gave bands of the appropriate size. Results are representative of at least three repeats.

5.7 STH2, NF-YC9, ANAC083, MYB31 and MYB61 interact preferentially with UV-B box2 in direct Y1H assays

The direct Y1H assays, which were employed for confirmation of the screening results, revealed that five out of the eleven candidate transcription factors are truly interacting with the "bait" DNAs. When both UV-B boxes were used in combination (bait b1.2), STH2, NF-YC9, ANAC083, MYB31 and MYB61 fusions with the GAL4-AD recognised and bound to the "bait" DNA, allowing growth of yeast cells on selective medium (SD-L-H) supplemented with up to 7.5 mM 3-AT (Fig 5-7). When the same yeast reporter strains were transformed with the empty pGADT7 vector, 2.5 mM 3-AT was sufficient to reduce growth resulting form the auto-activation of the *HIS3* reporter gene and 5 mM 3-AT completely restrained "leaky" growth (Fig 5-6 C.). Moreover, none of the above transcription factors recognised the mutated version (mb1.2) of the bait DNA (Fig 5-7), suggesting that the observed interactions are specific. In an attempt to investigate whether any of the two UV-B boxes is preferentially recognised by these TFs, the Y1H assays were repeated using each UV-B box individually as "target" DNA. All the aforementioned TFs were capable of recognising the b2 "bait" DNA, consisting of three tandem repeats of UV-B box2, allowing growth of yeast cells on selective medium containing 3-AT as high as 5 mM (Fig. 5-8), whereas the "leaky" growth for this yeast reporter strain could be effectively managed with only 2.5 mM of 3-AT (Fig 5-6 C.). In contrast, none of the TFs was able to recognise the mutated "bait" mb2 when 45 mM 3-AT was supplemented to restrain the background growth (Fig. 5-8 and Fig. 5-6 C.). When the UV-B box1 - derived bait (b1) was used as "target" DNA, none of the transcription factors was able to recognise it in the presence of 2.5 mM 3AT in the medium (Fig. 5-9), which is the lowest inhibitory concentration required to restrain "leaky" growth for this bait-reporter yeast strain (Fig. 5-6 C.). The relatively poor growth observed in the case of MYB31 might indicate a weak and/ or unstable interaction with the target DNA, but such an interaction, if true, is evidently on the limit of detection with this experimental setup. As for the rest of the transcription factors isolated from the three screens, no interactions were observed with any of the available "baits" (Fig 5-10). Taken together the results suggest that, at least in the heterologous Y1H system, STH2, NF-YC9, ANAC083, MYB31 and MYB61 are capable of interacting with the part of *HY5* promoter which consists of UV-B box1 , UV-B box2

and their native intermediate DNA sequence. This interaction seems to occur via a preferential binding with UV-B box2.

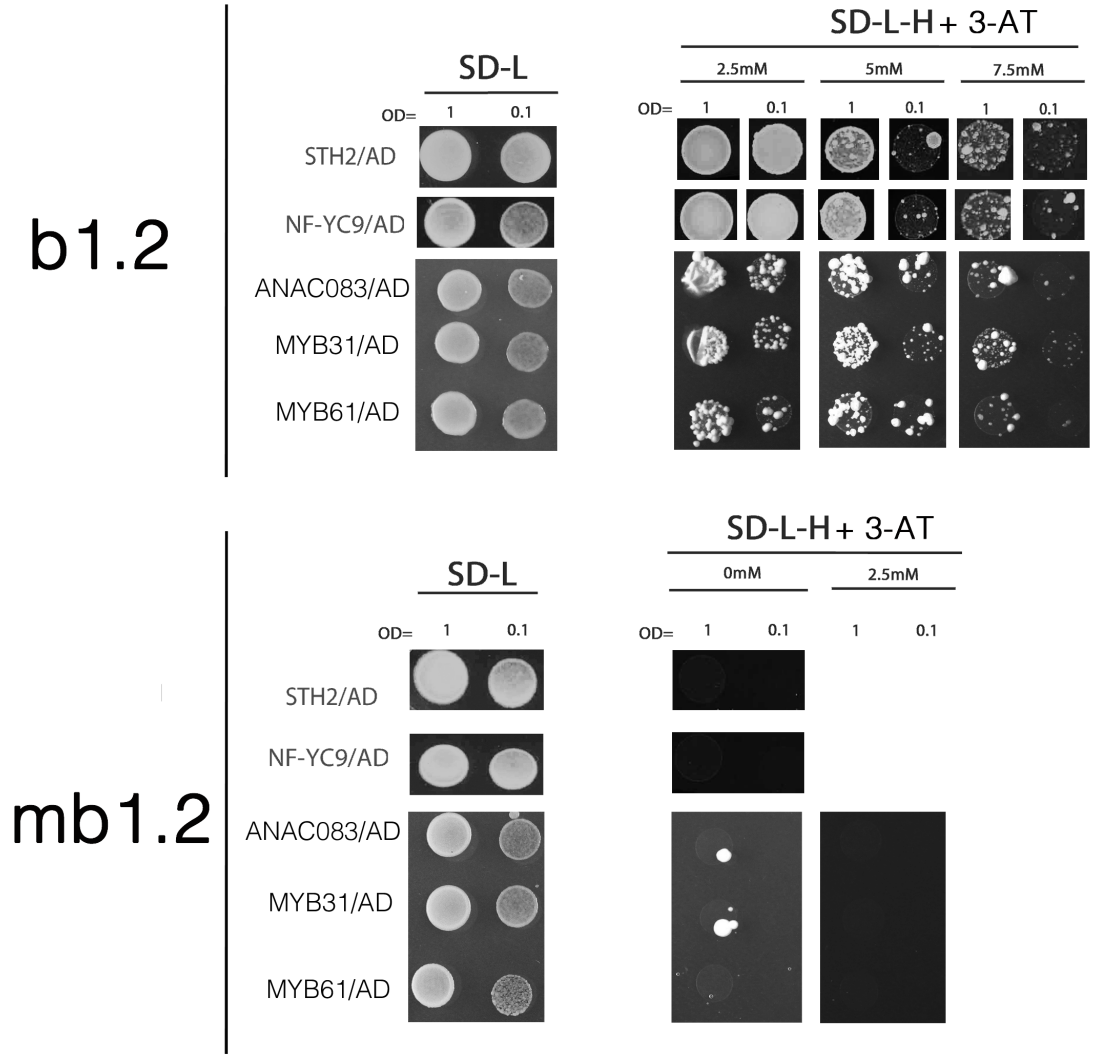

Fig. 5-7 : Y1H confirmation assay. STH2, NF-YC9, ANAC083, MYB31 and MYB61 interact specifically with the b1.2 "bait" DNA, consisting of UV-B box1, UV-B box2 and their native intermediate DNA sequence. No interaction is observed with the mutated version mb1.2. All different TFs were transformed in the corresponding yeast reporter strain as fusions with the GAL4-AD (STH2/AD, NF-YC9/AD, ANAC083/AD, MYB31/AD, MYB61/AD). SD-L medium was used as a control for the viability of the spotted cells. Interactions are assessed on His-lacking medium supplemented with different concentrations of the 3-AT inhibitor (SD-L-H + 3-AT). Spottings were performed from cell suspensions with two different cell densities (OD= 1 and 0.1). Results are representative of three repeats

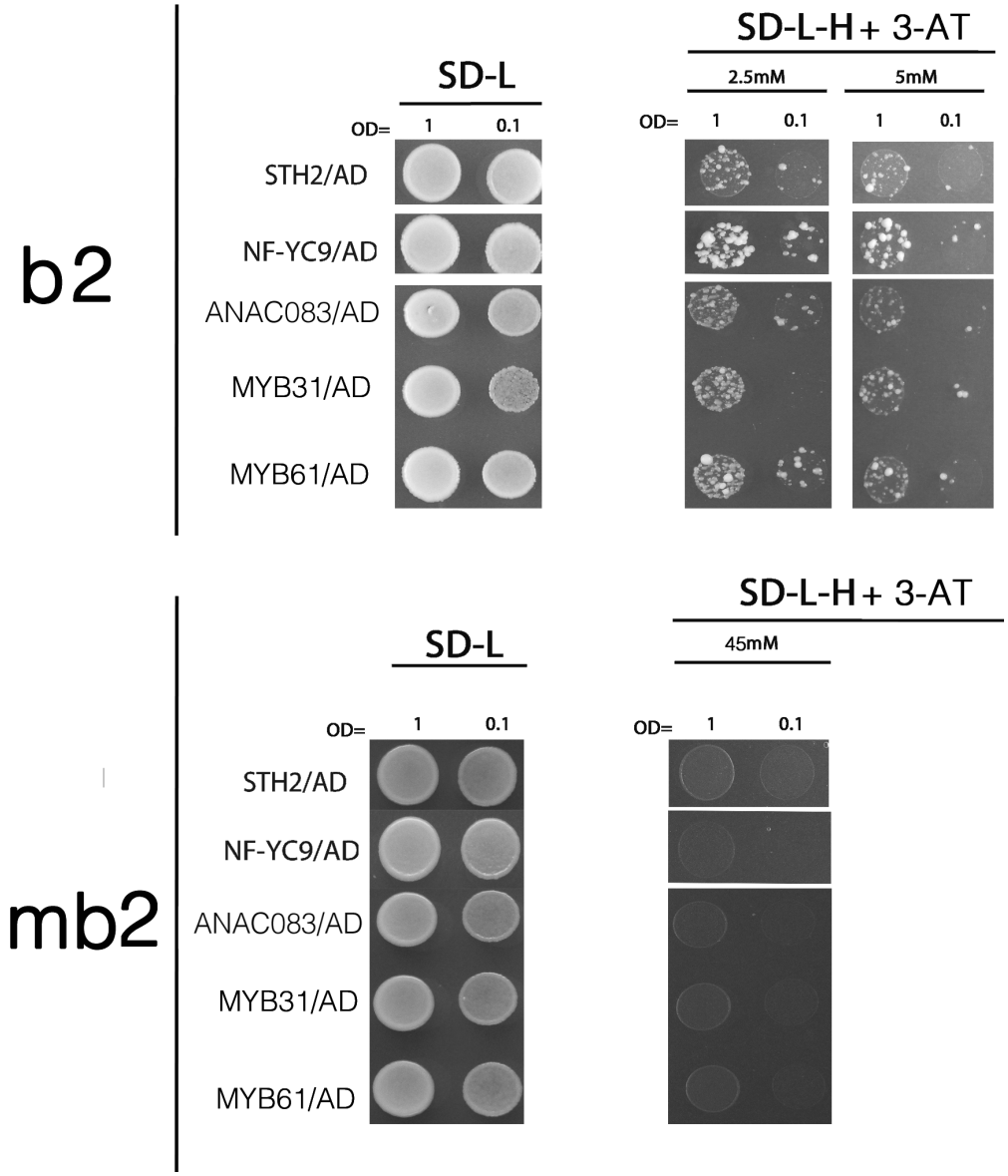

Fig. 5-8 : Y1H confirmation assay. STH2, NF-YC9, ANAC083, MYB31 and MYB61 interact specifically with the b2 "bait" DNA, consisting of tandem repeats of UV-B box2. No interaction is observed with the mutated version mb2. All different TFs were transformed in the corresponding yeast reporter strain as fusions with the GAL4-AD (STH2/AD, NF-YC9/AD, ANAC083/AD, MYB31/AD, MYB61/AD). SD-L medium was used as a control for the viability of the spotted cells. Interactions are assessed on His-lacking medium supplemented with different concentrations of the 3-AT inhibitor (SD-L-H + 3-AT). Spottings were performed from cell suspensions with two different cell densities (OD= 1 and 0.1). Results are representative of three repeats.

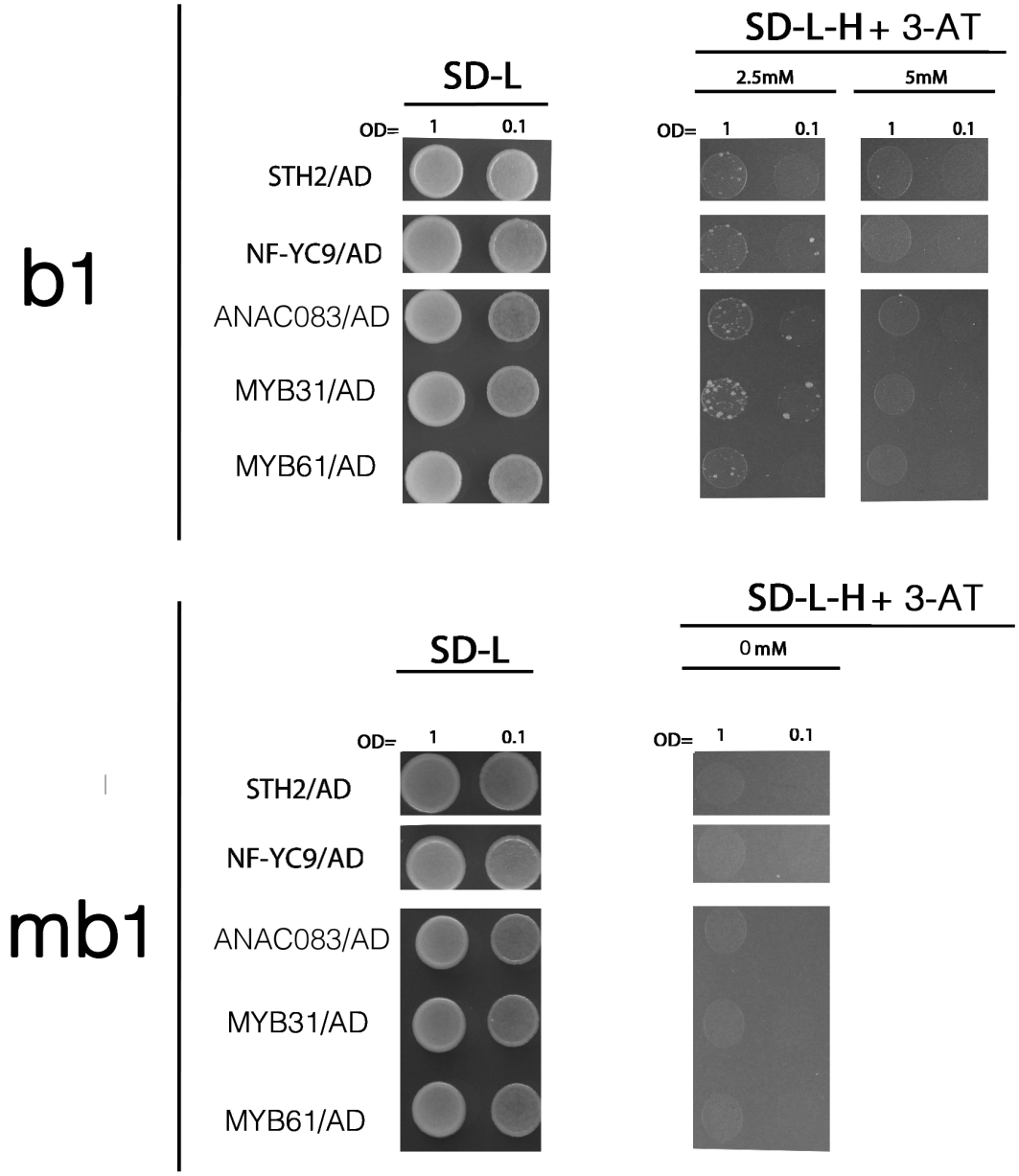

Fig. 5-9 : Y1H confirmation assay. STH2, NF-YC9, ANAC083, and MYB61 do not interact with the b1 "bait" DNA, consisting of tandem repeats of UV-B box1. No interaction is observed with the mutated version mb1 either. The relatively weak growth observed in the case of MYB31/AD might indicate a weak and/or unstable interaction of MYB31 with the target DNA, which however is on the limit of detection with this experimental setup. All different TFs were transformed in the corresponding yeast reporter strain as fusions with the GAL4-AD (STH2/AD, NF-YC9/AD, ANAC083/AD, MYB31/AD, MYB61/AD). SD-L medium was used as a control for the viability of the spotted cells. Interactions are assessed on His-lacking medium supplemented with different concentrations of the 3-AT inhibitor (SD-L-H + 3-AT). Spottings were performed from cell suspensions with two different cell densities (OD= 1 and 0.1). Results are representative of three repeats.

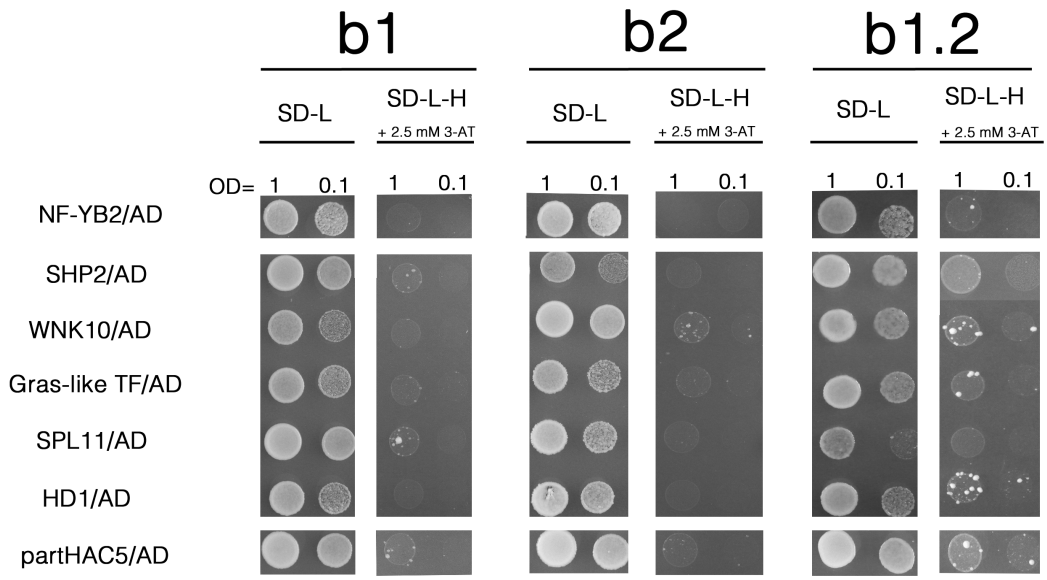

Fig. 5-10 : Y1H confirmation assay. NF-YB2, SHP2, WNK10, Gras-like TF, SPL11, HD1, partHAC5 do not interact with any of the DNA sequences used as "baits". All different TFs were transformed in the corresponding yeast reporter strain as fusions with the GAL4-AD (NF-YB2/ AD, SHP2/AD, WNK10AD, Gras-like TF/AD, SPL11/AD, HD1/AD, partHAC5/AD). SD-L medium was used as a control for the viability of the spotted cells. Interactions are assessed on His-lacking medium supplemented with 2.5 mM 3-AT. Spottings were performed from cell suspensions with two different cell densities (OD= 1 and 0.1). Results are representative of three repeats.

5.8 Discussion

Despite the wealth of information that has been accumulating during the past decade on how the UV-B-specific photoreceptor UVR8 regulates photomorphogenic UV-B responses of plants, remarkably little progress has been achieved in elucidating the events that follow the interaction with COP1 and lead to transcriptional regulation. A plausible scenario, emanating mainly from the fact that UVR8 has been found to associate with chromatin on loci occupied by some of the genes whose transcription it regulates, is that it promotes the activation/recruitment of specific transcription factors (Jenkins, 2014a). The latter has been a major working hypothesis throughout this project and a Yeast One Hybrid Screening approach was undertaken as a first step to address it. Time limitations imposed the screening to be confined to only one "target" promoter. Since the bZIP transcription factor HY5 is thought to be the key effector behind the photomorphogenic UV-B responses, the "bait" DNA sequences for the screens were all derived from the *HY5* promoter. Two putative cis-regulatory elements (Fig 5-1), identified via a promoter linker scan approach and found to be important in UV-B responses by a team of collaborating scientists, were employed either individually or in combination (Fig 5-2) as target DNAs for the isolation of TFs which specifically recognise them. Binding specificity was addressed by using mutated versions of the "bait" DNAs (Fig 5-5). This approach led to the singling out of five TFs, namely STH2, NF-YC9, ANAC083, MYB31 and MYB61 (Figs 5-7 and 5-8), which could be involved in UV-B signalling and should, therefore, be considered for further analysis. All candidates appeared to recognise preferentially UV-B box2 , while retaining the ability of binding to the "bait" DNA that consisted of both UV-B boxes and their native intermediate DNA sequence (Figs 5-7, 5-8 and 5-9). This was, in part, expected since none of these TFs was originally isolated via the screen against UV-B box1 (Table 5-1). Indeed, screen S1, in which UV-B box1 ("bait" b1) was used as target DNA sequence, resulted in the isolation of only one TF, namely SPL11, despite that this screen was the most saturated of all (Fig 5-4 A.). Moreover, SPL11 proved to be a false positive result during the subsequent confirmation assays (Fig 5-10). Thus, no TF could be found to specifically interact with UV-B box1 albeit the highest number of clones were screened against it. This observation could be explained by postulating a negative

regulatory role for UV-B box1, to which repressors of transcription bind naturally in vivo. In such case, no candidate TF would be expected to be found via a Y1H approach which relies methodologically on positive transcriptional effects on a reporter gene. Such explanation is consistent with unpublished data from our collaborators (Prof Ferenc Nagy's team) where UV-B box1, when mutated, leads to increased basal luminescence in promoter - reporter studies. Nevertheless, the negative regulatory function of any *cis*-regulatory element depends largely on the TF which acts in *trans*- by recognising and binding to it. It is possible that positive and negative regulators compete in planta for binding to the same DNA sequence and on that basis UV-B box1 was not excluded from the screening approach.

5.8.1 STH2 is a member of the BBX family of TFs

Among the five TFs isolated through the Y1H screens, STH2 appears to have the most striking involvement in photomorphogenesis. It is a member of the BBX family of transcription factors, which are known potent regulators of light dependent development (Sarmiento, 2013). STH2 in particular has been reported to interact genetically with HY5 as well as COP1 (Datta et al., 2008). However, Y2H assays and FRET experiments confirmed physical interaction only with HY5 whereas COP1 appeared to be important for recruiting STH2 in nuclear speckles, in which both proteins co-localised (Datta et al., 2007). Moreover, in the same study a hyposensitive hypocotyl elongation phenotype, partially dependent on HY5, was demonstrated for *sth2* mutants under various light qualities. The authors did not include UV-B light in their experimental design but interestingly they reported reduced levels of anthocyanin accumulation under blue light. Having no data to imply direct binding of STH2 onto the DNA itself, Datta et al. suggested a model for the positive regulatory function of STH2 in photomorphogenic signalling, in which HY5 is acting as a recruiting agent driving STH2 to various gene promoters. Since the presence of similar recruiting proteins in the yeast cells cannot be ruled out, the Y1H results presented in this chapter do not unequivocally demonstrate direct DNA binding activity of STH2. Nonetheless, our results are an additional line of evidence for direct interaction although more experiments are needed to clarify this point.

5.8.2 NF-YC9 is a member of the CCAAT-binding family of TFs

The CCAAT-box-binding family of TFs (which is also known as the Nuclear Factor Y family) is ubiquitously present in all higher eucaryotes. NF-Y transcription factors are known to exert their function as heterotrimeric complexes and studies, particularly in plants, have demonstrated that the genes encoding the different subunits belong to large multi-gene families rendering substantial functional diversification. A recently proposed nomenclature for the three subunits is AtNF-YAx , AtNF-YBy and AtNF-YCz. Although all three subunits have been shown to be essential for CCAAT-box binding *in vitro,* NF-YAx subunits are the ones responsible for the sequence specific association with the DNA (Laloum et al., 2013). However, it has been proposed (Wenkel et al., 2006) that proteins that possess the conserved CCT (CONSTANS, CONSTANS-like and TOC1) domain, some amino acids of which are common with those appearing in the DNA-binding domain of NF-YAx, can replace NF-YAx within the NF-Y complexes. In this context, NF-YC9 in particular has been reported to additively enhance the ability of CONSTANS (CO) to act as a transcriptional activator in the regulation of flowering time (Kumimoto et al., 2010). Two canonical CCAAT- boxes are present within the *HY5* promoter, one of which is immediately flanking the UV-B box2 (Fig5-1). Interestingly this CCAAT-box was mutated during the initial "linker scan" approach which led to the identification of UV-B box2 and the resulting mutant showed reduced sensitivity to UV-B (Data provided by the collaborating team of Prof Ferenc Nagy). It is therefore conceivable that NF-Y complexes could be important for the regulation of transcription of HY5 under UV-B, and NF-YC9 in particular might be an essential component of such regulatory heterotrimers.

5.8.3 ANAC083 is a member of the NAC domain-containing family of TFs

The NAC- family of transcription factors consists of proteins sharing the plant-specific NAC-domain (**N**AM, **A**TAF1 and **C**UC domain; NAM **N**o **A**pical **M**eristem, ATAF1 **A**rabidopsis **T**ranscription **A**ctivaton **F**actor1, CUC **Cu**p shaped **C**otyledon). In Arabidopsis, members are usually designated as ANAC (Arabidopsis NAC proteins) and comprise of more than a hundred TFs which are implicated in diverse processes, among

which are various growth and development responses as well as responses to environmental stress stimuli. So far, only ANAC13 has been implicated in UV-B signalling but via a UVR8- and COP1- independent pathway (Safrany et al., 2008). ANAC083 in particular has been reported to play a major role in leaf senescence regulation and xylem vessel formation (Yamaguchi et al., 2010; Yang et al., 2011). These processes do not have a direct link with UV-B signalling, however, gene ontology analysis presented in two databases (The Arabidopsis Information Resourse TAIR, and the Plant Transcription Factor Database PlantTFD) has placed ANAC083 amongst many candidate transcription factors which positively regulate flavonoid synthesis. Flavonoids are the sunscreen protective compounds which accumulate as the end products of the acclimatory photomorphogenic UV-B responses. It is not unlikely, therefore, taking into account the Y1H results presented in this chapter, that ANAC083 may participate in the early steps of UV-B signalling by contributing to the transcriptional up-regulation of *HY5*.

5.8.3 MYB31 and MYB61 are two R2R3 MYB transcription factors

The last two transcription factors isolated during the Y1H screens, namely MYB31 and MYB61, belong to one of the largest TF families in plants, the R2R3 MYB gene family. *MYB* genes are involved in the regulation of primary and secondary metabolism and in the fine-tuning of important developmental processes such as the control of cell fate and identity (Stracke et al., 2001). Interestingly, MYB31 from maize (ZmMYB31) has been reported to redirect phenylpropanoid metabolic flux and when overexpressed in Arabidopsis it affected the biosynthesis of flavonoids leading to accumulation of anthocyanins and increased sensitivity to UV-B radiation (Fornalé et al., 2010). MYB61 on the other hand, is a TF which is highly expressed in siliques and vascular tissue and has been implicated in the deposition of seed coat mucilage (Penfield et al., 2001; Romano et al., 2012). Morevoer, it is intriguing that MYB61 has also been linked to photomorphogenesis. Plants overexpressing this transcription factor were found to have a *det3*-like phenotype and it was demonstrated that MYB61 can account for at least some facets of the dark-photomorphogenic phenotype of the *det3* mutants (Newman et al., 2004).

5.8.4 Interpretation of the Y1H approach and the necessity of further functional characterisation of the isolated TFs

The Y1H screens were undertaken in an attempt to identify transcription factors with novel functional significance in the early steps of UV-B signalling, particularly in the UV-B regulation of *HY5* transcription. Transcripts of *HY5* increase rapidly after UV-B irradiation and it is unlikely that the TFs which mediate this accumulation are de-novo synthesised in response to UV-B. Probably these unknown transcription factors are already on the scene and are activated/recruited to the HY5 promoter as a result of the UV-B signalling process. For this reason, instead of utilising libraries prepared after specific UV-B treatments, the libraries chosen to perform the Y1H screens were commercial "Universal, Normalised Arabidopsis libraries" which offer the best possible representation of low abundance cDNAs. This, however, leaves the screening procedure with no elements of UV-B specificity other than the usage of "bait" DNA derived from *cis*-regulatory elements which are proposed to be involved in UV-B responses. Moreover, there is no reason to believe that a particular *cis*-regulatory element, important for any given response, will be exclusively involved in that particular process and no other. Given the diverse pleiotropic effects of HY5 in plant growth and development it is quite likely that some transcription factors, which drive the expression of *HY5* in response to non-UV-B related stimuli, could bind to the cis-regulatory elements which were employed as "baits" in our Y1H screens. Therefore, it was important to further characterise the isolated transcription factors and investigate their possible involvement in UV-B signalling. To that end, null or knock-down mutants of all five transcription factors were obtained and subjected to various treatments in search for altered UV-B responses. In addition, transgenic overexpressing lines for all five transcription factors fused with the GFP tag were generated for further functional analysis as well as *in planta* confirmation of the Y1H results via ChIP assays. Unfortunately, time limitations did not allow for exhaustive analysis of all transcription factors. However, some very interesting findings emerged along the way and they are reported in the the following two chapters.

CHAPTER 6: FUNCTIONAL ANALYSIS OF THE IDENTIFIED TRANSCRIPTION FACTORS - ADDRESSING THEIR POSSIBILE INVOLVEMENT IN UV-B SIGNALLING.

6.1 Introduction

As discussed in the previous chapter, the experimental setup of the Y1H screens was by necessity such, that the identified transcription factors could not be unequivocally associated with UV-B signalling. Further experimentation was needed in order to establish links, if any, with UVR8-dependent photomorphogenesis and the approaches undertaken are summarised here.

Initially, close attention was given to the B-Box containing transcription factor STH2, whose involvement in photomorphogenesis is well documented (Datta et al., 2008a). However, an inherent disadvantage of any screening approach is that important interacting partners may not be among the isolated candidates, either because their representation in the initial library stock is very low, or because they have been screened out under the particular technical parameters of the experimental setup. Thus, as the BBX subfamily IV, to which STH2 belongs, possesses many other members which have also been reported to play important roles in photomorphogenic responses (Sarmiento, 2013), it seemed reasonable to expand our focus to include several of them. Subsequently, Y2H assays were performed to assess whether there is physical interaction between the candidate TFs and UVR8. Moreover, a standard reverse genetics approach was employed for all the TFs. Mutant lines, each carrying a T-DNA insertion within the genetic locus occupied by the TF under investigation, were obtained and the plants were assessed for alterations in specific UV-B responses. From the diversity of such responses, the UV-B-induced inhibition of hypocotyl elongation, increase in the abundance of the transcripts of selected genes, and accumulation of the CHS protein were chosen as diagnostic assays for the involvement in UV-B signalling. Finally, translational fusions with GFP were produced for every TF. The resulting constructs were transiently expressed in *N. benthamiana* plants in order to ascertain satisfactory expression levels and proper nuclear localisation before proceeding to stable transformation of Arabidopsis plants.

6.2 STH3 and HY5, in contrast to BBX25 and BBX31, can recognise *HY5* promoter DNA by preferentially associating with UV-B box2

A recently described group of transcriptional regulators, which function as effectors of photomorphogenesis downstream of the photoreceptive events, are the family of B-Box containing zinc finger proteins (BBX family). Thirty two proteins are members of the BBX family (Khanna et al., 2009) and they can be subdivided in five clades designated by the latin numbers I-V. Subfamily IV consists of eight members (BBX18 - BBX25), with STH2 (also called BBX21) being one of them. Protein alignments between members of this clade show limited primary sequence conservation, and the closest amino acid identities are displayed between the pairs BBX18-BBX19 and BBX24-BBX25 (Sarmiento, 2013). During the Y1H screens performed in this project, and in the subsequent confirmation assays, STH2 was shown to be capable of driving the transcription of the reporter gene by preferentially associating with UV-B box2. This raised the question whether STH3 (another member of subfamily IV also known as LFZ1 or BBX22), which shares striking functional similarity with STH2, would behave in similar fashion. Both proteins have been characterised as positive regulators of photomorphogenesis (Datta et al., 2008b). On the contrary, BBX24 and BBX25 have been reported to exert negative regulatory function (Gangappa et al., 2013b). BBX24 in particular was recently implicated in UV-B signalling. A hypersensitivity phenotype under low doses of UV-B was observed for the *bbx24* mutants. Moreover, the protein was shown to interact in yeast and *in planta* with HY5, and *in planta* with COP1. Interestingly, the interaction with COP1 was found to be present upon UV-B illumination but not under control conditions (Jiang et al., 2012). It was worthwhile, therefore, to consider the above members of the BBX IV subfamily for subsequent analysis. In addition, data obtained via transcriptomic analysis (Brown et al., 2005), have unraveled interesting findings about BBX31, a member of the BBX V subfamily. *BBX31* transcripts were found elevated in Wt plants when treated with UV-B, although this up-regulation appears with a relatively high false discovery rate (FDR=10). In UV-B treated *uvr8-1* plants, however, when compared with UV-B treated Wt plants, BBX31 transcripts are much less abundant (FDR=0.4). This suggests involvement of UVR8 in the transcriptional regulation of *BBX31*. Furthermore, preliminary observations

by a colleague have implied that *bbx31* mutant plants might be sensitive to UV-B (Dr Bobby A. Brown unpublished data). On that basis BBX31 was also included in the ensuing experiments.

At first, it was assessed whether STH3 behaves similarly to STH2 in our Y1H system. To that end, the full length coding sequence of STH3 was fused to the GAL4/AD in the pGADT7 vector. The resulting construct was introduced in the yeast reporter strains carrying the three baits and in their mutant counterparts, and a direct Y1H assay was performed. The expression of STH3/AD in the yeast cells was confirmed via immunoblot against the HA epitope tag (Fig 6-1 A.). STH3/AD was capable of recognising "bait" b1.2 which consists of both UV-B boxes, and, like STH2, it appears to preferentially associate with UV-B box2. No recognition of UV-B box1 alone could be seen, as demonstrated by the lack of growth of the yeast cells when "bait" b1 was used (Fig 6-1 B.) Finally, as a model for the function of both STH2 and STH3 has been proposed (Datta et al., 2007), according to which the two proteins are recruited by HY5 to the promoters of the genes they regulate, rather than recognising specific sequences themselves, it was interesting to perform the Y1H assay with a HY5/AD fusion as well. The obtained result interestingly indicated that HY5 can recognise preferentially the UV-B box2 cis-regulatory elements of its own promoter (Fig 6-1 B.). This finding stands in agreement with recently published reports (Abbas et al., 2014; Binkert et. al., 2014) and it is suggestive of a positive regulatory loop via which HY5 regulates the transcription of its own gene.

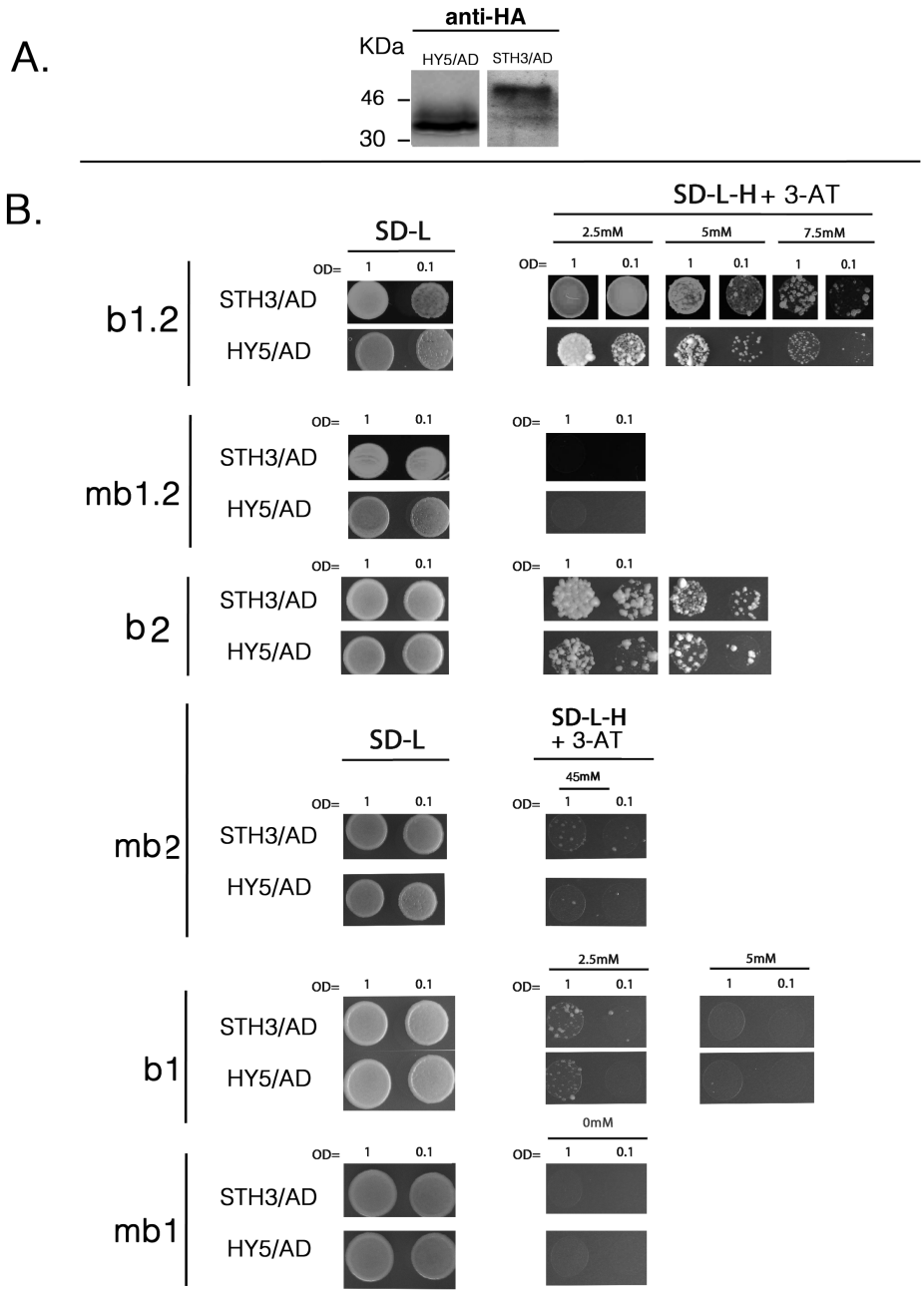

Fig. 6-1 : Y1H assay. STH3 and HY5 preferentially associate with UV-B box2.

A. Results of anti-HA antibody immunoblot assay on protein extracts of yeast transformed with the GAL4/AD fusions of STH3 or HY5 (STH3/AD, HY5/AD). **B.** STH3 and HY5 interact specifically with the b1.2 "bait" DNA, consisting of UV-B box1, UV-B box2 and their native intermediate DNA sequence, and with "bait" b2 which is derived from UV-B box2. No interaction is observed with the UV-B box1-derived "bait" b1. SD-L medium was used as a control for the viability of the spotted cells. Interactions are assessed on His-lacking medium supplemented with different concentrations of the 3-AT inhibitor (SD-L-H + 3-AT). Spottings were performed from cell suspensions with two different cell densities (OD= 1 and 0.1). Results are representative of three independent repeats.

In a following set of experiments, BBX25 and BBX31 were subjected to a Y1H assay. Unfortunately, for no evident reasons neither BBX25/AD nor BBX31/AD could be effectively transformed in the b1.2 yeast reporter strains. Repeated attempts, carried out along with control transformations which ruled out the possibility of problematic reagents, either failed to give any transformants at all, or resulted in cells with severely reduced growth rate, unreliable to be used in the assay. Thus, the experiment was performed with the b2 yeast reporter strain, which harbours the UV-B box2-derived "bait". It should be noted, however, that the transformation efficiency was still much lower compared to control transformations, suggesting that these particular fusions are tolerated with difficulty by the Y187 yeast strain used in these assays. No activity similar to that of STH2 and STH3 could be detected for either BBX25 or BBX31 (Fig 6-2 B.). The weak growth of yeast cells observed for BBX31/AD might indicate a transient and/or unstable interaction, but this needs further validation as the sensitivity of our experimental setup is clearly not sufficient to reliably detect such interactions. Moreover, whereas BBX31/AD could be faintly detected on immunoblots against the HA-epitope tag, no signal was visible for BBX25/AD (Fig 6-2 A.). Presumably, the reason is toxicity of the protein when produced in high amounts, as pGADT7 is a multiple copy vector. In their recent work Gangappa and coworkers managed to detect BBX25/AD in yeast protein extracts but they used a low copy vector and a different yeast strain (suppl Fig 1 in Gangappa et al., 2013a). In the same study, the authors showed that neither BBX25 nor its close homologue - and structurally very similar - BBX24 were capable of driving the transcription of the *LUC* reporter gene in promoter-reporter assays carried out in transfected Arabidopsis protoplasts. Although the promoter used by the authors was not that of *HY5,* their findings point against a direct DNA binding activity of BBX24 and BBX25. In that respect, the results reported here for BBX25, which was incapable of recognising the target DNA "bait" against which it was tested, are in agreement with those published by Gangappa et al. For economy of time, it was decided not to proceed with testing BBX24 in our Y1H system. The published literature, the high amino acid identity (70%) and the structural similarity with BBX25 are suggestive of a similar behaviour for the two homologues at least in terms of DNA binding activity.

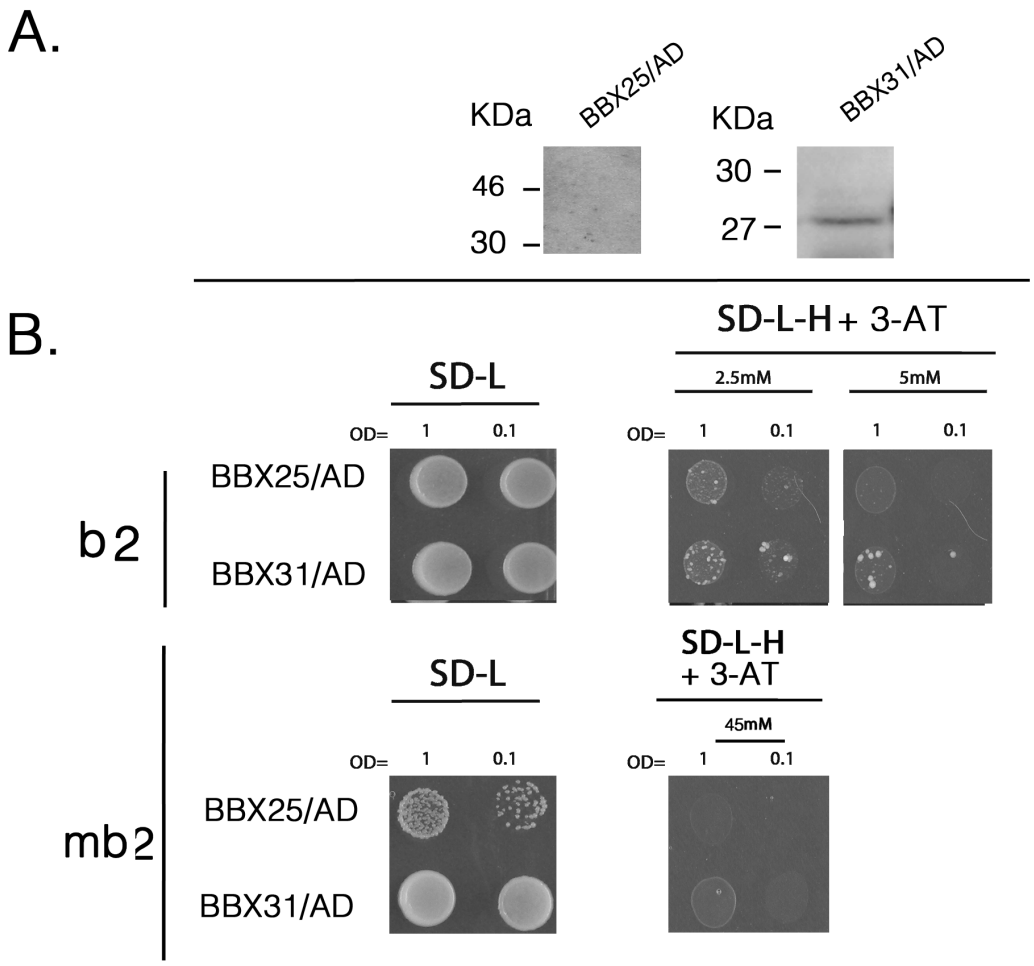

Fig. 6-2: Y1H assay. Neither BBX25 nor BBX31 recognise target DNA from the *HY5* promoter. **A.** anti-HA antibody immunoblot on protein extracts from yeast transformed with the GAL4-AD fusions of BBX25 or BBX31 (BBX25/AD, BBX31/AD). **B.** BBX25 does not recognise "bait" b2 which is derived from UV-B box2. A weak/transient interaction of BBX31 with the b2 "bait" DNA cannot be ruled out but confirmation with an alternative, more sensitive method is necessary. The yeast reporter strain carrying the mutated UV-B-box2-derived "bait" mb2 was used as a control. SD-L medium was used as a control for the viability of the spotted cells. Interactions are assessed on His-lacking medium supplemented with different concentrations of the 3-AT inhibitor (SD-L-H + 3-AT). Spottings were performed from cell suspensions with two different cell densities (OD= 1 and 0.1). Results are representative of two independent repeats.

6.3 BBX24 interacts with UVR8, both in the presence and absence of UV-B, in a Y2H assay

In the light of the results presented in the previous sections, it was interesting to address the possibility of a direct physical interaction between UVR8 and any of the BBX proteins under consideration. To that end, GAL4/AD fusions of all the aforementioned BBX proteins, except BBX24, were transformed in the AH109 yeast strain along with a GAL4/ BD fusion of UVR8. In the case of BBX24, it was decided to clone it in the pGBKT7 vector as a translational fusion with the GAL4/BD, so that it could be used in a control interaction against HY5/AD (Jiang et al., 2012), a construct already available from the Y1H assays. The well established interaction of UVR8 and COP1 in Y2H assays, observed only under UV-B, was employed as a control for the effectiveness of the UV-B treatment of the yeast cells. The results indicated that BBX24 interacts with UVR8 irrespective of whether the yeast cells are UV-B illuminated or not (Fig 6-3 B.). Intriguingly, no such interaction was observed for BBX25. It should be noted, however, that similarly to the Y1H assay, no visible band of the correct size could be detected for BBX25/AD in immunoblots (Fig 6-3 A.) The immunoblot experiments were carried out against the Myc-c epitope tag, for detection of the GAL4/BD fusions, and against the HA epitope tag, in order to detect the GAL4/AD fusions. All recombinant proteins gave signals at the expected size, except HY5/AD and BBX25/AD, for which no bands were visible. This result highlights two interesting technical limitations of the Y2H approach. Firstly, it demonstrates that the yeast strain of choice is important. Whereas the HY5/AD fusion could be readily detected from protein extracts of the Y187 yeast strain (Fig 6-1 A.), in which the Y1H assay was performed, we consistently failed to detect it in protein extracts from the AH109 yeast strain, which was the strain of choice for the Y2H assays. Revealingly, similar observations for the expression of HY5 in yeast have been reported previously in the literature (Holm et al., 2001). Nonetheless, when our HY5/AD construct was tested in a control Y2H interaction against BBX24 (Fig 6-3 B.), with which it has been reported to interact (Jiang et al., 2012), it behaved as expected. This suggests that the lack of visible bands is a consequence of expression levels lower than the limit of detection of the immunoblotting procedure, rather than of absolute absence of the protein.

Secondly, the fact that the BBX24/BD fusion could be detected, albeit faintly, contrary to the BBX25/AD fusion, implies that whether a protein of interest will be fused to the GAL4/AD or the GAL4/BD might actually be crucial for the outcome of the assay. BBX24 and BBX25 are structurally very similar and both pGBKT7 and pGADT7 are propagated in multiple copies within the yeast cells. The different fusions may fold differently in their tertiary structure, and it is possible that the BBX25/AD fusion protein folds in a way not tolerated by the yeast cells. If the cells manage to bypass the problem by keeping the expression levels low, the result would be faint signals or lack of visible bands in the immunoblots. Otherwise, the cells might experience an arrest of growth, which would explain the observations made during the attempts of transforming the yeast reporter strains for the Y1H assays.

Moreover, the discrepancy between the herein reported result and the findings of Jiang et al., who did not detect interaction between UVR8 and BBX24 in a Y2H assay using the same yeast strain (Jiang et al., 2012 suppl. fig S11) could be explained on the basis of the above rationale. The authors had UVR8 fused with the GAL4/BD domain and BBX24 fused with the GAL4/AD domain. Unfortunately, no data are provided on the expression levels of these recombinant proteins in the yeast cells, but it is possible that the BBX24/AD fusion renders expression of the recombinant protein in levels sufficient for detection of the interaction with HY5/BD, but too low for detection of any interaction with UVR8/BD. Moreover, the interaction of BBX24 with HY5 is not necessarily mediated by the same domain-region of the tertiary structure of the protein that effectuates the interaction with UVR8. It is conceivable, that the three dimensional folding of BBX24/AD might be such that the interaction interface with HY5 is not affected, whereas the interaction interface with UVR8 is masked leading to the results obtained by Jiang et al. Presumably the BBX24/BD fusion used in our work adopts a three dimensional folding pattern that leaves both interaction sites unaffected, thus allowing us to observe the interaction with UVR8. Nevertheless, instead of engaging in a time consuming domain swapping by generating different fusion combinations, BBX24-GFP plants were obtained by Jiang et al., and future CoIP experiments will hopefully help to resolve what is the true situation *in planta.*

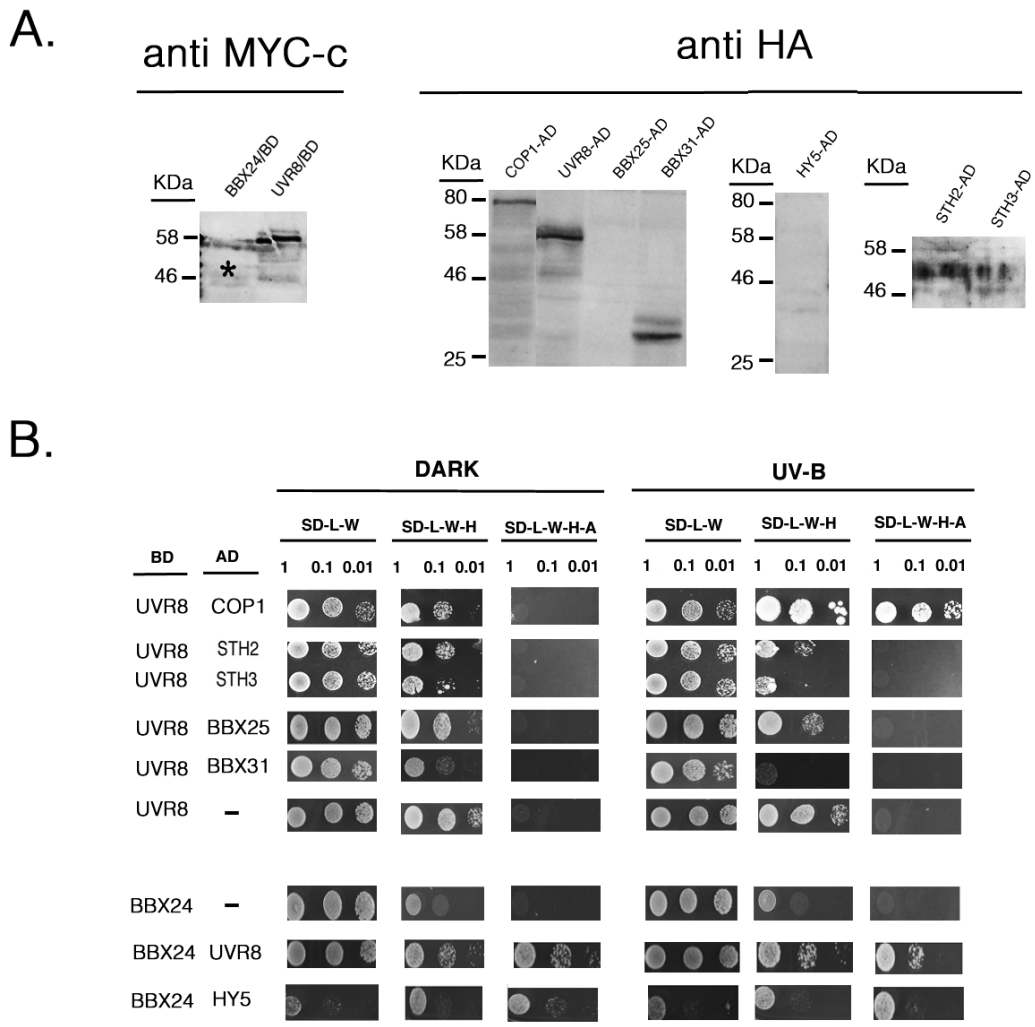

Fig. 6-3: Y2H assay. BBX24 interacts with UVR8 in a non UV-B-dependent manner. **A.** anti-MYC-c and anti-HA antibody immunoblots on protein extracts from yeast transformed with various GAL4-BD and GAL4-AD fusions respectively. The BBX24/BD fusion is detected faintly at ≈ 44 KDa (asterisk), whereas the band at ≈ 58 KDa is probably unspecific cross-reaction **B.** BBX24 interacts with UVR8 under both UV-B and UV-B-free conditions. The UVR8-COP1 interaction was used as a control for the effectiveness of the UV-B treatment. The BBX24-HY5 interaction was used as a control to demonstrate that both recombinant proteins are expressed in yeast, since the immunoblots gave extremely faint signals. SD-L-W medium was used as a control for the viability of the spotted cells. Interactions were assessed on low (SD-L-W-H) and high (SD-L-W-H-A) stringency selection plates. Spottings were performed from cell suspensions with three different cell densities (OD= 1 , 0.1 and 0.01). Results representative of two independent repeats are shown.

6.4 MYB61 interacts with UVR8 in a Y2H assay in the absence of UV-B

One of the working hypotheses of this project assumes a direct role of UVR8 in recruiting/ activating the transcription factors that mediate the expression of HY5 following UV-B illumination. In order to test that, a Y2H assay was performed with the aim of detecting any possible direct physical interactions between UVR8 and the TFs isolated from the Y1H screens. The experiments were carried out both in UV-B-supplemented and UV-B-free conditions. Moreover, as it is still unclear whether the UVR8-COP1 interaction is maintained while UVR8 exerts its gene regulatory function in the nucleus, possible interactions between the isolated TFs and COP1 were also investigated. A weak, though detectable under high stringency selection, interaction between UVR8 and MYB61 was observed (Fig 6-4). Interestingly, the interaction was abolished under UV-B illumination. As for the rest of the tested TFs, none was found to interact with UVR8 (Fig 6-4). In addition, no interactions between COP1 and the candidate TFs could be detected (Fig 6-5). The latter result is in agreement with previously published studies on the the roles of STH2 and STH3 in photomorphogenesis, where these proteins were found to co-localise with COP1 in nuclear speckles but no direct physical interaction was detected neither in yeast (Y2H experiments) nor in planta (FRET experiments) (Datta et al., 2008b).

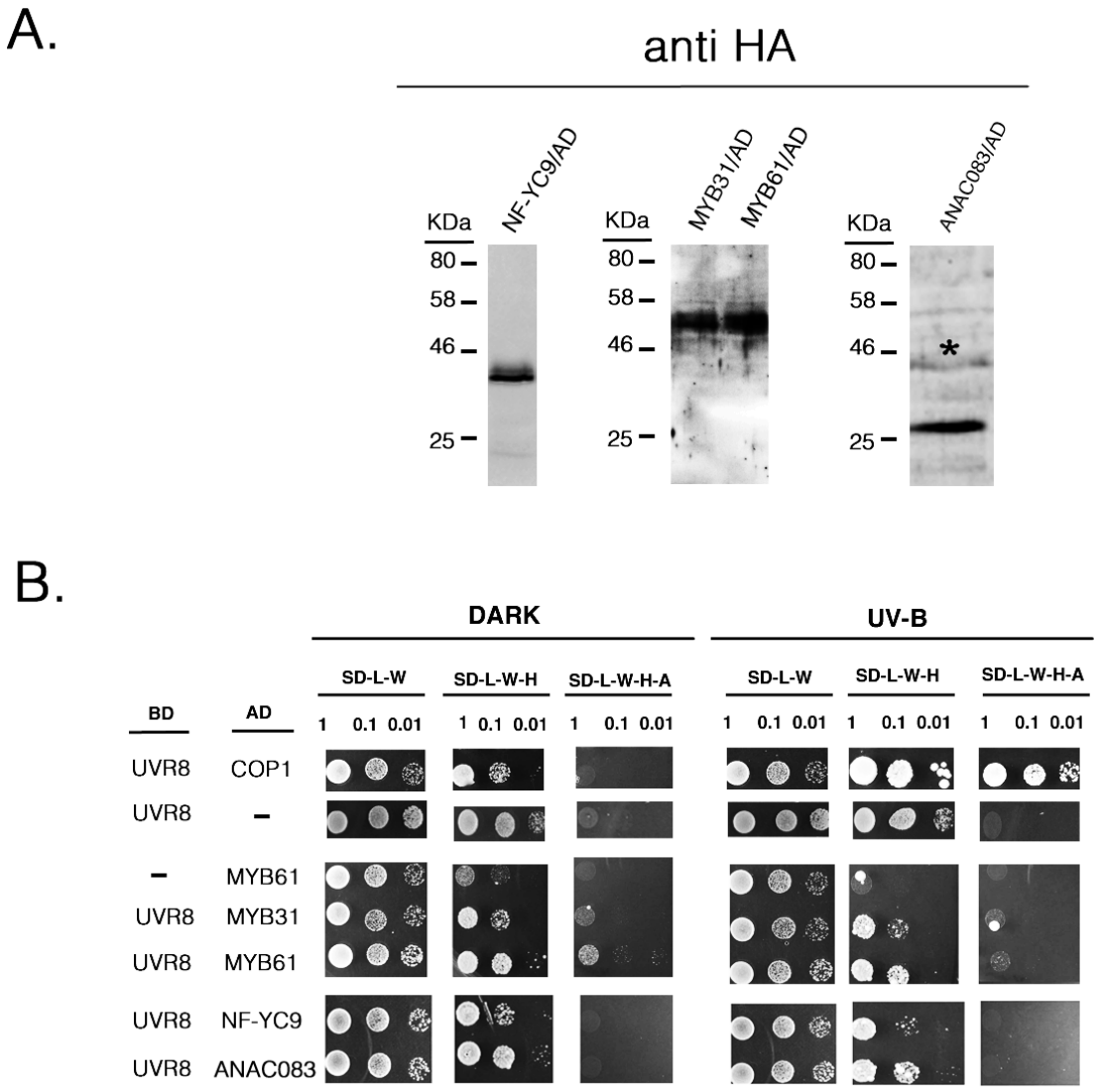

Fig. 6-4: Y2H assay. MYB61 interacts with UVR8 under UV-B-free conditions.
A. anti-HA antibody immunoblots on protein extracts from yeast transformed with various GAL4/AD fusions. The ANAC083/AD fusion is detected at ≈ 46 KDa (asterisk), whereas the band at ≈ 25 KDa might either be an unspecific signal or a degradation product of ANAC083/ AD **B.** Y2H assays for interaction between UVR8 and selected TFs. The UVR8-COP1 interaction was used as a control for the effectiveness of the UV-B treatment. SD-L-W medium was used as a control for the viability of the spotted cells. Interactions were assessed on low (SD-L-W-H) and high (SD-L-W-H-A) stringency selection plates. Spottings were performed from cell suspensions with three different cell densities (OD=1 , 0.1 and 0.01). The results are representative of three independent repeats.

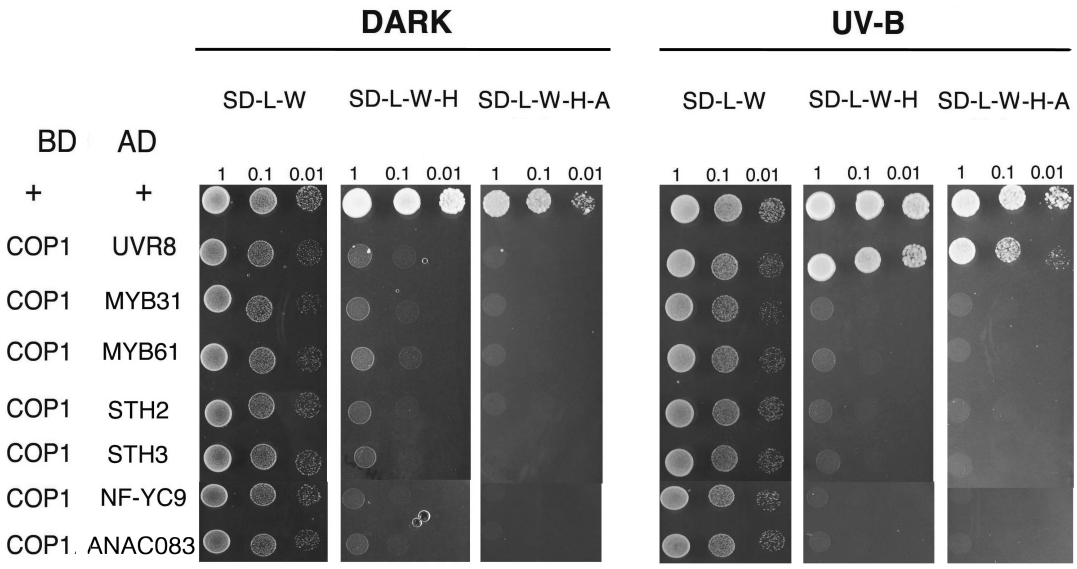

Fig. 6-5: Y2H assay. None of the TFs interacts with COP1 in yeast.

The interaction between the murine p53/GAL4BD fusion protein (+ve BD) and the SV40 large T-antigen/GAL4AD fusion protein (+ve AD) was used as a general positive control for the Y2H assay. The interaction between UVR8-COP1 interaction was used as a control for the effectiveness of the UV-B treatment. SD-L-W medium was used as a control for the viability of the spotted cells. Interactions were assessed on low (SD-L-W-H) and high (SD-L-W-H-A) stringency selection plates. Spottings were performed from cell suspensions with three different cell densities (OD= 1 , 0.1 and 0.01). The results are representative of two independent repeats.

6.5 Functional analysis of Arabidopsis T-DNA-insertion mutant lines for all the TFs isolated from the Y1H screens.

The binding of MYB61 to *cis*-regulatory elements of the *HY5* promoter, taken together with the physical interaction between UVR8 and MYB61 observed in yeast, were suggestive of a previously undescribed role of MYB61 in UV-B signalling. Thus, at least this TF was singled out for further analysis. However, at that stage of the project it was decided not to exclude the rest of the TFs from being considered candidates potentially involved in the early steps of the UVR8-mediated UV-B responses. The lack of interaction with UVR8 in a Y2H assay does not rule out such a possibility. Firstly, the situation *in planta* might be different from what is observed in yeast. Second, an important candidate does not necessarily need to physically interact with UVR8 itself. Its activation/recruitment by UVR8 might be taking place indirectly, via a bridging protein. Therefore, the *in planta* functional analyses were decided to be undertaken for all the candidate TFs. To that end, Arabidopsis T-DNA insertional "knock out" or "knock down" mutant lines were identified (Fig 6-6), all in the Col(0) ecotype background. For each line, homozygosity for the insertion was ascertained via PCR analysis (Fig 6-6 A.), and the severity of the insertional effect on each gene's transcript abundance was established via RT-PCR analysis (Fig 6-6 B.). More specifically, for *STH3* and *MYB31* T-DNA insertions residing between the ATG and the stop codon of each gene were identified from the SALK and the WiscDSLOx germ-plasm collections respectively. RT-PCR analysis suggested that both lines are "null" mutants for the corresponding genes (Fig 6-6, panel B for each gene). In addition, two T-DNA insertions were identified for *STH2* and one for *NF-YC9*, all from the SALK collection. For *STH2* in particular, one of the identified lines is the *sth2-1* mutant described previously (Datta et al., 2007) . Datta et al. also describe an *sth2-2* mutant which is in the L*er* ecotype background, and for this reason the second mutant line isolated in our study is designated *sth2-3*. RT-PCR results showed that *sth2-3* is not a "null" mutant, since the full length *STH2* transcript could be detected. In accordance with Datta et al., *sth2-1* appeared to be a "knock out" line (Fig 6-6 panel B for *STH2*). For *NF-YC9,* the isolated T-DNA line is the *nf-yc9-1* mutant described previously (Kumimoto et al.2010). In agreement with Kumimoto et al. we found this mutant to have reduced transcript abundance for the

affected gene. Additionally, one T-DNA insertion line from the SALK collection was obtained for *ANAC083* and one for *MYB61*. The *anac083* mutant appeared to have severely reduced ANAC083 transcript levels whereas *myb61* appeared to be a "knock down" mutant (Fig 6-6 panel B for each gene).

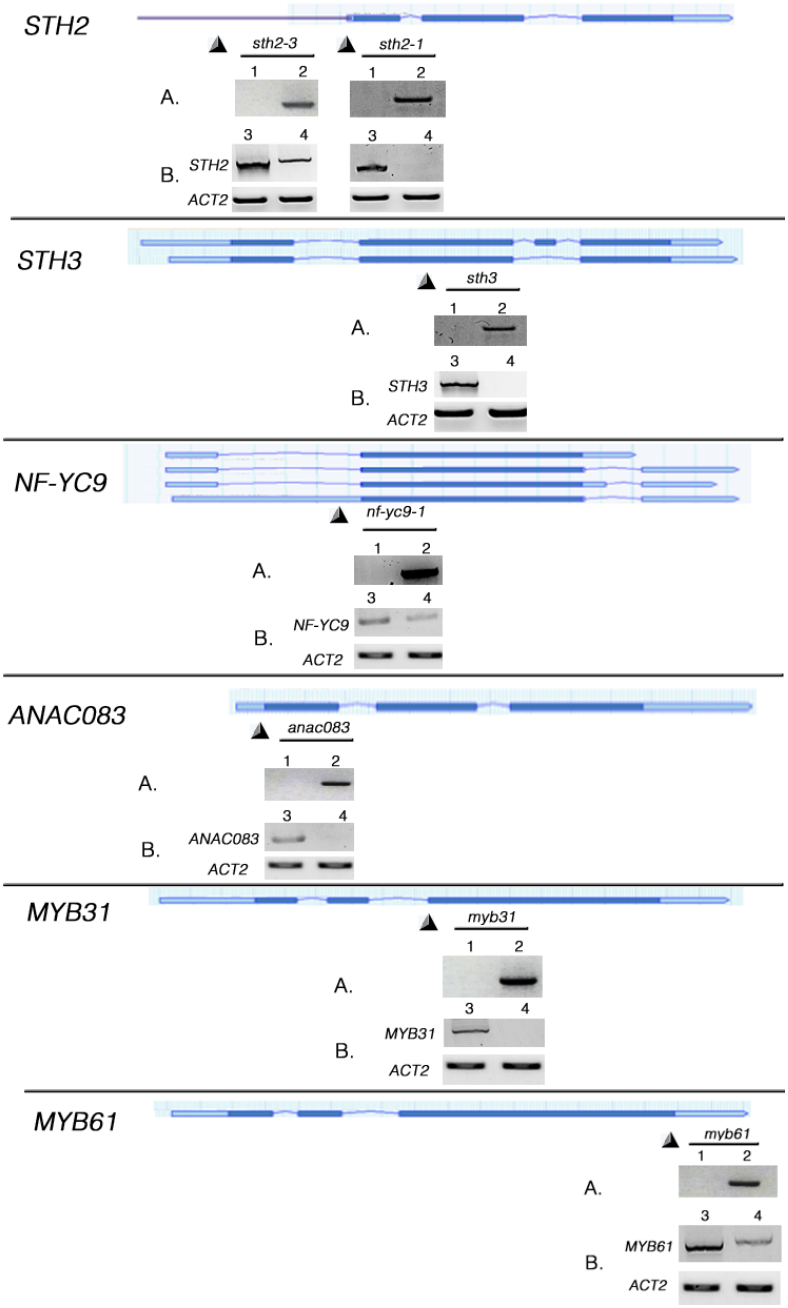

Fig. 6-6: Identification of T-DNA insertion mutant lines for the TFs of interest.

A genome browser view of each gene is presented, and the approximate location of every T-DNA insertion (according to TAIR database) is indicated with a triangle. Exons are depicted as dark blue thick lines, untranslated regions as light blue thick lines and promoters or introns as slim lines. For each gene, Panel A shows the genotyping results. Lane 1 corresponds to the PCR outcome when primers flanking either side of the T-DNA insertion were used, and it should not give product if an insertion is present; Lane 2 shows the PCR product when a Left Border T-DNA-specific primer and a locus-specific primer are used. Panel B shows the results of RT-PCR using gene specific primers, which amplify the full length coding sequence of each gene, and *ACT2* primers as a control. Lane 3 : WT cDNA Lane 4 : mutant line cDNA.

6.5.1 All mutant lines showed WT phenotypes in standard UV-B responses.

As soon as homozygous mutant lines for each of the TFs under investigation were isolated, their phenotype was assessed in a set of typical UVR8-mediated UV-B responses. At first, hypocotyl elongation assays were performed to monitor the effect of UV-B illumination on the rate of hypocotyl elongation. WT Col(0) plants were used as a positive control against which all mutant lines were compared, whereas *uvr8-1* mutant plants, which are known to be hypo-sensitive for this assay, were employed as a negative control. WT L*er* plants were also included to account for differences between the two ecotypes, as the *uvr8-1* mutants are in the L*er* background. Each genotype received two different light treatments, one in which the plants were germinated under low fluence white light without any measurable UV-B (-) and one supplemented with 1.5 μmol m^{-2} s^{-1} UV-B (+). Hypocotyl lengths were measured 5 days after germination. The mutant lines of all TFs appeared to be UV-B responsive, exhibiting at least 3-fold shorter hypocotyls under UV-B, similar to the WT Col(0) plants (Fig 6-7 A, B). As expected, the *uvr8-1* mutant plants displayed a hypo-sensitive response (1.3-fold shorter hypocotyls under UV-B) compared to Wt L*er* (2.3-fold shorter hypocotyls under UV-B). The differences in the hypocotyl lengths observed between different lines under the control UV-B-free conditions, could be attributed to slight differences in germination rates. Not all mutant lines were synchronically available during the project, as the genotyping required more than one generation for many lines. Hence, different seed batches were used for the experiment and this caused slight variation in germination time, even though an initial light treatment was applied in an attempt to induce synchronous germination. An alternative explanation could be that positional effects resulting from each T-DNA insertion might cause weak developmental phenotypes, rendering slightly taller or slightly shorter plants in general. Nevertheless, the aim of this experiment was to assess the UV-B responsiveness of each mutant line in terms of the inhibition of hypocotyl elongation. Thus, the meaningful comparison is the one between UV-B-free and UV-B supplemented conditions for each line, rather than a comparison of different lines under the same light quality.

In order to strengthen the findings from the hypocotyl length measurements, protein extracts from all seedlings were prepared, and immunoblots with antibody targeting the CHS protein were performed. Levels of CHS are normally elevated following UV-B illumination and this increase is UVR8-dependent. All genotypes, except *uvr8-1*, were found to have increased levels of CHS when subjected to UV-B light (Fig 6-7 C.).

Finally, the transcript abundance of some well known UV-B responsive genes, whose regulation is UVR8-dependent, was examined in gene expression assays. Three weeks old seedlings of all different genotypes, grown under continuous low fluence rate white light ($\leq$ 20 μmol m^{-2} s^{-1}), were transferred to 3 μmol m^{-2} s^{-1} UV-B for 4 hours. Total RNA was then isolated, cDNA was synthesised and the transcript abundance of *HY5, ELIP.1* and *CHS* was determined via semi-quantitative RT-PCR. Only the *uvr8-1* mutants did not show the UV-B-induced accumulation of the aforementioned transcripts (Fig 6-8). Taken together, our data imply that neither of STH2, STH3, ANAC083, or MYB31 is essential for the UV-B responses which were tested, since the loss of function mutants (Fig 6-6) behaved similarly to the WT. For NF-YC9 and MYB61, no such claim can be made from our data, because the mutant lines that were used had detectable levels of each gene's transcript (Fig 6-6). Hence, it is possible that a fully or partly functional protein is synthesised in these mutants and the residual activity might be sufficient for mediating the responses. Further experiments are needed to clarify this point.

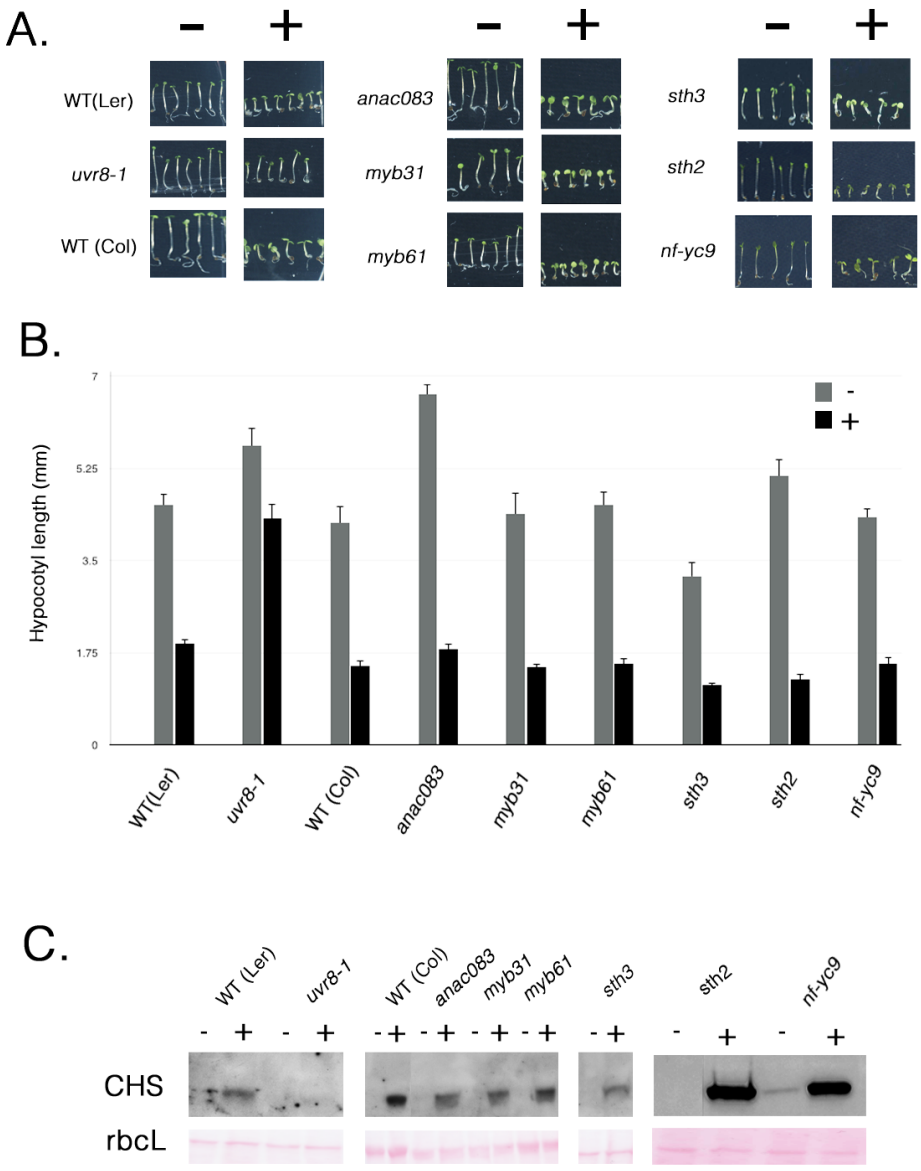

Fig. 6-7: Hypocotyl assay. All tested lines appeared UV-B responsive.

- : Low fluence rate white light, no measurable UV-B ; + : Low white light supplemented with 1.5 µmol m^{-2} s^{-1} narrow band UV-B. **A.** Photographs of representative seedlings from each line, which were germinated and grown for 5 days under UV-B-supplemented or UV-B-free light. **B.** Bar-chart of the average hypocotyl length values for each line, under the two distinct light conditions of the assay, 5 days after germination. Error bars represent SE ($n \geq 25$) . **C.** Anti-CHS antibody immunoblots on protein samples prepared from crude protein extracts of 5 days-old seedlings, subjected to the light treatments described above. Ponceau staining of the large subunit of RuBisCo (rbcL) is presented as a loading control. All tested lines, except *uvr8-1* which served as negative control, displayed the UVR8-dependent, UV-B stimulated increase of the levels of immunoreactive CHS protein. Results are representative of three independent repeats.

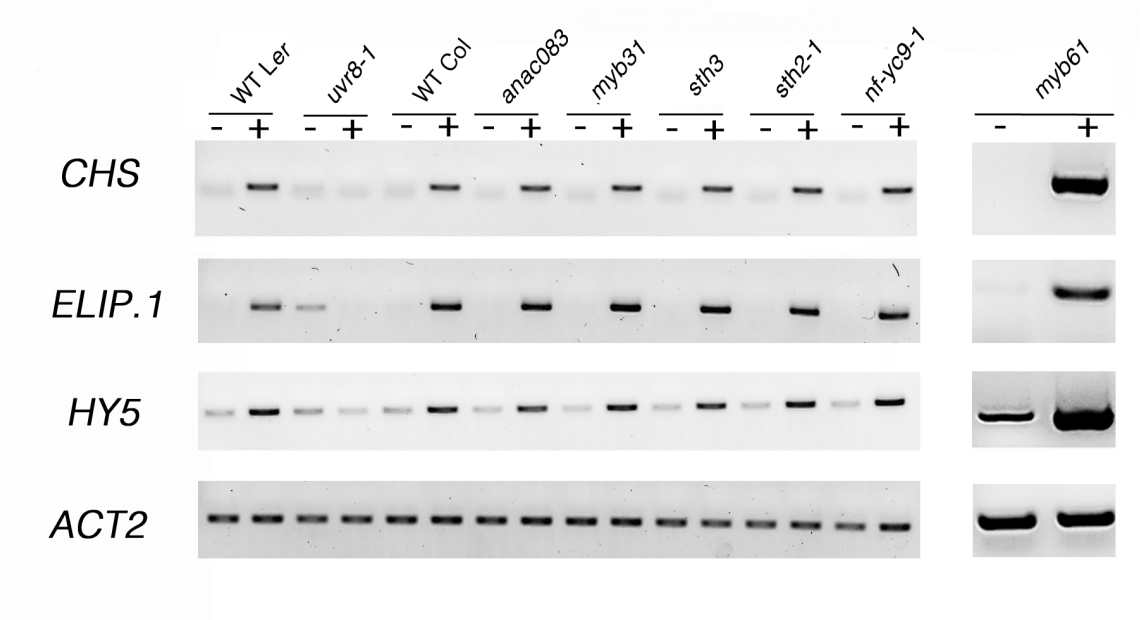

Fig. 6-8: Gene expression assay using semiquantitative RT-PCR. All tested lines appeared UV-B responsive.

- : Low fluence rate white light, no measurable UV-B ; + : 3 μmol m^{-2} s^{-1} narrow band UV-B for 4 hours.The transcript abundance of three genes, which respond to UV-B in a UVR8-dependent manner, was determined. All tested lines, except *uvr8-1* which was employed as a negative control, displayed accumulation of *HY5*, *ELIP.1* and *CHS* transcripts following UV-B exposure. *ACT2* was used as a control to demonstrate that equal amounts of starting cDNA template was used for the PCRs. Results are representative of three independent repeats.

6.6 Generation of stably transformed transgenic lines over-expressing each TF as a translational fusion with the EGFP fluorescent tag.

One of the disadvantages of the usage of single mutant lines, when attempting functional characterisation of specific TFs in relation to particular physiological responses, is that redundancy within large gene families may compensate for the loss of function of individual members. In such cases, overexpression of a specific TF might be useful in deciphering its involvement in the physiological response of interest. For this reason, it was decided to generate transgenic Arabidopsis lines which would overexpress each of the TFs isolated from the Y1H screens (including STH3, which was shown in this chapter to behave similarly to STH2 in the Y1H assays). Moreover, instead of overexpressing the native forms, we chose to produce recombinant proteins consisting of translational fusions of each TF with the **E**nhanced form of the **G**reen **F**luorescent **P**rotein (EGFP, hereafter referred to as GFP), under the transcriptional control of the *35S* CaMV promoter. In this way, the tagged proteins' subcellular localisation could be traced and certain *in planta* assays, which would fortify our results obtained in yeast, would be facilitated. In principle, the GFP-fusions may be either N-terminal or C-terminal. If no data are available as to which fusion will affect least the function of the protein, it is advisable to produce both fusions. However, time limitations did not allow to proceed with the generation of both alternative forms for every single TF we were interested in. Instead, the preferred fusions were chosen on the basis of published structural information. For example, if an annotated domain, important for either DNA binding or protein protein interactions, is reported to reside close to the N-terminal region of the protein, then a C-terminal GFP fusion was produced, so that the domain of interest would be least affected. Obviously, a similar argument could be made against the C-terminal fusion in the above case. The function of every protein is a consequence of its tertiary structure, and it is by no means guaranteed that a C-terminal fusion will not affect the three-dimensional folding in a way detrimental to the protein's function. Hence, the productive fusions would essentially need to be determined on a trial and error basis. An easy way to demonstrate the functionality of the recombinant proteins is to generate the transgenic lines in knock out mutant backgrounds for the respective genes, which allows to observe whether the mutant phenotypes are rescued via functional complementation. However, this was not possible, because at the

time none of the single mutant lines were available and their identification was still at the stage of genotyping the material obtained from the germ-plasm stock centres. Therefore, all transgenic lines were generated in the WT Col(0) background. As an indirect, rough estimation of unimpaired function, the subcellular localisation of each recombinant protein was determined in transient transformations of *N. benthamiana* plants. Transcription factors exert their function in the nucleus, to which they are targeted via specific **N**uclear **L**ocalisation **S**equences (NLS). The NLS can either be a single amino acid sequence or it may be comprised of many sequences distributed throughout the entire protein. In both cases, proper three dimensional folding is essential for the protein to be correctly targeted to the nucleus. A mis-folded (hence functionally impaired) recombinant protein would either be quickly degraded by the proteasome, causing no detectable GFP fluorescence, or it would be ectopically expressed in the cell, retained in the wrong subcellular compartment. On the other hand, a properly folded protein (likely to be functionally intact) would be readily detected in the nucleus. Nevertheless, it should be noted that proper subcellular localisation in transient transformations is not an unequivocal proof of functional sufficiency and further validation must be provided on this point in the future.

All GFP- translational fusions generated in this project were C-terminal. Before proceeding to stable transformation of Arabidopsis, expression was assayed in transient transformations of *Nicotiana benthamiana* (Fig 6-9). All constructs, except NF-YC9-GFP, showed satisfactory expression levels and the expected nuclear localisation of the recombinant proteins. The NF-YC9-GFP fusion showed very high levels of expression in all transient transformations, resulting in detection of the protein ubiquitously in the cell as well as in the nucleus. This, however, might be an artefact of the transient transformation approach and this construct was not excluded from the generation of stably transformed Arabidopsis lines. Stably transformed Arabidopsis often exhibit varying levels of expression. If mildly expressing lines show proper nuclear-only localisation, they may be considered for further analysis. If, in contrast, a similar ubiquitous expression is displayed, then it might be worth testing an N-terminal GFP fusion for this particular transcription factor.

Currently, T2 seeds have been obtained from different lines of all TFs-GFP fusions, except MYB61-GFP, and are in the stage of segregation analysis for identification of single-insertion lines. For MYB61-GFP, as the Y2H assay (Fig 6-4 B.) singled out MYB61 for more thorough analysis, the GFP-fusion lines were handled with priority and three independent single-locus insertion T3 homozygous lines were identified. Results from experiments performed on these plants are presented in the following chapter.

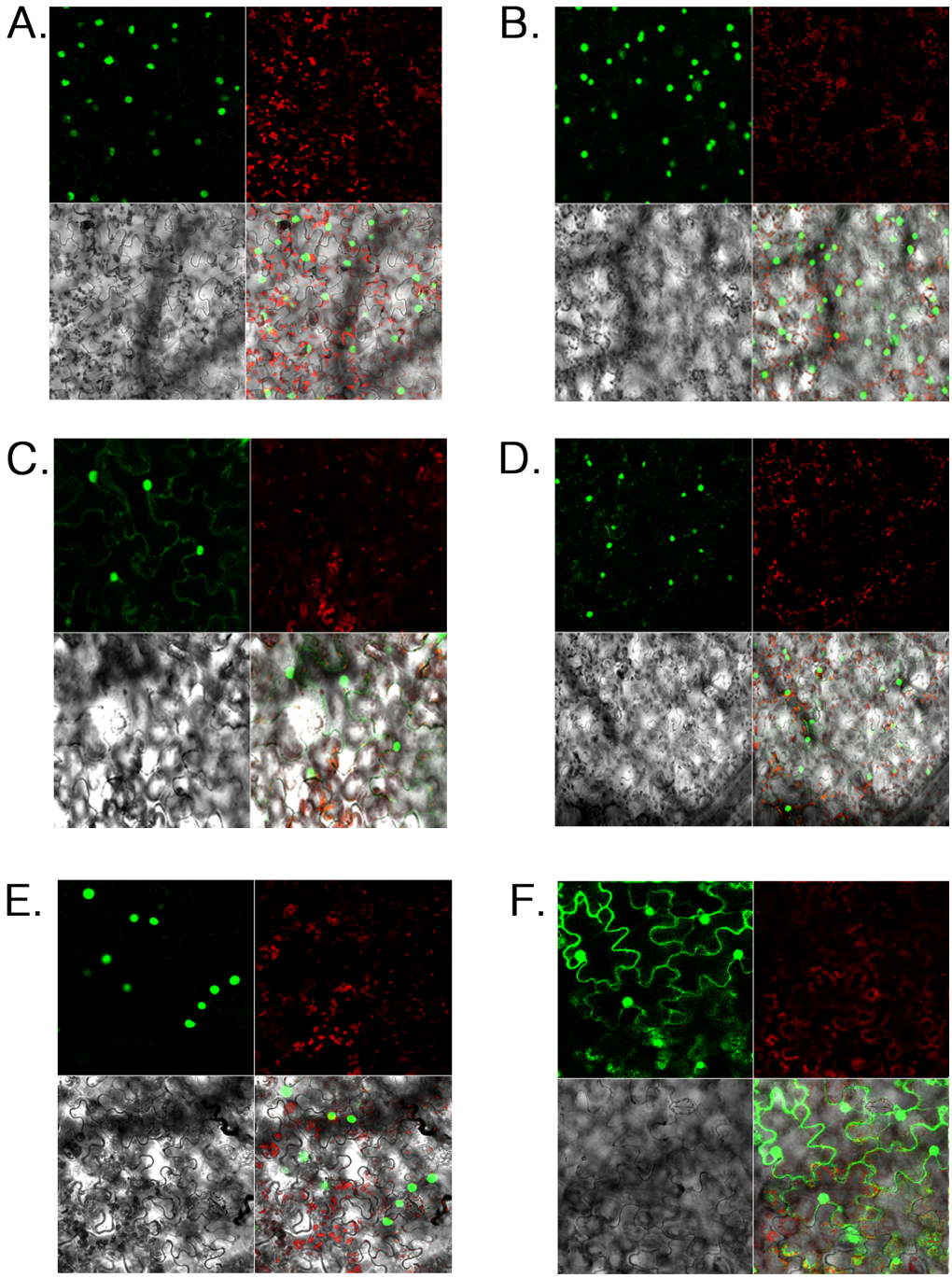

Fig. 6-9: Sub-cellular localisation of the GFP-fusions of all TFs, via Confocal Laser Scanning Microscopy, following transient transformation of *N. benthamiana* plants.
Each panel represents a different GFP- fusion. A: STH2-GFP; B: STH3-GFP; C: MYB31-GFP; D: MYB61-GFP; E: ANAC083-GFP; F: NF-YC9-GFP. For each panel, the upper two quartiles correspond to the GFP-detecting channel (left) and the autofluorescence detecting channel (right). The lower two quartiles represent the bright-field image (left) and the merged version all three quartiles (right).

6.7 Discussion

Following the results of the Y1H screens, further experiments were performed in yeast and *in planta* with the aim of deciphering the possible links, if any, of the isolated clones with photomorphogenic UVR8-dependent UV-B signalling. For STH2, focus was also expanded to several other family members, which according to published literature appeared to be worthy of testing. The obtained results did not reveal any of the tested candidates to be essential for the studied responses. Nevertheless, interesting insights were gained on the molecular behaviour of some clones and further studies will be needed to better characterise their potential role in UV-B signalling.

6.7.1 Members of the BBX family of zing-finger proteins might be involved in complex transcriptional and/or protein interaction regulatory networks important for UV-B signalling.

As mentioned previously, the BBX family consists of thirty two members (Khanna et al., 2009) which are further classified in five subfamilies. Recently, members of subfamily IV were described to have positive (STH2/BBX21 and STH3/BBX22) and negative (BBX24 and BBX25) roles in photomorphogenic cascades, by strongly associating with HY5 and COP1 (Sarmiento, 2013). Involvement in UV-B signalling, however, has to date been reported only for BBX24, which was proposed to be a negative regulator that binds to COP1 and represses *HY5* transcriptional activity (Jiang et al., 2012). Our interest on the BBX IV subfamily was sparked when one of its members, namely STH2, was isolated during the Y1H screens described in chapter 5. STH2 had been described as a transcriptional activator that interacts with HY5 and positively mediates light regulated development (Datta et al., 2007). Later, STH3, a close homologue of STH2 and functionally a very similar protein, was reported to be involved in gene expression processes that underpin light dependent development (Datta et al., 2008b). We therefore decided to subject STH3 to the same Y1H assays that had been performed for STH2. Unsurprisingly, the two proteins behaved in a similar way, showing preferential association with the UV-B box2 *cis*-regulatory element of the *HY5* promoter. It should be noted, however, that as is the case for all BBX IV subfamily members, STH2 and STH3 lack the

C-terminal **C**onstans **C**onstans-like and **T**OC1 (CCT) domain believed to modulate DNA binding (Tiwari et al., 2010; Sarmiento, 2013). No direct DNA binding activity has ever been reported for either STH2, STH3 or indeed any of the BBX IV subfamily members. Instead, a model has been proposed (Datta et al., 2007), according to which HY5 is believed to act on the cis-regulatory elements it recognises via heterodimeric complexes with STH2 or STH3. This hypothesis was based on observations made during promoter-reporter studies performed in Arabidopsis protoplasts, where it was found that STH2 and STH3 can activate transcription of the *LUC* reporter gene, which was under the transcriptional control of well known HY5-binding promoters (Datta et al., 2007; Datta et al., 2008b). Interestingly, this activity was compromised when mutations of the BBX domains, which mediate interactions with other proteins, were introduced. In our Y1H experimental set up, the yeast reporter strains were transformed solely with STH2/AD or STH3/AD fusions, and this appeared to suffice for yeast growth on selective media. This points towards a direct DNA binding activity but does not provide an undoubted proof. As discussed briefly in the previous chapter, the existence of yeast proteins which might recognise the "bait" promoter sequences and at the same time interact with STH2 and STH3, thereby recruiting them to the cis-regulatory elements we used as targets, cannot be ruled out. In fact, the UV-B box2 cis regulatory element with its flanking sequences is very similar to the plant G-Box element (C/A-CACGTGGCA), for which it has been long known that it can activate transcription in *Sacharomyces cerevisiae,* and it is bound in vitro by a yeast activity similar to the plant **G**-box **B**inding **F**actor (GBF) (Donald et al., 1990). On that basis, although STH2 and STH3 have been for convenience referred to as TFs throughout this thesis, the term should be used with caution and "transcriptional co-activators" is probably a more accurate description.

Driven by the model described above, we tested the ability of HY5 to recognise its own promoter via direct Y1H assays (Fig 6-1). Not surprisingly, as HY5 is known to act in *trans*- on G-box containing **L**ight-**R**esponsive **E**lements (LREs), we observed that HY5 preferentially associates with UV-B box 2 driving yeast growth on selective media. This finding provides an additional line of evidence towards a positive regulatory loop via which HY5 might regulate its own transcription during photomorphogenic UV-B

responses. Interestingly, HY5 has been found essential albeit not sufficient for the light-dependent induction of *STH3* expression (Chang et al., 2008), and has also been reported to induce *STH3* transcripts upon UV-B illumination (Ulm et al., 2004). It is conceivable that the aforementioned feedback loop might involve UVR8 and/or COP1 as recruiting agents, although neither of them was found to physically interact with STH2 or STH3 in Y2H assays (Fig 6-3 and 6-5). If the above hypothesis is true, and if the yeast results truly reflect the *in planta* situation, other yet unidentified proteins are probably directly responsible for the recruitment. An interesting future approach would be to perform promoter-reporter studies using *HY5* promoter fused to the *LUC* reporter gene, in Arabidopsis protoplasts derived from WT and *uvr8-1* plants. By co-transfecting HY5 with STH2 or STH3 and monitoring the activity of the reporter gene under plus or minus UV-B conditions, it could be possible to determine firstly whether HY5/STH2 or HY5/STH3 heterodimers associate with the *HY5* promoter *in planta*, and secondly whether this association is UVR8-dependent. Using protoplasts derived from different mutant backgrounds, the same experimental set up could be used to test the involvement of any supposed recruiting protein. Such experiments might need extensive and tedious optimisation, as issues related to high basal fluorescence levels or increased signals when single effectors are used would have to be overcome. Protoplasts derived from *hy5,hyh,sth2* and *hy5,hyh,sth3* triple mutants, and effectors carrying mutations in the domains important for their heterodimerisation might help to tackle the above hurdles. Overall this strategy seems a rather long shot, but in principle it could lead to informative data.

BBX24 and BBX25 are another pair of close homologues in the BBX IV subfamily, and they are emerging as potent negative regulators of light dependent development. BBX24 was first linked to photomorphogenic signalling when it was reported to physically interact with COP1 in Y2H assays (Holm et al., 2001). This interaction was mediated by a conserved amino acid motif, which is shared among BBX24, BBX25 and HY5, and appeared essential for the interaction with the WD40 domain of COP1. Later, it was found that BBX24 co-localises with COP1 in the nucleus, and undergoes a COP1-dependent degradation in the dark, even though it appeared not to have any obvious role during skotomorphogenesis (Indorf et al., 2007). In a subsequent study, BBX24 was reported to

accumulate transiently throughout the first few hours of light exposure during de-etiolation of young seedlings. However, prolonged light irradiation led to a decrease, which again appeared to be COP1-dependent (Yan et al., 2011). Interestingly, Yan et al. have additionally suggested that COP1 does not only regulate BBX24 turnover, but is also crucial for a functional modulation of BBX24 during light, which they propose is conferred via a ubiquitination activity of COP1 distinct from the one exerted when proteins are targeted for proteasomal degradation. Recently, BBX24 was correlated with UV-B signalling (Jiang et al., 2012). The interaction with COP1 was confirmed via CoIP experiments, which clearly demonstrated that in the presence of UV-B BBX24 and COP1 interact *in planta.* Although the authors claimed that the interaction is UV-B dependent, the lack of input signals for COP1 in the CoIP experiments (Fig 2A in Jiang et al., 2012) suggests that a possible UV-B dependence of the interactions needs further justification. In the same study, UV-B light caused accumulation of the BBX24 protein levels and BBX24 was found to physically interact with HY5 both in yeast and *in planta.* This interaction appeared to be mediated by the bZIP domain of HY5, and this finding was suggestive of a direct suppression of HY5 transcriptional activity which could explain the observed hypersensitivity of *bbx24* plants in low intensity UV-B light. Moreover, although the UV-B-stimulated BBX24 expression pattern appeared to be similar to that of the RUPs, Jiang et al. did not observe interaction between UVR8 and BBX24 in Y2H experiments, in contrast to the results reported here (Fig 6-4). Probable reasons for this discrepancy were discussed in the relevant results section of this chapter. As the true *in planta* situation may be different from what is revealed via Y2H experiments, further investigation of this issue is necessary via alternative methodologies. If the UVR8-BBX24 interactions turns out to be real, this would place BBX24 higher in the hierarchy of the known negative regulators of UV-B responses.

The homologue of BBX24, BBX25, has also been reported to interact with HY5 and to suppress seedling photomorphogenesis by negatively regulating the expression of STH3. On the basis of an observed, auto-activating in nature, transcriptional activation by BBX24 when it was fused with a GAL4/BD in yeast (Yan et al., 2011), BBX24 and BBX25 had been speculated to have roles in positive transcriptional regulation of various target genes (Sarmiento, 2013). Such auto-activation was not observed for BBX24 in our Y2H

experiments, although it should be noted that different yeast strain and different selection conditions were employed compared to Yan et al. Moreover, neither BBX24 nor BBX25 could activate the transcription of reporter genes in promoter-reporter studies carried out in Arabidopsis protoplasts, and both impaired the ability of HY5 to activate the transcription of the reporter genes (Gangappa et al., 2013a). Consistently, our data showed that BBX25 could not associate with the target DNA against which it was tested (Fig 6-2). Nevertheless, the positive role in transcription, proposed by Sarmiento, 2013, via other promoters cannot be ruled out. Finally, the implication of BBX24 with UV-B signalling raised questions about a similar, maybe additive role of BBX25. No interaction of BBX25 and UVR8 was observed but, unlike BBX24, BBX25 was fused with the GAL4/AD domain. For reasons briefly outlined in the results section, it remains possible that a GAL4/ BD - GAL4/AD domain swapping might show interaction with UVR8. Nonetheless, since the physiologically relevant interactions are only those observed *in planta,* further analysis should be undertaken in the future with non-yeast based approaches.

6.7.2 None of the Y1H screen - isolated TFs is essential for some standard UVR8-dependent UV-B responses.

The Y2H assays (Fig 6-3, 6-4 and 6-5) revealed that only MYB61, among the tested TFs, was capable of interacting with UVR8, and this interaction was only observable under UV-B-free conditions. However, a possible involvement in UV-B signalling does not necessarily have to include direct physical interactions with the UV-B photoreceptor. Therefore, it was decided that the putative role of all candidates in UVR8-dependent photomorphogenesis should be examined using T-DNA insertion mutant Arabidopsis lines for the corresponding genes. Single mutant lines were identified by PCR genotyping, and the mutant status (“knock out” vs “knock down” mutations) was determined with semiquantitative RT-PCR (Fig 6-6). For subsequent analysis, “null” mutants were used if available. In the hypocotyl elongation assays that followed (Fig 6-7), all tested lines behaved similarly to the WT control in terms of hypocotyl length phenotypes and UV-B induction of CHS. Similarly, the gene expression studies (Fig 6-8) revealed that all tested lines displayed elevated transcript abundances for three well known UVR8-dependent UV-

B responsive genes. For STH2, STH3, ANAC083 and MYB31, for which "loss of function" mutant lines were used, the result implies that they are not essential for the particular responses. Nevertheless, these TFs are members of large multi-gene families in which functional redundancy may hinder unequivocal phenotypic characterisation using single mutants. It is not unlikely for close homologues of the mutated TFs to take over their role in the studied responses, thus masking any effects of a single member loss of function. As for NF-YC9 and MYB61, the respective mutant lines had detectable levels of the full length transcripts (Fig 6-6). This, however, does not imply that these transcripts are stable enough to undergo translation. It is possible that either no protein is produced, or some protein is produced but the levels do not suffice for its activity to be comparable to that of a WT plant. Unfortunately, no antibodies were available to check the protein expression levels, and time constraints did not allow for a comprehensive analysis of the expression patterns of known downstream targets of NF-YC9 and MYB61 in their respective mutant lines, which would be an indirect way of assessing their activity. Obviously, the functional redundancy argument described above is equally applicable to these "knock down" mutants. Thus, further studies need to be undertaken to unravel a role in UV-B signalling, if such role is present. In an attempt to bypass the hurdles outlined above, it was decided to proceed with the generation of transgenic lines overexpressing a GFP-fused recombinant form of every candidate transcription factor. The GFP-fusions were placed under the transcriptional control of the *35S* CaMV promoter and the transgenic lines were generated in the WT Col(0) background. As already mentioned, a judgement call had to be made as to which lines would be more thoroughly followed, as it was practically impossible to exhaustively investigate them all within the defined time frame of this project. The interaction of MYB61 with UVR8 in yeast, albeit weak (Fig 6-4), was a very intriguing result which needed further fortification via an alternative approach. Subsequently, if more evidence was to be added in support of such interaction, further analysis would have to be undertaken in order to elucidate its functional significance. Therefore, the MYB61-GFP overexpressing lines were treated on a first priority basis, as they might be useful for the planned experiments. The most interesting findings from these attempts are summarised in the forthcoming, final results chapter of this thesis.

CHAPTER 7: IN SEARCH OF THE FUNCTIONAL SIGNIFICANCE BEHIND THE ASSOCIATION OF MYB61 WITH THE *HY5* PROMOTER AND ITS INTERACTION WITH THE UV-B PHOTORECEPTOR UVR8.

7.1 Introduction

MYB61 is a member of the large R2-R3 MYB family of Arabidopsis transcription factors. In the course of this project, two findings were interpreted as suggestive of its possible involvement in photomorphogenic UV-B responses. First, MYB61 was found capable of associating with the *HY5* promoter via a preferential binding to a particular UV-B responsive *cis*-regulatory element. Second, Y2H assays revealed a weak but consistently observable physical interaction with UVR8, the plant UV-B-specific photoreceptor. Preliminary attempts to assess *in planta* the functional connection between MYB61 and UVR8-mediated signalling were based on the utilisation of a SALK T-DNA insertion line, which was unfortunately found to retain detectable levels of the full length *MYB61* transcript. Thus, no strong conclusions could be drawn as to whether MYB61 is implicated in the tested responses. As discussed in the previous chapter, the lack of an interesting phenotype or of any intriguing deviations from expected UV-B-elicited molecular patterns might be attributed to functional redundancy, and/or to residual MYB61 activity sufficient to fulfil its physiological role. Therefore, having no sufficient data to reject our working hypothesis and being aware that more results were needed to support it, we decided to proceed with a more thorough investigation.

A bona fide loss-of-function *myb61* mutant line was identified from a different collection of T-DNA insertional Arabidopsis mutants. In addition, plants overexpressing MYB61 conditionally, and others displaying a constitutive overexpression, were obtained and assayed for altered UV-B responses. In the case of the constitutively overexpressing lines, they were designed to produce a MYB61-GFP recombinant protein so that they could be utilised in ChIP assays with the aim of testing the *HY5* promoter binding *in planta*. Moreover, co-immunoprecipitation assays were performed in order to provide an additional line of evidence in support of the physical interaction between MYB61 and UVR8. Eventually, the closest homologue of MYB61 in Arabidopsis, namely MYB50, was

also considered for analysis. The results were interesting but indicative of a rather complex picture, the full understanding of which will require further research. This chapter summarises our findings.

7.2 The C27 region of UVR8 is important for the interaction with MYB61 in yeast

The C-terminus of UVR8 contains a 27 amino acids region (amino acids 397 to 423, hereafter referred to as C27) which has been shown to be important in the signalling events orchestrated by UVR8. It mediates the interaction with COP1 in yeast and in plants, and it is necessary for UVR8 function in the regulation of gene expression and hypocotyl growth suppression in Arabidopsis (Cloix et al., 2012). In addition, the negative regulators of photomorphogenic UV-B responses RUP1 and RUP2 interact with UVR8 via the same C27 region. Consistently, UVR8 that lacks this particular stretch of amino acids has been reported to have a reduced rate of dimer regeneration *in vivo* (Heilmann and Jenkins, 2013). Given this apparently key role of C27 in UVR8 function, it was desirable to assess its significance for the interaction with MYB61 in yeast. Two distinct mutant variants of UVR8 which are impaired in photoreception and have been demonstrated to be altered in terms of the interaction with COP1 in Y2H assays were also included in the analysis. $UVR8^{W285A}$ and $UVR8^{W285F}$ have the functionally crucial "triad" tryptophan W285 substituted with alanine and phenylalanine respectively. The first mutant is a weak dimer which is most likely to occur as a monomer under the conditions found within the plant cell (O'Hara and Jenkins, 2012), and is constitutively monomeric in yeast (Heijde et al., 2013; Huang et al., 2014). Moreover, $UVR8^{W285A}$ interacts with COP1 in both yeast and plants irrespective of UV-B illumination conditions. On the other hand, $UVR8^{W285F}$ is constitutively dimeric in plants and yeast and fails to interact with COP1.

With regard to MYB61, the interaction with UVR8 was observed only in non-UV-B-irradiated yeast cells and was abolished when the C27 region was removed (Fig 7-1). Intriguingly, none of the two W285 substitutions affected the physical association of the two proteins. This was a rather puzzling outcome considering the differential dimer/ monomer status of the two variants within the yeast cells, and it will be discussed in more

detail in a following section in the light of additional data obtained from co-immunoprecipitation experiments.

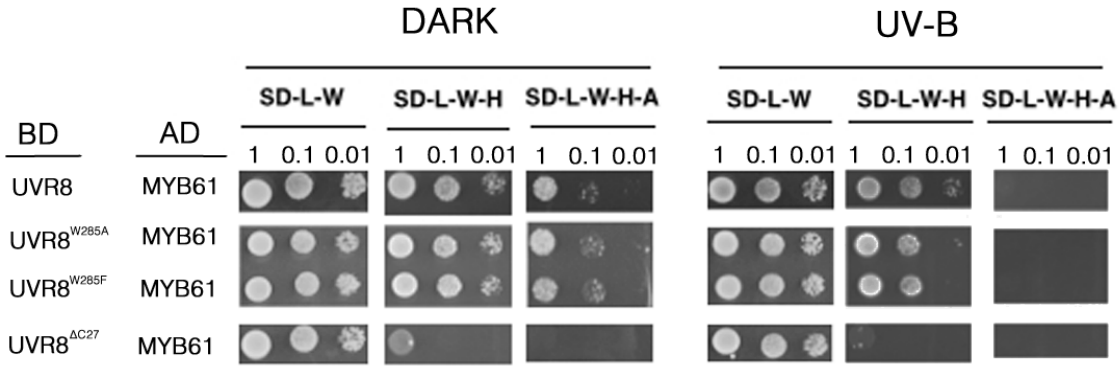

Fig. 7-1: The C27 region of UVR8 is important for the interaction with MYB61 in yeast. $UVR8^{W285A}$ and $UVR8^{W285F}$ represent two single-amino-acid-substitution mutant variants of UVR8 in which the "triad" photoreceptive tryptophan W285 has been replaced by an Ala and a Phe residue respectively. $UVR8^{\Delta C27}$ corresponds to UVR8 lacking the C27 region. SD-L-W medium was used as a control for the viability of the spotted cells. Interactions were assessed on low (SD-L-W-H) and high (SD-L-W-H-A) stringency selection plates. Spottings were performed from cell suspensions with three different cell densities (OD=1 , 0.1 and 0.01). Results are representative of at least two independent biological replicates.

7.3 Identification of a genuine loss-of-function *myb61* mutant Arabidopsis line

The SALK T-DNA insertion line described in the previous chapter was found to be a "knock down" mutant which maintained detectable levels of the full length *MYB61* transcript. This allele was previously reported as *myb61-3* (Meissner et al., 1999), hence for consistency it will be hereafter referred to using the same designation. The initial description of *myb61-3* placed the T-DNA insertion within the ORF of *MYB61* and towards its 3' end. According to the TAIR database, the sequence identified as mapping close to the insertion site is located approximately 135 bp upstream of the *MYB61* STOP codon. These positions however are approximate and according to the data obtained in the course of our research it is unlikely that this particular T-DNA insertion is located within the *MYB61* ORF. If that were the case, no full length *MYB61* transcript would be detected (Fig. 6-6 in previous chapter and Fig. 7-2 here). Most probably the insertion in the *myb61-3* allele is disrupting the 3' untranslated region of *MYB61,* which could additionally explain why the full length transcript from *myb61-3* plants appeared slightly larger than the full length transcript detected in WT plants (Fig. 7-2). Splicing and processing of 3' untranslated regions have been reported to be functionally coordinated in eucaryotes (Millevoi et al., 2006), and it is conceivable that in *myb61-3* plants the *MYB61* transcript is not spliced correctly leading to a somewhat larger variant.

For the functional characterisation of MYB61 in relation to photomorphogenic UV-B responses the identification of an authentic loss-of-function mutant line would be imperative. To that end, Arabidopsis seeds from plants carrying a previously described (Penfield et al., 2001) mutant allele of *MYB61* were obtained from the **S**ainsbury **L**aboratory ***A****rabidopsis* ***t****haliana* (SLAT) population. The resulting seedlings were genotyped and found to be homozygous for the mutant allele (Fig 7-2 Aα), which was designated *myb61-1* in consistency with Penfield and co-workers. At the transcript level, *myb61-1* plants appeared to be "null" (Fig 7-2 Aβ.). As an additional validation of the bona fide loss-of-function of the *myb61-1* plants, a simple phenotypic assay was performed. MYB61 is required for mucilage deposition and extrusion in the Arabidopsis seed coat. In mature seeds, each epidermal cell possesses mucilage in a dehydrated form. Upon contact with water, mucilage is quickly hydrated and extruded from the seed coat as it expands

outwards rupturing the primary cell wall. At this stage mucilage forms a pectin hydrogel that encapsulates the whole seed and can be readily observed under the microscope following staining with ruthenium red (Penfield et al., 2001). Whereas WT seeds displayed this gel-like envelope, *myb61-3* seeds had a much reduced and faintly stained layer of mucilage, which was completely absent in *myb61-1* seeds (Fig 7-2 B) consistent with the "knock down" and "null" nature of the respective mutations. Conversely, *uvr8-1* seeds were indistinguishable from WT suggesting that the mucilage extrusion deficiency in *myb61* mutants is not dependent on a functional UVR8 protein.

7.4 MYB61 is not required for suppression of hypocotyl elongation, UVR8-mediated transcriptional up-regulation of certain UV-B-induced genes, or CHS accumulation upon UV-B irradiation

After obtaining a true "knock out" *myb61* mutant line, it was desirable to assess its behaviour under the standard UV-B responses we've been employing throughout this project as diagnostic assays for the identification of potentially crucial mediators of UVR8-mediated signalling. Hypocotyl elongation assays revealed that *myb61-1* plants are similarly responsive to UV-B as the WT plants (Fig 7-3 A and B). In particular the the UV-B (-) / UV-B (+) ratios of hypocotyl lengths were ~ 2.4 , 2,2 and 1.9 for WT, *myb61-3* and *myb61-1* respectively. Control *uvr8-1* plants on the other hand displayed the anticipated lack of UV-B responsiveness. Furthermore, immunoblots with antibody against CHS on protein extracts from the seedlings subjected to the hypocotyl elongation assay, revealed that in both *myb61-3* and *myb61-1* UV-B illumination leads to increased steady state levels of CHS, similar to WT plants and in contrast to the *uvr8-1* control plants (Fig 7-3 C). Finally, gene expression analysis demonstrated that UV-B irradiation causes accumulation of *HY5, CHS* and *ELIP.1* transcripts in the *myb61-1* mutant comparably to WT plants. It can be therefore concluded that MYB61 is not essential for the tested UV-B responses.

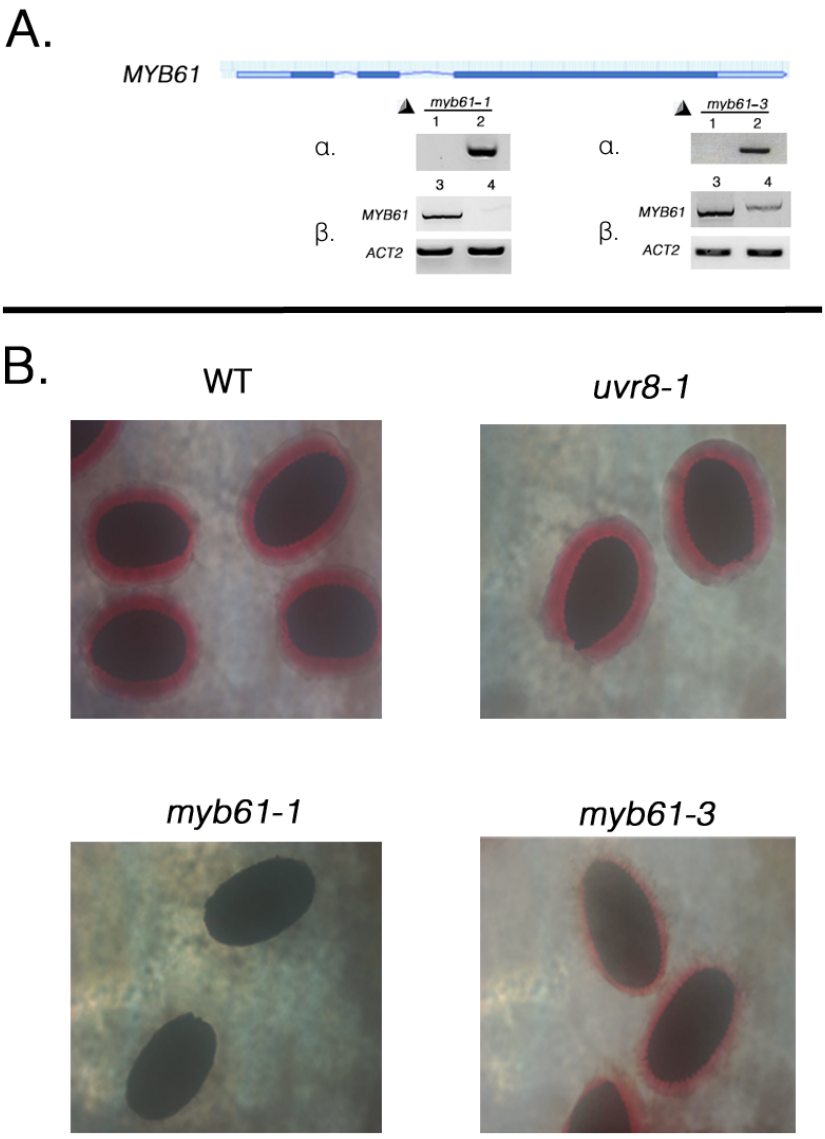

Fig. 7-2: Identification of a genuine loss-of-function *myb61* mutant.

A. Genome browser view of *MYB61* and the approximate locations of the T-DNA insertions in *myb61-1* and *myb61-3*. Exons are depicted as dark blue thick lines, untranslated regions as light blue thick lines and promoters or introns as slim lines. Panel α. shows the genotyping results; lane 1 corresponds to the PCR outcome when primers flanking the T-DNA insertion were used, and it should not give product if an insertion is present; lane 2 shows the PCR product when a Left Border T-DNA-specific primer and a locus-specific primer were used. Panel β. shows the results of RT-PCR using *MYB61*-specific primers, which amplify the full length coding sequence. *ACT2* primers were used as controls. Lane 3 : WT cDNA Lane 4 : mutant line cDNA.

B. Mucilage staining with ruthenium red showing that *myb61-1* is a functionally "null" mutant. (Observation under the 10X objective lens of a conventional light microscope.)

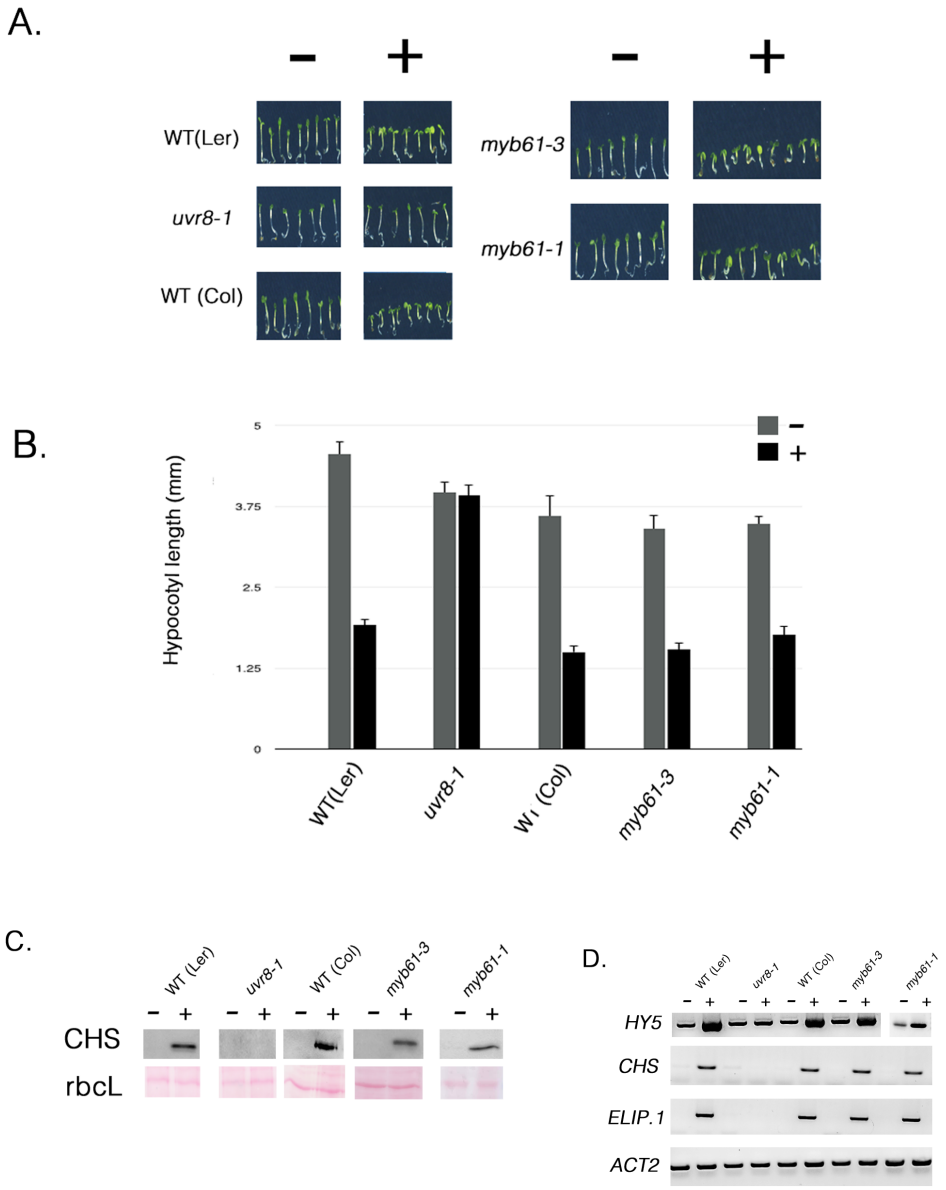

Fig. 7-3: Functional characterisation of *myb61-1* mutant plants in relation to standard UVR8-mediated responses. A. and **B.** Hypocotyl elongation assay. For the quantitative analysis at least 25 seedlings were measured and error bars represent SE. **C.** CHS protein accumulation in seedlings subjected to the hypocotyl elongation assay; rbcL: Rubisco Large subunit, -/+ : absence/presence of UV-B. **D.** Gene expression analysis from 3 weeks-old plants treated with UV-B light. -/+ : absence/presence of UV-B. Results are representative of three independent biological repetitions

7.5 MYB61 overexpressing lines display WT phenotypes in standard UV-B responses

The *R2-R3 MYB* family is one of the largest transcription factor gene families of Arabidopsis (Stracke et al., 2001). An unfortunate consequence of this fact is that the use of single mutants when attempting functional characterisation of individual members is rarely informative. Commonly, the loss-of-function of a particular member can be counterbalanced by another related transcription factor leading to no observable phenotypic output. A strategy that has often helped scientists to circumvent this problem is the use of plants which overexpress the TF of interest. Hoping that such an approach would provide some insights into the functional involvement of MYB61 in UVR8-mediated signalling, MYB61:GFP overexpressing lines were constructed. The fusion construct was placed under the transcriptional control of the *35S CaMV* promoter and the entire cassette was introduced into WT Col (0) plants (see chapter 6). Four independent, homozygous, single-locus insertion lines were obtained as described in the "materials and methods" section and were designated L9, L24, L26 and L37. RT- PCR analysis performed with two different primer pairs, one targeting the 5' and the other the 3' region of the *MYB61* ORF, demonstrated that L26 and L37 are overexpressing profoundly compared to WT whereas L9 and L24 represent milder overexpressors (Fig 7-4 A.). Observation under the laser scanning confocal microscope allowed detection of the nuclear-localised MYB61-GFP in all four transgenic lines (Fig 7-4 C.). Unfortunately, the detection of the recombinant protein in immunoblots proved to be problematic to a certain extent, because at least two commercially available anti-GFP antibodies gave a non-specific cross-reacting band at about the same size as MYB61-GFP. To overcome this, a highly specific monoclonal HRP-conjugated anti-GFP antibody was used, which nonetheless resulted in weaker signals as the whole procedure lacked the signal-amplifying step of secondary antibodies. Even so, a band of the correct size was detected for L26 and L37, the two strongly overexpressing transgenic lines (Fig 7-4 B), whereas no signal could be obtained for L9 and L24 under the defined conditions of these immunoblotting experiments. For subsequent functional characterisation of the MYB61-GFP lines in relation to UV-B responses, it was decided to use line L9 (a mild overexpressor) and lines L26 and L37 (strong overexpressors). Line

L24 was excluded at the time, because the initial amount of the recovered homozygous seeds was very low and it was reserved for bulking up more material.

While the generation of our MYB61-GFP overexpressing transgenic lines was under way, a study was published reporting the public availability of the TRANSPLANTA collection of Arabidopsis lines (Coego et al., 2014). This collection is a resource for the functional characterisation of Arabidopsis transcription factors, and it offers the advantage of a chemically induced conditional overexpression as opposed to a stable constitutive overexpression. The authors cloned numerous Arabidopsis TFs under the control of an estradiol-inducible promoter, thus allowing time-controlled overexpression by applying an estradiol treatment to the plants. Luckily, three such transgenic lines in the TRANSPLANTA collection, designated TPT53, TPT54 and TPT55, were claimed to offer an estradiol-induced overexpression of MYB61. We obtained these three lines from NASC, the European Arabidopsis Stock Centre, and we subjected them to an estradiol treatment as described in Coego et al (2014). In contrast to TPT53, TPT54 and TPT55 exhibited the expected elevation in *MYB61* transcripts after the application of the inducing agent (Fig 7-4 D.) Hence, both lines were included in subsequent analysis.

Sadly, neither our constitutively overexpressing lines nor the TRANSPLANTA collection conditional overexpressors differed from the WT plants with regard to the UV-B-induced suppression of hypocotyl elongation phenotype (Fig 7-5 A and B). In addition, all tested lines displayed accumulation of CHS protein following UV-B illumination (Fig 7-5 C). It could be argued, however, that the dose of UV-B (1.5 μmoles m^{-1} s^{-1}) used for the hypocotyl elongation assays is already saturating, thus not allowing the detection of a supposedly hypersensitive response from the overexpressing lines. Therefore, it might be worth performing carefully optimised hypocotyl elongation assays with varying fluence rates of UV-B in the future, as such assays could reveal mild differences which were not observable under the experimental setup reported here. Moreover, the immunoblots as performed in this study were not quantitative. Hence, future efforts could employ more sensitive, suitable for quantitative comparisons kits, thereby providing more reliable information as to wether certain MYB61 overexpressing lines (e.g the TPT lines) accumulate more CHS protein following UV-B.

Finally, as evidenced by gene expression analysis (Fig 7-6 A. and B.), UV-B-irradiated MYB61-GFP overexpressing lines accumulated *HY5, CHS* and *ELIP.1* transcripts indistinguishably from the WT plants. Interestingly, as one might anticipate for plants that overexpress strongly and constitutively a TF that binds to the *HY5* promoter, the basal expression of *HY5* in lines L26 and L37 was found higher (~7 fold difference) when compared to WT Col (0) plants (Fig 7-6 B.). Conversely, the mildly overexpressing lines L9 and L24 displayed basal steady-state levels of the *HY5* transcript which were comparable to those observed in WT plants. The quantitative PCR analysis was performed relatively late during this project and only one biological repeat was assayed. Nonetheless, the fact that four independent transgenic lines were analysed, taken together with the good correlation between *MYB61* overexpression (Fig 7-4 B), MYB61 accumulation (Fig 7-4 D), and *HY5* transcript basal abundance (Fig 7-6 B.), gave confidence for inclusion of this result in the thesis.

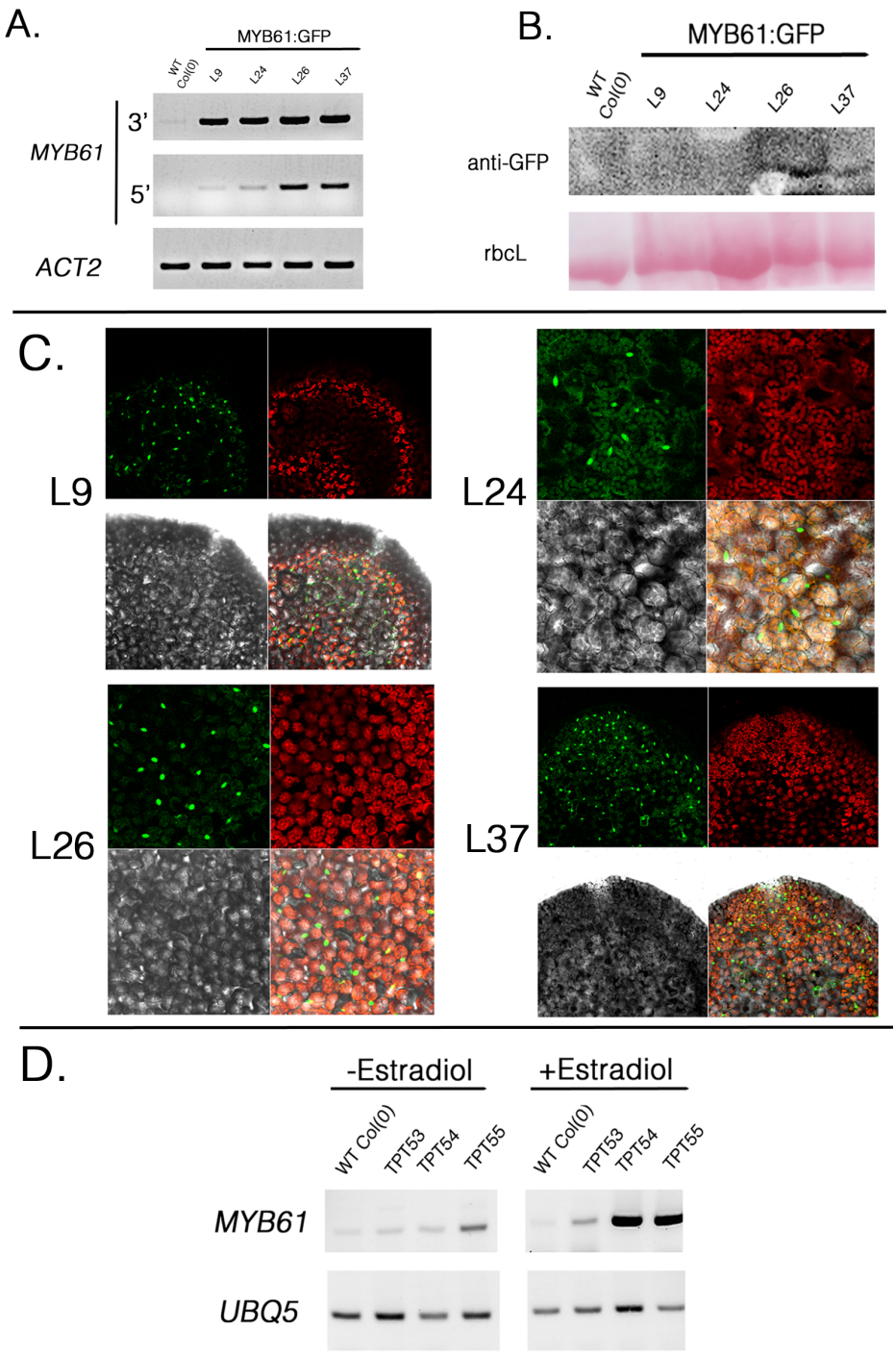

Fig. 7-4: Characterisation of MYB61 OE lines. A. Estimation of total *MYB61* (native plus transgene) transcript abundance in four MYB61-GFP overexpressing lines, using two distinct primer combinations, one annealing to the 3' region and one to the 5' region. *ACT 2* was used as a normalisation control. **B.** MYB61-GFP detection in protein extracts from the overexpressing lines L9, L24, L26 and L37, through immunoblotting using Ab against the GFP tag. Ponceau staining of the Rubisco Large subunit (rbcL) is provided as control for equal loading. Results are representative of at least two independent biological repetition. **C.** Nuclear localisation of MYB61-GFP in the four MYB61 overexpressing lines., as observed via laser scanning confocal microscopy. **D.** Assessment of the estradiol-induced overexpression of *MYB61* in TPT lines via RT-PCR. *UBQ5* was used as normalisation control

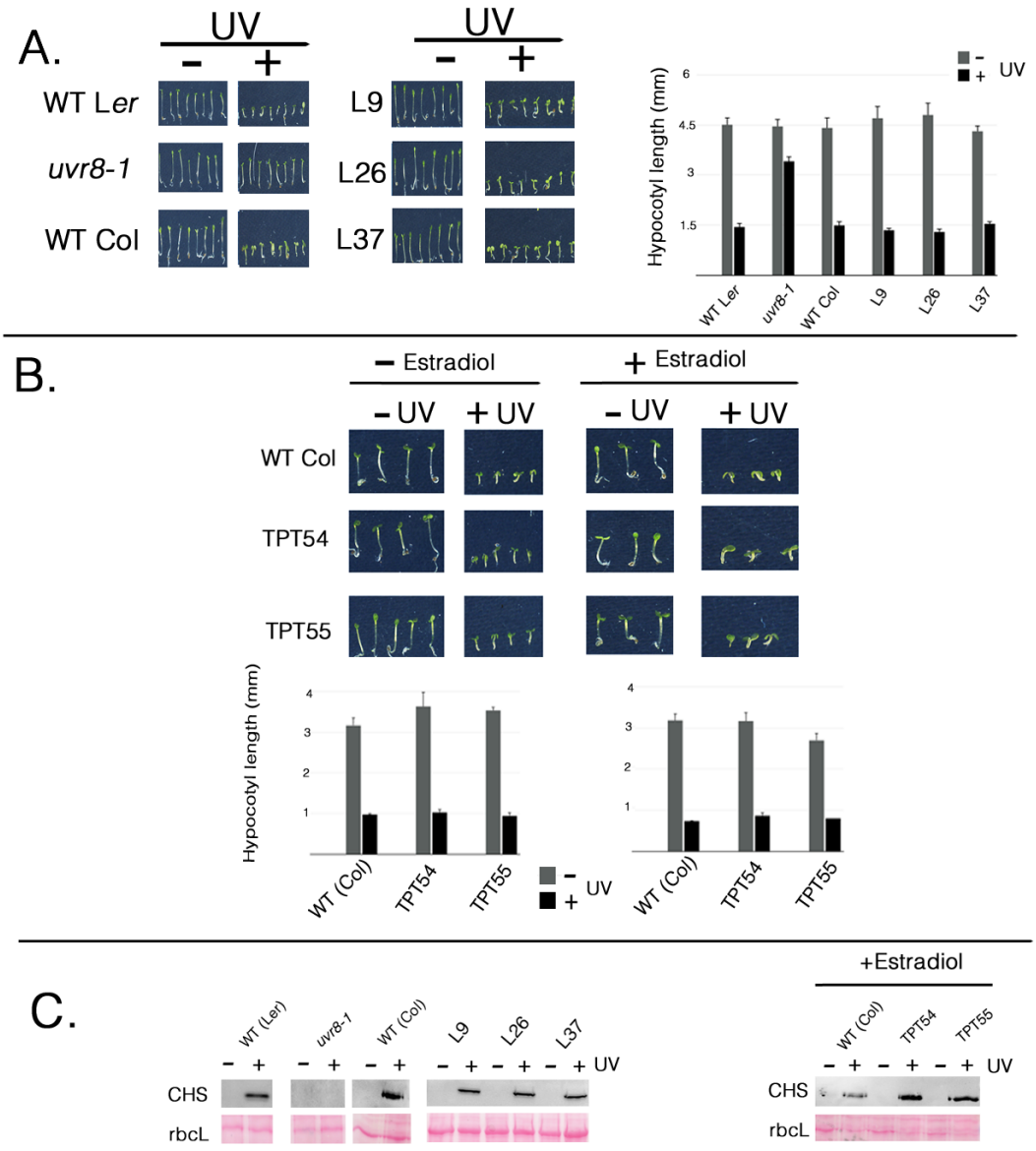

Fig. 7-5: Functional characterisation of MYB61-OE plants in relation to standard UVR8-mediated responses. A. Hypocotyl elongation assay for three individual MYB61-GFP OE lines (L9, L26 and L37). For the quantitative analysis error bars represent SE ($n \geq 25$). **B.** Hypocotyl elongation assay for two TPT lines (TPT54, TPT55) conditionally overexpressing MYB61 only after treatment with Estradiol. For the quantitative analysis error bars represent SE ($n \geq 12$). **C.** CHS protein accumulation in seedlings subjected to the hypocotyl elongation assays of **A.** and **B.**, measured via immunoblotts with anti-CHS antibody. rbcL: Rubisco Large subunit. Results are representative of two independent biological repeats.

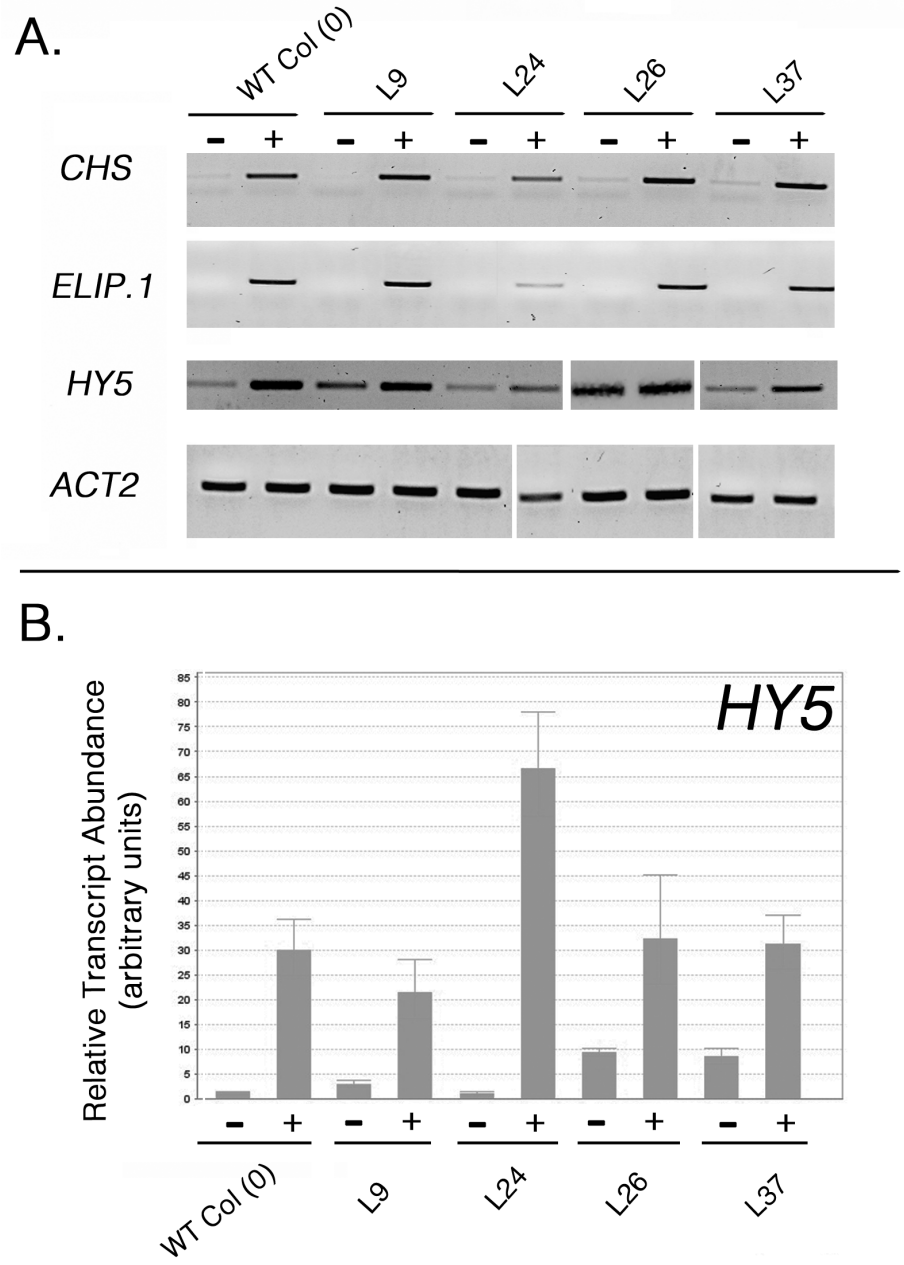

Fig. 7-6: Gene expression analysis in the MYB61-GFP OE lines for certain UVR8-regulated UV-B induced genes. A. The transcript abundance of *HY5*, *ELIP.1* and *CHS* was determined via semiquantitative RT-PCR. *ACT2* was used as a control to demonstrate that equal amounts of starting cDNA template was used. **B.** Real time quantitative PCR for *HY5* transcript accumulation, estimated as relative enrichment normalised against *ACT2,* performed for obtaining a clearer and more accurate picture compared to the one obtained in A. Error bars represent SD form three technical replicates.

- : Low fluence rate white light, no measurable UV-B ; + : 3 µmol m^{-2} s^{-1} narrow band UV-B for 4 hours. Panel A results are representative of two independent biological repeats, whereas the qPCR analysis (Panel B) was performed for only one biological repeat.

7.6 MYB50, the closest homologue of MYB61, associates with the HY5 promoter and interacts with UVR8 in yeast

Soon after obtaining of the experimental findings presented thus far, there was a growing suspicion that other members of the R2-R3 MYB family of transcription factors might share specific UV-B-related molecular functions with MYB61, thereby hindering a comprehensive understanding of its physiological role through the approaches that had been undertaken. There are numerous R2-R3 MYB family subgroups, categorised on the basis of the conservation of the N-terminal DNA binding domains and according to particular C-terminal amino acid motifs (Dubos et al., 2010). MYB61 belongs to the S13 subgroup together with MYB86, MYB55 and MYB50, with the latter being its closest homologue. Hence, it was decided to investigate whether MYB50 could bind to the *HY5* promoter and whether it could associate physically with UVR8. To that end, Y1H and Y2H assays were undertaken (Fig 7-7). It was revealed that MYB50 can associate with the b1.2 DNA "bait" sequence, which as described in chapter 5 consists of both the UV-B box1 and the UV-B box2 cis-regulatory elements of the *HY5* promoter (Fig 7-7 A). The lack of yeast growth when a reporter strain carrying the mutated "bait" mb1.2 (see chapter 5) was used, indicated that the aforementioned interaction was specific. Whether the DNA binding occurs via the preferential recognition of UV-B box2 remains to be demonstrated, but the high sequence similarity between the MYB50 and MYB61 DNA-binding domains suggests that this is most likely the case. The Y2H assay showed that MYB50 can interact with UVR8 regardless of the illumination conditions (Fig 7-7 B.) in contrast to MYB61 whose physical association with UVR8 in yeast was only observed when the cells were not UV-B irradiated (Fig 6-4. and Fig 7-1).

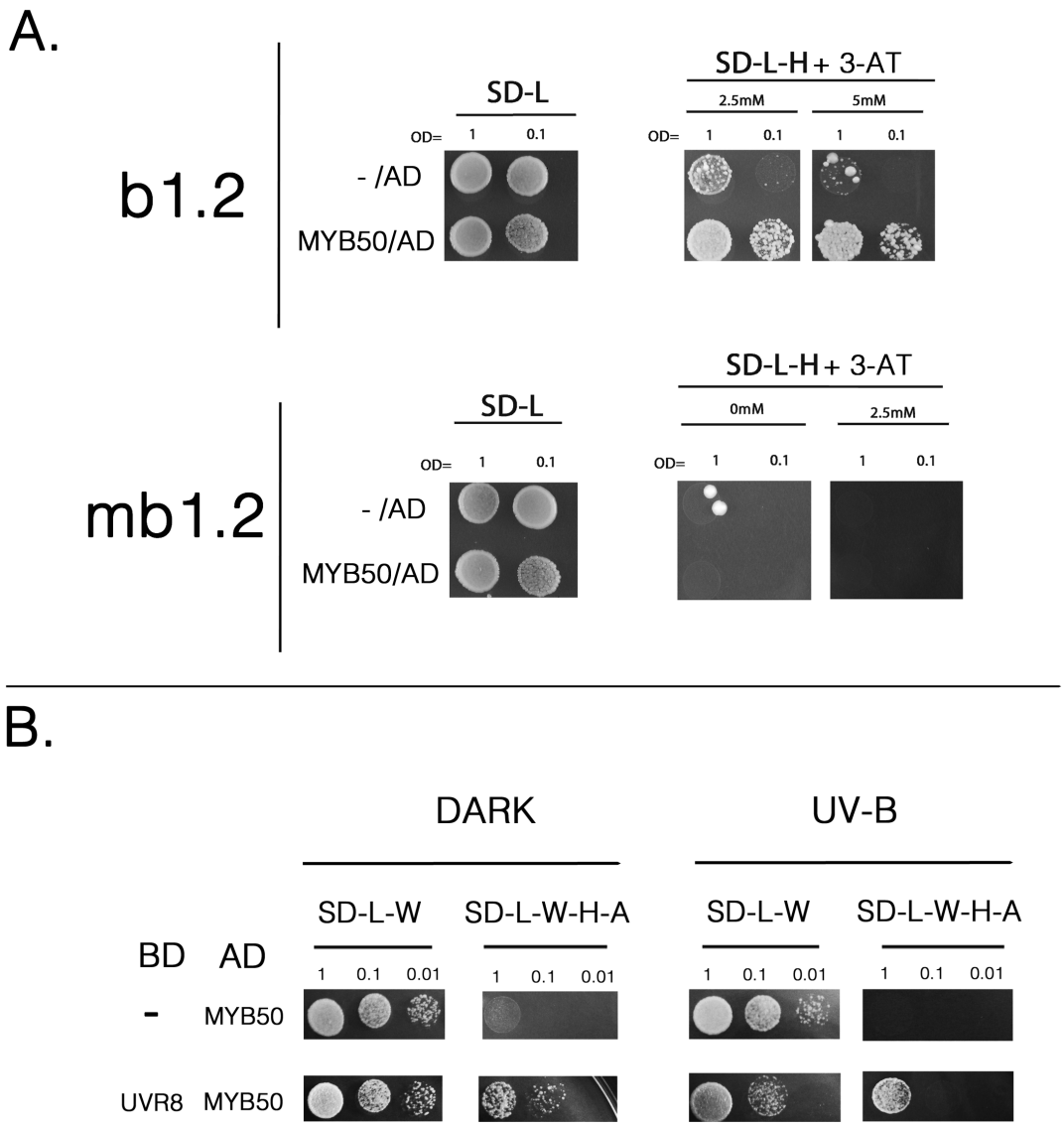

Fig. 7-7: Interaction of MYB50 with the *HY5* promoter and with UVR8. A. Direct Y1H assay . MYB50 interacts specifically with the b1.2 "bait" DNA, consisting of UV-B box1, UV-B box2 and their native intermediate DNA sequence. No interaction is observed with the mutated version mb1.2.. SD-L medium was used as a control for the viability of the spotted cells. Interactions were assessed on His-lacking medium supplemented with different concentrations of the 3-AT inhibitor (SD-L-H + 3-AT). Spottings were performed from cell suspensions with two different cell densities (OD= 1 and 0.1). **B.** Y2H assay showing the interaction of MYB50 with UVR8 regardless of UV-B illumination conditions. SD-L-W medium was used as a control for the viability of the spotted cells. Interactions were assessed only on high (SD-L-W-H-A) stringency selection plates. Spottings were performed from cell suspensions with three different cell densities (OD= 1 , 0.1 and 0.01). Results representative of two independent biological repeats are shown.

7.7 Both MYB61 and MYB50 co-precipitate with UVR8 in protein extracts from leaves of transiently transformed *Nicotiana benthamiana* plants

Informative as it is, the Y2H assay for assessing interactions between plant-specific proteins is a heterologous system and it can occasionally be misleading. Therefore, for claims of such interactions to be persuasive, the physical association of the proteins of interest needs to be demonstrated via at least one alternative approach and, if possible, *in vivo*. Two widely used procedures are the **Bi**molecular **F**luorescence **C**omplementation (BiFC) and the **Co**-**i**mmuno**p**recipitation assay (Co-IP). Although performing both these assays would provide greater rigour in our analysis, concerns about the time consuming optimisations that might be necessary led to the decision of proceeding only with the CoIP, which was chosen over BiFC as the latter required extensive re-cloning for obtaining the desired constructs, whereas for the co-immunoprecipitations some of the materials were already available.

A *MYB50-GFP* fusion, similar to the one described for MYB61 in chapter 6, was constructed in the pEZRL(N) binary vector. Additionally, an *HA-UVR8* fusion cassette in a GATEWAY Entry clone was kindly provided by a colleague in the laboratory (Dr Monika Heilmann) and it was subcloned in a GATEWAY destination vector following the recommended protocols, leading to the generation of a binary expression vector encoding for the HA-UVR8 fusion protein. Subsequently, leaves of 4-5 weeks old *Nicotiana benthamiana* plants were co-transformed with both a MYB-GFP fusion (either one of the two) and the HA-UVR8 fusion. After 1.5 days the transiently transformed plants were assessed for satisfactory expression of both fusion proteins, following which some were irradiated for 4h with 3 μmol m^{-2} s^{-1} narrow band UV-B whereas others were kept under low fluence rate white light (~15 μmol m^{-2} s^{-1}) for the same period of time. The Co-IPs were performed as described in "materials and methods" and the results revealed that regardless of the light treatment both MYB TFs were capable of associating with UVR8 (Fig 7-8). For MYB50 this finding is in complete agreement with the Y2H assay (Fig 7-7 B.), while for MYB61 it demonstrates that UV-B does not affect the interaction contrary to what was observed in yeast. This discrepancy nicely highlights the importance of addressing a particular research question by undertaking independent experimental

approaches, as the puzzling results shown in Fig. 7-1 can be now rationalised in the light of the CoIP findings. The Y2H assay had revealed that MYB61 can interact with UVR8 only under UV-B-free conditions. UV-B treatment did not seem to impair yeast growth in general, therefore one would anticipate to observe a light-independent persistent interaction with the constitutively dimeric ($UVR8^{W285F}$) variant and no interaction at all with the constitutively monomeric ($UVR8^{W285A}$) form. Contrary to these expectations however, the interaction in yeast appeared not to depend on the dimer-monomer status of the photoreceptor, although it was affected by UV-B light. Conversely, the CoIP experiments seem to suggest that an alternative scenario might be at play *in planta,* where plant-specific factors are probably contributing to the stability of the MYB61-UVR8 complex upon UV-B, but this stabilising effect is lost in the heterologous yeast system.

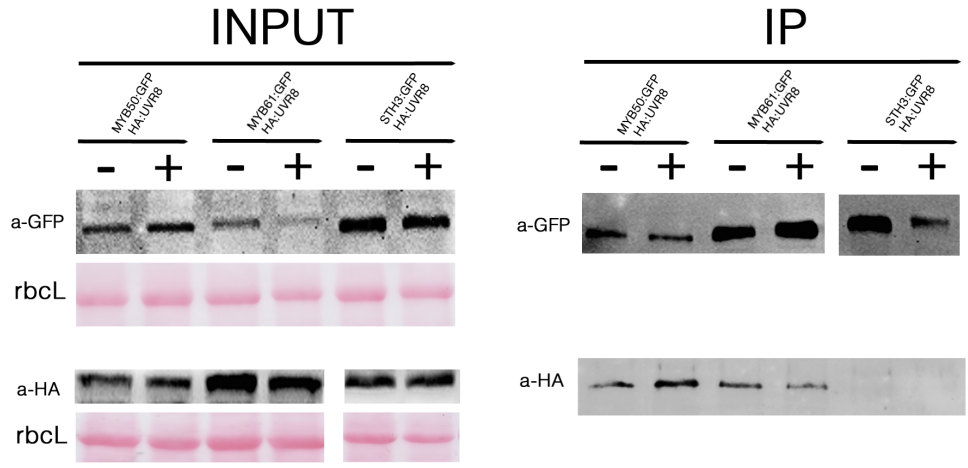

Fig. 7-8: Interaction of MYB61 and MYB50 with UVR8 in plant protein extracts.
Nicotiana benthamiana leaf protein extracts (INPUT) were first assessed for satisfactory expression of both -GFP and HA- fusion constructs via immunoblot analysis. Subsequently, immunoprecipitations (IP) were performed with anti GFP ab, and the recovered material was assessed for the enriched presence of the GFP-fusion protein to evaluate the success of the IP. Eventually, IP samples were subjected to immunoblot analysis with anti-HA antibody to determine whether the HA- fusion protein has been Co-immunoprecipitated.. STH3-GFP was used as a negative control, as it was found to display high expression levels and exclusively nuclear localisation in transiently transformed *Nicotiana benthamiana* plants, and it did not interact with UVR8 in Y2H assays (chapter 6.). -/+ : absence/presence of UV-B. Results are representative of two independent biological repetitions.

7.8 MYB61 interacts with FVE in yeast

It has been suggested that the recruitment of chromatin modifiers is a common mechanistic attribute behind the regulatory function of many transcription factors. In a Y2H screen performed in search of interacting partners for the histone acetyltransferase GCN5, MYB106 was among the identified proteins (Servet et al., 2008). Not long ago, it was shown that the MYB-domain-containing protein **A**lways Ear**ly 2** (ALY2) interacts with the **S**I**N**3-**L**IKE **1** (SNL1) Arabidopsis orthologue of the yeast transcriptional co-regulator SIN3. Like its yeast counterpart, SNL1 was demonstrated to have an HDAC-dependent transcriptional repression activity, and it was suggested that ALY2 might be a direct recruiter of the SNL1-containing complexes onto their target genes (Bowen et al., 2010). Recently, a study investigating the antagonistic effects of UV-B illumination and pathogen attack mimicry in the regulation of flavonol biosynthesis genes put forward for consideration a working model which emphasised the interplay of certain UV-B-responses-related MYBs, namely MYB12 (Stracke et al. 2010) and MYB4 (Jin et al., 2000), with yet unidentified HATs and HDACs (Schenke et al., 2014). FVE, a protein involved in histone deacetylation in Arabidopsis (Ausín et al., 2004) and important in DNA repair following UV-B damage (Campi et al., 2012), was found to interact weakly with UVR8 (Fig 4-3 Chapter 4) but the lack of consistency between independent repetitions of the assay raised suspicions that this might be a weak/transient interaction. It was therefore decided, first to investigate whether MYB61 and MYB50 could interact with FVE, and if that were the case a presumable stabilising effect of MYB61 and/or MYB50 on the UVR8-FVE interaction would be assessed via a Y3H assay. Unlike MYB50, MYB61 was found to associate with FVE in a Y2H assay (Fig 7-9). Unfortunately, however, the Y3H (Fig 7-10) approach revealed that MYB61 does not act as a stabilising bridge between UVR8 and FVE.

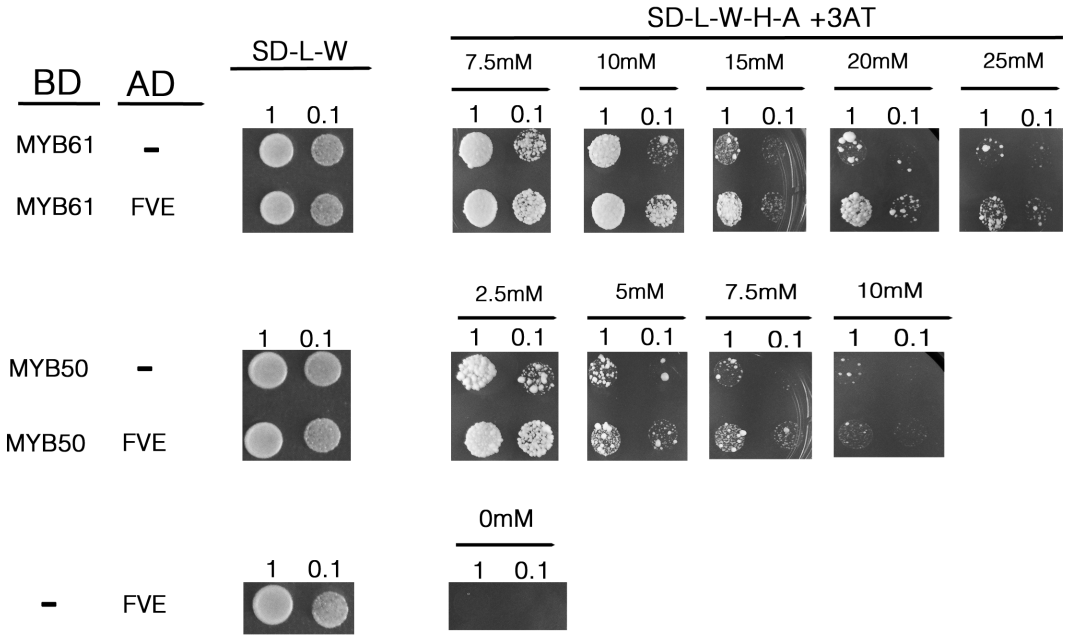

Fig. 7-9: Interaction of MYB61 with FVE

SD-L-W medium was used as a control for the viability of the spotted cells. Interactions were assessed only on high (SD-L-W-H-A) stringency selection plates, supplemented with various concentrations of 3-AT to control the auto-activation of MYB61 and MYB50 when fused with the GAL4-BD domain. Spottings were performed from cell suspensions with three different cell densities (OD= 1 , 0.1 and 0.01). Results are representative of two independent biological repetitions

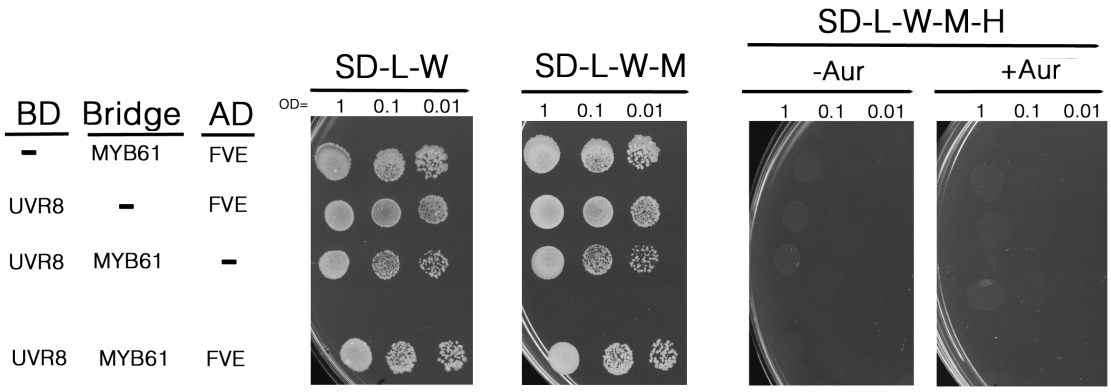

Fig. 7-10: Y3H assay

SD-L-W medium was used as a control for the viability of the spotted cells. Interactions were assessed only on low (SD-L-W-M-A) and high stringency (SD-L-W-M-A+Aur) selection plates. Spottings were performed from cell suspensions with three different cell densities (OD= 1 , 0.1 and 0.01). Results are representative of two independent biological repetitions.

7.9 Chromatin immunoprecipitation with a MYB61-GFP overexpressing line was performed but it appears that some optimisation will be required to obtain conclusive results

Various routine assays were performed with the MYB61-GFP overexpressing lines throughout this project, but the main objective for their generation in the first place was to eventually utilise them for ChIP assays, via which the association of MYB61 with the *HY5* promoter could be demonstrated *in planta.* Unfortunately, time was not an ally in this effort, as attention to MYB61 itself was only turned after lengthy Y1H screens, which left a very limited period during which homozygous transgenic lines would have to be identified, characterised, and grown for successive generations in order to bulk up sufficient seed material for the amount of tissue required for ChIP experiments. Nevertheless, while the writing of this thesis was close to completion, everything needed for a first attempt was at hand and a ChIP experiment was performed with line L26. Two biological controls were included in the analysis, apart from the standard technical controls. First, transgenic lines expressing a SCL33-GFP fusion protein (kindly provided by Dr Eirini Kaiserli, University of Glasgow), and generated in the same background as line L26 -WT Col (0)-, were used to compensate for any unspecific binding of the anti-GFP antibody and to demonstrate that GFP-tagging does not confer a gain-of-function DNA binding activity to a random nuclear protein which is normally not anticipated to associate with the *HY5* promoter. This purpose would be better served if the GFP-tagged protein was a transcription factor with documented inability to bind to the *HY5* promoter, but as such lines were not available we resorted to using SCL33 (**SC**35-**L**IKE SPLICING FACTOR **33**) , which is involved in splicing. Second, primers annealing to promoters which have been reported to contain MYB61-binding consensus sequences, such as the ***P****ECTIN* ***ME****THYLESTERASE (PME)* and ***C****AFEOYL-****CoA*** *3-****O****-****m****ethyl****t****ransferase* ***7*** (*CcoAOMT)* promoters (Prouse and Campbell, 2013), were employed as positive controls. The experimental set up and the technical details of the ChIP procedure were identical to those followed in the epigenetic analysis described in Chapter 3, except that the immunoprecipitated DNA was analysed via end-point PCR. Sadly, we were unable to detect any signal, persuasively stronger than that of the mock technical control, in the

immunoprecipitates of interest derived from the L26 line (Fig 7-11). This was true even when the IP samples were analysed for the presence of positive control sequences, suggesting that the ChIP protocol might need to be subjected to some optimising changes before drawing any conclusions. Efforts in that direction will be highly prioritised in the near future, as it is imperative to assess the binding of MYB61 to the *HY5* promoter *in planta*.

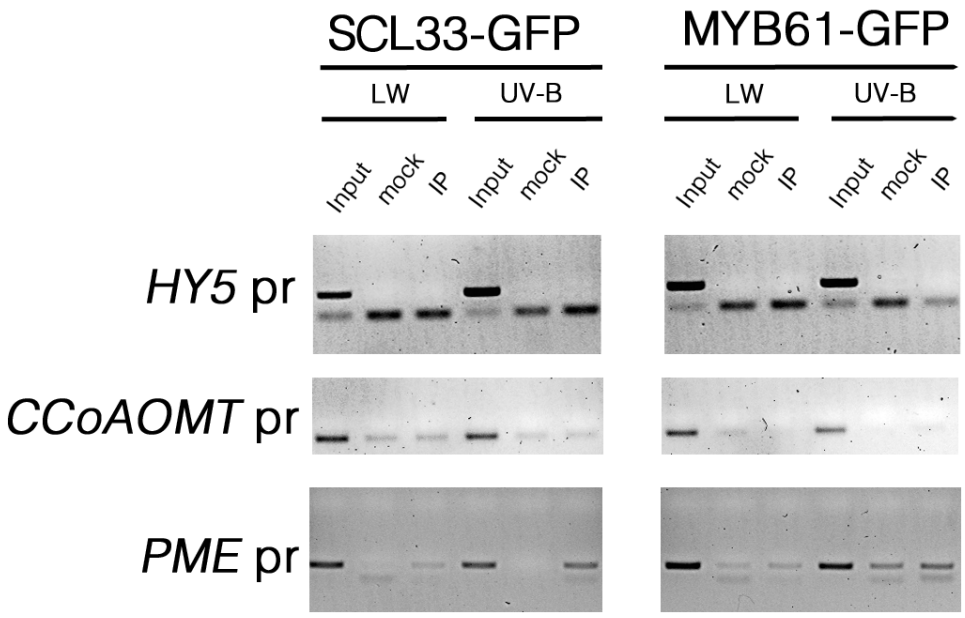

Fig. 7-11: End point PCR analysis of the DNA recovered following ChIP with anti-GFP antibody. The MYB61-GFP line assayed was L26, whereas SCL33-GFP corresponds to a splisosome-associated protein, normally not anticipated to associate with the *HY5* promoter, which was used as a negative control. Apart from the target *HY5* promoter, two additional promoters (*CoAOMT* pr and *PME* pr) were included in the analysis as positive controls. Input: Non immunoprecipitated DNA; mock: No antibody control; IP: immunoprecipitated DNA. LW: low fluence rate white light (15 μmol m^{-2} s^{-1}). UVB: 1.5 μmol m^{-2} s^{-1} narrow band UV-B

7.10 Discussion

The experimental findings presented in this chapter summarise the attempts made in the the final stages of this project towards elucidating the functional relevance of the R2R3 MYB family TF MYB61 to UVR8-mediated photomorphogenic UV-B responses. No groundbreaking discovery came out of these attempts, but some of the findings may be helpful in putting together the pieces of this puzzle with future research.

The C27 region of UVR8, well established for its importance in UVR8-mediated signalling (Cloix et al., 2012; Heijde and Ulm, 2013; Heilmann and Jenkins, 2013; Jenkins, 2014a), was found to be important for the interaction with MYB61 (Fig 7-1). From our results, however, it cannot be concluded whether the C27 region is also sufficient for this interaction and it would be worth testing this possibility in the future. Indeed, a more thorough domain mapping of the physical association between UVR8 and MYB61 could provide further insights into its functional significance, as it might reveal possible mechanisms for the fine tuning of the signalling output through the competition of different proteins for the same interaction sites. Moreover, it would be informative to assess *in planta* whether $UVR8^{W285A}$ and $UVR8^{W285F}$ retain the ability to interact with MYB61. As already mentioned, $UVR8^{285A}$ is most probably a constitutive monomer in plants whereas $UVR8^{W285F}$ is dimeric. Current structural data suggest that the C-terminal region of UVR8 could be flexible and its conformational position in relation to the core of the protein is unknown for both the native UVR8 and the above mutant variants (Jenkins, 2014b). Nevertheless, it has been suggested that the C27 region lies hidden from COP1 when UVR8 is in its homodimeric form, and UV-B-induced monomerisation together with concomitant conformational changes expose the C27 so that it becomes accessible for interaction (Cloix et al., 2012). For $UVR8^{W285A}$ particularly, it has been hypothesised that the C27 is accessible independently of UV-B (Heijde et al., 2013). Therefore, investigating *in planta* how these variants behave with regard to MYB61 binding would be insightful for the formulation of working hypotheses that subsequent research can be based on. For more rigorous analysis, additional UVR8 mutants known to be constitutively monomeric but presumably having different conformations in their C terminus - e.g $UVR8^{R146A/R286A}$, $UVR8^{R286A/R338A}$ and $UVR8^{D96N/D107N}$ (Christie et al., 2012) - may also be incorporated in the suggested experiments. The approach of choice could be CoIPs, simply because they

were optimised for MYB61 binding during this project, but for precise interpretation of the results it should be kept in mind that the co-immunoprecipitation experiments do not unequivocally reflect what the true situation is within the plant cell, as it is quite possible that the immunocomplexes are being formed in vitro, after the protein extraction, under the stabilising effects of the particular buffer conditions used. For definite proof that the interactions appear within the plant, BiFC would have to be included in the experimental investigations.

The functional characterisation of the *myb61* mutant plants as well as of the MYB61 overexpressors did not reveal any interesting phenotypes (Fig 7-2 and 7-4) apart from the fact that two strongly overexpressing MYB61-GFP lines displayed higher basal abundance of *HY5* transcript (Fig 7-6 B) which might be interpreted as an indirect indication that MYB61 associates with the *HY5* promoter in vivo. The lack of observable phenotypic deviations from the WT might be a result of functional redundancy of MYB61 with its close homologue MYB50, which was also found to associate with the *HY5* promoter (Fig 7-7 A) and to interact with UVR8 (Fig 7-7 B and Fig 7-8). To address this possibility in the future, *myb50* mutant plants were obtained from the Gabi Kat T-DNA collection and after identification of homozygous individuals crosses were performed to obtain *myb61myb50* double mutants. Currently, plants that are heterozygous for both genetic loci have been identified and are being grown. Genotyping will be carried out in the next generation in order to identify the individuals that will be homozygous for both mutant alleles. With regard to the overexpressing lines, an important concern that has not been addressed directly in our work is whether the MYB61-GFP fusion is fully functional. The easily observable phenotype of the *myb61-1* loss-of function mutants (Fig 7-2), however, provides a convenient and easy assay to perform functional complementation studies. To that end, MYB61-GFP overexpressing lines were generated in the *myb61-1* background and three independent single-locus-insertion T2 lines were identified. Currently, these plants are being grown to obtain the T3 homozygous lines, which will soon allow the functional complementation assays to be performed.

The interaction of MYB61, but not of MYB50, with FVE (Fig 7-9) is intriguing as well as enigmatic at present. The finding definitely needs to be strengthened via an alternative methodology and a CoIP would be the most straight forward approach as the necessary

constructs are already available. The Y3H assay (Fig 7-10) revealed no stabilising effect of MYB61 in the presumable weak/transient interaction between UVR8 and FVE, but, as discussed in Chapter 4, the latter has yet to be demonstrated in plants.

An important issue that needs to be taken into consideration is that the responses that were looked at during this project as diagnostic tools for unraveling possible roles of a given protein in UV-B signalling, may have not been the appropriate ones for every candidate. Indeed, HY5 is the master transcriptional regulator for the majority of the gene-regulatory networks that orchestrate UVR8-mediated physiological responses. It might be, that MYB61 is involved in processes parallel with, dependent on, yet downstream of and/or distinct from the UV-B-induced accumulation of CHS, induction of *HY5, ELIP.1* and *CHS* transcripts, and suppression of hypocotyl elongation. Hence, the whole question might need to be addressed from a different perspective. Obviously, functional redundancy may as always pose difficulties in such an attempt, but it is nevertheless true that R2R3 MYB family TFs have also undergone an extensive functional diversification, such that homologous members display very distinct spatiotemporal expression patterns and regulate quite distinct processes (Dubos et al., 2010). In fact, there are numerous studies reporting phenotypes in which MYB61 is the master regulator without any interference from MYB50 (Liang et al., 2005; Newman et al., 2004; Penfield et al., 2001; Romano et al., 2012). Therefore, while it is undoubtedly interesting for future research to address in more detail the UV-B-signalling-related role, if any, of MYB50 for which there is not much information in the literature, one may hope that the elucidation of the role of MYB61 could be relatively straightforward provided that the analysis will focus on the appropriate UVR8-regulated response. Hints as to which this response might be came recently with the report of Tossi et al. (2014), where evidence was presented that the UV-B induced, UVR8-regulated stomatal closure is brought about via a Nitric Oxide (NO) - dependent mechanism. MYB61 has been long known to be a necessary and sufficient TF for the stomatal closure in Arabidopsis (Chen et al., 2012; Liang et al., 2005). NO is known to be produced through many pathways in plants (Moreau et al., 2010) but the one involved in UV-B regulated stomatal closure is proposed to involve the enzyme **N**itrate **R**eductase (NR) (Tossi et al., 2014). Intriguingly, the promoters of both genes encoding for the two isoenzymes of NR in Arabidopsis (NR1 and NR2) have several repeats of the AC-element

ACCACA, to which MYB61 binds with high affinity according to a recent report (Prouse and Campbell, 2013). Moreover, Prouse and Campbell identified a consensus binding sequence (ACCTAC) for MYB61, which is itself present on the *NR1* promoter at the position -213 from the transcription start site. It is tempting to speculate that MYB61 binds to both the *HY5* and *NR1* promoters in order to mediate the UV-B induced UVR8-regulated stomatal closure. Relatively straightforward experiments measuring the stomatal aperture of WT, *uvr8-1, myb61-1* and MYB61 OE plants plus and minus UV-B, in the presence or absence of NO inhibitors, should provide a quick test for the above working hypothesis. With the optimisation of the ChIP experiments for the MYB61-GFP lines, it may be possible to detect MYB61 on the *NR1* promoter, thus revealing a novel transcriptional network operating under photomorphogenic UV-B light.

CHAPTER 8: FINAL DISCUSSION

8.1 Introduction

Plants are immobile autotrophs whose optimal growth and development relies heavily on light. In addition to its role as an energy source, light provides regulatory signals for the fine-tuning of numerous events throughout the plant life cycle from germination to flowering (Kami et al., 2010). UV-B (280-315 nm) is a minor component of the solar spectrum that reaches the Earth's surface (Jenkins, 2009), but it has the highest energy and its impact on the biosphere is remarkable. Low fluence rates of UV-B illumination elicit photomorphogenic responses in plants that modify biochemical composition, photosynthetic competence, morphogenesis and defence (Jenkins, 2014a). To date, the only known UV-B photoreceptor is UVR8, which employs a unique photosensory mechanism to mediate light absorption and initiate the signalling events that eventually lead to the manifestation of particular physiological responses (Tilbrook et al., 2013). The exploration of the *in vivo* function of UVR8 is still at an early stage, but since research has been disproportionately focusing on the photoreceptive mechanism, on signalling initiation and UVR8 regulation, it is an ironic fact that currently the largest gap of knowledge is our poor understanding of how UVR8 mediates gene expression, an area that initial studies had concentrated on. The main objective of this project was to address the above question by approaching it on the basis of a central working hypothesis: that the mysterious association of UVR8 with chromatin (Brown et al., 2005; Cloix et al., 2012; Cloix and Jenkins, 2008; Favory et al., 2009; Kaiserli and Jenkins, 2007) might be a functional necessity for the recruitment and/or activation of chromatin modifiers and/or transcription factors, that would then underlie the transcriptional events. In this chapter, the most important findings from our research have been summarised, major discussion points are reminded, but an attempt is also made to reflect upon the data from a different perspective, highlighting weaknesses of the approaches that were undertaken and suggesting directions for future research efforts.

8.2 Histone acetylation appears to be involved in the UVR8-mediated regulation of transcription

Histone acetylation usually influences transcriptional activity positively by favouring an "open" euchromatic conformation under which the accessibility of DNA by the basal transcriptional machinery and various specific effectors is facilitated (Barneche et al., 2014). Predominantly, histone acetylation occurs on lysine residues and in Arabidopsis it has been detected on various positions of the H3, H4 and H2B histone isoforms. With regard to light-induced transcription, pioneering work was done on pea (*Pisum sativum*) with a study that focused on the plastocyanin *PetE* gene in green and etiolated shoots (Chua et al., 2001). Increased expression of *PetE* correlated with hyperacetylation of H3 and H4 at enhancer/promoter regions and was preceded by an organ-specific reduced nucleosome occupancy. In a follow-up study, the authors utilised an inhibitor of HDAC activity to provide the first lines of evidence that histone acetylation enhances transcriptional activity in plants (Chua et al., 2003). In subsequent years, as research expanded to include Arabidopsis and maize, a growing body of evidence suggested that the chromatin loci of various light responsive genes undergo light-mediated enrichments in H3 and H4 acetylation (Charron et al., 2009; Guo et al., 2008; Jang et al., 2011; Offermann et al., 2006; Offermann et al., 2008). A particular histone mark that regularly appeared in the relevant literature was H3K9ac. Studies that concentrated on comparing dark- versus light-grown seedlings demonstrated that H3K9ac levels at selected light-responsive genes accumulate in a developmentally dependent manner, correlate with the fluctuations of mRNA and are affected by light intensity and wavelength (Guo et al., 2008). A succeeding genome-wide survey of H3 acetylation dynamics during de-etiolation revealed massive variations in the acetylation profiles of light-regulated loci with regard to H3K9ac and the co-occurring H3K27ac mark (Charron et al., 2009). The latter, together with the bivalent modification H3K9/14diac, has been reported to underlie the activation of *phyA* in darkness (Jang et al., 2011). Earlier reports had already highlighted the potential significance of H3K9/14diac in UV-B responses (Casati et al., 2008; Cloix and Jenkins, 2008). In consonance with these observations, our results revealed that UV-B illumination leads to accumulation of H3K9/14diac over the chromatin loci of selected UVR8-regulated genes, and that this enrichment requires a functional UVR8 photoreceptor (Chapter 3).

Nevertheless, a recent study provided a cautionary note regarding ChIP analyses that rely on antibodies raised against this bivalent histone mark, as it demonstrated their inability to discriminate between the two acetylated residues (Schenke et al., 2014). By using antibodies raised specifically against H3K9ac or H3K14ac, and by employing UV-B illumination conditions that are just sufficient to trigger the photomorphogenic responses (Schenke et al., 2011), the authors concluded that the UV-B-associated increases in H3 acetylation over the loci of certain genes of interest are a consequence of H3K9ac. Among the genes that Schenke et al. (2014) investigated was *CHS,* and their findings were very similar to those reported in this study. Therefore, it is most likely that our observations are also an effect of H3K9ac rather than H3K14ac, although clearly for this claim to be fully justified the specific antibodies must be used.

After obtaining the first promising results with H3K9/14diac, it was decided to investigate whether the findings could be expanded to include other histone marks. Candidate modifications that would be anticipated to co-occur with H3K9/14 were sought in epigenomic mapping reports and among marks that appeared consistently in studies on light-regulated chromatin remodelling. The modifications which were eventually selected for investigation were H2Bub, H3K4me3, H3K9me3, H3K36me3, and H3K56ac. With the exception of the latter, no interesting observations were made after ChIP assays with antibodies raised against the corresponding histone marks. In the case of H3K56ac, the data suggested that UVR8 might be linked to a locus-specific accumulation for only a subset of the tested UVR8-dependent UV-B responsive genes. Although two biological repetitions were sufficient to highlight the clear differences in the enrichment for this particular mark, more experiments would be necessary to reveal borderline fluctuations. A valid criticism against some of the data presented in this thesis, as ChIPs are notoriously variable, would be that two independent repeats are hardly sufficient to justify claims of significant dissimilarities in the observations or to dismiss a result as “not interesting”. It must be appreciated, however, that it was practically impossible to perform for every histone modification of interest as many independent biological repetitions as it would be enough for the results to satisfy the rigorous statistical conventions. Instead, each histone mark was initially assayed in two independent biological ChIP replicates, and the investigation was taken further only if promising patterns were observed. In the

interpretation of the results (Chapter 3) it has been repeatedly acknowledged that lack of statistical significance does not necessarily mean that two values are the same, that mild but biologically important differences may lie hidden within the data, and that more experiments are necessary to uncover them.

The nature of UVR8 involvement in the UV-B-elicited increases in histone acetylation is currently unclear. Our investigations revealed no evidence that UVR8 is the direct recruiter of enzymes with HAT or HDAC activity (Chapter 4), although a weak/transient interaction with FVE was detected in Y2H experiments. As already argued, this interaction will need to be validated via a plant-based assay. Various candidate acetyltransferases and deacetylases with documented involvement in light signalling, such as GCN5, TAF1, HD1, FVE, were explored for a potentially crucial involvement in UV-B signalling but no data in support of such claim were obtained. In principle, downstream signalling effectors of UVR8-initiated signalling could fulfil the role of attracting histone modifying enzymes at their respective sites of action, and HY5 appears a good candidate (Barneche et al., 2014; Charron et al., 2009; Guo et al., 2008). Experiments that could address this possibility have been discussed previously, therefore here attention is brought on the possible usefulness of the diverse mutant variants of UVR8 which have become available in recent years, and provide a convenient molecular toolkit for investigating the likelihood of UVR8 itself being the physical recruiter.

It has been reported that the association of UVR8 with chromatin is independent of UV-B but insufficient on its own to trigger transcriptional responses (Cloix and Jenkins, 2008). Moreover, depletion of the C27 region of the photoreceptor impairs its ability to initiate signalling but does not affect chromatin association (Cloix et al., 2012). $UVR8^{W285A}$ and $UVR8^{W285F}$ (O'Hara and Jenkins, 2012) are two mutant variants with distinct properties *in vitro* and *in vivo*, but in theory both should be capable of binding to chromatin. Histone acetylation on the other hand is known to be independent of transcription, as at least occasionally light-induced enrichment has been reported without concomitant increase in gene expression (Fisher and Franklin, 2011; Offermann et al., 2006). It would be interesting, therefore, to assess how plants expressing the aforementioned mutant variants of UVR8 would behave with regard to acetylation levels under the experimental conditions used in this study. If the role of UVR8 is purely structural in providing a scaffold for the

assembly of the chromatin modifying machinery, then one would anticipate that no differences would be observed compared to the WT. Of course, it could alternatively be that an operational UVR8-initiated signalling pathway is imperative for these chromatin-based events, in which case lines expressing the constitutively active variants UVR8^{W285A} and UVR8^{R338A} (Heijde et al., 2013; Huang et al., 2014) would have to be employed. The first is impaired in photoreception whereas the latter retains the ability to sense UV-B light. Both are most likely monomeric *in planta* and there are no reasons to believe that they would differ in their chromatin-association properties. If the recruitment of the chromatin modifiers is triggered by the light signal, then the two variants should display markedly different enrichment signatures. Conversely, if the histone modifying activities are attracted to their target genes as a result of a later signalling event, then acetylation patterns similar in trend would be expected. Moreover, as the constitutively active variants described by Hunag et al (2014) differed remarkably in the severity of the transcriptional responses, quantitative ChIP measurements could provide hints as to whether UVR8 is the actual physical recruiter or this role is undertaken by a downstream signalling mediator. For example, the YFP-UVR8^{W285A} plants were reported to accumulate much lower levels of *HY5* and *ELIP.1* transcripts upon UV-B induction compared to YFP-UVR8^{R338A} . As mentioned above, UVR8^{W285A} and UVR8^{R338A} would be expected to bind chromatin in similar fashion, therefore if qChIP signals are found to differ significantly, then it is most likely that UVR8 itself is not the physical recruiter.

8.3 A Y1H screen led to the identification of a set of transcription factors, brought into attention a specific family of transcriptional regulators, and opened new directions for future research on UVR8-regulated gene expression

The principal transcriptional effector of UVR8-regulated responses is the bZIP TF HY5, which acting in partial redundancy with its close homologue HYH mediates photomorphogenic-UV-B-elicited gene expression. Transcription factor-encoding genes can be found among the downstream targets of HY5/HYH (Brown et al., 2005; Ulm and Nagy, 2005), and *MYB12* and *FHY3* are notable examples (Huang et al., 2012; Stracke et al., 2010). Particularly the transposon-derived TF FHY3 was recently placed on a higher hierarchical position amongst the known positive transcriptional regulators of UV-B responses, as it was demonstrated to act together with HY5, but by binding to a distinct *cis*-regulatory element, in setting in operation a positive regulatory loop on the *COP1* promoter (Huang et al., 2012). Nevertheless, HY5/HYH-independent pathways downstream of the photoreceptive event have been reported as well, and these are implicated in processes relating to the UV-B-promoted entrainment of the circadian clock (Feher et al., 2011), and inhibition of shade avoidance (Hayes et al., 2014).

With regard to stimuli other than UV-B, extensive research was performed during the past decade with the aim of addressing questions related to the integrative function of HY5 in orchestrating gene expression networks. For example, numerous studies have attempted to shed light on the crosstalk between light and hormonal signalling and all have converged towards reporting a central role for HY5 (Alabadi et al., 2008; Chen et al., 2008; Cluis et al., 2004; Sibout et al., 2006; Vandenbussche et al., 2007). Moreover, it has been shown that HY5 participates in the feedback downregulation of *FAR1* expression, which is brought about in a phyA-dependent fashion following FR exposure (Li et al., 2010). Furthermore, HY5 has been reported to bind to the G-box present in close proximity to the CCA1- binding site on the ***L****IGHT* ***H****ARVESTING* ***C****HLOROPHYL* ***b*** (*Lhcb*) promoter (Andronis et al., 2008). The undoubtedly high significance of HY5 for photomorphogenesis has been the motivation for scientists to put substantial effort into identifying HY5-binding sites on a genome wide scale (Gao et al., 2004; Lee et al., 2007; Zhang et al., 2011). Yet, the transcriptional regulation of *HY5* itself remains largely unknown. *HY5* expression can be detected in various tissues, including roots, hypocotyl,

cotyledons, leaves, stems and flowers (Oyama et al., 1997). The abundance of HY5 reaches a peak three days after germination and then protein levels decline steadily, being, however, detectable for at least four more days. During the transition to flowering HY5 accumulates again (Hardtke et al., 2000). Therefore, photomorphogenic UV-B responses in older seedlings and adult plants depend crucially on the re-engagement of HY5 through its UVR8-mediated transcriptional stimulation and post-translational stabilisation. Whereas significant advances have been made towards understanding the mechanistic basis of the latter (Huang et al., 2013), the details of the molecular events preceding *HY5* upregulation are largely unresolved.

Two studies were published recently reporting among other things a functional dissection of the *HY5* promoter. Firstly, Abbas and co-workers (2014) focused on the molecular connectivity between HY5 and CAM7, a recently recognised important transcriptional regulator of Arabidopsis seedling development (Kushwaha et al., 2008). They identified two closely residing *cis*-regulatory elements which were designated as T/G- box (the UV-B box2 of our study, see Chapter 5) and E- box. It was revealed that *HY5* expression is regulated under diverse light conditions and across various developmental stages by both HY5 and CAM7, which were found to interact physically with each other and to associate with different binding specificities with the T/G- and E-box cis-acting elements, respectively (Abbas et al., 2014). Expanding the above observations to include photomorphogenic UV-B responses, Binkert et al. (2014) demonstrated that the T/G-box (UV-B box2) is required for UV-B responsiveness, and that both HY5 and HYH associate with it in order to effect redundantly the induction of *HY5* expression. The authors also concluded that for full UV-B induction an intact E-box is required but its functional significance is minor in the absence of HY5/HYH or the T/G- box. Moreover, a third *cis*-regulatory element, designated ACG-box (UV-B box1 of our study) and located ~13 bases upstream of the T/G- box was identified and compelling evidence was presented that it attracts a negative transcriptional regulator active under continuous visible light (Binkert et al., 2014). Notably, whereas chromatin occupancy of HY5 at selected target UV-B-responsive genes was enhanced by UV-B in a UVR8-dependent manner, the association per se with the *HY5* promoter itself appeared independent of the presence of a functional UVR8.

As explained in Chapter 5 of this thesis, the identification of the ACG- and T/G-box elements as putative UV-B-responsive cis-regulatory sequences of the *HY5* promoter was shared with us as unpublished information (Prof Ferenc Nagy, personal communication). At the time, the two elements had been designated as UV-B box1 and UV-B box2 respectively, and these terms were preferred throughout this project as they highlight the functional relevance of the two sequences. With the aim of discovering novel transcription factors that might mediate the UV-B-elicited activation of *HY5* expression, Y1H screens were performed using various combinations of UV-B box1 and UV-B box2 as "bait" DNA. These efforts led to the identification of a set of TFs (MYB31, MYB61, NF-YC9, ANAC83) which belong to various known families. A member of the BBX family of transcriptional regulators, namely STH2/BBX21, was also pulled out from the screens. Notably, during the confirmations of the screening results all candidates appeared to recognise preferentially UV-B box2 (the T/G-box) but none was capable of associating with "bait" DNA consisting of UV-B box1 (the ACG-box) alone. In follow-up investigations (Chapter 6) we observed that HY5 recognises and binds to UV-B box2, although not to UV-B box1, thus providing an additional line of evidence, consistent with the literature, for its ability to regulate the expression of its own gene. Moreover, the documented involvement of STH2 in light signalling (Datta et al., 2007) prompted us to expand the analysis and include various other members of the BBX family. This resulted in some very intriguing observations, as STH3/BBX22, a functional homologue of STH2, was found to associate with the *HY5* promoter via UV-B box2 (Chapter 6). HY5 is known to regulate the expression of *STH3* during de-etiolation (Chang et al., 2008) and following UV-B irradiation (Ulm et al., 2004). In addition, the two proteins interact physically in vivo (Datta et al., 2008b). It is conceivable, therefore, that during photomorphogenic UV-B responses HY5 and STH3 form a cyclic positive feedback loop, whereby a heterodimeric HY5/STH3 complex mediates the activation of *HY5* and *STH3*. As already discussed, fusions of the *HY5* and *STH3* promoters with the *LUC* reporter gene in Arabidopsis protoplasts could be utilised in transfection assays to determine wether HY5, STH2, STH3, or their respective heterodimers associate with the target promoters *in planta.* Moreover, by employing protoplasts derived from various mutant Arabidopsis backgrounds valuable

information could be extracted as to whether these associations are dependent on particular recruiting candidates. Such candidates could be identified by performing HY5-STH3 CoIPs, preferably with the addition of cross-linking agents so that any other proteins participating in the complex could be retained in the immunoprecipitates, and then mass spectrometry could be employed to identify all the proteins that have been pulled down.

Finally, an intriguing physical interaction between UVR8 and BBX24 was observed in Y2H assays, but this contradicts the findings reported by Jiang et al. (2012). Possible explanations for this discrepancy have been already discussed and it is important that a plant-based protein interaction assay is performed to reveal what the truth of the matter is. If UVR8 and BBX24 can truly bind each other *in planta*, this will provide additional insights into the inhibitory action of BBX24 in UV-B responses.

8.4 Limitations/weaknesses of the Y1H screens and suggestions for alternative ways of addressing the research questions

Although the screening approach that was undertaken during this project was successful in identifying interesting candidates to focus on, there are a few issues that have probably prevented further discoveries.

Firstly, despite the fact that all three screens were saturating and the stringency of the selection conditions was balanced after careful control experiments, it is possible that TFs which interact weakly, yet sufficiently for an important biological output, were simply screened out. Second, from the clones that actually grew on the selective plates, there is a practical limit to the number of those that can be handled and it is not unlikely that an important candidate has been missed simply by chance. Moreover, during the first round of eliminating false positives (blue-white selection) very few clones were clearly either blue or white. The majority could be described as blue-white with varying degrees of pigment formation, therefore an inevitably subjective judgment call had to be made as to whether a particular clone would be taken further for analysis or discarded. Nevertheless, all the above issues are technicalities inherent in the experimental methodology and as such they are largely unavoidable.

While selecting the clones that the post-screen analysis would concentrate on, it was decided that annotated, known TFs would be treated with priority. However, it is worth

mentioning that among the sequenced clones there were a few proteins of unknown function, which nonetheless contained DNA-binding motifs. Merely the time limitations of the project dictated the exclusion of these candidates from subsequent investigations, but it would be interesting for future efforts to characterise them further. For example, *AT1G15350* stands out intriguingly as its function is unknown but it resides in a genomic cluster of at least three genes encoding for nucleic acids-binding proteins. Operon-like gene clusters have been predicted for Arabidopsis (Wada et al., 2012), hence interesting novel research directions might open if the product of *AT1G15350* is confirmed to associate with the *HY5* promoter.

Strikingly, the Y1H screens failed to identify any TFs binding to the UV-B box1 (the ACG-box), although the highest number of clones were screened when the respective "bait" DNA was used. It has been suggested that this *cis*-element attracts a negatively acting TF (Binkert et al., 2014), therefore it is not surprising that the Y1H approach, which methodologically relies on the activation of a reporter gene, failed to retrieve any transcriptional repressors. One would anticipate that the native function of a transcription factor in Arabidopsis should not matter in the heterologous yeast system, since in any case all clones are translationally fused with the GAL4-AD. Indeed, repressors have been identified previously with Y1H screens (Pruneda-Paz et al., 2009). However, it should be kept in mind that transcriptional repression in eukaryotes is delivered through a range of mechanisms (Latchman and Latchman, 2010), some of which involve chromatin stabilisation and/or negative regulation of RNA pol II and are therefore conserved among distinct phylogenetic clades (Sridhar et al., 2004). Thus, if the elusive transcriptional repressor that binds to the UV-B box1 interferes with the yeast's basal transcriptional machinery, its detection through a Y1H assay would be improbable.

In order to overcome the difficulty outlined above, standard forward genetics screens might be performed. According to Binkert et al. (2014), the transcriptional repressor of interest down-regulates *HY5* transcription under continuous visible light. Stable *UV-B box1*:*LUC* transgenic Arabidopsis lines could be subjected to EMS-mediated mutagenesis and then screened for increased *LUC* activity. A loss-of-function allele of the sought-after TF might be among the obtained mutants. Alternatively, an elegant but slightly more complicated approach could be employed. Back in 1989, Elledge and co-workers described

a clever transcriptional interference assay in *E.coli* cells, which they designed to facilitate the cloning of genes encoding for sequence-specific-DNA-binding proteins. A strong synthetic promoter is placed downstream of an adjacent drug resistance gene. The orientation of this promoter is chosen to be such, that the transcription controlled by it interferes with the transcription of the drug resistance gene from its native promoter. Thus, bacterial cells harbouring this molecular cassette do not survive in drug-supplemented medium. Subsequently, a *cis*-element of interest is inserted between the strong synthetic promoter and the drug resistance gene, so that if a protein binds to that *cis*-element the synthetic-promoter-driven transcription is impaired. In this way the expression of the drug resistance gene is no longer interfered with, and the cells survive on drug supplemented medium (Elledge et al., 1989). In principle, this system could be taken advantage of for "fishing" the elusive UV-B box1-binding repressor out of a library of Arabidopsis proteins, if the latter is screened in appropriately engineered *E. coli* cells. Subsequently, the identified candidates can be easily assayed for negative regulation of transcription by performing standard yeast-based and/or plant based transcriptional repression assays (Sridhar et al., 2004).

8.5 MYB61 is a TF which seems to be involved in UVR8-mediated photomorphogenic UV-B responses, but the functional details remain to be clarified

MYB61 was identified in the Y1H screens as capable of associating with the UV-B box2 *cis*-element of the *HY5* promoter (Chapter 5). Intriguingly, it was also shown to interact with UVR8 in yeast (Chapter 6) and co-immunoprecipitation assays performed with plant protein extracts suggested that this physical association might also reflect a true *in planta* situation (Chapter 7). Sadly, no interesting phenotypes were observed when standard UV-B responses were assayed in a loss-of-function *myb61* mutant and MYB61 overexpressing plants. As argued previously though, this might simply be a result of concentrating our analysis to the "wrong" responses. MYB50, the closest homologue of MYB61, was also found to interact with the *HY5* promoter in a Y1H assay and was additionally demonstrated to associate physically with UVR8 in yeast and, presumably, in plants. The functional significance of these events is currently unknown, but it would be interesting for future

research to take a closer look at the role of MYB50, if there is such a role, in UV-B signalling. Single *myb50* mutant plants were obtained late in this project (noted in Chapter 7) and currently the generation of *myb50myb61* double mutants is under way as these plants may be valuable for future functional characterisations with regard to UV-B responses. Nonetheless, despite undoubted partial overlapping redundancies, R2R3 MYB family TFs also display extensive functional diversification (Dubos et al., 2010). Homologous members frequently show differential spatiotemporal expression patterns and regulate distinct processes. Several studies, for example, report phenotypes in which MYB61 is the key regulator without any observable contribution by MYB50 (Liang et al., 2005; Newman et al., 2004; Penfield et al., 2001; Romano et al., 2012). Provided that the investigation would concentrate on a suitable UV-B-mediated response, establishing the in vivo function of MYB61 could be relatively easy. In chapter 7 it was explained why looking at UV-B-regulated stomatal closure might be informative. To the discussion points presented there, it can be added that not only is it possible that MYB61 is involved as a transcriptional activator in the NO generation pathway by stimulating *HY5,* and presumably *NR* expression, but it might also act pleiotropically by repressing the expression of genes whose products are involved in stomatal opening. This latter claim may seem far too speculative, but at the very least it provides a working hypothesis for addressing the functional significance of the physical interaction between MYB61 and FVE, provided that this will be further validated via an alternative non-yeast based approach. MYB61 is a key transcriptional regulator of stomatal closure (Chen et al., 2012; Liang et al., 2005) and FVE is involved in the deposition/removal of repressing/activating histone marks on target loci (Ausín et al., 2004; Pazhouhandeh et al., 2011). We propose the model depicted in Fig 8-1 as a basis for future efforts to address the role of MYB61 in UVR8-regulated UV-B signalling. It would be interesting to examine UV-B induced stomatal closure in WT, *uvr8-1, myb61-1, myb61-1/myb50* and the various MYB61 OE lines, in the presence/absence of NO inhibitors.

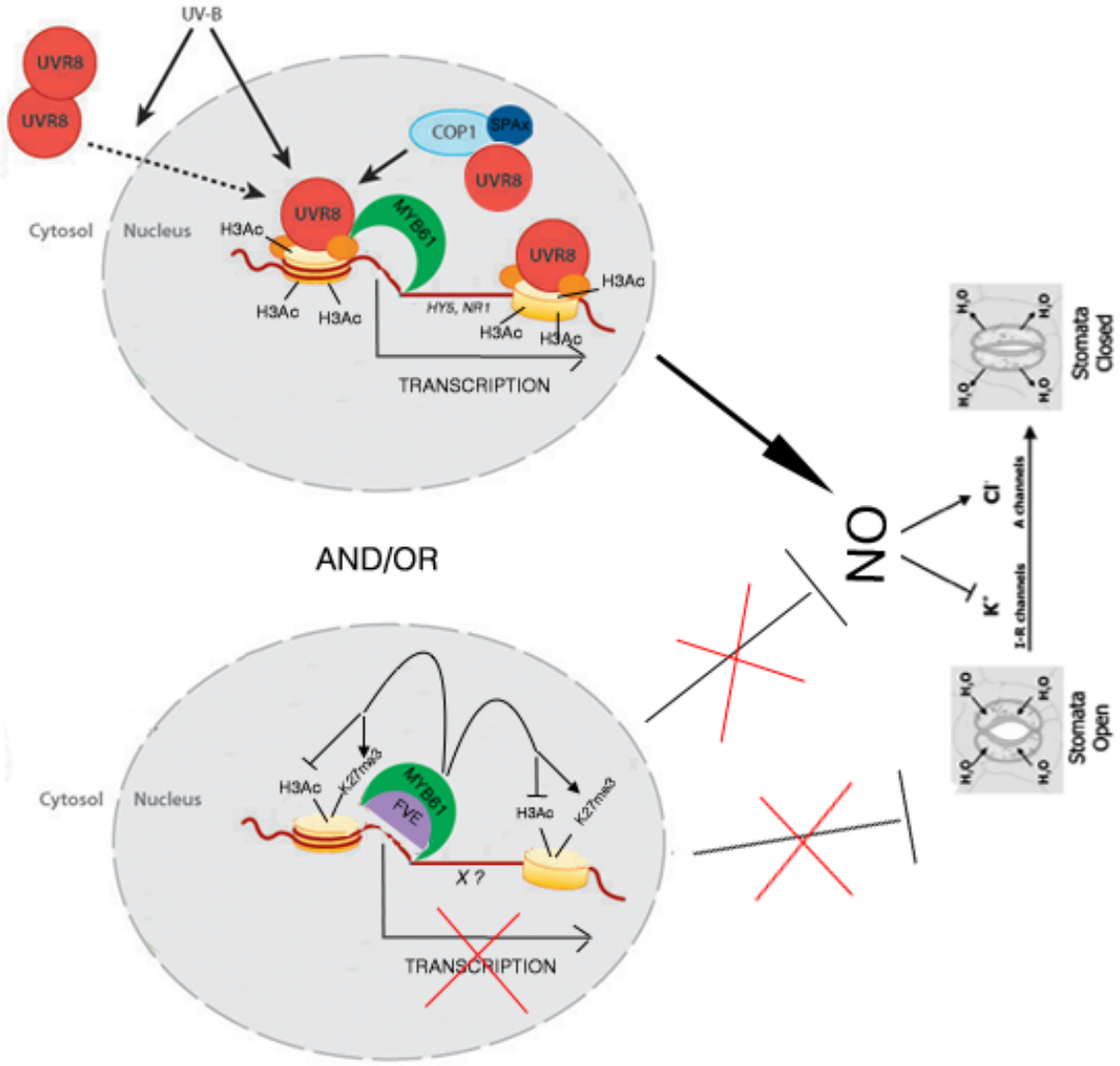

Fig 8-1 Proposed Model for the role that MYB61 might play in UVR8-regulated UV-B signalling. Photomorphogenic doses of UV-B are perceived by the homodimeric form of the UVR8 photoreceptor. Light sensing causes monomerisation and accumulation in the nucleus, where by signalling events involving UVR8-COP-SPA complexes, and presumably through the contribution of UVR8-mediated accumulation of transcription-activating histone marks and recruitment of TFs, target genes are expressed. One of the early responsive genes is *HY5,* on the promoter of which response-specific TFs associate with particular *cis*-regulatory elemet/s. Conceivably, MYB61 is one such example. By mediating *HY5* activation, and supposedly activation of *NR* as well, MYB61 contributes to UV-B-elicited NO accumulation and effectuates stomatal closure. Alternatively, or additively, MYB61 might be recruiting chromatin-modifying complexes consisting of FVE in order to mediate chromatin-based silencing of genes whose products participate in signalling pathways that result in stomatal opening. Not all features appearing in the above picture have been proven to be true during this project. The model is simply a suggestion that could be taken into consideration in future research efforts.

REFERENCES

A−H−Mackerness, S., Surplus, S.L., Blake, P., John, C.F., Buchanan−Wollaston, V., Jordan, B.R., and Thomas, B. (1999). Ultraviolet−B−induced stress and changes in gene expression in *Arabidopsis thaliana*: role of signalling pathways controlled by jasmonic acid, ethylene and reactive oxygen species. Plant, Cell & Environment **22**: 1413–1423.

Abbas, N., Maurya, J.P., Senapati, D., Gangappa, S.N., and Chattopadhyay, S. (2014). Arabidopsis CAM7 and HY5 physically interact and directly bind to the HY5 promoter to regulate its expression and thereby promote photomorphogenesis. Plant Cell **26**: 1036–1052.

Alabadi, D., Gallego-Bartolome, J., Orlando, L., Garcia-Carcel, L., Rubio, V., Martinez, C., Frigerio, M., Iglesias-Pedraz, J.M., Espinosa, A., Deng, X.W., and Blazquez, M.A. (2008). Gibberellins modulate light signaling pathways to prevent Arabidopsis seedling de-etiolation in darkness. The Plant Journal **53**: 324–335.

Andronis, C., Barak, S., Knowles, S.M., Sugano, S., and Tobin, E.M. (2008). The clock protein CCA1 and the bZIP transcription factor HY5 physically interact to regulate gene expression in Arabidopsis. Molecular Plant **1**: 58–67.

Arguello-Astorga, G., and Herrera-Estrella, L. (1998). EVOLUTION OF LIGHT-REGULATED PLANT PROMOTERS. Annual Review of Plant Physiology and Plant Molecular Biology **49**: 525–555.

Arguello-Astorga, G.R., and Herrera-Estrella, L.R. (1996). Ancestral multipartite units in light-responsive plant promoters have structural features correlating with specific phototransduction pathways. Plant Physiology **112**: 1151–1166.

Ausín, I., Alonso-Blanco, C., Jarillo, J.A., Ruiz-García, L., and Martínez-Zapater, J.M. (2004). Regulation of flowering time by FVE, a retinoblastoma-associated protein. Nature genetics **36**: 162–166.

Ballaré, C.L., Barnes, P.W., and Flint, S.D. (1995). Inhibition of hypocotyl elongation by ultraviolet−B radiation in de−etiolating tomato seedlings. I. The photoreceptor. Physiologia Plantarum **93**: 584–592.

Barneche, F., Malapeira, J., and Mas, P. (2014). The impact of chromatin dynamics on plant light responses and circadian clock function. Journal of Experimental Botany **65**: 2895–2913.

Bauer, D., Viczian, A., Kircher, S., Nobis, T., Nitschke, R., Kunkel, T., Panigrahi, K.C., Adam, E., Fejes, E., Schafer, E., and Nagy, F. (2004). Constitutive photomorphogenesis 1 and multiple photoreceptors control degradation of phytochrome interacting factor 3, a transcription factor required for light signaling in Arabidopsis. Plant Cell **16**: 1433–1445.

Benhamed, M., Bertrand, C., Servet, C., and Zhou, D.-X. (2006). Arabidopsis GCN5, HD1, and TAF1/HAF2 interact to regulate histone acetylation required for light-responsive gene expression. Plant Cell **18**: 2893–2903.

Benhamed, M., Martin−Magniette, M., Taconnat, L., Bitton, F., Servet, C., De Clercq, R., De Meyer, B., Buysschaert, C., Rombauts, S., and Villarroel, R. (2008). Genome−scale Arabidopsis promoter array identifies targets of the histone acetyltransferase GCN5. The Plant Journal **56**: 493–504.

Benvenuto, G., Formiggini, F., Laflamme, P., Malakhov, M., and Bowler, C. (2002). The photomorphogenesis regulator DET1 binds the amino-terminal tail of histone H2B in a nucleosome context. Current biology **12**: 1529–1534.

Berger, S.L., Pina, B., Silverman, N., Marcus, G.A., Agapite, J., Regier, J.L., Triezenberg, S.J., and Guarente, L. (1992). Genetic isolation of ADA2: a potential transcriptional adaptor required for function of certain acidic activation domains. Cell **70**: 251–265.

Bernhardt, A., Lechner, E., Hano, P., Schade, V., Dieterle, M., Anders, M., Dubin, M.J., Benvenuto, G., Bowler, C., and Genschik, P. (2006). CUL4 associates with DDB1 and DET1 and its downregulation affects diverse aspects of development in *Arabidopsis thaliana*. The Plant Journal **47**: 591–603.

Bertrand, C., Benhamed, M., Li, Y.-F., Ayadi, M., Lemonnier, G., Renou, J.-P., Delarue, M., and Zhou, D.-X. (2005). Arabidopsis HAF2 gene encoding TATA-binding protein (TBP)-associated factor TAF1, is required to integrate light signals to regulate gene expression and growth. Journal of Biological Chemistry **280**: 1465–1473.

Biedermann, S., and Hellmann, H. (2010). The DDB1a interacting proteins ATCSA−1 and DDB2 are critical factors for UV−B tolerance and genomic integrity in *Arabidopsis thaliana*. The Plant Journal **62**: 404–415.

Biever, J.J., Brinkman, D., and Gardner, G. (2014). UV-B inhibition of hypocotyl growth in etiolated *Arabidopsis thaliana* seedlings is a consequence of cell cycle arrest initiated by photodimer accumulation. Journal of Experimental Botany **65**: 2949–2961.

Binkert, M., Kozma-Bognar, L., Terecskei, K., De Veylder, L., Nagy, F., and Ulm, R. (2014). UV-B-Responsive Association of the Arabidopsis bZIP Transcription Factor ELONGATED HYPOCOTYL5 with Target Genes, Including Its Own Promoter. Plant Cell **26**: 4200–4213.

Block, A., Dangl, J.L., Hahlbrock, K., and Schulze-Lefert, P. (1990). Functional borders, genetic fine structure, and distance requirements of cis elements mediating light responsiveness of the parsley chalcone synthase promoter. Proceedings of the National Academy of Sciences of the United States of America **87**: 5387–5391.

Boccalandro, H.E., Mazza, C.A., Mazzella, M.A., Casal, J.J., and Ballare, C.L. (2001). Ultraviolet B radiation enhances a phytochrome-B-mediated photomorphogenic response in Arabidopsis. Plant Physiol **126**: 780–788.

Bouly, J.P., Giovani, B., Djamei, A., Mueller, M., Zeugner, A., Dudkin, E.A., Batschauer, A., and Ahmad, M. (2003). Novel ATP-binding and autophosphorylation activity associated with Arabidopsis and human cryptochrome-1. European Journal of Biochemistry **270**: 2921–2928.

Bourbousse, C., Ahmed, I., Roudier, F., Zabulon, G., Blondet, E., Balzergue, S., Colot, V., Bowler, C., and Barneche, F. (2012). Histone H2B monoubiquitination facilitates the rapid modulation of gene expression during Arabidopsis photomorphogenesis. PLoS genetics **8**: e1002825.

Bowen, A.J., Gonzalez, D., Mullins, J.G., Bhatt, A.M., Martinez, A., and Conlan, R.S. (2010). PAH-domain-specific interactions of the Arabidopsis transcription coregulator SIN3-LIKE1 (SNL1) with telomere-binding protein 1 and ALWAYS EARLY2 Myb-DNA binding factors. Journal of Molecular Biology **395**: 937–949.

Boycheva, I., Vassileva, V., and Iantcheva, A. (2014). Histone acetyltransferases in plant development and plasticity. Current Genomics **15**: 28–37.

Briggs, W.R., and Christie, J.M. (2002). Phototropins 1 and 2: versatile plant blue-light receptors. Trends in Plant Science **7**: 204–210.

Brosche, M., Schuler, M.A., Kalbina, I., Connor, L., and Strid, A. (2002). Gene regulation by low level UV-B radiation: identification by DNA array analysis. Photochemical and Photobiological Sciences **1**: 656–664.

Brown, B.A., Cloix, C., Jiang, G.H., Kaiserli, E., Herzyk, P., Kliebenstein, D.J., and Jenkins, G.I. (2005). A UV-B-specific signaling component orchestrates plant UV protection. Proceedings of the National Academy of Sciences of the United States of America **102**: 18225–18230.

Brown, B.A., Headland, L.R., and Jenkins, G.I. (2009). UV−B Action Spectrum for UVR8−Mediated HY5 Transcript Accumulation in Arabidopsis. Photochemistry and photobiology **85**: 1147–1155.

Brown, B.A., and Jenkins, G.I. (2008). UV-B signaling pathways with different fluence-rate response profiles are distinguished in mature Arabidopsis leaf tissue by requirement for UVR8, HY5, and HYH. Plant Physiology **146**: 576–588.

Bu, Q., Zhu, L., Dennis, M.D., Yu, L., Lu, S.X., Person, M.D., Tobin, E.M., Browning, K.S., and Huq, E. (2011). Phosphorylation by CK2 enhances the rapid light-induced degradation of phytochrome interacting factor 1 in Arabidopsis. Journal of Biological Chemistry **286**: 12066–12074.

Bustin, S.A., Benes, V., Garson, J.A., Hellemans, J., Huggett, J., Kubista, M., Mueller, R., Nolan, T., Pfaffl, M.W., Shipley, G.L., Vandesompele, J., and Wittwer, C.T. (2009). The MIQE guidelines: minimum information for publication of quantitative real-time PCR experiments. Clinical Chemistry **55**: 611–622

Caldwell, M.M., Robberecht, R., and Flint, S.D. (1983). Internal filters: prospects for UV−acclimation in higher plants. Physiologia Plantarum **58**: 445–450.

Campi, M., D'Andrea, L., Emiliani, J., and Casati, P. (2012). Participation of chromatin-remodeling proteins in the repair of ultraviolet-B-damaged DNA. Plant physiology **158**: 981–995.

Campos, E.I., and Reinberg, D. (2009). Histones: annotating chromatin. Annual review of genetics **43**: 559–599.

Carrozza, M.J., Li, B., Florens, L., Suganuma, T., Swanson, S.K., Lee, K.K., Shia, W.-J., Anderson, S., Yates, J., and Washburn, M.P. (2005). Histone H3 methylation by Set2 directs deacetylation of coding regions by Rpd3S to suppress spurious intragenic transcription. Cell **123**: 581–592.

Casal, J.J. (2013). Photoreceptor signaling networks in plant responses to shade. Annual Review of Plant Biology **64**: 403–427

Casal, J.J., Candia, A.N., and Sellaro, R. (2014). Light perception and signalling by phytochrome A. Journal of Experimental Botany **65**: 2835–2845.

Casati, P., and Walbot, V. (2003). Gene expression profiling in response to ultraviolet radiation in maize genotypes with varying flavonoid content. Plant Physiology **132**: 1739–1754

Casati, P., and Walbot, V. (2004a). Crosslinking of ribosomal proteins to RNA in maize ribosomes by UV-B and its effects on translation. Plant physiology **136**: 3319–3332.

Casati, P., and Walbot, V. (2004b). Rapid transcriptome responses of maize (Zea mays) to UV-B in irradiated and shielded tissues. Genome Biology **5**: R16.

Casati, P., Campi, M., Chu, F., Suzuki, N., Maltby, D., Guan, S., Burlingame, A.L., and Walbot, V. (2008). Histone acetylation and chromatin remodeling are required for UV-B–dependent transcriptional activation of regulated genes in maize. Plant Cell **20**: 827–842.

Casati, P., Stapleton, A.E., Blum, J.E., and Walbot, V. (2006). Genome−wide analysis of high−altitude maize and gene knockdown stocks implicates chromatin remodeling proteins in response to UV−B. The Plant Journal **46**: 613–627.

Chang, C.J., Li, Y., Chen, L., Chen, W., Hsieh, W., Shin, J., Jane, W., Chou, S., Choi, G., and Hu, J. (2008). LZF1, a HY5−regulated transcriptional factor, functions in Arabidopsis de−etiolation. The Plant Journal **54**: 205–219.

Charron, J.-B.F., He, H., Elling, A.A., and Deng, X.W. (2009). Dynamic landscapes of four histone modifications during deetiolation in Arabidopsis. Plant Cell **21**: 3732–3748.

Chattopadhyay, S., Ang, L.-H., Puente, P., Deng, X.-W., and Wei, N. (1998b). Arabidopsis bZIP protein HY5 directly interacts with light-responsive promoters in mediating light control of gene expression. Plant Cell **10**: 673–683.

Chattopadhyay, S., Puente, P., Deng, X.W., and Wei, N. (1998a). Combinatorial interaction of light-responsive elements plays a critical role in determining the response characteristics of light-regulated promoters in Arabidopsis. The Plant Journal **15**: 69–77.

Chaves, I., Pokorny, R., Byrdin, M., Hoang, N., Ritz, T., Brettel, K., Essen, L.O., van der Horst, G.T., Batschauer, A., and Ahmad, M. (2011). The cryptochromes: blue light photoreceptors in plants and animals. Annual Review of Plant Biology **62**: 335–364.

Chen, C., Xiao, Y.G., Li, X., and Ni, M. (2012). Light-regulated stomatal aperture in Arabidopsis. Molecular Plant **5**: 566–572.

Chen, F., Li, B., Demone, J., Charron, J.B., Shi, X., and Deng, X.W. (2014). Photoreceptor partner FHY1 has an independent role in gene modulation and plant development under far-red light. Proceedings of the National Academy of Sciences of the United States of America **111**: 11888–11893.

Chen, F., Shi, X., Chen, L., Dai, M., Zhou, Z., Shen, Y., Li, J., Li, G., Wei, N., and Deng, X.W. (2012). Phosphorylation of FAR-RED ELONGATED HYPOCOTYL1 is a key mechanism defining signaling dynamics of phytochrome A under red and far-red light in Arabidopsis. Plant Cell **24**: 1907–1920.

Chen, H., Zhang, J., Neff, M.M., Hong, S.W., Zhang, H., Deng, X.W., and Xiong, L. (2008). Integration of light and abscisic acid signaling during seed germination and early seedling development. Proceedings of the National Academy of Sciences of the United States of America **105**: 4495–4500.

Chen, H., Huang, X., Gusmaroli, G., Terzaghi, W., Lau, O.S., Yanagawa, Y., Zhang, Y., Li, J., Lee, J.-H., and Zhu, D. (2010). Arabidopsis CULLIN4-damaged DNA binding protein 1 interacts with CONSTITUTIVELY PHOTOMORPHOGENIC1-SUPPRESSOR OF PHYA complexes to regulate photomorphogenesis and flowering time. Plant Cell **22**: 108–123.

Chen, H., Shen, Y., Tang, X., Yu, L., Wang, J., Guo, L., Zhang, Y., Zhang, H., Feng, S., and Strickland, E. (2006). Arabidopsis CULLIN4 forms an E3 ubiquitin ligase with RBX1 and the CDD complex in mediating light control of development. Plant Cell **18**: 1991–2004.

Chen, M., and Chory, J. (2011). Phytochrome signaling mechanisms and the control of plant development. Trends in Cell Biology **21**: 664–671.

Christie, J.M. (2007). Phototropin blue-light receptors. Annual Review of Plant Biology **58**: 21–45.

Christie, J.M., Reymond, P., Powell, G.K., Bernasconi, P., Raibekas, A.A., Liscum, E., and Briggs, W.R. (1998). Arabidopsis NPH1: a flavoprotein with the properties of a photoreceptor for phototropism. Science **282**: 1698–1701.

Christie, J.M., Yang, H., Richter, G.L., Sullivan, S., Thomson, C.E., Lin, J., Titapiwatanakun, B., Ennis, M., Kaiserli, E., Lee, O.R., Adamec, J., Peer, W.A., and Murphy, A.S. (2011). phot1 inhibition of ABCB19 primes lateral auxin fluxes in the shoot apex required for phototropism. PLoS Biology **9**: e1001076.

Christie, J.M., Arvai, A.S., Baxter, K.J., Heilmann, M., Pratt, A.J., O'Hara, A., Kelly, S.M., Hothorn, M., Smith, B.O., and Hitomi, K. (2012). Plant UVR8 photoreceptor senses UV-B by tryptophan-mediated disruption of cross-dimer salt bridges. Science **335**: 1492–1496.

Christie, J.M., and Jenkins, G.I. (1996). Distinct UV-B and UV-A/blue light signal transduction pathways induce chalcone synthase gene expression in Arabidopsis cells. Plant Cell **8**: 1555–1567.

Chua, Y.L., Brown, A.P.C., and Gray, J.C. (2001). Targeted histone acetylation and altered nuclease accessibility over short regions of the pea plastocyanin gene. Plant Cell **13**: 599–612.

Chua, Y.L., Watson, L.A., and Gray, J.C. (2003). The transcriptional enhancer of the pea plastocyanin gene associates with the nuclear matrix and regulates gene expression through histone acetylation. Plant Cell **15**: 1468–1479.

Clack, T., Shokry, A., Moffet, M., Liu, P., Faul, M., and Sharrock, R.A. (2009). Obligate heterodimerization of Arabidopsis phytochromes C and E and interaction with the PIF3 basic helix-loop-helix transcription factor. Plant Cell **21**: 786–799.

Cloix, C., Kaiserli, E., Heilmann, M., Baxter, K.J., Brown, B.A., O'Hara, A., Smith, B.O., Christie, J.M., and Jenkins, G.I. (2012). C-terminal region of the UV-B photoreceptor UVR8 initiates signaling through interaction with the COP1 protein. Proceedings of the National Academy of Sciences of the United States of America **109**: 16366–16370.

Cloix, C., and Jenkins, G.I. (2008). Interaction of the Arabidopsis UV-B-specific signaling component UVR8 with chromatin. Molecular plant **1**: 118–128.

Clough, R.C., and Vierstra, R.D. (1997). Phytochrome degradation. Plant, Cell & Environment **20**: 713–721.

Cluis, C.P., Mouchel, C.F., and Hardtke, C.S. (2004). The Arabidopsis transcription factor HY5 integrates light and hormone signaling pathways. The Plant Journal **38**: 332–347.

Coego, A., Brizuela, E., Castillejo, P., Ruiz, S., Koncz, C., del Pozo, J.C., Pineiro, M., Jarillo, J.A., Paz-Ares, J., and Leon, J. (2014). The TRANSPLANTA collection of Arabidopsis lines: a resource for functional analysis of transcription factors based on their conditional overexpression. The Plant Journal **77**: 944–953.

Crevillen, P., Yang, H., Cui, X., Greeff, C., Trick, M., Qiu, Q., Cao, X., and Dean, C. (2014). Epigenetic reprogramming that prevents transgenerational inheritance of the vernalized state. Nature **515**: 587–590.

Crosson, S., Rajagopal, S., and Moffat, K. (2003). The LOV domain family: photoresponsive signaling modules coupled to diverse output domains. Biochemistry **42**: 2–10.

Datta, A., Bagchi, S., Nag, A., Shiyanov, P., Adami, G.R., Yoon, T., and Raychaudhuri, P. (2001). The p48 subunit of the damaged-DNA binding protein DDB associates with the CBP/p300 family of histone acetyltransferase. Mutation Research/DNA Repair **486**: 89–97.

Datta, S., Hettiarachchi, C., Johansson, H., and Holm, M. (2007). SALT TOLERANCE HOMOLOG2, a B-box protein in Arabidopsis that activates transcription and positively regulates light-mediated development. Plant Cell **19**: 3242–3255.

Datta, S., Johansson, H., Hettiarachchi, C., and Holm, M. (2008a). STH2 has 2 B there: An insight into the role of B-box containing proteins in Arabidopsis. Plant signaling & behavior **3**: 547–548.

Datta, S., Johansson, H., Hettiarachchi, C., Irigoyen, M.L., Desai, M., Rubio, V., and Holm, M. (2008b). LZF1/SALT TOLERANCE HOMOLOG3, an Arabidopsis B-box protein involved in light-dependent development and gene expression, undergoes COP1-mediated ubiquitination. Plant Cell **20**: 2324–2338.

Davey, M.P., Susanti, N.I., Wargent, J.J., Findlay, J.E., Paul Quick, W., Paul, N.D., and Jenkins, G.I. (2012). The UV-B photoreceptor UVR8 promotes photosynthetic efficiency in *Arabidopsis thaliana* exposed to elevated levels of UV-B. Photosynthesis Research **114**: 121–131.

Davis, A.M., Hall, A., Millar, A.J., Darrah, C., and Davis, S.J. (2009). Protocol: Streamlined sub-protocols for floral-dip transformation and selection of transformants in *Arabidopsis thaliana*. Plant Methods **5**: 3.

de Carbonnel, M., Davis, P., Roelfsema, M.R., Inoue, S., Schepens, I., Lariguet, P., Geisler, M., Shimazaki, K., Hangarter, R., and Fankhauser, C. (2010). The Arabidopsis PHYTOCHROME KINASE SUBSTRATE2 protein is a phototropin signaling element that regulates leaf flattening and leaf positioning. Plant Physiology **152**: 1391–1405.

Demarsy, E., and Fankhauser, C. (2009). Higher plants use LOV to perceive blue light. Current Opinion in Plant Biology **12**: 69–74.

Demarsy, E., Schepens, I., Okajima, K., Hersch, M., Bergmann, S., Christie, J., Shimazaki, K., Tokutomi, S., and Fankhauser, C. (2012). Phytochrome Kinase Substrate 4 is phosphorylated by the phototropin 1 photoreceptor. The EMBO Journal **31**: 3457–3467.

Demkura, P.V., and Ballare, C.L. (2012). UVR8 mediates UV-B-induced Arabidopsis defense responses against Botrytis cinerea by controlling sinapate accumulation. Molecular Plant **5**: 642–652.

Dinman, J.D., Ruiz-Echevarria, M.J., Czaplinski, K., and Peltz, S.W. (1997). Peptidyl-transferase inhibitors have antiviral properties by altering programmed -1 ribosomal frameshifting efficiencies: development of model systems. Proceedings of the National Academy of Sciences of the United States of America **94**: 6606–6611.

Donald, R.G., Schindler, U., Batschauer, A., and Cashmore, A.R. (1990). The plant G box promoter sequence activates transcription in *Saccharomyces cerevisiae* and is bound in vitro by a yeast activity similar to GBF, the plant G box binding factor. The EMBO journal **9**: 1727.

Dubos, C., Stracke, R., Grotewold, E., Weisshaar, B., Martin, C., and Lepiniec, L. (2010). MYB transcription factors in Arabidopsis. Trends in Plant Science **15**: 573–581.

Elledge, S.J., Sugiono, P., Guarente, L., and Davis, R.W. (1989). Genetic selection for genes encoding sequence-specific DNA-binding proteins. Proceedings of the National Academy of Sciences of the United States of America **86**: 3689–3693.

Faktor, O., Kooter, J.M., Loake, G.J., Dixone, R.A., and Lamb, C.J. (1997a). Differential utilization of regulatory< i> cis-elements for stress-induced and tissue-specific activity of a French bean chalcone synthase promoter. Plant Science **124**: 175–182.

Faktor, O., Loake, G., Dixon, R.A., and Lamb, C.J. (1997b). The G−box and H−box in a 39 bp region of a French bean chalcone synthase promoter constitute a tissue−specific regulatory element. The Plant Journal **11**: 1105–1113.

Fankhauser, C., and Ulm, R. (2011). Light-regulated interactions with SPA proteins underlie cryptochrome-mediated gene expression. Genes and Development **25**: 1004–1009.

Fankhauser, C., Yeh, K.C., Lagarias, J.C., Zhang, H., Elich, T.D., and Chory, J. (1999). PKS1, a substrate phosphorylated by phytochrome that modulates light signaling in Arabidopsis. Science **284**: 1539–1541.

Favory, J.-J., Stec, A., Gruber, H., Rizzini, L., Oravecz, A., Funk, M., Albert, A., Cloix, C., Jenkins, G.I., and Oakeley, E.J. (2009). Interaction of COP1 and UVR8 regulates UV-B-induced photomorphogenesis and stress acclimation in Arabidopsis. The EMBO journal **28**: 591–601.

Feher, A. (2014). Somatic embryogenesis - Stress-induced remodeling of plant cell fate. Biochim Biophys Acta (in press)

Feher, B., Kozma-Bognar, L., Kevei, E., Hajdu, A., Binkert, M., Davis, S.J., Schafer, E., Ulm, R., and Nagy, F. (2011). Functional interaction of the circadian clock and UV RESISTANCE LOCUS 8-controlled UV-B signaling pathways in *Arabidopsis thaliana*. The Plant Journal **67**: 37–48.

Feldbrugge, M., Sprenger, M., Dinkelbach, M., Yazaki, K., Harter, K., and Weisshaar, B. (1994). Functional analysis of a light-responsive plant bZIP transcriptional regulator. Plant Cell **6**: 1607–1621.

Fisher, A.J., and Franklin, K.A. (2011). Chromatin remodelling in plant light signalling. Physiologia plantarum **142**: 305–313.

Folta, K.M., and Maruhnich, S.A. (2007). Green light: a signal to slow down or stop. Journal of Experimental Botany **58**: 3099–3111.

Fornalé, S., Shi, X., Chai, C., Encina, A., Irar, S., Capellades, M., Fuguet, E., Torres, J., Rovira, P., and Puigdomènech, P. (2010). ZmMYB31 directly represses maize lignin genes and redirects the phenylpropanoid metabolic flux. The Plant Journal **64**: 633–644.

Fortunato, A.E., Annunziata, R., Jaubert, M., Bouly, J.P., and Falciatore, A. (2014). Dealing with light: The widespread and multitasking cryptochrome/photolyase family in photosynthetic organisms. Journal of Plant Physiology (in press)

Franco-Zorrilla, J.M., López-Vidriero, I., Carrasco, J.L., Godoy, M., Vera, P., and Solano, R. (2014). DNA-binding specificities of plant transcription factors and their potential to define target genes. Proceedings of the National Academy of Sciences of the United States of America **111**: 2367–2372.

Franklin, K.A., and Quail, P.H. (2010). Phytochrome functions in Arabidopsis development. Journal of experimental botany **61**: 11–24.

Frohnmeyer, H., Loyall, L., Blatt, M.R., and Grabov, A. (1999). Millisecond UV-B irradiation evokes prolonged elevation of cytosolic-free Ca2+ and stimulates gene expression in transgenic parsley cell cultures. The Plant Journal **20**: 109–117.

Frohnmeyer, H., Bowler, C., Zhu, J., Yamagata, H., Schäfer, E., and Chua, N. (1998). Different roles for calcium and calmodulin in phytochrome−and UV−regulated expression of chalcone synthase. The Plant Journal **13**: 763–772.

Gadjev, I., Vanderauwera, S., Gechev, T.S., Laloi, C., Minkov, I.N., Shulaev, V., Apel, K., Inze, D., Mittler, R., and Van Breusegem, F. (2006). Transcriptomic footprints disclose specificity of reactive oxygen species signaling in Arabidopsis. Plant Physiology **141**: 436–445.

Gangappa, S.N., and Chattopadhyay, S. (2013). MYC2 differentially regulates GATA-box containing promoters during seedling development in Arabidopsis. Plant Signalling and Behaviour **8**: e25679

Gangappa, S.N., Crocco, C.D., Johansson, H., Datta, S., Hettiarachchi, C., Holm, M., and Botto, J.F. (2013a). The Arabidopsis B-BOX protein BBX25 interacts with HY5, negatively regulating BBX22 expression to suppress seedling photomorphogenesis. Plant Cell **25**: 1243–1257.

Gangappa, S.N., Holm, M., and Botto, J.F. (2013b). Molecular interactions of BBX24 and BBX25 with HYH, HY5 HOMOLOG, to modulate Arabidopsis seedling development. Plant Signalling and Behaviour **8**: e25208

Gangappa, S.N., Maurya, J.P., Yadav, V., and Chattopadhyay, S. (2013c). The regulation of the Z- and G-box containing promoters by light signaling components, SPA1 and MYC2, in Arabidopsis. PLoS One **8**: e62194.

Gangappa, S.N., Srivastava, A.K., Maurya, J.P., Ram, H., and Chattopadhyay, S. (2013d). Z-box binding transcription factors (ZBFs): a new class of transcription factors in Arabidopsis seedling development. Molecular Plant **6**: 1758–1768.

Gao, Y., Li, J., Strickland, E., Hua, S., Zhao, H., Chen, Z., Qu, L., and Deng, X.W. (2004). An arabidopsis promoter microarray and its initial usage in the identification of HY5 binding targets in vitro. Plant Molecular Biology **54**: 683–699.

Genoud, T., Schweizer, F., Tscheuschler, A., Debrieux, D., Casal, J.J., Schafer, E., Hiltbrunner, A., and Fankhauser, C. (2008). FHY1 mediates nuclear import of the light-activated phytochrome A photoreceptor. PLoS Genetics **4**: e1000143.

Georgakopoulos, T., and Thireos, G. (1992). Two distinct yeast transcriptional activators require the function of the GCN5 protein to promote normal levels of transcription. The EMBO journal **11**: 4145.

Gilmartin, P.M., and Chua, N.H. (1990a). Localization of a phytochrome-responsive element within the upstream region of pea rbcS-3A. Molecular and cellular biology **10**: 5565–5568.

Gilmartin, P.M., and Chua, N.-H. (1990b). Spacing between GT-1 binding sites within a light-responsive element is critical for transcriptional activity. Plant Cell **2**: 447–455.

Gilmartin, P.M., Memelink, J., Hiratsuka, K., Kay, S.A., and Chua, N.-H. (1992). Characterization of a gene encoding a DNA binding protein with specificity for a light-responsive element. Plant Cell **4**: 839–849.

Gonzalez Besteiro, M.A., Bartels, S., Albert, A., and Ulm, R. (2011). Arabidopsis MAP kinase phosphatase 1 and its target MAP kinases 3 and 6 antagonistically determine UV-B stress tolerance, independent of the UVR8 photoreceptor pathway. The Plant Journal **68**: 727–737.

Grant, P.A., Duggan, L., Côté, J., Roberts, S.M., Brownell, J.E., Candau, R., Ohba, R., Owen-Hughes, T., Allis, C.D., and Winston, F. (1997). Yeast Gcn5 functions in two multisubunit complexes to acetylate nucleosomal histones: characterization of an Ada complex and the SAGA (Spt/Ada) complex. Genes & development **11**: 1640–1650.

Gruber, H., Heijde, M., Heller, W., Albert, A., Seidlitz, H.K., and Ulm, R. (2010). Negative feedback regulation of UV-B-induced photomorphogenesis and stress acclimation in Arabidopsis. Proceedings of the National Academy of Sciences of the United States of America **107**: 20132–20137.

Gu, X., Jiang, D., Yang, W., Jacob, Y., Michaels, S.D., and He, Y. (2011). Arabidopsis homologs of retinoblastoma-associated protein 46/48 associate with a histone deacetylase to act redundantly in chromatin silencing. PLoS Genetics **7**: e1002366.

Guo, L., Zhou, J., Elling, A.A., Charron, J.-B.F., and Deng, X.W. (2008). Histone modifications and expression of light-regulated genes in Arabidopsis are cooperatively influenced by changing light conditions. Plant physiology **147**: 2070–2083.

Gupta, N., Prasad, V.B., and Chattopadhyay, S. (2014). LeMYC2 acts as a negative regulator of blue light mediated photomorphogenic growth, and promotes the growth of adult tomato plants. BMC Plant Biology **14**: 38.

Ha, M., Ng, D.W.K., Li, W.-H., and Chen, Z.J. (2011). Coordinated histone modifications are associated with gene expression variation within and between species. Genome research **21**: 590–598.

Hahlbrock, K., and Scheel, D. (1989). Physiology and molecular biology of phenylpropanoid metabolism. Annual review of plant biology **40**: 347–369.

Hao, Y., Oh, E., Choi, G., Liang, Z., and Wang, Z.Y. (2012). Interactions between HLH and bHLH factors modulate light-regulated plant development. Molecular Plant **5**: 688–697.

Hardtke, C.S., Gohda, K., Osterlund, M.T., Oyama, T., Okada, K., and Deng, X.W. (2000). HY5 stability and activity in Arabidopsis is regulated by phosphorylation in its COP1 binding domain. The EMBO journal **19**: 4997–5006.

Haring, M., Offermann, S., Danker, T., Horst, I., Peterhansel, C., and Stam, M. (2007). Chromatin immunoprecipitation: optimization, quantitative analysis and data normalization. Plant methods **3**: 11.

Harper, S.M., Neil, L.C., and Gardner, K.H. (2003). Structural basis of a phototropin light switch. Science **301**: 1541–1544.

Hartmann, U., Sagasser, M., Mehrtens, F., Stracke, R., and Weisshaar, B. (2005). Differential combinatorial interactions of cis-acting elements recognized by R2R3-MYB, BZIP, and BHLH factors control light-responsive and tissue-specific activation of phenylpropanoid biosynthesis genes. Plant molecular biology **57**: 155–171.

Hartmann, U., Valentine, W.J., Christie, J.M., Hays, J., Jenkins, G.I., and Weisshaar, B. (1998). Identification of UV/blue light-response elements in the *Arabidopsis thaliana* chalcone synthase promoter using a homologous protoplast transient expression system. Plant molecular biology **36**: 741–754.

Hayes, S., Velanis, C.N., Jenkins, G.I., and Franklin, K.A. (2014). UV-B detected by the UVR8 photoreceptor antagonizes auxin signaling and plant shade avoidance. Proceedings of the National Academy of Sciences of the United States of America **111**: 11894–11899.

Hectors, K., Prinsen, E., De Coen, W., Jansen, M.A., and Guisez, Y. (2007). *Arabidopsis thaliana* plants acclimated to low dose rates of ultraviolet B radiation show specific changes in morphology and gene expression in the absence of stress symptoms. New Phytologist **175**: 255–270.

Heijde, M., Binkert, M., Yin, R., Ares-Orpel, F., Rizzini, L., Van De Slijke, E., Persiau, G., Nolf, J., Gevaert, K., De Jaeger, G., and Ulm, R. (2013). Constitutively active UVR8 photoreceptor variant in Arabidopsis. Proceedings of the National Academy of Sciences of the United States of America **110**: 20326–20331.

Heijde, M., and Ulm, R. (2012). UV-B photoreceptor-mediated signalling in plants. Trends in Plant Science **17**: 230–237.

Heijde, M., and Ulm, R. (2013). Reversion of the Arabidopsis UV-B photoreceptor UVR8 to the homodimeric ground state. Proceedings of the National Academy of Sciences of the United States of America **110**: 1113–1118.

Heilmann, M. (2013). Structure-Function Studies Of The UV-B Photoreceptor Uvr8 In *Arabidopsis thaliana.* Phd Dissertation, University of Glasgow

Heilmann, M., and Jenkins, G.I. (2013). Rapid reversion from monomer to dimer regenerates the ultraviolet-B photoreceptor UV RESISTANCE LOCUS8 in intact Arabidopsis plants. Plant Physiology **161**: 547–555.

Hill, C., and Jones, R.L. (2000). Absorption of solar radiation by water vapor in clear and cloudy skies: Implications for anomalous absorption. Journal of Geophysical Research: Atmospheres (1984–2012) **105**: 9421–9428.

Holm, M., Hardtke, C.S., Gaudet, R., and Deng, X. (2001). Identification of a structural motif that confers specific interaction with the WD40 repeat domain of Arabidopsis COP1. The EMBO journal **20**: 118–127.

Hornitschek, P., Lorrain, S., Zoete, V., Michielin, O., and Fankhauser, C. (2009). Inhibition of the shade avoidance response by formation of non-DNA binding bHLH heterodimers. The EMBO Journal **28**: 3893–3902.

Huala, E., Oeller, P.W., Liscum, E., Han, I.S., Larsen, E., and Briggs, W.R. (1997). Arabidopsis NPH1: a protein kinase with a putative redox-sensing domain. Science **278**: 2120–2123.

Huang, X., Ouyang, X., and Deng, X.W. (2014a). Beyond repression of photomorphogenesis: role switching of COP/DET/FUS in light signalling. Current Opinion in Plant Biology **21**: 96–103.

Huang, X., Ouyang, X., Yang, P., Lau, O.S., Chen, L., Wei, N., and Deng, X.W. (2013). Conversion from CUL4-based COP1-SPA E3 apparatus to UVR8-COP1-SPA complexes underlies a distinct biochemical function of COP1 under UV-B. Proceedings of The National Academy of Sciences of the United States of America **110**: 16669–16674.

Huang, X., Yang, P., Ouyang, X., Chen, L., and Deng, X.W. (2014b). Photoactivated UVR8-COP1 module determines photomorphogenic UV-B signaling output in Arabidopsis. PLoS Genetics **10**: e1004218.

Huang, X., Ouyang, X., Yang, P., Lau, O.S., Li, G., Li, J., Chen, H., and Deng, X.W. (2012). Arabidopsis FHY3 and HY5 positively mediate induction of COP1 transcription in response to photomorphogenic UV-B light. Plant Cell **24**: 4590–4606.

Hudson, M.E., and Quail, P.H. (2003). Identification of promoter motifs involved in the network of phytochrome A-regulated gene expression by combined analysis of genomic sequence and microarray data. Plant physiology **133**: 1605–1616.

Hughes, J. (2013). Phytochrome cytoplasmic signaling. Annual Review of Plant Biology **64**: 377–402.

Huq, E., and Quail, P.H. (2002). PIF4, a phytochrome-interacting bHLH factor, functions as a negative regulator of phytochrome B signaling in Arabidopsis. The EMBO Journal **21**: 2441–2450.

Indorf, M., Cordero, J., Neuhaus, G., and Rodríguez−Franco, M. (2007). Salt tolerance (STO), a stress−related protein, has a major role in light signalling. The Plant Journal **51**: 563–574.

Inoue, H., Nojima, H., and Okayama, H. (1990). High efficiency transformation of< i> Escherichia coli with plasmids. Gene **96**: 23–28.

Jang, I.C., Henriques, R., and Chua, N.H. (2013). Three transcription factors, HFR1, LAF1 and HY5, regulate largely independent signaling pathways downstream of phytochrome A. Plant Cell Physiology **54**: 907–916.

Jang, I.-C., Chung, P.J., Hemmes, H., Jung, C., and Chua, N.-H. (2011). Rapid and reversible light-mediated chromatin modifications of Arabidopsis phytochrome A locus. Plant Cell **23**: 459–470.

Jenkins, G.I. (2009). Signal transduction in responses to UV-B radiation. Annual review of plant biology **60**: 407–431.

Jenkins, G.I., Long, J.C., Wade, H.K., Shenton, M.R., and Bibikova, T.N. (2001). UV and blue light signalling: pathways regulating chalcone synthase gene expression in Arabidopsis. New Phytologist **151**: 121–131.

Jenkins, G.I. (2014b). Structure and function of the UV-B photoreceptor UVR8. Current Opinion in Structural Biology **29**: 52–57.

Jenkins, G.I. (2014a). The UV-B photoreceptor UVR8: from structure to physiology. Plant Cell **26**: 21–37

Jenuwein, T., and Allis, C.D. (2001). Translating the histone code. Science **293**: 1074–1080.

Jeon, J., and Kim, J. (2011). FVE, an Arabidopsis homologue of the retinoblastoma-associated protein that regulates flowering time and cold response, binds to chromatin as a large multiprotein complex. Molecules and Cells **32**: 227–234.

Jiang, L., Wang, Y., Bjorn, L.O., and Li, S. (2009). Arabidopsis radical-induced cell death1 is involved in UV-B signaling. Photochemical and Photobiological Sciences **8**: 838–846.

Jiang, L., Wang, Y., Li, Q.F., Bjorn, L.O., He, J.X., and Li, S.S. (2012). Arabidopsis STO/BBX24 negatively regulates UV-B signaling by interacting with COP1 and repressing HY5 transcriptional activity. Cell Research **22**: 1046–1057.

Jiao, Y., Lau, O.S., and Deng, X.W. (2007). Light-regulated transcriptional networks in higher plants. Nature Reviews in Genetics **8**: 217–230.

Jiao, Y., Yang, H., Ma, L., Sun, N., Yu, H., Liu, T., Gao, Y., Gu, H., Chen, Z., Wada, M., Gerstein, M., Zhao, H., Qu, L.J., and Deng, X.W. (2003). A genome-wide analysis of blue-light regulation of Arabidopsis transcription factor gene expression during seedling development. Plant Physiology **133**: 1480–1493.

Jiao, Y., Ma, L., Strickland, E., and Deng, X.W. (2005). Conservation and divergence of light-regulated genome expression patterns during seedling development in rice and Arabidopsis. Plant Cell **17**: 3239–3256.

Jin, H., Cominelli, E., Bailey, P., Parr, A., Mehrtens, F., Jones, J., Tonelli, C., Weisshaar, B., and Martin, C. (2000). Transcriptional repression by AtMYB4 controls production of UV−protecting sunscreens in Arabidopsis. The EMBO journal **19**: 6150–6161.

Jing, Y., Zhang, D., Wang, X., Tang, W., Wang, W., Huai, J., Xu, G., Chen, D., Li, Y., and Lin, R. (2013). Arabidopsis Chromatin Remodeling Factor PICKLE Interacts with Transcription Factor HY5 to Regulate Hypocotyl Cell Elongation. Plant Cell **25**: 242–256.

Josse, E.M., and Halliday, K.J. (2008). Skotomorphogenesis: the dark side of light signalling. Current Biology **18**: R1144–R1146.

Kaiser, T., Emmler, K., Kretsch, T., Weisshaar, B., Schafer, E., and Batschauer, A. (1995). Promoter elements of the mustard CHS1 gene are sufficient for light regulation in transgenic plants. Plant Molecular Biology **28**: 219–229.

Kaiserli, E., and Jenkins, G.I. (2007). UV-B promotes rapid nuclear translocation of the Arabidopsis UV-B–specific signaling component UVR8 and activates its function in the nucleus. Plant Cell **19**: 2662–2673.

Kami, C., Lorrain, S., Hornitschek, P., and Fankhauser, C. (2010). Chapter two-light-regulated plant growth and development. Current topics in developmental biology **91**: 29–66.

Khanna, R., Kronmiller, B., Maszle, D.R., Coupland, G., Holm, M., Mizuno, T., and Wu, S.-H. (2009). The Arabidopsis B-box zinc finger family. Plant Cell **21**: 3416–3420.

Kilian, J., Whitehead, D., Horak, J., Wanke, D., Weinl, S., Batistic, O., D'Angelo, C., Bornberg-Bauer, E., Kudla, J., and Harter, K. (2007). The AtGenExpress global stress expression data set: protocols, evaluation and model data analysis of UV-B light, drought and cold stress responses. The Plant Journal **50**: 347–363.

Kim, B.C., Tennessen, D.J., and Last, R.L. (1998). UV-B-induced photomorphogenesis in *Arabidopsis thaliana*. The Plant Journal **15**: 667–674.

Kim, J., Yi, H., Choi, G., Shin, B., Song, P.S., and Choi, G. (2003). Functional characterization of phytochrome interacting factor 3 in phytochrome-mediated light signal transduction. Plant Cell **15**: 2399–2407.

Kim, W.Y., Fujiwara, S., Suh, S.S., Kim, J., Kim, Y., Han, L., David, K., Putterill, J., Nam, H.G., and Somers, D.E. (2007). ZEITLUPE is a circadian photoreceptor stabilized by GIGANTEA in blue light. Nature **449**: 356–360.

Kircher, S., Ledger, S., Hayashi, H., Weisshaar, B., Schäfer, E., and Frohnmeyer, H. (1998). CPRF4a, a novel plant bZIP protein of the CPRF family: comparative analyses of light-dependent expression, post-transcriptional regulation, nuclear import and heterodimerisation. Molecular and General Genetics MGG **257**: 595–605.

Kleine, T., Lockhart, P., and Batschauer, A. (2003). An Arabidopsis protein closely related to Synechocystis cryptochrome is targeted to organelles. The Plant Journal **35**: 93–103.

Kliebenstein, D.J., Lim, J.E., Landry, L.G., and Last, R.L. (2002). Arabidopsis UVR8 regulates ultraviolet-B signal transduction and tolerance and contains sequence similarity to human regulator of chromatin condensation 1. Plant Physiology **130**: 234–243.

Koga, A., Ishibashi, T., Kimura, S., Uchiyama, Y., and Sakaguchi, K. (2006). Characterization of T-DNA insertion mutants and RNAi silenced plants of *Arabidopsis thaliana* UV-damaged DNA binding protein 2 (AtUV-DDB2). Plant molecular biology **61**: 227–240.

Koini, M.A., Alvey, L., Allen, T., Tilley, C.A., Harberd, N.P., Whitelam, G.C., and Franklin, K.A. (2009). High temperature-mediated adaptations in plant architecture require the bHLH transcription factor PIF4. Current Biology **19**: 408–413.

Kotchoni, S.O., and Gachomo, E.W. (2009). A rapid and hazardous reagent free protocol for genomic DNA extraction suitable for genetic studies in plants. Molecular Biology Reports **36**: 1633–1636.

Kumar, S.V., and Wigge, P.A. (2010). H2A. Z-Containing Nucleosomes Mediate the Thermosensory Response in< i> Arabidopsis. Cell **140**: 136–147.

Kumimoto, R.W., Zhang, Y., Siefers, N., and Holt, B.F. (2010). NF–YC3, NF–YC4 and NF–YC9 are required for CONSTANS‐mediated, photoperiod‐dependent flowering in *Arabidopsis thaliana*. The Plant Journal **63**: 379–391.

Kuo, M.H., Brownell, J.E., Sobel, R.E., Ranalli, T.A., Cook, R.G., Edmondson, D.G., Roth, S.Y., and Allis, C.D. (1996). Transcription-linked acetylation by Gcn5p of histones H3 and H4 at specific lysines. Nature **383**: 269–272.

Kushwaha, R., Singh, A., and Chattopadhyay, S. (2008). Calmodulin7 plays an important role as transcriptional regulator in Arabidopsis seedling development. Plant Cell **20**: 1747–1759.

Laloum, T., De Mita, S., Gamas, P., Baudin, M., and Niebel, A. (2013). CCAAT-box binding transcription factors in plants: Y so many? Trends in Plant Science **18**: 157–166.

Latchman, D., and Latchman, D.S. (2010). Eukaryotic transcription factors. Academic press.

Lau, O.S., and Deng, X.W. (2012). The photomorphogenic repressors COP1 and DET1: 20 years later. Trends in plant science **17**: 584–593.

Lee, C.-K., Shibata, Y., Rao, B., Strahl, B.D., and Lieb, J.D. (2004). Evidence for nucleosome depletion at active regulatory regions genome-wide. Nature genetics **36**: 900–905.

Lee, J., and Zhou, P. (2007). DCAFs, the missing link of the CUL4-DDB1 ubiquitin ligase. Molecular cell **26**: 775–780.

Lee, J., He, K., Stolc, V., Lee, H., Figueroa, P., Gao, Y., Tongprasit, W., Zhao, H., Lee, I., and Deng, X.W. (2007). Analysis of transcription factor HY5 genomic binding sites revealed its hierarchical role in light regulation of development. Plant Cell **19**: 731–749.

Leivar, P., Monte, E., Oka, Y., Liu, T., Carle, C., Castillon, A., Huq, E., and Quail, P.H. (2008). Multiple phytochrome-interacting bHLH transcription factors repress premature seedling photomorphogenesis in darkness. Current Biology **18**: 1815–1823.

Leivar, P., Tepperman, J.M., Monte, E., Calderon, R.H., Liu, T.L., and Quail, P.H. (2009). Definition of early transcriptional circuitry involved in light-induced reversal of PIF-imposed repression of photomorphogenesis in young Arabidopsis seedlings. Plant Cell **21**: 3535–3553.

Leivar, P., and Quail, P.H. (2011). PIFs: pivotal components in a cellular signaling hub. Trends in plant science **16**: 19–28.

Li, B., Carey, M., and Workman, J.L. (2007). The role of chromatin during transcription. Cell **128**: 707–719.

Li, J., Li, G., Gao, S., Martinez, C., He, G., Zhou, Z., Huang, X., Lee, J.H., Zhang, H., Shen, Y., Wang, H., and Deng, X.W. (2010). Arabidopsis transcription factor ELONGATED HYPOCOTYL5 plays a role in the feedback regulation of phytochrome A signaling. Plant Cell **22**: 3634–3649.

Li, J., Terzaghi, W., and Deng, X.W. (2012). Genomic basis for light control of plant development. Protein Cell **3**: 106–116.

Li, J., Yang, L., Jin, D., Nezames, C.D., Terzaghi, W., and Deng, X.W. (2013). UV-B-induced photomorphogenesis in Arabidopsis. Protein Cell **4**: 485–492.

Liang, Y.K., Dubos, C., Dodd, I.C., Holroyd, G.H., Hetherington, A.M., and Campbell, M.M. (2005). AtMYB61, an R2R3-MYB transcription factor controlling stomatal aperture in *Arabidopsis thaliana*. Current Biology **15**: 1201–1206.

Lin, C., and Shalitin, D. (2003). Cryptochrome structure and signal transduction. Annual Review of Plant Biology **54**: 469–496.

Liscum, E., Hodgson, D.W., and Campbell, T.J. (2003). Blue light signaling through the cryptochromes and phototropins. So that's what the blues is all about. Plant Physiology **133**: 1429–1436.

Liu, H., Wang, Q., Liu, Y., Zhao, X., Imaizumi, T., Somers, D.E., Tobin, E.M., and Lin, C. (2013). Arabidopsis CRY2 and ZTL mediate blue-light regulation of the transcription factor CIB1 by distinct mechanisms. Proceedings of the National Academy of Sciences of the United States of America **110**: 17582–17587.

Liu, X., Chen, C.-Y., Wang, K.-C., Luo, M., Tai, R., Yuan, L., Zhao, M., Yang, S., Tian, G., and Cui, Y. (2013). PHYTOCHROME INTERACTING FACTOR3 associates with the histone deacetylase HDA15 in repression of chlorophyll biosynthesis and photosynthesis in etiolated Arabidopsis seedlings. Plant Cell **25**: 1258–1273.

Liu, Z., Li, X., Zhong, F.W., Li, J., Wang, L., Shi, Y., and Zhong, D. (2014). Quenching Dynamics of Ultraviolet-Light Perception by UVR8 Photoreceptor. The Journal of Physical Chemistry Letters **5**: 69–72.

Loake, G.J., Faktor, O., Lamb, C.J., and Dixon, R.A. (1992). Combination of H-box [CCTACC (N) 7CT] and G-box (CACGTG) cis elements is necessary for feed-forward stimulation of a chalcone synthase promoter by the phenylpropanoid-pathway intermediate p-coumaric acid. Proceedings of the National Academy of Sciences of the United States of America **89**: 9230–9234.

Lopato, S., Bazanova, N., Morran, S., Milligan, A.S., Shirley, N., and Langridge, P. (2006). Isolation of plant transcription factors using a modified yeast one-hybrid system. Plant Methods **2**: 3.

Ma, L., Gao, Y., Qu, L., Chen, Z., Li, J., Zhao, H., and Deng, X.W. (2002). Genomic evidence for COP1 as a repressor of light-regulated gene expression and development in Arabidopsis. Plant Cell **14**: 2383–2398.

Ma, X., Lv, S., Zhang, C., and Yang, C. (2013). Histone deacetylases and their functions in plants. Plant Cell Reports **32**: 465–478.

Martinez, E. (2002). Multi-protein complexes in eukaryotic gene transcription. Plant molecular biology **50**: 925–947.

Martínez-García, J.F., Huq, E., and Quail, P.H. (2000). Direct targeting of light signals to a promoter element-bound transcription factor. Science **288**: 859–863.

Mas, P., Kim, W.Y., Somers, D.E., and Kay, S.A. (2003). Targeted degradation of TOC1 by ZTL modulates circadian function in *Arabidopsis thaliana*. Nature **426**: 567–570.

McKenzie, R.L., Björn, L.O., Bais, A., and Ilyasd, M. (2003). Changes in biologically active ultraviolet radiation reaching the Earth's surface. Photochemical & Photobiological Sciences **2**: 5–15.

Meissner, R.C., Jin, H., Cominelli, E., Denekamp, M., Fuertes, A., Greco, R., Kranz, H.D., Penfield, S., Petroni, K., Urzainqui, A., Martin, C., Paz-Ares, J., Smeekens, S., Tonelli, C., Weisshaar, B., Baumann, E., Klimyuk, V., Marillonnet, S., Patel, K., Speulman, E., Tissier, A.F., Bouchez, D., Jones, J.J., Pereira, A., Wisman, E., and et, A. (1999). Function search in a large transcription factor gene family in Arabidopsis: assessing the potential of reverse genetics to identify insertional mutations in R2R3 MYB genes. Plant Cell **11**: 1827–1840.

Meshi, T., and Iwabuchi, M. (1995). Plant transcription factors. Plant and cell physiology **36**: 1405–1420.

Millevoi, S., Loulergue, C., Dettwiler, S., Karaa, S.Z., Keller, W., Antoniou, M., and Vagner, S. (2006). An interaction between U2AF 65 and CF I(m) links the splicing and 3' end processing machineries. The EMBO Journal **25**: 4854–4864.

Möglich, A., Yang, X., Ayers, R.A., and Moffat, K. (2010). Structure and function of plant photoreceptors. Annual review of plant biology **61**: 21–47.

Monte, E., Tepperman, J.M., Al-Sady, B., Kaczorowski, K.A., Alonso, J.M., Ecker, J.R., Li, X., Zhang, Y., and Quail, P.H. (2004). The phytochrome-interacting transcription factor, PIF3, acts early, selectively, and positively in light-induced chloroplast development. Proceedings of the National Academy of Sciences of the United States of America **101**: 16091–16098.

Morales, L.O., Brosche, M., Vainonen, J., Jenkins, G.I., Wargent, J.J., Sipari, N., Strid, A., Lindfors, A.V., Tegelberg, R., and Aphalo, P.J. (2013). Multiple roles for UV RESISTANCE LOCUS8 in regulating gene expression and metabolite accumulation in Arabidopsis under solar ultraviolet radiation. Plant Physiology **161**: 744–759.

Moreau, M., Lindermayr, C., Durner, J., and Klessig, D.F. (2010). NO synthesis and signaling in plants–where do we stand? Physiologia Plantarum **138**: 372–383.

Morohashi, K., Xie, Z., and Grotewold, E. (2009). Gene-specific and genome-wide ChIP approaches to study plant transcriptional networks. Methods in Molecular Biology **553**: 3–12.

Motchoulski, A., and Liscum, E. (1999). Arabidopsis NPH3: A NPH1 photoreceptor-interacting protein essential for phototropism. Science **286**: 961–964.

Nagy, F., and Schäfer, E. (2002). Phytochromes control photomorphogenesis by differentially regulated, interacting signaling pathways in higher plants. Annual review of plant biology **53**: 329–355.

Newman, L.J., Perazza, D.E., Juda, L., and Campbell, M.M. (2004). Involvement of the R2R3-MYB, AtMYB61, in the ectopic lignification and dark-photomorphogenic components of the det3 mutant phenotype. The Plant Journal **37**: 239–250.

Ni, M., Tepperman, J.M., and Quail, P.H. (1998). PIF3, a phytochrome-interacting factor necessary for normal photoinduced signal transduction, is a novel basic helix-loop-helix protein. Cell **95**: 657–667.

Ni, M., Tepperman, J.M., and Quail, P.H. (1999). Binding of phytochrome B to its nuclear signalling partner PIF3 is reversibly induced by light. Nature **400**: 781–784.

O'Hara, A., and Jenkins, G.I. (2012). In vivo function of tryptophans in the Arabidopsis UV-B photoreceptor UVR8. Plant Cell **24**: 3755–3766.

Offermann, S., Danker, T., Dreymüller, D., Kalamajka, R., Töpsch, S., Weyand, K., and Peterhänsel, C. (2006). Illumination is necessary and sufficient to induce histone acetylation independent of transcriptional activity at the C4-specific phosphoenolpyruvate carboxylase promoter in maize. Plant physiology **141**: 1078–1088.

Offermann, S., Dreesen, B., Horst, I., Danker, T., Jaskiewicz, M., and Peterhansel, C. (2008). Developmental and environmental signals induce distinct histone acetylation profiles on distal and proximal promoter elements of the C4-Pepc gene in maize. Genetics **179**: 1891–1901.

Ohgishi, M., Saji, K., Okada, K., and Sakai, T. (2004). Functional analysis of each blue light receptor, cry1, cry2, phot1, and phot2, by using combinatorial multiple mutants in Arabidopsis. Proceedings of the National Academy of Sciences of the United States of America **101**: 2223–2228.

Oravecz, A., Baumann, A., Máté, Z., Brzezinska, A., Molinier, J., Oakeley, E.J., Ádám, É., Schäfer, E., Nagy, F., and Ulm, R. (2006). CONSTITUTIVELY PHOTOMORPHOGENIC1 is required for the UV-B response in Arabidopsis. Plant Cell **18**: 1975–1990.

Osterlund, M.T., Hardtke, C.S., Wei, N., and Deng, X.W. (2000). Targeted destabilization of HY5 during light-regulated development of Arabidopsis. Nature **405**: 462–466.

Ouwerkerk, P.B., and Meijer, A.H. (2001). Yeast one-hybrid screening for DNA-protein interactions. Current Protocols in Molecular Biololgy **Chapter 12**: Unit 12.12.

Ouwerkerk, P.B., and Meijer, A.H. (2011). Yeast one-hybrid screens for detection of transcription factor DNA interactions. Methods in Molecular Biology **678**: 211–227.

Oyama, T., Shimura, Y., and Okada, K. (1997). The Arabidopsis HY5 gene encodes a bZIP protein that regulates stimulus-induced development of root and hypocotyl. Genes & Development **11**: 2983–2995.

Panchal, C.J., Whitney, G.K., and Stewart, G.G. (1984). Susceptibility of Saccharomyces spp. and Schwanniomyces spp. to the aminoglycoside antibiotic G418. Applied and Environmental Microbiology **47**: 1164–1166

Pandey, R., MuÈller, A., Napoli, C.A., Selinger, D.A., Pikaard, C.S., Richards, E.J., Bender, J., Mount, D.W., and Jorgensen, R.A. (2002). Analysis of histone acetyltransferase and histone deacetylase families of *Arabidopsis thaliana* suggests functional diversification of chromatin modification among multicellular eukaryotes. Nucleic acids research **30**: 5036–5055.

Pazhouhandeh, M., Molinier, J., Berr, A., and Genschik, P. (2011). MSI4/FVE interacts with CUL4–DDB1 and a PRC2-like complex to control epigenetic regulation of flowering time in Arabidopsis. Proceedings of the National Academy of Sciences of the United States of America **108**: 3430–3435.

Penfield, S., Meissner, R.C., Shoue, D.A., Carpita, N.C., and Bevan, M.W. (2001). MYB61 is required for mucilage deposition and extrusion in the Arabidopsis seed coat. Plant Cell **13**: 2777–2791.

Perez-Burgos, L., Peters, A.H.F.M., Opravil, S., Kauer, M., Mechtler, K., and Jenuwein, T. (2004). Generation and characterization of methyl-lysine histone antibodies. Methods in enzymology **376**: 234–254.

Perrella, G., Lopez-Vernaza, M.A., Carr, C., Sani, E., Gosselé, V., Verduyn, C., Kellermeier, F., Hannah, M.A., and Amtmann, A. (2013). Histone deacetylase complex1 expression level titrates plant growth and abscisic acid sensitivity in Arabidopsis. Plant Cell **25**: 3491–3505

Possart, A., Fleck, C., and Hiltbrunner, A. (2014). Shedding (far-red) light on phytochrome mechanisms and responses in land plants. Plant Science **217-218**: 36–46.

Prouse, M.B., and Campbell, M.M. (2013). Interactions between the R2R3-MYB Transcription Factor, AtMYB61, and Target DNA Binding Sites. PloS one **8**: e65132.

Pruneda-Paz, J.L., Breton, G., Para, A., and Kay, S.A. (2009). A functional genomics approach reveals CHE as a component of the Arabidopsis circadian clock. Science **323**: 1481–1485.

Puente, P., Wei, N., and Deng, X.W. (1996). Combinatorial interplay of promoter elements constitutes the minimal determinants for light and developmental control of gene expression in Arabidopsis. The EMBO Journal **15**: 3732–3743.

Pyvovarenko, T., and Lopato, S. (2011). Isolation of plant transcription factors using a yeast one-hybrid system. Methods in Molecular Biology **754**: 45–66.

Renault, L., Nassar, N., Vetter, I., Becker, J., Klebe, C., Roth, M., and Wittinghofer, A. (1998). The 1.7 A crystal structure of the regulator of chromosome condensation (RCC1) reveals a seven-bladed propeller. Nature **392**: 97–101.

Riechmann, J.L., Heard, J., Martin, G., Reuber, L., Keddie, J., Adam, L., Pineda, O., Ratcliffe, O.J., Samaha, R.R., and Creelman, R. (2000). Arabidopsis transcription factors: genome-wide comparative analysis among eukaryotes. Science **290**: 2105–2110.

Rizzini, L., Favory, J.-J., Cloix, C., Faggionato, D., O'Hara, A., Kaiserli, E., Baumeister, R., Schäfer, E., Nagy, F., and Jenkins, G.I. (2011). Perception of UV-B by the Arabidopsis UVR8 protein. Science **332**: 103–106.

Rockwell, N.C., Su, Y.-S., and Lagarias, J.C. (2006). Phytochome structure and signaling mechanisms. Annual review of plant biology **57**: 837.

Romano, J.M., Dubos, C., Prouse, M.B., Wilkins, O., Hong, H., Poole, M., Kang, K., Li, E., Douglas, C.J., and Western, T.L. (2012). AtMYB61, an R2R3−MYB transcription factor, functions as a pleiotropic regulator via a small gene network. New Phytologist **195**: 774–786.

Rosenfeldt, G., Viana, R.M., Mootz, H.D., von Arnim, A.G., and Batschauer, A. (2008). Chemically induced and light-independent cryptochrome photoreceptor activation. Molecular Plant **1**: 4–14.

Roudier, F., Ahmed, I., Bérard, C., Sarazin, A., Mary-Huard, T., Cortijo, S., Bouyer, D., Caillieux, E., Duvernois-Berthet, E., and Al-Shikhley, L. (2011). Integrative epigenomic mapping defines four main chromatin states in Arabidopsis. The EMBO journal **30**: 1928–1938.

Roudier, F., Teixeira, F.K., and Colot, V. (2009). Chromatin indexing in< i> Arabidopsis: an epigenomic tale of tails and more. Trends in genetics **25**: 511–517.

Ruban, A.V. (2014). Evolution under the sun: optimizing light harvesting in photosynthesis. Journal of Experimental Botany (in press, doi:10.1093/jxb/eru400)

Rufiange, A., Jacques, P.-E., Bhat, W., Robert, F., and Nourani, A. (2007). Genome-wide replication-independent histone H3 exchange occurs predominantly at promoters and implicates H3 K56 acetylation and Asf1. Molecular cell **27**: 393–405.

Ryan, K.G., Swinny, E.E., Winefield, C., and Markham, K.R. (2001). Flavonoids and UV photoprotection in Arabidopsis mutants. Z Naturforsch C **56**: 745–754.

Safrany, J., Haasz, V., Mate, Z., Ciolfi, A., Feher, B., Oravecz, A., Stec, A., Dallmann, G., Morelli, G., and Ulm, R. (2008). Identification of a novel cis−regulatory element for UV−B−induced transcription in Arabidopsis. The Plant Journal **54**: 402–414.

Salomon, M., Christie, J.M., Knieb, E., Lempert, U., and Briggs, W.R. (2000). Photochemical and mutational analysis of the FMN-binding domains of the plant blue light receptor, phototropin. Biochemistry **39**: 9401–9410.

Sambrook, J., Russell, D.W., and Russell, D.W. (2001). Molecular cloning: a laboratory manual (3-volume set). Cold spring harbor laboratory press Cold Spring Harbor, New York).

Sang, Y., Li, Q.H., Rubio, V., Zhang, Y.C., Mao, J., Deng, X.W., and Yang, H.Q. (2005). N-terminal domain-mediated homodimerization is required for photoreceptor activity of Arabidopsis CRYPTOCHROME 1. Plant Cell **17**: 1569–1584.

Sarmiento, F. (2013). The BBX subfamily IV: additional cogs and sprockets to fine-tune light-dependent development. Plant Signalling and Behaviour **8**: e23831.

Schafer, E., and Bowler, C. (2002). Phytochrome-mediated photoperception and signal transduction in higher plants. EMBO Reports **3**: 1042–1048.

Schenke, D., Cai, D., and Scheel, D. (2014). Suppression of UV-B stress responses by flg22 is regulated at the chromatin level via histone modification. Plant Cell and Environment **37**: 1716–1721.

Schenke, D., Boettcher, C., and Scheel, D. (2011). Crosstalk between abiotic ultraviolet-B stress and biotic (flg22) stress signalling in Arabidopsis prevents flavonol accumulation in favor of pathogen defence compound production. Plant, cell & environment **34**: 1849–1864.

Schmitz, R.J., Tamada, Y., Doyle, M.R., Zhang, X., and Amasino, R.M. (2009). Histone H2B deubiquitination is required for transcriptional activation of FLOWERING LOCUS C and for proper control of flowering in Arabidopsis. Plant physiology **149**: 1196–1204.

Schroeder, D.F., Gahrtz, M., Maxwell, B.B., Cook, R.K., Kan, J.M., Alonso, J.M., Ecker, J.R., and Chory, J. (2002). De-Etiolated 1 and Damaged DNA Binding Protein 1 Interact to Regulate< i> Arabidopsis Photomorphogenesis. Current Biology **12**: 1462–1472.

Schulze-Lefert, P., Becker-Andre, M., Schulz, W., Hahlbrock, K., and Dangl, J.L. (1989a). Functional architecture of the light-responsive chalcone synthase promoter from parsley. Plant Cell **1**: 707–714.

Schulze-Lefert, P., Dangl, J.L., Becker-Andre, M., Hahlbrock, K., and Schulz, W. (1989b). Inducible in vivo DNA footprints define sequences necessary for UV light activation of the parsley chalcone synthase gene. The EMBO Journal **8**: 651–656.

Schwammle, V., Aspalter, C.M., Sidoli, S., and Jensen, O.N. (2014). Large scale analysis of co-existing post-translational modifications in histone tails reveals global fine structure of cross-talk. Molecular and Cellular Proteomics **13**: 1855–1865.

Servet, C., Benhamed, M., Latrasse, D., Kim, W., Delarue, M., and Zhou, D.X. (2008). Characterization of a phosphatase 2C protein as an interacting partner of the histone acetyltransferase GCN5 in Arabidopsis. Biochimica et Biophysica Acta **1779**: 376–382.

Sethi, V., Raghuram, B., Sinha, A.K., and Chattopadhyay, S. (2014). A Mitogen-Activated Protein Kinase Cascade Module, MKK3-MPK6 and MYC2, Is Involved in Blue Light-Mediated Seedling Development in Arabidopsis. Plant Cell **26**: 3343–3357.

Shalitin, D., Yang, H., Mockler, T.C., Maymon, M., Guo, H., Whitelam, G.C., and Lin, C. (2002). Regulation of Arabidopsis cryptochrome 2 by blue-light-dependent phosphorylation. Nature **417**: 763–767.

Sharrock, R.A., and Clack, T. (2002). Patterns of expression and normalized levels of the five Arabidopsis phytochromes. Plant Physiology **130**: 442–456.

Sharrock, R.A., and Clack, T. (2004). Heterodimerization of type II phytochromes in Arabidopsis. Proceedings of the National Academy of Sciences of the United States of America **101**: 11500–11505.

Shin, J., Kim, K., Kang, H., Zulfugarov, I.S., Bae, G., Lee, C.H., Lee, D., and Choi, G. (2009). Phytochromes promote seedling light responses by inhibiting four negatively-acting phytochrome-interacting factors. Proceedings of the National Academy of Sciences of the United States of America **106**: 7660–7665.

Shin, J., Park, E., and Choi, G. (2007). PIF3 regulates anthocyanin biosynthesis in an HY5-dependent manner with both factors directly binding anthocyanin biosynthetic gene promoters in Arabidopsis. The Plant Journal **49**: 981–994.

Shinkle, J.R., Atkins, A.K., Humphrey, E.E., Rodgers, C.W., Wheeler, S.L., and Barnes, P.W. (2004). Growth and morphological responses to different UV wavebands in cucumber (Cucumis sativum) and other dicotyledonous seedlings. Physiologia Plantarum **120**: 240–248.

Shinkle, J.R., Edwards, M.C., Koenig, A., Shaltz, A., and Barnes, P.W. (2010). Photomorphogenic regulation of increases in UV-absorbing pigments in cucumber (*Cucumis sativus*) and *Arabidopsis thaliana* seedlings induced by different UV-B and UV-C wavebands. Physiologia Plantarum **138**: 113–121.

Sibout, R., Sukumar, P., Hettiarachchi, C., Holm, M., Muday, G.K., and Hardtke, C.S. (2006). Opposite root growth phenotypes of hy5 versus hy5 hyh mutants correlate with increased constitutive auxin signalling. PLoS Genetics **2**: e202.

Singh, A., Ram, H., Abbas, N., and Chattopadhyay, S. (2012). Molecular interactions of GBF1 with HY5 and HYH proteins during light-mediated seedling development in *Arabidopsis thaliana*. Journal of Biological Chemistry **287**: 25995–26009.

Singh, S., Agrawal, S.B., and Agrawal, M. (2014). UVR8 mediated plant protective responses under low UV-B radiation leading to photosynthetic acclimation. Journal of Photochemistry and Photobiology B **137**: 67–76.

Squazzo, S.L., O'Geen, H., Komashko, V.M., Krig, S.R., Jin, V.X., Jang, S.-, Margueron, R., Reinberg, D., Green, R., and Farnham, P.J. (2006). Suz12 binds to silenced regions of the genome in a cell-type-specific manner. Genome research **16**: 890–900.

Sridhar, V.V., Surendrarao, A., Gonzalez, D., Conlan, R.S., and Liu, Z. (2004). Transcriptional repression of target genes by LEUNIG and SEUSS, two interacting regulatory proteins for Arabidopsis flower development. Proceedings of the National Academy of Sciences of the United States of America **101**: 11494–11499.

Stirnimann, C.U., Petsalaki, E., Russell, R.B., and Muller, C.W. (2010). WD40 proteins propel cellular networks. Trends in Biochemical Sciences **35**: 565–574.

Stockinger, E.J., Mao, Y., Regier, M.K., Triezenberg, S.J., and Thomashow, M.F. (2001). Transcriptional adaptor and histone acetyltransferase proteins in Arabidopsis and their interactions with CBF1, a transcriptional activator involved in cold-regulated gene expression. Nucleic acids research **29**: 1524–1533.

Stracke, R., Favory, J.J., Gruber, H., Bartelniewoehner, L., Bartels, S., Binkert, M., Funk, M., Weisshaar, B., and Ulm, R. (2010). The Arabidopsis bZIP transcription factor HY5 regulates expression of the PFG1/MYB12 gene in response to light and ultraviolet-B radiation. Plant Cell and Environment **33**: 88–103.

Stracke, R., Werber, M., and Weisshaar, B. (2001). The< i> R2R3-MYB gene family in< i> *Arabidopsis thaliana.* Current opinion in plant biology **4**: 447–456.

Strahl, B.D., and Allis, C.D. (2000). The language of covalent histone modifications. Nature **403**: 41–45.

Struhl, K. (2007). Interpreting chromatin immunoprecipitation experiments. Evaluating Techniques in Biochemical Research, D. Zuk, ed 29–33.

Suganuma, T., and Workman, J.L. (2008). Crosstalk among Histone Modifications. Cell **135**: 604–607.

Sullivan, A.M., Arsovski, A.A., Lempe, J., Bubb, K.L., Weirauch, M.T., Sabo, P.J., Sandstrom, R., Thurman, R.E., Neph, S., Reynolds, A.P., Stergachis, A.B., Vernot, B., Johnson, A.K., Haugen, E., Sullivan, S.T., Thompson, A., Neri, F.V., Weaver, M., Diegel, M., Mnaimneh, S., Yang, A., Hughes, T.R., Nemhauser, J.L., Queitsch, C., and Stamatoyannopoulos, J.A. (2014). Mapping and dynamics of regulatory DNA and transcription factor networks in A. thaliana. Cell Reports **8**: 2015–2030.

Surplus, S.L., Jordan, B.R., Murphy, A.M., Carr, J.P., Thomas, B., and Mackerness, S.A. (1998). Ultraviolet−B−induced responses in *Arabidopsis thaliana*: role of salicylic acid and reactive oxygen species in the regulation of transcripts encoding photosynthetic and acidic pathogenesis−related proteins. Plant, Cell & Environment **21**: 685–694.

Takemiya, A., Sugiyama, N., Fujimoto, H., Tsutsumi, T., Yamauchi, S., Hiyama, A., Tada, Y., Christie, J.M., and Shimazaki, K. (2013). Phosphorylation of BLUS1 kinase by phototropins is a primary step in stomatal opening. Nature Communications **4**: 2094.

Tang, W., Wang, W., Chen, D., Ji, Q., Jing, Y., Wang, H., and Lin, R. (2012). Transposase-derived proteins FHY3/FAR1 interact with PHYTOCHROME-INTERACTING FACTOR1 to regulate chlorophyll biosynthesis by modulating HEMB1 during deetiolation in Arabidopsis. Plant Cell **24**: 1984–2000.

Tanurdzic, M., Vaughn, M.W., Jiang, H., Lee, T.-J., Slotkin, R.K., Sosinski, B., Thompson, W.F., Doerge, R.W., and Martienssen, R.A. (2008). Epigenomic consequences of immortalized plant cell suspension culture. PLoS biology **6**: e302

Tepperman, J.M., Hudson, M.E., Khanna, R., Zhu, T., Chang, S.H., Wang, X., and Quail, P.H. (2004). Expression profiling of phyB mutant demonstrates substantial contribution of other phytochromes to red−light−regulated gene expression during seedling de−etiolation. The Plant Journal **38**: 725–739.

Tepperman, J.M., Zhu, T., Chang, H.S., Wang, X., and Quail, P.H. (2001). Multiple transcription-factor genes are early targets of phytochrome A signaling. Proceedings of the National Academy of Sciences of the United States of America **98**: 9437–9442.

Terzaghi, W.B., and Cashmore, A.R. (1995). Light-regulated transcription. Annual review of plant biology **46**: 445–474.

Tian, L., Wang, J., Fong, M.P., Chen, M., Cao, H., Gelvin, S.B., and Chen, Z.J. (2003). Genetic control of developmental changes induced by disruption of Arabidopsis histone deacetylase 1 (AtHD1) expression. Genetics **165**: 399–409.

Tilbrook, K., Arongaus, A.B., Binkert, M., Heijde, M., Yin, R., and Ulm, R. (2013). The UVR8 UV-B Photoreceptor: Perception, Signaling and Response. Arabidopsis Book **11**: e0164.

Tiwari, S.B., Shen, Y., Chang, H., Hou, Y., Harris, A., Ma, S.F., McPartland, M., Hymus, G.J., Adam, L., and Marion, C. (2010). The flowering time regulator CONSTANS is recruited to the FLOWERING LOCUS T promoter via a unique cis-element. New Phytologist **187**: 57–66.

Toledo-Ortiz, G., Johansson, H., Lee, K.P., Bou-Torrent, J., Stewart, K., Steel, G., Rodriguez-Concepcion, M., and Halliday, K.J. (2014). The HY5-PIF regulatory module coordinates light and temperature control of photosynthetic gene transcription. PLoS Genetics **10**: e1004416.

Tong, H., Leasure, C.D., Hou, X., Yuen, G., Briggs, W., and He, Z.H. (2008). Role of root UV-B sensing in Arabidopsis early seedling development. Proceedings of the National Academy of Sciences of the United States of America **105**: 21039–21044.

Tossi, V., Lamattina, L., Jenkins, G.I., and Cassia, R.O. (2014). Ultraviolet-B-Induced Stomatal Closure in Arabidopsis Is Regulated by the UV RESISTANCE LOCUS8 Photoreceptor in a Nitric Oxide-Dependent Mechanism. Plant Physiology **164**: 2220–2230.

Tsai, H.L., Li, Y.H., Hsieh, W.P., Lin, M.C., Ahn, J.H., and Wu, S.H. (2014). HUA ENHANCER1 is involved in post-transcriptional regulation of positive and negative regulators in Arabidopsis photomorphogenesis. Plant Cell **26**: 2858–2872.

Tucker, C.L., Peteya, L.A., Pittman, A.M., and Zhong, J. (2009). A genetic test for yeast two-hybrid bait competency using RanBPM. Genetics **182**: 1377–1379.

Turck, F., Roudier, F., Farrona, S., Martin-Magniette, M.L., Guillaume, E., Buisine, N., Gagnot, S., Martienssen, R.A., Coupland, G., and Colot, V. (2007). Arabidopsis TFL2/LHP1 specifically associates with genes marked by trimethylation of histone H3 lysine 27. PLoS Genetics **3**: e86.

Ulm, R., and Nagy, F. (2005). Signalling and gene regulation in response to ultraviolet light. Current Opinion in Plant Biology **8**: 477–482.

Ulm, R., Baumann, A., Oravecz, A., Máté, Z., Ádám, É., Oakeley, E.J., Schäfer, E., and Nagy, F. (2004). Genome-wide analysis of gene expression reveals function of the bZIP transcription factor HY5 in the UV-B response of Arabidopsis. Proceedings of the National Academy of Sciences of the United States of America **101**: 1397–1402.

Vakoc, C.R., Mandat, S.A., Olenchock, B.A., and Blobel, G.A. (2005). Histone H3 lysine 9 methylation and HP1γ are associated with transcription elongation through mammalian chromatin. Molecular cell **19**: 381–391.

Van Buskirk, E.K., Decker, P.V., and Chen, M. (2012). Photobodies in light signaling. Plant Physiology **158**: 52–60.

Vandenbussche, F., Habricot, Y., Condiff, A.S., Maldiney, R., Van der Straeten, D., and Ahmad, M. (2007). HY5 is a point of convergence between cryptochrome and cytokinin signalling pathways in *Arabidopsis thaliana*. The Plant Journal **49**: 428–441.

Vandenbussche, F., Tilbrook, K., Fierro, A.C., Marchal, K., Poelman, D., Van Der Straeten, D., and Ulm, R. (2014). Photoreceptor-mediated bending towards UV-B in Arabidopsis. Molecular Plant **7**: 1041–1052.

Voityuk, A.A., Marcus, R.A., and Michel-Beyerle, M.E. (2014). On the mechanism of photoinduced dimer dissociation in the plant UVR8 photoreceptor. Proceedings of the National Academy of Sciences of the United States of America **111**: 5219–5224.

Wada, M., Takahashi, H., Altaf-Ul-Amin, M., Nakamura, K., Hirai, M.Y., Ohta, D., and Kanaya, S. (2012). Prediction of operon-like gene clusters in the< i> *Arabidopsis thaliana* genome based on co-expression analysis of neighbouring genes. Gene **503**: 56–64.

Wang, H., Ma, L.G., Li, J.M., Zhao, H.Y., and Deng, X.W. (2001). Direct interaction of Arabidopsis cryptochromes with COP1 in light control development. Science **294**: 154–158.

Wang, Y., Maruhnich, S.A., Mageroy, M.H., Justice, J.R., and Folta, K.M. (2013). Phototropin 1 and cryptochrome action in response to green light in combination with other wavelengths. Planta **237**: 225–237.

Wargent, J.J., Gegas, V.C., Jenkins, G.I., Doonan, J.H., and Paul, N.D. (2009). UVR8 in *Arabidopsis thaliana* regulates multiple aspects of cellular differentiation during leaf development in response to ultraviolet B radiation. New Phytologist **183**: 315–326.

Weake, V.M., and Workman, J.L. (2008). Histone ubiquitination: triggering gene activity. Molecular cell **29**: 653–663.

Weigel, D., and Glazebrook, J. (2005). Setting up Arabidopsis crosses. CSH protocols **2006**: 436–440.

Weisshaar, B., Armstrong, G.A., Block, A., da Costa e Silva, O., and Hahlbrock, K. (1991). Light-inducible and constitutively expressed DNA-binding proteins recognizing a plant promoter element with functional relevance in light responsiveness. The EMBO Journal **10**: 1777–1786.

Weisshaar, B., and Jenkins, G.I. (1998). Phenylpropanoid biosynthesis and its regulation. Current Opinion in Plant Biology **1**: 251–257.

Wellmann, E. (1976). Specific ultraviolet effects in plant morphogenesis. Photochem Photobiol **24**: 659–660.

Wenkel, S., Turck, F., Singer, K., Gissot, L., Le Gourrierec, J., Samach, A., and Coupland, G. (2006). CONSTANS and the CCAAT box binding complex share a functionally important domain and interact to regulate flowering of Arabidopsis. Plant Cell **18**: 2971–2984.

West, J.A., Cook, A., Alver, B.H., Stadtfeld, M., Deaton, A.M., Hochedlinger, K., Park, P.J., Tolstorukov, M.Y., and Kingston, R.E. (2014). Nucleosomal occupancy changes locally over key regulatory regions during cell differentiation and reprogramming. Nature Communications **5**: 4719.

Wu, D., Hu, Q., Yan, Z., Chen, W., Yan, C., Huang, X., Zhang, J., Yang, P., Deng, H., and Wang, J. (2012). Structural basis of ultraviolet-B perception by UVR8. Nature **484**: 214–219.

Wu, M., Grahn, E., Eriksson, L.A., and Strid, A. (2011). Computational evidence for the role of *Arabidopsis thaliana* UVR8 as UV-B photoreceptor and identification of its chromophore amino acids. J Chem Inf Model **51**: 1287–1295.

Wu, M., Strid, A., and Eriksson, L.A. (2013). Interactions and stabilities of the UV RESISTANCE LOCUS8 (UVR8) protein dimer and its key mutants. J Chem Inf Model **53**: 1736–1746.

Wu, M., Strid, A., and Eriksson, L.A. (2014). Photochemical reaction mechanism of UV-B-induced monomerization of UVR8 dimers as the first signaling event in UV-B-regulated gene expression in plants. J Phys Chem B **118**: 951–965.

Wu, S.-H. (2014). Gene Expression Regulation in Photomorphogenesis from the Perspective of the Central Dogma. Annual review of plant biology **65**: 311–333.

Xu, C., and Min, J. (2011). Structure and function of WD40 domain proteins. Protein Cell **2**: 202–214.

Xu, F., Zhang, K., and Grunstein, M. (2005). Acetylation in histone H3 globular domain regulates gene expression in yeast. Cell **121**: 375–385.

Yamaguchi, M., Ohtani, M., Mitsuda, N., Kubo, M., Ohme-Takagi, M., Fukuda, H., and Demura, T. (2010). VND-INTERACTING2, a NAC domain transcription factor, negatively regulates xylem vessel formation in Arabidopsis. Plant Cell **22**: 1249–1263.

Yan, H., Marquardt, K., Indorf, M., Jutt, D., Kircher, S., Neuhaus, G., and Rodríguez-Franco, M. (2011). Nuclear localization and interaction with COP1 are required for STO/BBX24 function during photomorphogenesis. Plant physiology **156**: 1772–1782.

Yang, H.Q., Tang, R.H., and Cashmore, A.R. (2001). The signaling mechanism of Arabidopsis CRY1 involves direct interaction with COP1. Plant Cell **13**: 2573–2587.

Yang, S.W., Jang, I.-C., Henriques, R., and Chua, N.-H. (2009). FAR-RED ELONGATED HYPOCOTYL1 and FHY1-LIKE associate with the Arabidopsis transcription factors LAF1 and HFR1 to transmit phytochrome A signals for inhibition of hypocotyl elongation. Plant Cell **21**: 1341–1359.

Yang, S.-D., Seo, P.J., Yoon, H.-K., and Park, C.-M. (2011). The Arabidopsis NAC transcription factor VNI2 integrates abscisic acid signals into leaf senescence via the COR/RD genes. Plant Cell **23**: 2155–2168.

Yi, C., and Deng, X.W. (2005). COP1–from plant photomorphogenesis to mammalian tumorigenesis. Trends in cell biology **15**: 618–625.

Zhang, H., He, H., Wang, X., Wang, X., Yang, X., Li, L., and Deng, X.W. (2011). Genome-wide mapping of the HY5-mediated gene networks in Arabidopsis that involve both transcriptional and post-transcriptional regulation. The Plant Journal **65**: 346–358.

Zhang, T., Maruhnich, S.A., and Folta, K.M. (2011). Green light induces shade avoidance symptoms. Plant Physiology **157**: 1528–1536.

Zhang, X., Bernatavichute, Y.V., Cokus, S., Pellegrini, M., and Jacobsen, S.E. (2009). Genome-wide analysis of mono-, di-and trimethylation of histone H3 lysine 4 in *Arabidopsis thaliana*. Genome Biology **10**: R62.

Zhang, Y., Mayba, O., Pfeiffer, A., Shi, H., Tepperman, J.M., Speed, T.P., and Quail, P.H. (2013). A quartet of PIF bHLH factors provides a transcriptionally centered signaling hub that regulates seedling morphogenesis through differential expression-patterning of shared target genes in Arabidopsis. PLoS genetics **9**: e1003244.

Zhu, Y.Y., Machleder, E.M., Chenchik, A., Li, R., and Siebert, P.D. (2001). Reverse transcriptase template switching: A SMART™ approach for full-length cDNA library construction. Biotechniques **30**: 892–897.

Zirak, P., Penzkofer, A., Moldt, J., Pokorny, R., Batschauer, A., and Essen, L.O. (2009). Photocycle dynamics of the E149A mutant of cryptochrome 3 from *Arabidopsis thaliana*. J Photochem Photobiol B **97**: 94–108.